NCEER-TAISEI CORPORATION RESEARCH PROGRAM ON SLIDING SEISMIC ISOLATION SYSTEMS FOR BRIDGES:

EXPERIMENTAL AND ANALYTICAL STUDY OF A SYSTEM CONSISTING OF SLIDING BEARINGS AND FLUID RESTORING FORCE/DAMPING DEVICES

By

T. Tsopelas and M.C. Constantinou

State University of New York at Buffalo
Department of Civil Engineering
Buffalo, New York 14260

Technical Report NCEER-94-0014

July 13, 1994

This research was conducted at the State University of New York at Buffalo and was partially supported by the National Science Foundation under Grant Number BCS 90-25010 and the New York State Science and Technology Foundation under Grant Number NEC-91029

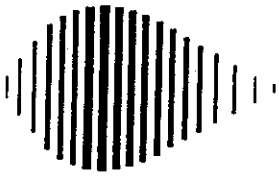

NCEER-Taisei Corporation Research Program on Sliding Seismic Isolation Systems for Bridges:

Experimental and Analytical Study of a System Consisting of Sliding Bearings and Fluid Restoring Force/Damping Devices

by

P. Tsopelas[1] and M.C. Constantinou[2]

June 13, 1994

Technical Report NCEER-94-0014

NCEER Task Numbers 90-2101 and 91-5411B
and
Taisei Corporation Grant 150-6889A

NSF Master Contract Number BCS 90-25010
and
NYSSTF Grant Number NEC-91029

1 Research Assistant, Department of Civil Engineering, State University of New York at Buffalo
2 Professor, Department of Civil Engineering, State University of New York at Buffalo

NATIONAL CENTER FOR EARTHQUAKE ENGINEERING RESEARCH
State University of New York at Buffalo
Red Jacket Quadrangle, Buffalo, NY 14261

PREFACE

The National Center for Earthquake Engineering Research (NCEER) was established to expand and disseminate knowledge about earthquakes, improve earthquake-resistant design, and implement seismic hazard mitigation procedures to minimize loss of lives and property. The emphasis is on structures in the eastern and central United States and lifelines throughout the country that are found in zones of low, moderate, and high seismicity.

NCEER's research and implementation plan in years six through ten (1991-1996) comprises four interlocked elements, as shown in the figure below. Element I, Basic Research, is carried out to support projects in the Applied Research area. Element II, Applied Research, is the major focus of work for years six through ten. Element III, Demonstration Projects, have been planned to support Applied Research projects, and will be either case studies or regional studies. Element IV, Implementation, will result from activity in the four Applied Research projects, and from Demonstration Projects.

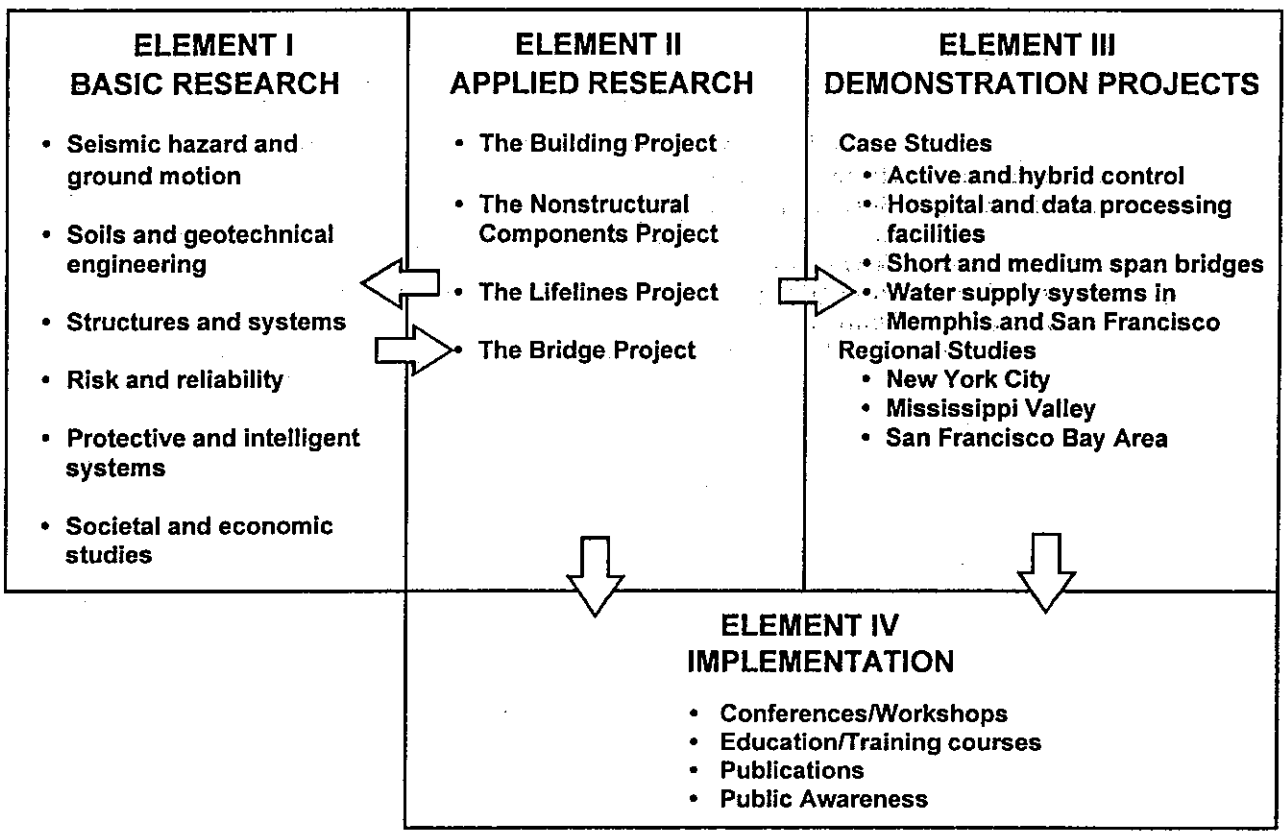

Research tasks in the **Bridge Project** expand current work in the retrofit of existing bridges and develop basic seismic design criteria for eastern bridges in low-to-moderate risk zones. This research parallels an extensive multi-year research program on the evaluation of gravity-load design concrete buildings. Specifically, tasks are being performed to:

1. Determine the seismic vulnerability of bridge structures in regions of low-to-medium seismicity, and in particular of those bridges in the eastern and central United States.
2. Develop concepts for retrofitting vulnerable bridge systems, particularly for typical bridges found in the eastern and central United States.
3. Develop improved design and evaluation methodologies for bridges, with particular emphasis on soil-structure mechanics and its influence on bridge response.
4. Review seismic design criteria for new bridges in the eastern and central United States.

The end product of the **Bridge Project** will be a collection of design manuals, pre-standards and design aids which will focus on typical eastern and central United States highway bridges. Work begun in the **Bridge Project** has now been incorporated into the **Highway Project.**

The **protective and intelligent systems program** constitutes one of the important areas of research in the **Bridge Project**. Current tasks include the following:

1. Evaluate the performance of full-scale active bracing and active mass dampers already in place in terms of performance, power requirements, maintenance, reliability and cost.
2. Compare passive and active control strategies in terms of structural type, degree of effectiveness, cost and long-term reliability.
3. Perform fundamental studies of hybrid control.
4. Develop and test hybrid control systems.

The design of earthquake resistant structures should always consider the possible use of protective and intelligent devices to enhance their energy absorbing capacity or isolate their dynamic characteristics away from the damaging frequency range of an earthquake.

This report describes the results of an experimental study of the behavior of a bridge seismic sliding isolation system consisting of flat sliding bearings and fluid restoring force/damping devices. Earthquake simulator tests have been performed on a model bridge structure both isolated with this system and non-isolated. The experimental results demonstrate a marked increase of the capacity of the isolated bridge to withstand earthquake forces. Analytical techniques are used to predict the dynamic response of the system and the obtained results are in very good agreement with the experimental results.

ABSTRACT

This report describes the results of an experimental study of the behavior of a bridge seismic sliding isolation system consisting of flat sliding bearings and fluid restoring force/damping devices. Earthquake simulator tests have been performed on a model bridge structure both isolated with this system and non-isolated. The experimental results demonstrate a marked increase of the capacity of the isolated bridge to withstand earthquake forces. Analytical techniques are used to predict the dynamic response of the system and the obtained results are in very good agreement with the experimental results.

ACKNOWLEDGMENTS

Financial support for this project has been provided by Taisei Corporation, Japan and the National Center for Earthquake Engineering Research, Projects No. 902101 and 915411B.

The sliding bearings used in the study were manufactured by Watson Bowman Acme Corporation, Amherst, NY.

The fluid restoring force/damping devices were manufactured by Taylor Devices, Inc., North Tonawanda, NY.

TABLE OF CONTENTS

LIST OF ILLUSTRATIONS

LIST OF ILLUSTRATIONS (cont'd)

LIST OF ILLUSTRATIONS (cont'd)

LIST OF ILLUSTRATIONS (cont'd)

LIST OF TABLES

SECTION 1

INTRODUCTION

Seismic isolation systems are typified by the use of either elastomeric or sliding bearings. Elastomeric isolation systems have been used in the seismic isolation of buildings in Japan and the United States (Buckle 1990, Soong 1992, Kelly 1993). Several other countries, such as New Zealand and Italy among others, have a number of applications of elastomeric isolation systems in buildings (Buckle 1990, Martelli 1993).

Sliding isolation systems in buildings have been widely used in the former Soviet Union, where over 200 buildings are now seismically isolated (Constantinou 1991a, Eisenberg 1992). In Japan, Taisei Corporation constructed three buildings on the TASS sliding isolation system (Kawamura 1988, Constantinou 1991a). In the United States, sliding isolation systems have recently been selected for the retrofit of three buildings (Soong 1992, Kelly 1993). In particular, spherical sliding or FPS bearings (Zayas 1987, Mokha 1990b and 1991) have been selected for the retrofit of the U.S. Court of Appeals building in San Francisco. This historic structure with a floor area of 31500m^2, will be, when completed, the largest base-isolated structure in the U.S. and one of the largest in the world (Soong 1992, Palfalvi 1993).

Seismic isolation of bridge structures has been widely implemented in New Zealand and Italy (Buckle 1990, Medeot 1991, Martelli 1993). While in New Zealand the application is exclusively with elastomeric systems, in Italy the application is primarily with sliding systems. Over 150 km of isolated bridge deck in Italy is supported by sliding bearings together with various forms of restoring force and energy dissipation devices (Medeot 1991, Constantinou 1991a).

Japan has over 100 concrete railway bridges of the Shinkansen supported by sliding bearings together with viscous fluid devices, called the KP-stoppers, for restricting displacements within acceptable limits (Buckle 1990, Constantinou 1991a). This system is regarded as an early form of sliding isolation system.

More recently, Japan moved towards a cautious implementation of modern seismic isolation systems in bridges. So far, the application is restricted to only longitudinal isolation using elastomeric systems (Kawashima 1991).

The application of seismic isolation to bridges in the U.S. followed an interesting development. Until 1989, only six bridges were isolated, of which five were retrofit projects in California and one was a new construction in Illinois (Buckle 1990). While the 1989 Loma Prieta earthquake resulted in an accelerated implementation of seismic isolation systems to buildings, this has not been the case in bridges. Rather, we observe a renewed interest and new applications of bridge seismic isolation following the development of specifications for seismic isolation design (ICBO 1991, AASHTO 1991) and the adoption of seismic design guidelines for bridges in the entire U.S. The lack of specifications for the design of seismic isolated structures was regarded as an impediment to the application of the technology (Mayes 1990). Today (January 1994), 57 isolated bridges of total deck length exceeding 11 km are opened to traffic or they are in either the construction or in the design process in the U.S. The isolation system of these bridges consists of either lead-rubber bearings or sliding bearings with restoring force devices and sliding bearings with yielding steel devices. Interestingly, the majority of these bridges are located in the Eastern United States.

While seismic isolation systems found application to over 200 bridges, large scale testing of bridge isolation systems has been so far limited to three studies which concentrated on elastomeric systems (Kelly 1986, Kawashima 1991) and one specific sliding system (Constantinou 1991a). All three studies were restricted to models with rigid piers or abutments and rigid decks. The effects of pier flexibility, pier strength, deck flexibility and distribution of isolation elements could not be studied in these experimental programs. Rather, these effects were studied by analytical techniques and found to be significant (Constantinou 1991a, Kartoum 1992).

The study reported herein was carried out as part of the NCEER-Taisei Corporation research project on bridge seismic isolation systems. This project included the

development of advanced sliding isolation systems for bridges and a comprehensive testing program utilizing a flexible pier model. This report concentrates on one of these systems, which consists of flat sliding bearings and fluid restoring force/damping devices. Results for other sliding isolation systems studied under this project have been reported by Constantinou 1993 and Tsopelas 1994.

(d) Fluid restoring force/damping devices.

(2) Spherically shaped FPS sliding bearings.

(3) Flat lubricated PTFE-stainless steel sliding bearings in combination with yielding E-shaped mild steel devices.

This report contains the results of the experimental study, interpretation of the results and analytical modeling of systems consisting of flat sliding bearings and fluid restoring force/damping devices.

SECTION 2

NCEER-TAISEI CORPORATION RESEARCH PROJECT ON BRIDGE SLIDING SEISMIC ISOLATION SYSTEMS

In 1991, the National Center for Earthquake Engineering Research and Taisei Corporation began a collaborative research project on the development and verification of advanced sliding seismic isolation systems for bridges (Constantinou 1992). The project included also the study of established sliding isolation systems such as the Friction Pendulum (or FPS) system (Zayas 1987, Mokha 1990b and 1991, Constantinou 1993) and the lubricated sliding bearing/hysteretic steel damper system used in a large number of bridges in Italy (Medeot 1991, Marioni 1991).

The project had two portions: one concentrated on active systems and was carried out at Taisei Corporation and Princeton University, and the other concentrated on passive systems and was carried out at the University at Buffalo and Taisei Corporation. The Buffalo/Taisei portion of the project had the objective of producing a class of advanced passive sliding seismic isolation systems by modifying and/or adapting existing technology. Particular emphasis has been given to the adaptation and use of aerospace and military hardware in either the form of restoring force and damping devices or in the form of high performance composite materials in the construction of sliding bearings. The following systems were experimentally studied:

(1) Flat sliding bearings consisting of PTFE or PTFE-based composites in contact with polished stainless steel (coefficient of sliding friction at high velocity of sliding in the range of 0.07 to 0.15) and in combination with

   (a) Rubber restoring force devices,

   (b) Rubber restoring force devices and fluid viscous dampers,

   (c) Wire rope restoring force devices, and

SECTION 3

ISOLATION SYSTEM

3.1 Design Requirements

The studied isolation systems consisted of two components :

(1) Flat sliding bearings to support the weight of the deck and provide a mechanism for energy dissipation.

(2) Restoring force/damping devices for providing restoring force, that is, recentering capability and preload for eliminating permanent displacements.

The two components of the isolation system provided load carrying capacity, restoring force capability and hysteretic and viscous damping which were not interrelated. This facilitated optimum performance for specific design requirements.

The specific design requirements of the isolation system were to minimize the transmission of force to the substructure, that is piers and foundation, while bearing displacements in the scale of the model (length scale factor equal to 4) did not exceed 50 mm and permanent displacements were nearly zero. These requirements were to be met for seismic motions representative of bridge design spectra in California (CalTrans) (Gates 1979) and in Japan (Level 2) (CERC 1992) for all ground conditions. Furthermore, the performance of the isolated bridge should be better, in terms of transmission of force to the substructure, than a comparable non-isolated bridge under weak seismic excitation, such as the Japanese Level 1 motions (CERC 1992).

The severe requirement on the maximum bearing displacement (50 mm in the scaled model or 200 mm in prototype scale) under strong seismic excitation reflects some design and economic considerations in bridge seismic isolation. A maximum bearing displacement of 200 mm allows the use of short multidirectional expansion joints and eliminates the need for knock-off elements. Short expansion joints are less expensive, require less maintenance and produce less noise on automobile crossing than long ones.

3.2 Sliding Bearings

Four multidirectional sliding bearings of the disc type were used. Illustrated in Figures 3-1 and 3-2, this bearing consisted of a bottom plate which was supported by a high hardness Adiprene disc and a shear restriction mechanism. The disc provided rotational capability to the bottom plate so that the sliding interface was always in full contact.

The sliding interface consisted of austenitic stainless steel, conforming to ASTM A-240, type 304 requirements and polished to mirror finish. The roughness of the polished stainless steel surface was measured with a Surtronic 3P instrument (stylus radius=2.5 μm, cutoff length=0.8 mm, traverse length=4.5 mm) and found to be 0.04 μm R_a (Arithmetic Average, AA, or Center Line Average, CLA).

The bottom plate of the sliding bearing was delivered with a circular recess, which could accept plates faced with PTFE or other materials. This facilitated easy replacement of the sliding interface in order to achieve friction coefficients at large velocity of sliding in the range of 0.07 to 0.15. Specifically, three different interfaces were used in the NCEER-TAISEI research program (Tsopelas 1994). However, in the testing of this isolation system only the high friction interface was used. The material was unfilled PTFE under pressure of 5 MPa (designated as bearing T1). Prior to conducting the tests of the system with fluid restoring force/damping devices, the bearings were used in about 100 seismic and identification tests which were reported in Tsopelas, 1994. During these tests the coefficient of friction at high velocity of sliding dropped gradually from an initial value of 0.15 to a final value of 0.14. This is illustrated in Figure 3-3 which depicts recorded values of the coefficient of sliding friction as function of sliding velocity. It may be seen that in the initial identification tests and during testing of the test series IDRUN (reported in Tsopelas 1994) the coefficient of friction at high velocity of sliding is 0.15. However, during the tests that followed (series TDRUN for the system reported herein) the friction coefficient has the value of 0.14. This behavior is consisted with observations made by Mokha, 1988.

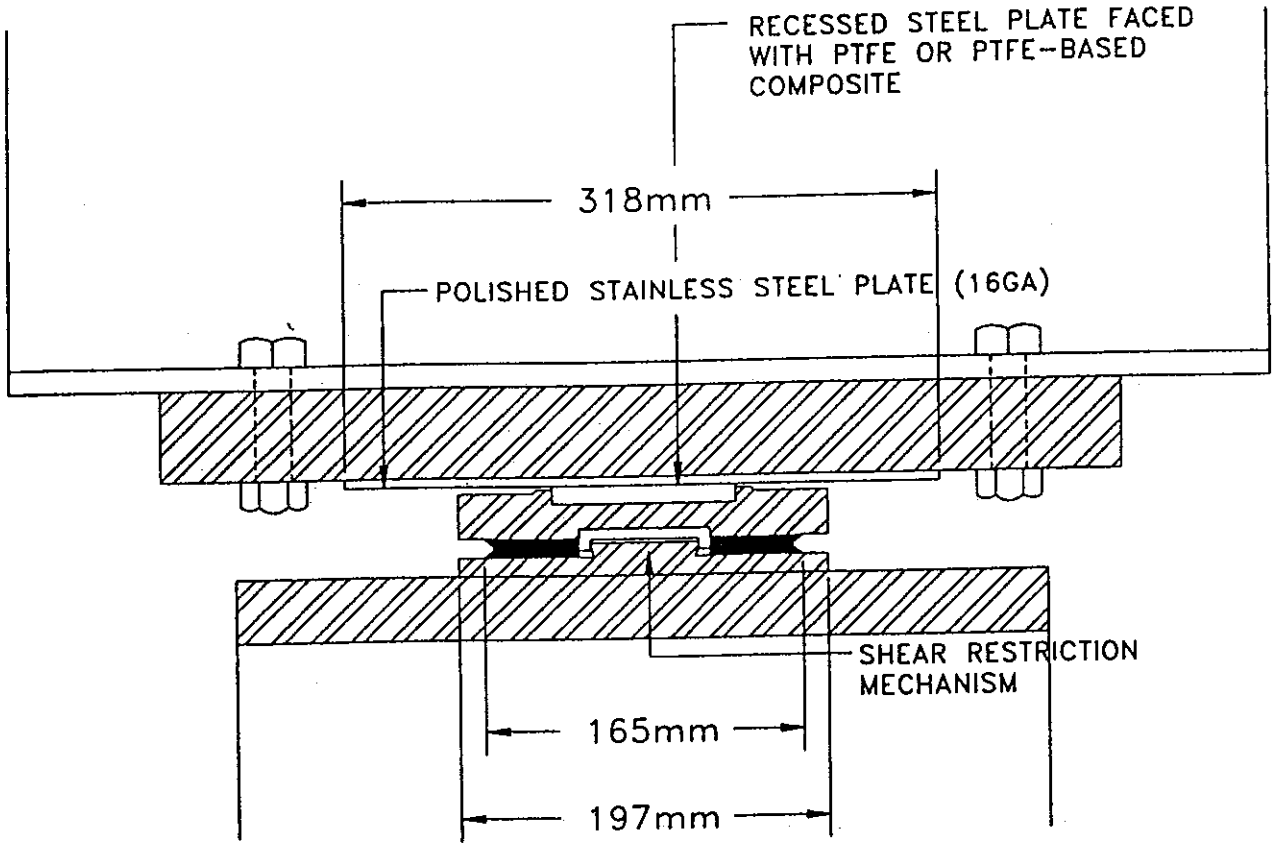

Figure 3-1 Sliding Disc Bearing Design.

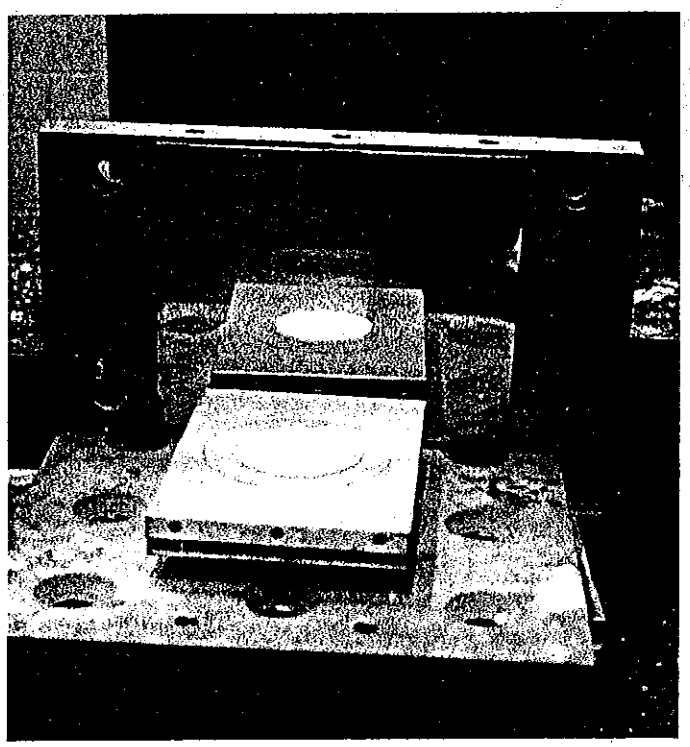

Figure 3-2 View of Sliding Disc Bearing.

The coefficient of sliding friction, μ, followed the relation (Constantinou 1990a)

$$\mu = f_{\max} - (f_{\max} - f_{\min})\exp(-a|\dot{u}|) \qquad (3\text{-}1)$$

where f_{max} is the coefficient of friction at high velocity of sliding, f_{min} is the coefficient of friction at essentially zero velocity of sliding, a is a parameter controlling the variation of the coefficient of friction with velocity of sliding and $\dot{u}$ is the velocity of sliding. A comparison of experimental results on the coefficient of friction to predictions of the calibrated model of Equation (3-1) is presented in Figure 3-3. The parameters are listed in Table 3-I.

Table 3-I Properties of Sliding Disc Bearings

Bearing	Characterization of Friction	Condition	Material	Contact Area (mm^2)	Bearing Pressure (MPa)	f_{max}	f_{min}	a (s/m)
T1	High Friction (HF)	First 100 Tests	Unfilled PTFE	7090	5.0	0.150	0.055	23.7
T1	High Friction (HF)	Subsequent Tests	Unfilled PTFE	7090	5.0	0.140	0.060	24.0

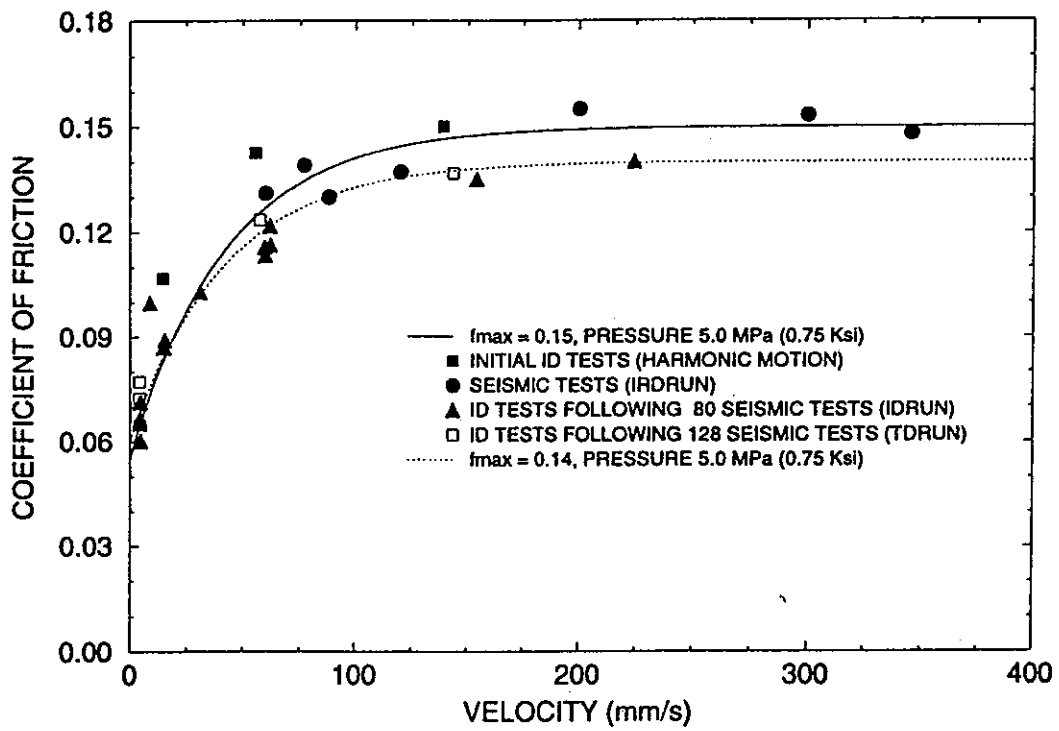

Figure 3-3 Coefficient of Friction as Function of Sliding Velocity of Sliding Disc Bearings.

3.3 Fluid Restoring Force/Damping Devices

Two fluid restoring force/damping devices were connected between the deck and the two piers. The construction of these devices is illustrated in Figure 3-4. Each device had a pin-to-pin length of 380 mm, outside diameter equal to 44 mm, weight equal to 1.7 Kg, stroke of ±50 mm and output force of about 13.5 kN at peak stroke under dynamic conditions. Typical force-displacement loops of one device under static and dynamic loading conditions are shown in Figure 3-5.

Each device features a preload F_o=4.75 kN, stiffness K_o (slope for forces exceeding the preload) of about 100 N/mm and a viscous force component. Furthermore, the device is double-acting with identical properties in tension and compression. The preload was selected to be slightly more than the minimum friction force in the isolation system. That is, $2F_o$ (for two devices) equals 9.5 kN, whereas the minimum friction force is $f_{min} W_d$ (W_d=143 kN, deck weight) or $0.06 \times 143 = 8.58$ kN. Under these conditions the two devices were capable of recentering the bridge and eliminate permanent displacements.

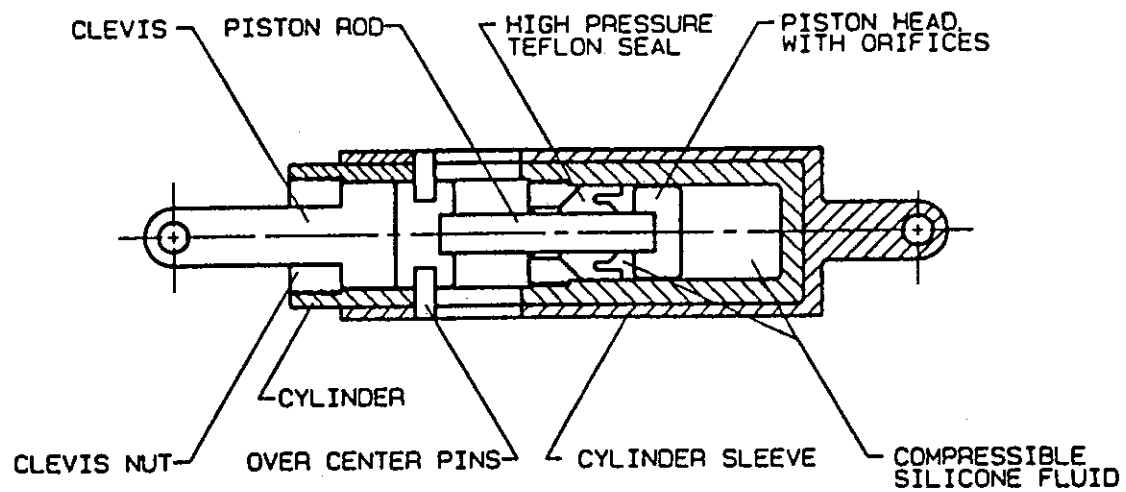

Figure 3-4 Construction of Fluid Restoring Force/Damping Device.

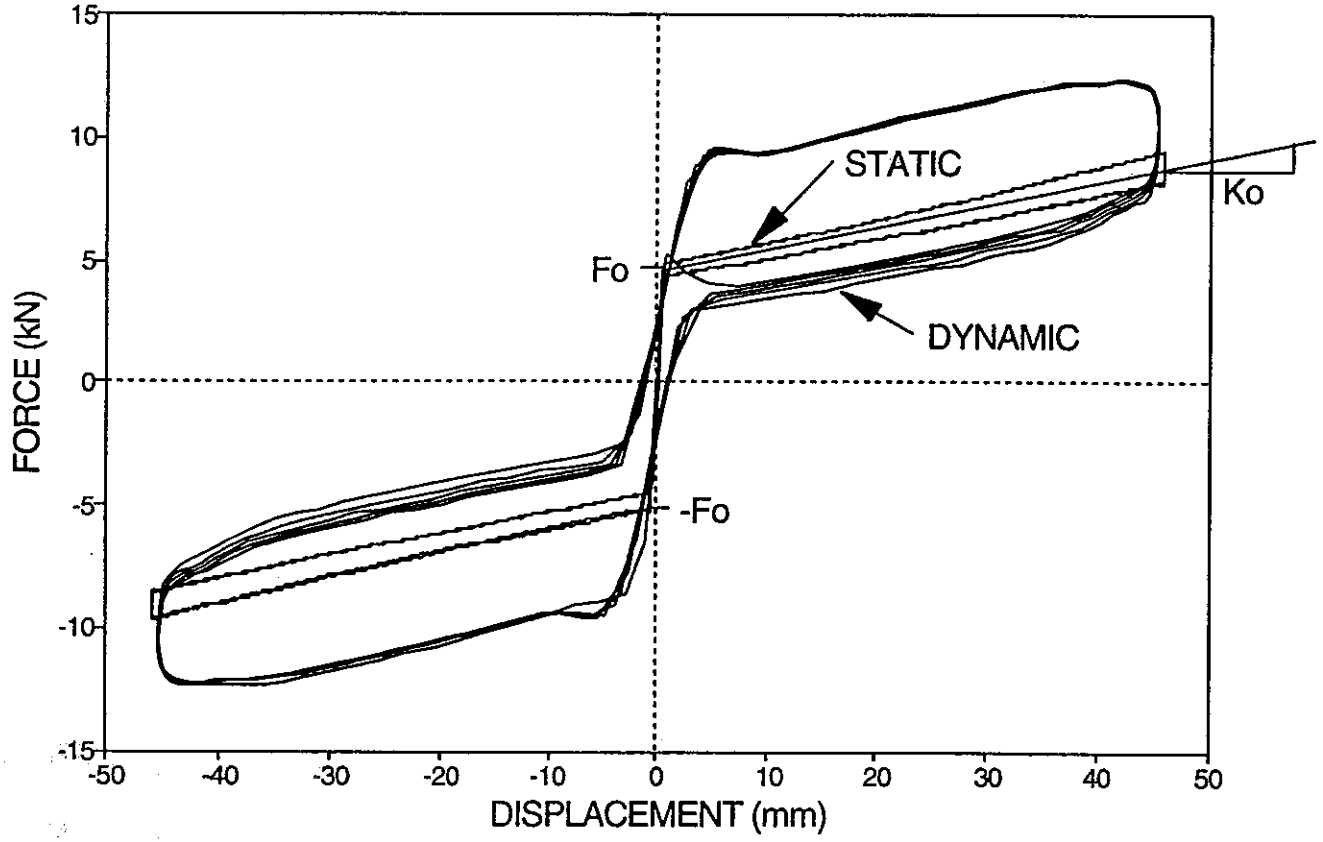

Figure 3-5 Force-Displacement Relationship of Fluid Restoring Force/Damping Device.

The devices are compressible fluid springs which are pressurized in order to develop the preload. Furthermore, fluid orificing is utilized to produce viscous damping force. The principles of operation of the devices are illustrated in Figure 3-6. A hydraulic cylinder is completely filled with silicone oil. A rod of area A_r is forced into the cylinder. Thus, the volume of the fluid is reduced by $A_r u$, u being the imposed rod motion. The overpressure p in the cylinder is

$$p = \frac{F}{A_r} \tag{3-2}$$

and is related to the volume change $\Delta V = A_r u$

$$p = K\frac{\Delta V}{V} \tag{3-3}$$

where K is the fluid bulk modulus and V is the fluid volume.

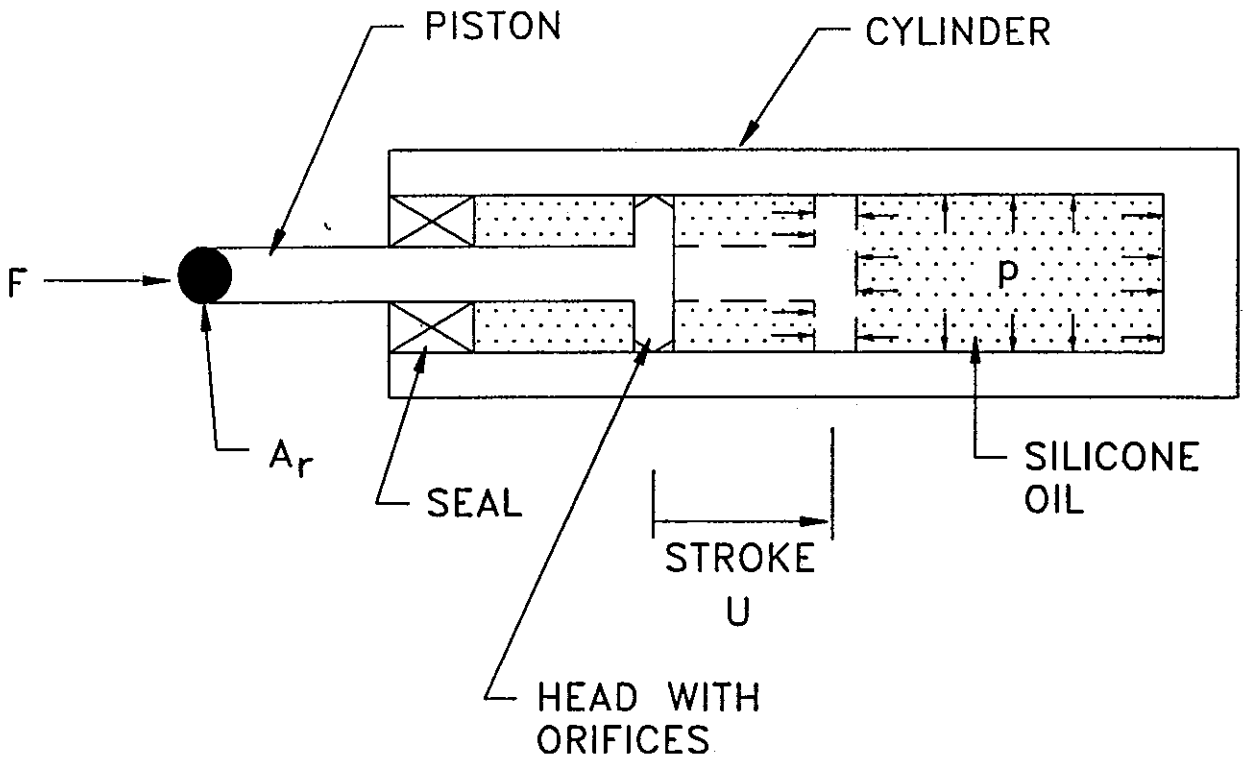

Figure 3-6 Principles of Operation of Fluid Restoring Force/Damping Device.

Therefore,

$$F = \frac{KA_r^2}{V}u \tag{3-4}$$

This relation is depicted in Figure 3-7(a). In general, this relation is nonlinear due to the dependency of the bulk modulus to the total pressure p_T and the fact that volume V is not constant but rather equal to V_o-A_r u, where V_o is the fluid volume at zero displacement. More accurately, Equation (3-4) should be written as

$$F = \int \frac{K(p_T)A_r^2}{V_o - A_r u}du \tag{3-5}$$

where $K(p_T)$ is the pressure dependent bulk modulus.

Friction in the seal of the devices alters the force-displacement relation to the form depicted in Figure 3-7(b). By pressurizing the device to an initial pressure of p_o, a

preload F_o develops

$$F_o = A_r p_o \tag{3-5}$$

This preload must be exceeded for the rod to move. The resulting force-displacement relation is shown in Figure 3-7 (c).

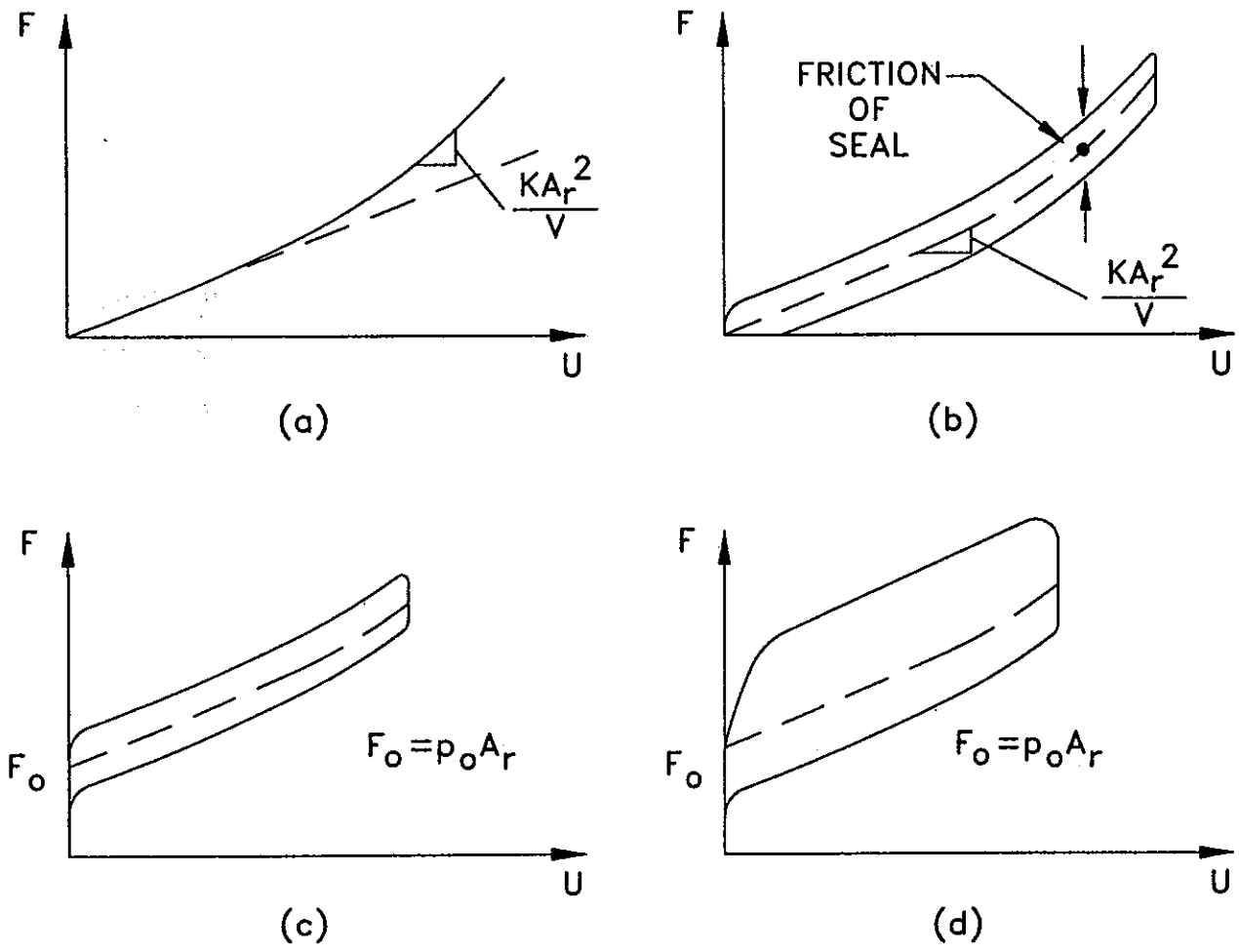

Figure 3-7 Components of Force in Fluid Restoring Force/Damping Device.

The piston head supports the rod and provides resistance to fluid transfer across the head during stroking. The area and shape of the orifices on the piston head determine the level and nature of the developed viscous force. This viscous force is, of course, related to the velocity of the piston rod. A complete force-displacement loop is depicted in Figure 3-7(d). It may be noted that the loop in this figure is shown with the viscous force being more in one direction than the opposite direction (this may be also seen in actual loops of the tested device in Figure 3-5). This behavior is produced by utilizing additional orifice area in only one direction. The behavior is desirable because it provides high damping force when the stroke increases, that is when needed, while it provides low damping force on return.

This type of compressible fluid restoring force/damping device has been used by the U.S. Military since the 1970's. The device that was used in these tests is virtually the same as that used as the arresting hook centering spring-damper on the carrier based Lockheed S-3 Viking aircraft. Other applications include those of weapons grade shock isolation systems for the NATO MK49 ring laser gyro navigator, the shipboard version of the sparrow missile, the MX missile and the Seawolf submarine. Output force ranges for these applications are between 1 and 1500 kN.

Furthermore, compression-only versions of these devices with designs dating prior to 1970 are still used as shock absorbers in industrial applications. Moreover, such compression-only shock absorbers have been used in a number of bridge applications in Italy (Grenier 1991). The devices were used as shock absorbers for preventing impact of the deck on the abutments. One application described by Grenier, 1991 is on a 25000 ton bridge which utilizes four compression only shock absorbers, each with 500 ton peak output force at displacement of 500 mm. Thus, the peak force exerted by the shock absorbers on the deck is 1000/25000 = 0.04 times the weight. This force is very small but probably appropriate for the rather weak seismisity of the area of application and the allowed large displacement (500 mm). In contrast, the design of the isolation system in the tests described herein was based on a peak force of nearly 0.19 times the weight at displacement (in prototype scale) of 200 mm. These differences are the result of the

significantly stronger seismic motions utilized in the tested system and the stringent displacement constraints.

The design of the isolation system in the tested model was based on the following considerations:

(a) Preload of 9.5 kN (for two devices) for eliminating permanent displacements. This was based on the assumption that f_{min} equals to 0.06.

(b) Peak force in the isolation system at displacement of 50 mm equal to about 0.33 of the deck weight. For force of 13.5 kN in each device and assumed value of f_{max}= 0.15, the peak force is equal to about 0.33W (W = 143 kN, deck weight). Thus, for displacements of up to 50 mm (or 200 mm in prototype scale) the force in the isolation system should be close to the minimum value specified in the Japanese design specifications for the Level 2 earthquake (CERC 1992). It should be noted that the Japanese specifications require the pier design to be based on a minimum force of 0.3W even when pier inelastic behavior occurs.

3.4 Behavior of Isolation System

A number of identification tests were conducted in order to determine the force-displacement characteristics of the isolation system. For this purpose the piers of the bridge model were braced for increasing their stiffness and the deck was connected to a nearby erected reaction frame, while on the shake table. The shake table was then driven at specified sinusoidal motion. Load cells measured the force developed in each restoring force/damping device. Furthermore, load cells, which supported the sliding bearings, monitored the friction force.

Figures 3-8 to 3-10 show recorded loops of friction force in each of the sliding bearings, the force in the two restoring force/damping devices and of the total force. Tests were conducted at frequencies of 0.03, 0.4 and 1.0 Hz, amplitude of 25 mm and for five cycles. The force in Figures 3-8 to 3-10 is normalized either by the axial load on each sliding bearing (35.75 kN), in order to directly give the friction coefficient, or by the

deck weight (143 kN) in the case of the force in the two devices and the total isolation system force.

It may be seen in Figures 3-8 to 3-10 that the friction force-displacement loops exhibit a wavy form which has not been observed in the seismic test (see Appendix A). This is not the actual behavior of the sliding bearings but rather it is the result of flexibilities in the piers and the laterally supporting reaction frame. In the higher frequency testing, these flexibilities induced additional high frequency components on the imposed sinusoidal motion, which caused the irregular wavy form in the friction and total force loops.

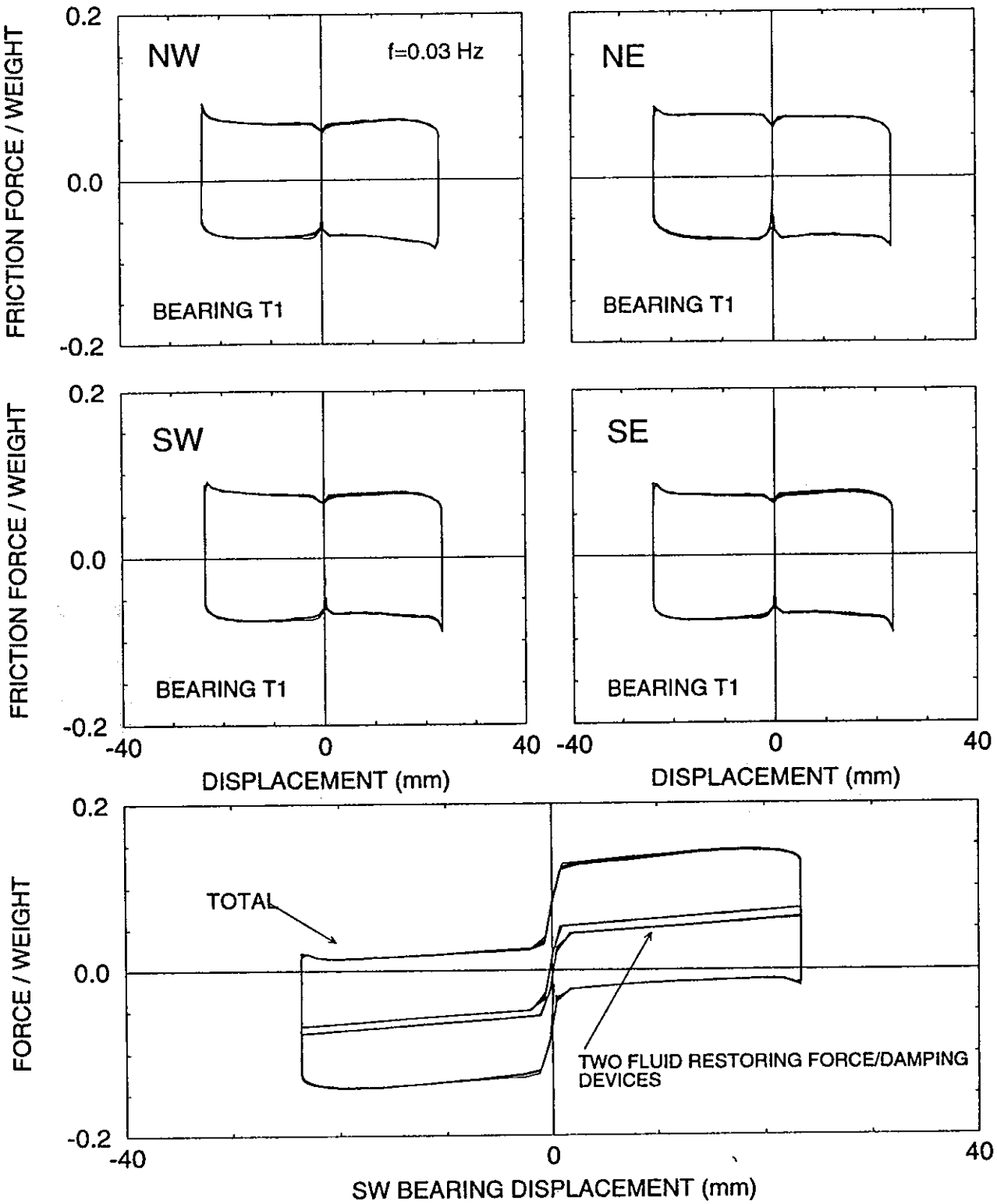

Figure 3-8 Friction Force and Total Force Versus Displacement Loops of Isolation System for Harmonic Excitation at 0.03 Hz.

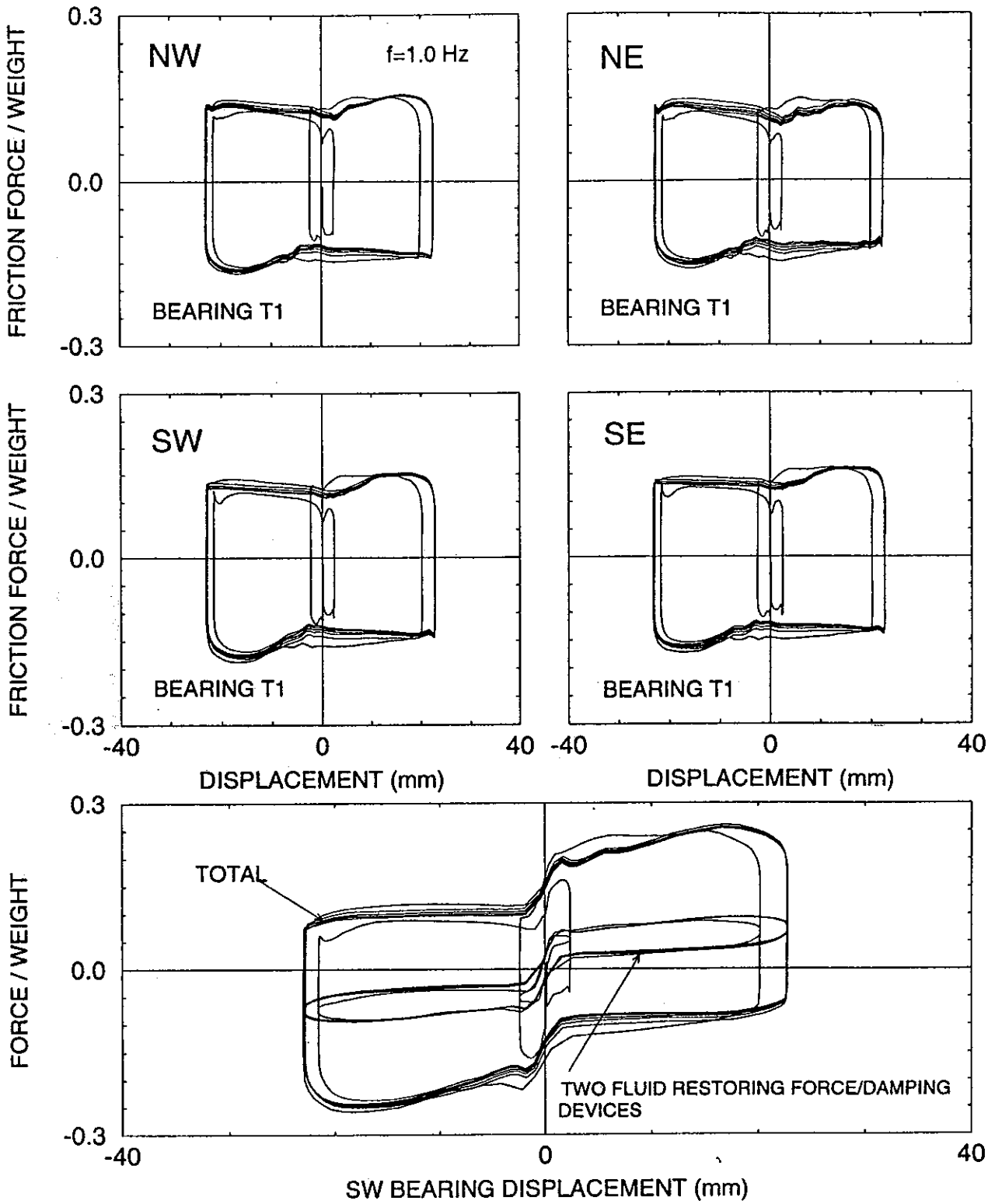

Figure 3-10 Friction Force and Total Force Versus Displacement Loops of Isolation System for Harmonic Excitation at 1.0 Hz.

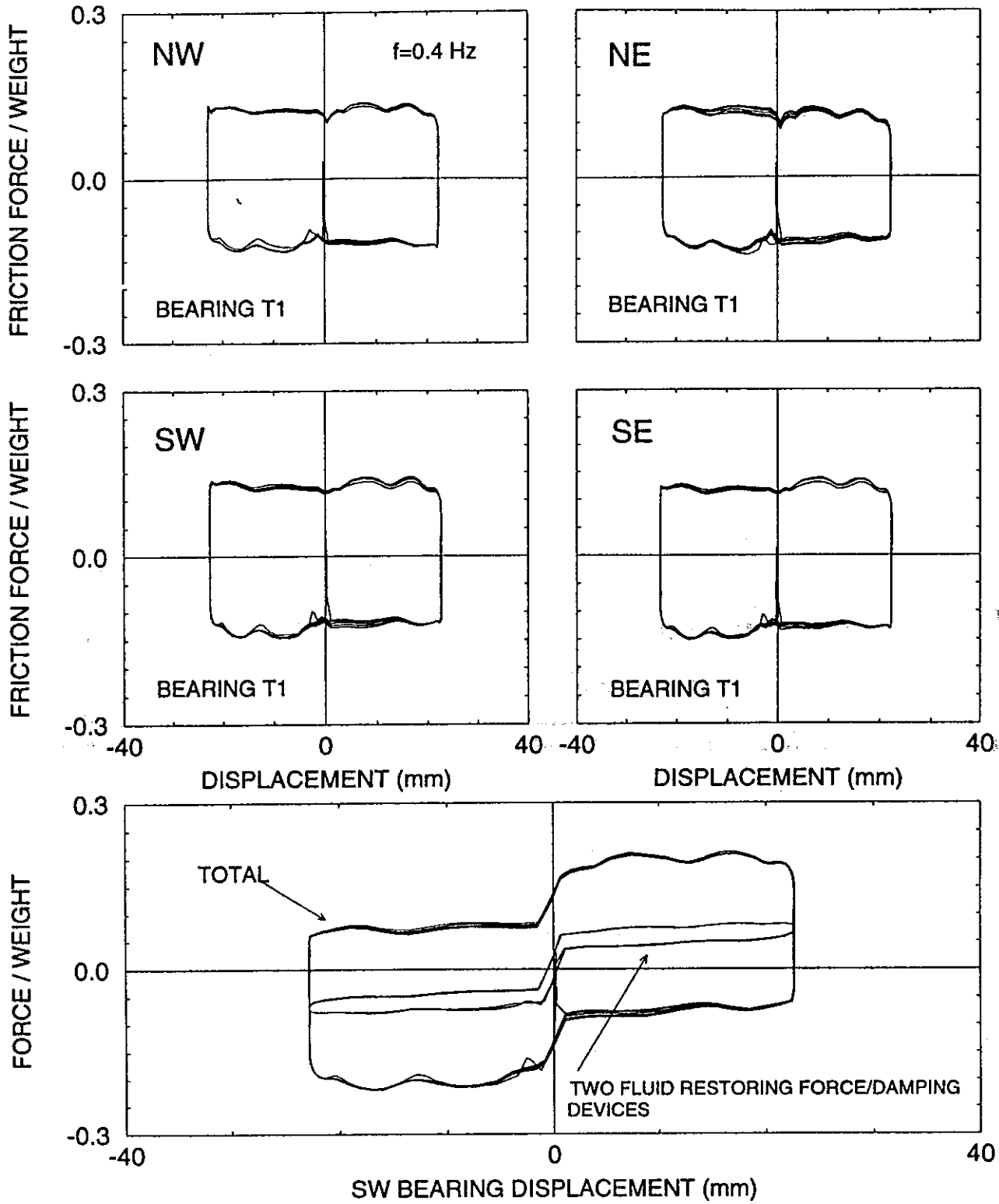

Figure 3-9 Friction Force and Total Force Versus Displacement Loops of Isolation System for Harmonic Excitation at 0.4 Hz.

SECTION 4

MODEL FOR EARTHQUAKE SIMULATOR TESTING

4.1 Bridge Model

The bridge model was designed to have flexible piers so that under non-isolated conditions the fundamental period of the model in the longitudinal direction is 0.25s (or 0.5s in prototype scale).

The bridge model is shown in Figure 4-1. At quarter length scale, it had a clear span of 4.8m (15.7 feet), height of 2.53m (8.3 feet) and total weight of 157.8 kN (35.5 kips). The deck consisted of two AISC W14x90 sections which were transversely connected by beams. Additional steel and lead weights were added to reach the model deck weight of 143 kN (32.1 kips), as determined by the similitude requirements. Each pier consisted of two AISC TS 6 x 6 x 5/16 columns with a top made of a channel section which was detailed to have sufficient torsional rigidity. The tube columns were connected to beams which were bolted to a concrete extension of the shake table. In this configuration, the column loads were transferred at a point located 0.57 m (1.87 ft) beyond the edge of the shake table. While the overhangs of the concrete shake table extension could safely carry the column load of over 80 kN (18 kips), they had some limited vertical flexibility which during seismic testing resulted in vertical motion of the piers and the supported deck.

The piers were designed to have in their free standing cantilever position a period of 0.1 s (0.2 s in prototype scale) when fully loaded (load cells and bottom part of bearings). Furthermore, the piers were detailed to yield under the combined effects of gravity load (40 kN each column) and 50 percent of the gravity load applied as horizontal load at each bearing location. The stiffness of each pier was verified by pulling the piers against each other on the shake table. During the test the piers were also proof-loaded to their rated capacity and the results were used to calibrate the strain gage load cell of each column.

Identification of the model was conducted by exciting the shake table with a 0-20 Hz banded white noise of 0.03g peak acceleration. Acceleration transfer functions of each

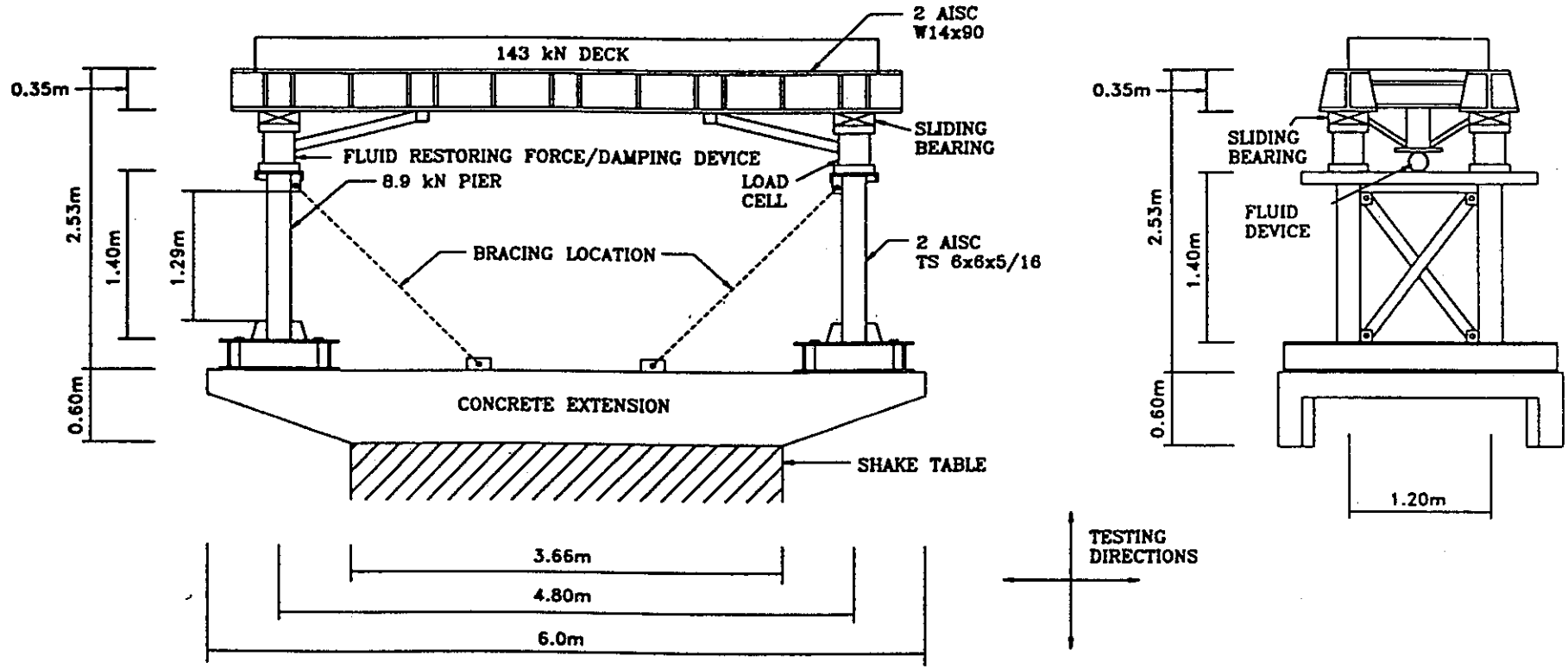

Figure 4-1 Schematic of Quarter Scale Bridge Model.

free standing pier and of the assembled bridge model with all bearings fixed against translational movement (but not rotation) revealed the following properties: fundamental period of free standing pier equal to 0.096s and fundamental period of non-isolated bridge in the longitudinal direction equal to 0.26s. These values are in excellent agreement with the design values of 0.1s and 0.25s, respectively.

Damping in the model was estimated to be 0.015 of critical for the free standing piers and 0.02 of critical for the entire model in its non-isolated condition. Identification tests of the model were also conducted with white noise input of 0.1g peak table acceleration to obtain a fundamental period of 0.25s and corresponding damping ratio of 0.04 of critical. The increased damping was the result of hysteretic action, not in the columns of the model but in the overhangs of the concrete extension of the shake table. During shake table testing of the non-isolated model, the recorded loops of shear force versus displacement of the piers displayed hysteretic action (see Section 5). Estimates of damping ratio from these loops were in the range of 0.04 to 0.08 of critical. Thus while the columns of the piers remained elastic, the pier system displayed realistic hysteretic action with equivalent damping ratio of at least 5 percent of critical.

The design of the model bridge was based in the similitude laws for artificial mass simulation (Sabnis 1983). A summary of the scale factors in the model is presented in Table 4-I.

4.2 Instrumentation

The instrumentation consisted of load cells, accelerometers and displacement transducers. Figure 4-2 shows the overall instrumentation diagram, whereas Figures 4-3 and 4-4 show the instrumentation diagrams for accelerometers and displacement transducers, respectively. A list of monitored channels and their corresponding descriptions are given in Table 4-II. A total of 55 channels were monitored.

Table 4-I : Summary of Scale Factors in Bridge Model

QUANTITY	DIMENSION	SCALE FACTOR[1]
Linear Dimension	L	4
Displacement	L	4
Velocity	LT^{-1}	2
Acceleration	LT^{-2}	1
Time	T	2
Frequency	T^{-1}	0.5
Force	F	16
Pressure	FL^{-2}	1
Strain	---	1

[1] PROTOTYPE/MODEL

4.3 Test Configurations

Testing of the bridge model was performed in four different bridge configurations. Figure 4-5 shows the four bridge configurations. They were :

(1) The sliding bearings were locked by side plates to represent a non-isolated bridge, as shown in Figure 4-6. In this configuration, the structure was identified in tests with banded white noise table motion. Furthermore, a selected number of seismic tests was conducted.

(2) Braces were installed to stiffen the piers (see Figure 4-7) and the deck was connected by stiff rods to a nearby reaction frame. In this configuration, the shake table was driven in displacement-controlled mode with specified frequency and amplitude of harmonic motion. This motion was nearly the motion experienced by the sliding bearings. Loops of bearing horizontal force versus bearing displacement were recorded and used to extract the frictional properties of the sliding bearings.

(3) Both piers were stiffened by braces so that they represented stiff abutments. In this configuration, the model resembled a single span isolated bridge (see Figure 4-7).

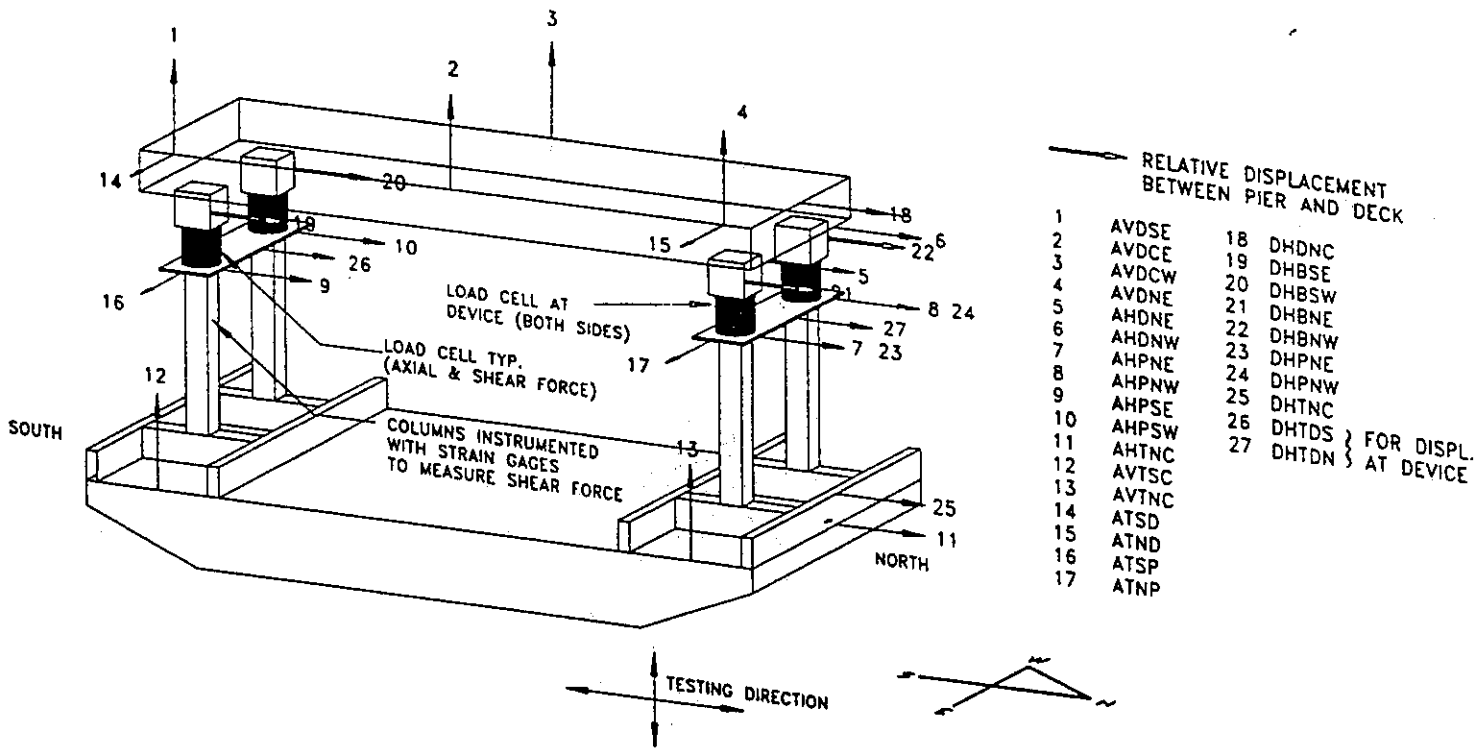

Figure 4-2 Overall Instrumentation Diagram.

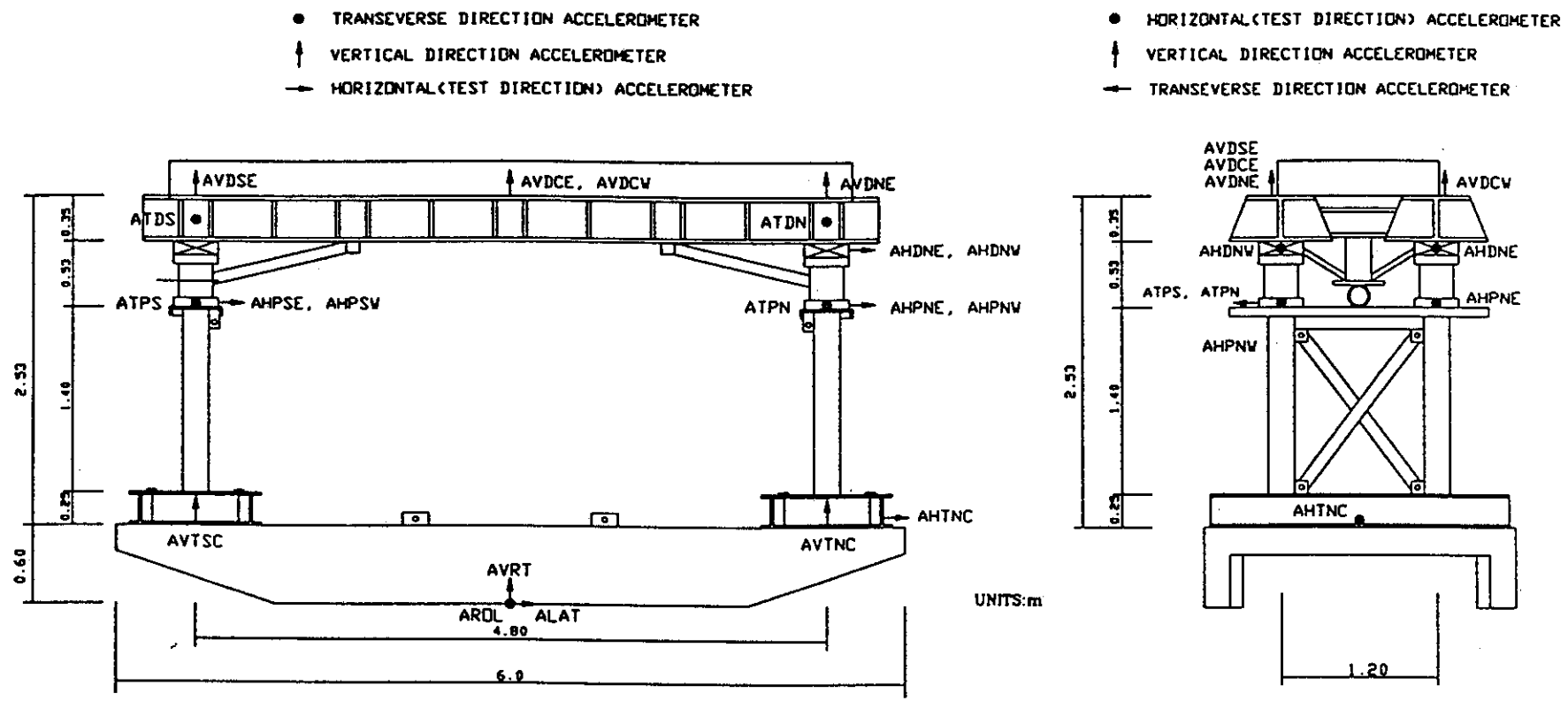

Figure 4-3 Location of Accelerometers (Units:m)

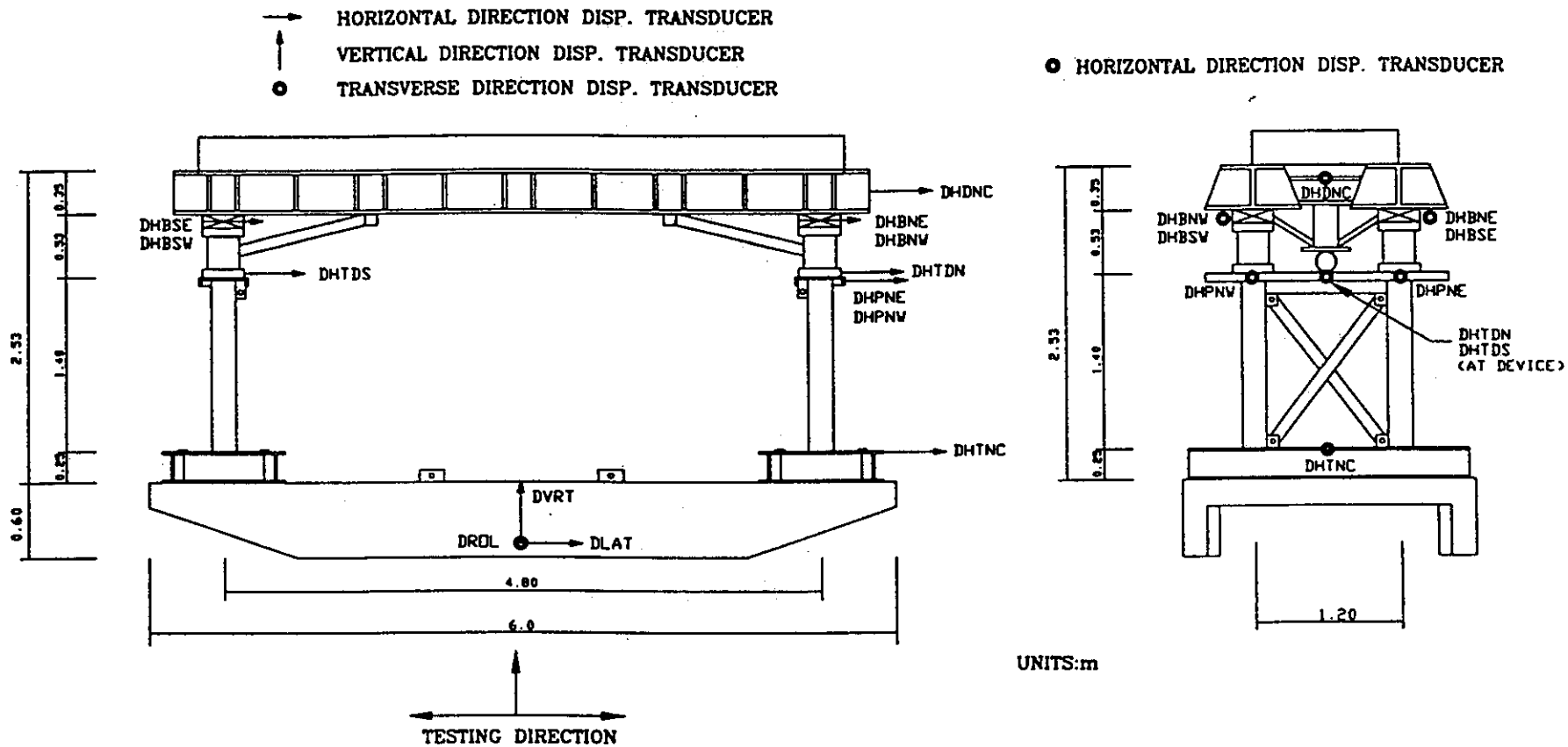

Figure 4-4 Location of Displacement Transducers (Units:m)

Table 4-II List of Channels (with reference to Figures 4-2 to 4-4)

CHANNEL	NOTATION	INSTRUMENT	RESPONSE MEASURED
1	AVDSE	ACCL	Deck Vertical Accel.-South East Corner
2	AVDCE	ACCL	Deck Vertical Accel.-East Side at Center
3	AVDCW	ACCL	Deck Vertical Accel.-West Side at Center
4	AVDNE	ACCL	Deck Vertical Accel.-North East Corner
5	AHDNE	ACCL	Deck Horizontal Accel.-North East Corner
6	AHDNW	ACCL	Deck Horizontal Accel.-North West Corner
7	AHPNE	ACCL	Pier Horizontal Accel.-North East
8	AHPNW	ACCL	Pier Horizontal Accel.-North West
9	AHPSE	ACCL	Pier Horizontal Accel.-South East
10	AHPSW	ACCL	Pier Horizontal Accel.-South West
11	AHTNC	ACCL	Table Horizontal Accel.-North Side at Center
12	AVTSC	ACCL	Table Vertical Accel.-South Side at Center
13	AVTNC	ACCL	Table Vertical Accel.-North Side at Center
14	ATSD	ACCL	Deck Transverse Accel.-South Side
15	ATND	ACCL	Deck Transverse Accel.-North Side
16	ATSP	ACCL	Pier Transverse Accel.-South
17	ATNP	ACCL	Pier Transverse Accel.-North
18	DHDNC	DT	Deck Total Horizontal Displ.-North Side Center
19	DHBSE	DT	Bearing Horizontal Displ.-South East
20	DHBSW	DT	Bearing Horizontal Displ.-South West
21	DHBNE	DT	Bearing Horizontal Displ.-North East
22	DHBNW	DT	Bearing Horizontal Displ.-North West
23	DHPNE	DT	Pier Total Horizontal Displ.-North East
24	DHPNW	DT	Pier Total Horizontal Displ.-North West
25	DHTNC	DT	Table Horizontal Displ.-North Side at Center
26	DHTDS	DT	Displ. of Rest. Force/Damping Device South Pier
27	DHTDN	DT	Displ. of Rest. Force/Damping Device North Pier
28	DHBAV	DT	Bearing Horizontal Average Displ.
29	DLAT	DT	Table Horizontal Displ.
30	ALAT	ACCL	Table Horizontal Accel.
31	DVRT	DT	Table Vertical Displ.
32	AVRT	ACCL	Table Vertical Accel.
33	DROL	DT	Table Rolling Displ.
34	AROL	ACCL	Table Rolling Accel.

ACCEL=Accelerometer, DT=Displacement Transducer

Table 4-II (Cont'd)

CHANNEL	NOTATION	INSTRUMENT	RESPONSE MEASURED
35	SX1	LOAD CELL	Shear Bearing Force-South West
36	SX2	LOAD CELL	Shear Bearing Force-South East
37	SX3	LOAD CELL	Shear Bearing Force-North West
38	SX4	LOAD CELL	Shear Bearing Force-North East
39	SCNE	LOAD CELL	Column Shear Force-North East
40	SCSE	LOAD CELL	Column Shear Force-South East
41	SCNW	LOAD CELL	Column Shear Force-North West
42	SCSW	LOAD CELL	Column Shear Force-South West
43	N1SW	LOAD CELL	Axial Bearing Force-South West
44	N2SE	LOAD CELL	Axial Bearing Force-South East
45	N3NW	LOAD CELL	Axial Bearing Force-North West
46	N4NE	LOAD CELL	Axial Bearing Force-North East
47	SCN	LOAD CELL	Average Column Shear Force-North
48	SCS	LOAD CELL	Average Column Shear Force-South
49	DHDSW	DT	Deck Total Horizontal Displ.-South West Corner
50	DHDSE	DT	Deck Total Horizontal Displ.-South East Corner
51	LCTDS	LOAD CELL	Force of Rest Force/Damping Device at South Pier
52	LCTDN	LOAD CELL	Force of Rest Force/Damping Device at North Pier
53	LCNE	LOAD CELL	East Friction Force-North East Corner(ID-test)
54	LCNW	LOAD CELL	West Friction Force-North West Corner(ID-Test)
55	LCTOT	LOAD CELL	Average Friction Force(ID-Test)

ACCEL=Accelerometer, DT=Displacement Transducer

(4) A configuration with two flexible piers which resembled portion of a multiple span bridge between expansion joints. A view of this configuration on the shake table is shown in Figure 4-8.

A view of the isolation system with details of installation is shown in Figure 4-9. A total of 55 seismic tests were conducted with two combinations of bridge configurations. These combinations are listed in Table 4-III.

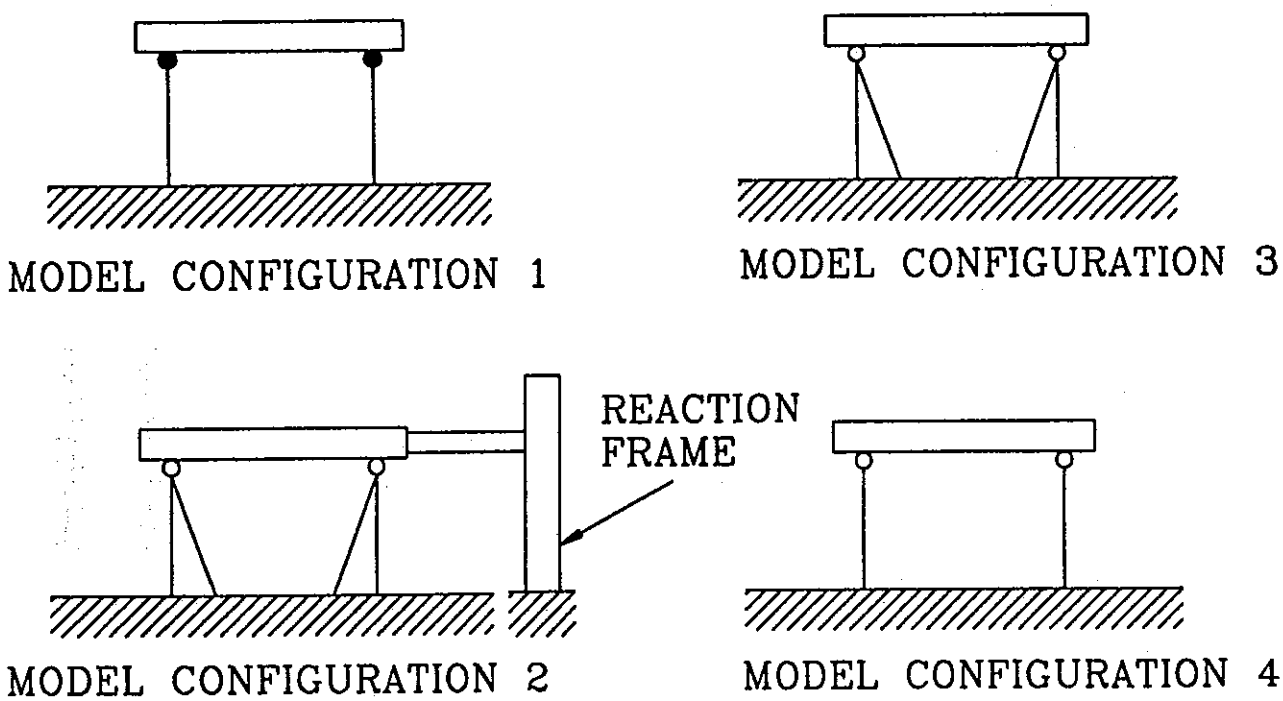

Figure 4-5 Model Configurations in Testing (1:Non-isolated Bridge, 2:Identification of Frictional Properties, 3:Single Span Model, 4:Multiple Span Model).

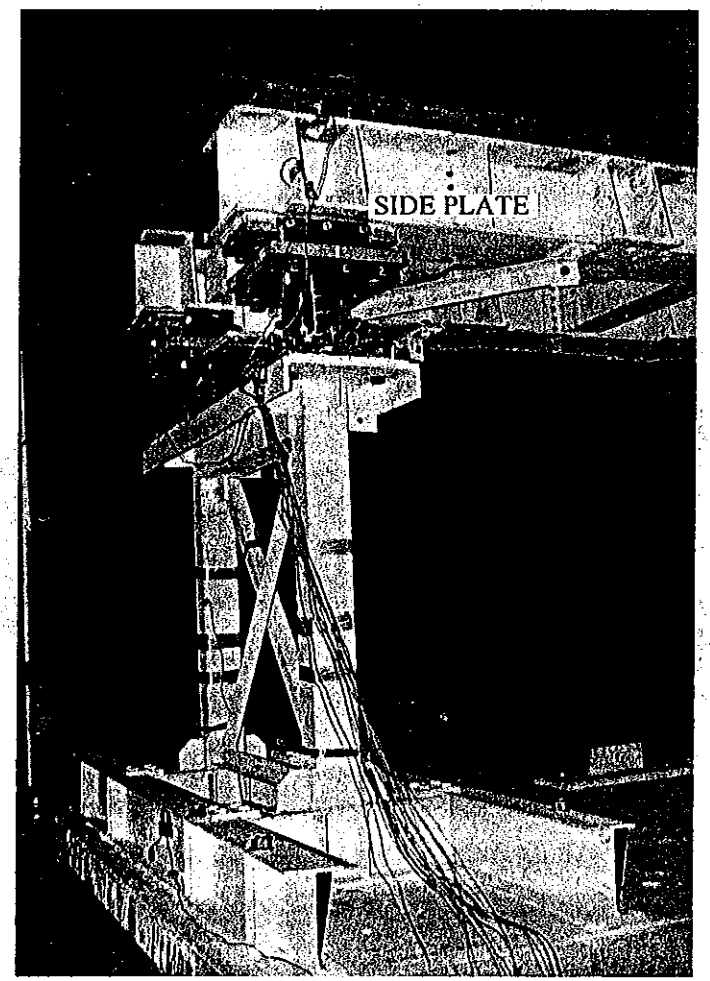

Figure 4-6 View of Bridge Model with Sliding Bearings Locked by Side Plates (Configuration No. 1).

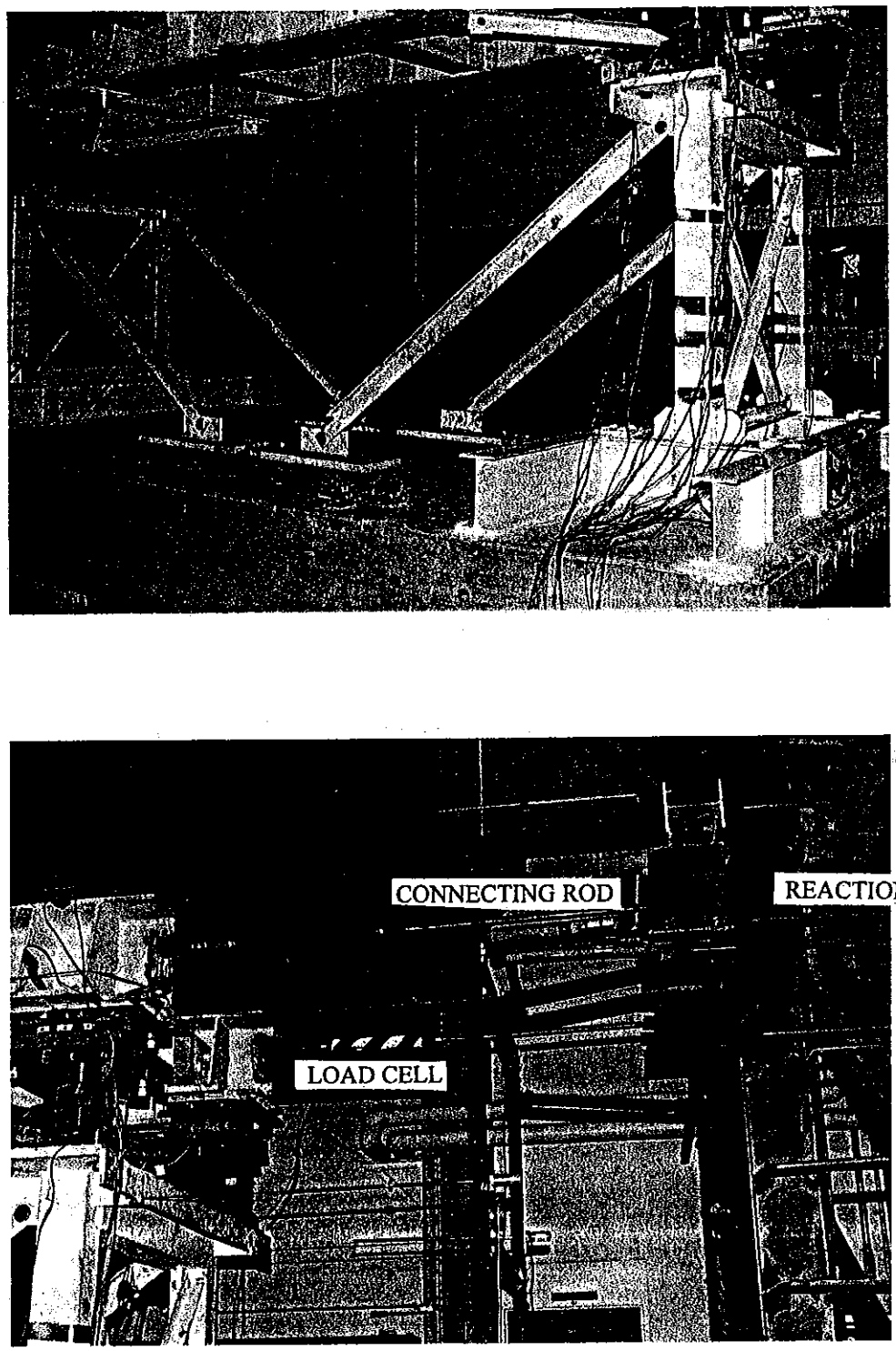

Figure 4-7 Views of Bridge Model in Configuration No. 2 (Identification of Frictional Properties of Sliding Bearings).

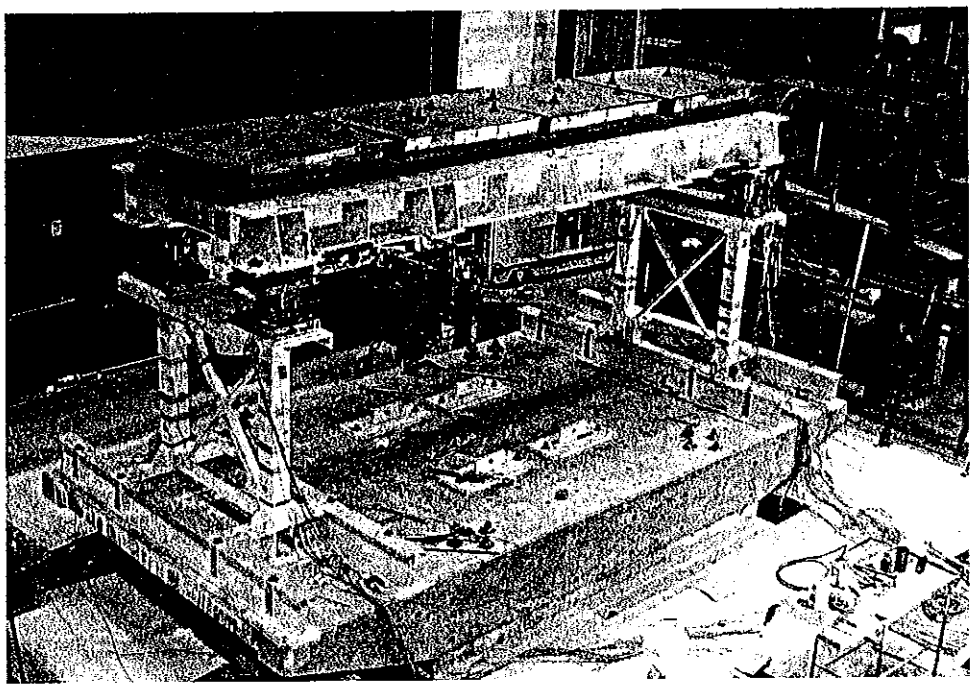

Figure 4-8 View of Bridge Model in Configuration with Two Flexible Piers.

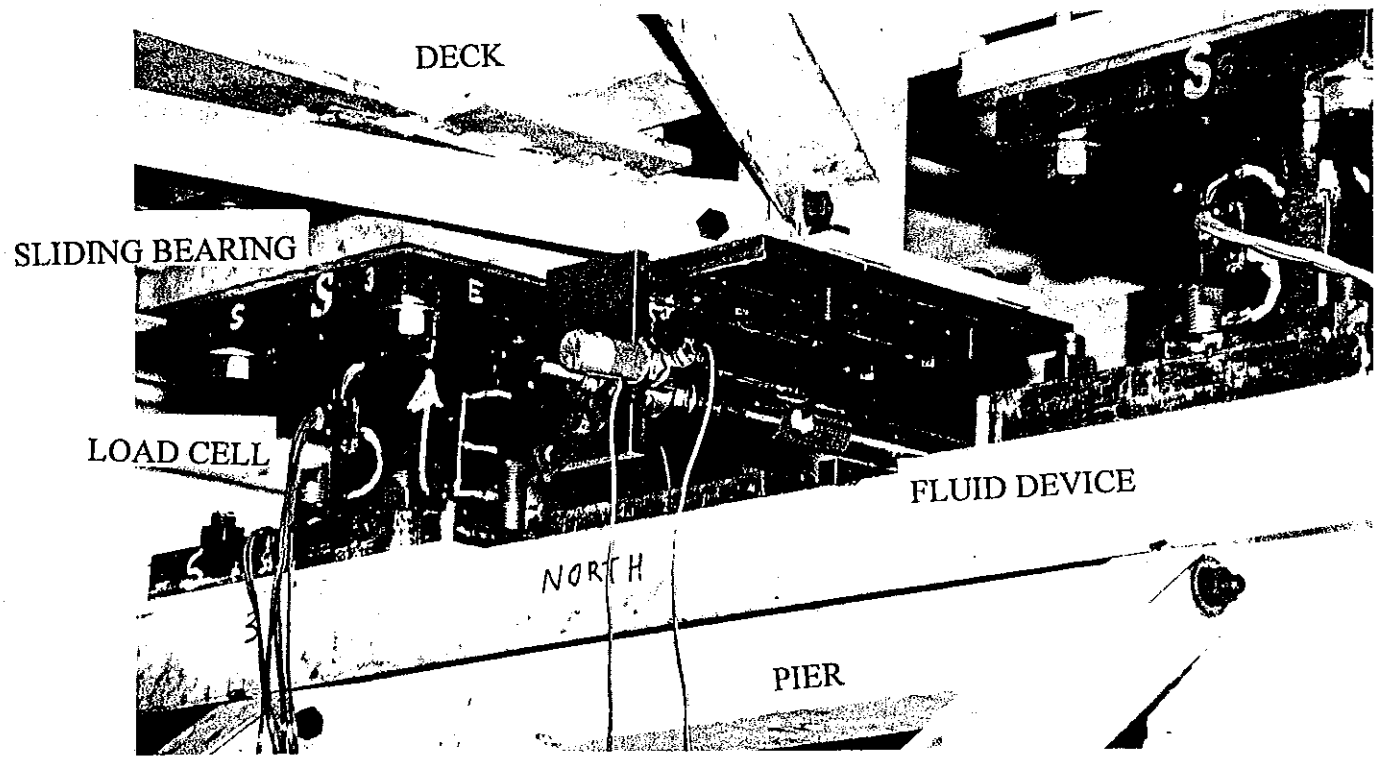

Figure 4-9 View of Isolation System with Details of Installation of Fluid Restoring Force/Damping Devices.

Table 4-III Bridge and Isolation System Configurations

TEST No.	NUMBER OF TESTS	PIER CONDITION		SLIDING BEARINGS (Type)		RESTORING FORCE / DAMPING DEVICES (Number)	
		SOUTH	NORTH	SOUTH PIER	NORTH PIER	SOUTH PIER	NORTH PIER
TDRUN01-24	24	STIFF	STIFF	T1	T1	1	1
TDRUN25-55	31	FLEXIBLE	FLEXIBLE	T1	T1	1	1

4.4 Test Program

A total of 55 earthquake simulation tests were performed on the model bridge. Tests were conducted with only horizontal input and with combined horizontal and vertical input. The earthquake signals and their characteristics are listed in Table 4-IV. The earthquake signals consisted of historic earthquakes and artificial motions compatible with:

(a) The Japanese bridge design spectra for Level 1 and Level 2 and ground conditions 1 (rock), 2 (alluvium) and 3 (deep alluvium) (CERC 1992). In Japan, it is required that bridges are designed for two levels of seismic loading. In Level 1 seismic loading, it is required that the bridge remains undamaged and fully elastic. In Level 2 seismic loading, inelastic behavior is permitted. Tables 4-V and 4-VI describe the shapes of the 5%-damped acceleration spectra of the Japanese Level 1 and 2 motions.

(b) The California Department of Transportation (CalTrans) bridge spectra (Gates 1979). These motions were identical to those used in the testing of another bridge model by Constantinou, 1991a.

Each record was compressed in time by a factor of two to satisfy the similitude requirements. Figure 4-10 to 4-26 show recorded time histories of the table motion in tests with input being the earthquake signals of Table 4-IV. The acceleration and displacement records were directly measured, whereas the velocity record was obtained by numerical differentiation of the displacement record. It may be observed that the peak ground motion was reproduced well, but not exactly, by the table generated motion.

Figures 4-10 to 4-26 also show the response spectra of acceleration of the table motions. The 5% damped acceleration spectrum is compared to the spectrum of the target record to demonstrate the good reproduction of the motion by the table.

Table 4-IV Earthquake Motions Used in Test Program and Characteristics in Prototype Scale

NOTATION	RECORD	PEAK ACC. (g)	PEAK VEL. (mm/sec)	PEAK DIS. (mm)
EL CENTRO S00E	Imperial Valley, May 18 1940, Component S00E	0.34	334.50	108.70
TAFT N21E	Kern County, July 21,1952, Component N21E	0.16	157.20	67.10
MEXICO N90W	Mexico City, September 19, 1985 SCT building, Component N90W	0.17	605.00	212.00
PACOIMA S16E	San Fernando, February 9, 1971, Component S16E	1.17	1132.30	365.30
PACOIMA S74W	San Fernando, February 9, 1971, Component S74E	1.08	568.20	108.20
HACHINOHE N-S	Tokachi, Japan, May 16, 1968 Hachinohe, Component N-S	0.23	357.10	118.90
MIYAGIKEN OKI	Miyaki, Japan, June 12, 1978 Ofunato-Bochi, Component E-W	0.16	141.00	50.80
AKITA N-S	Nihonkai Chuubu, Japan, May 23, 1983 Component N-S	0.19	292.00	146.00
JP. L1G1	Artificial Compatible with Japanese Level 1 Ground Condition 1	0.10	215.00	90.00
JP. L1G2	Artificial Compatible with Japanese Level 1 Ground Condition 2	0.12	251.00	69.00
JP. L1G3	Artificial Compatible with Japanese Level 1 Ground Condition 3	0.14	274.00	132.00
JP. L2G1	Artificial Compatible with Japanese Level 2 Ground Condition 1	0.37	864.00	526.00
JP. L2G2	Artificial Compatible with Japanese Level 2 Ground Condition 2	0.43	998.00	527.00
JP. L2G3	Artificial Compatible with Japanese Level 2 Ground Condition 3	0.45	1121.00	700.00
CALTRANS 0.6g A2	Artificial Compatible with CalTrans 0.6g 80'-150'Alluvium Spectrum, No.2	0.60	836.40	282.90
CALTRANS 0.6g S3	Artificial Compatible with CalTrans 0.6g 10'-80'Alluvium Spectrum, No.3	0.60	778.00	438.90
CALTRANS 0.6g R3	Artificial Compatible with CalTrans 0.6g Rock Spectrum, No.3	0.60	571.00	342.40

Table 4-V Spectral Acceleration of Japanese Bridge Design Spectra, Level 1

G.C.	Spectral Acceleration (S_{10}) in units of cm/sec^2 as Function of Period T_i in units of seconds		
1	$T_i < 0.1$ $S_{10} = 431T_i^{1/3}$ $S_{10} \geq 160$	$0.1 \leq T_i \leq 1.1$ $S_{10}=200$	$1.1 < T_i$ $S_{10}=220/T_i$
2	$T_i < 0.2$ $S_{10} = 427T_i^{1/3}$ $S_{10} \geq 200$	$0.2 \leq T_i \leq 1.3$ $S_{10}=250$	$1.3 < T_i$ $S_{10}=325/T_i$
3	$T_i < 0.34$ $S_{10} = 430T_i^{1/3}$ $S_{10} \geq 240$	$0.34 \leq T_i \leq 1.5$ $S_{10}=300$	$1.5 < T_i$ $S_{10}=450/T_i$

Table 4-VI Spectral Acceleration of Japanese Bridge Design Spectra, Level 2

G.C.	Spectral Acceleration (S_{20}) in units of cm/sec^2 as Function of Period T_i in units of seconds		
1	$T_i \leq 1.4$ $S_{20}=700$		$1.4 < T_i$ $S_{20}=980/T_i$
2	$T_i < 0.18$ $S_{20} = 1506T_i^{1/3}$ $S_{20} \geq 700$	$0.18 \leq T_i \leq 1.6$ $S_{20}=850$	$1.6 < T_i$ $S_{20}=1360/T_i$
3	$T_i < 0.29$ $S_{20} = 1511T_i^{1/3}$ $S_{20} \geq 700$	$0.29 \leq T_i \leq 2.0$ $S_{20}=1000$	$2.0 < T_i$ $S_{20}=2000/T_i$

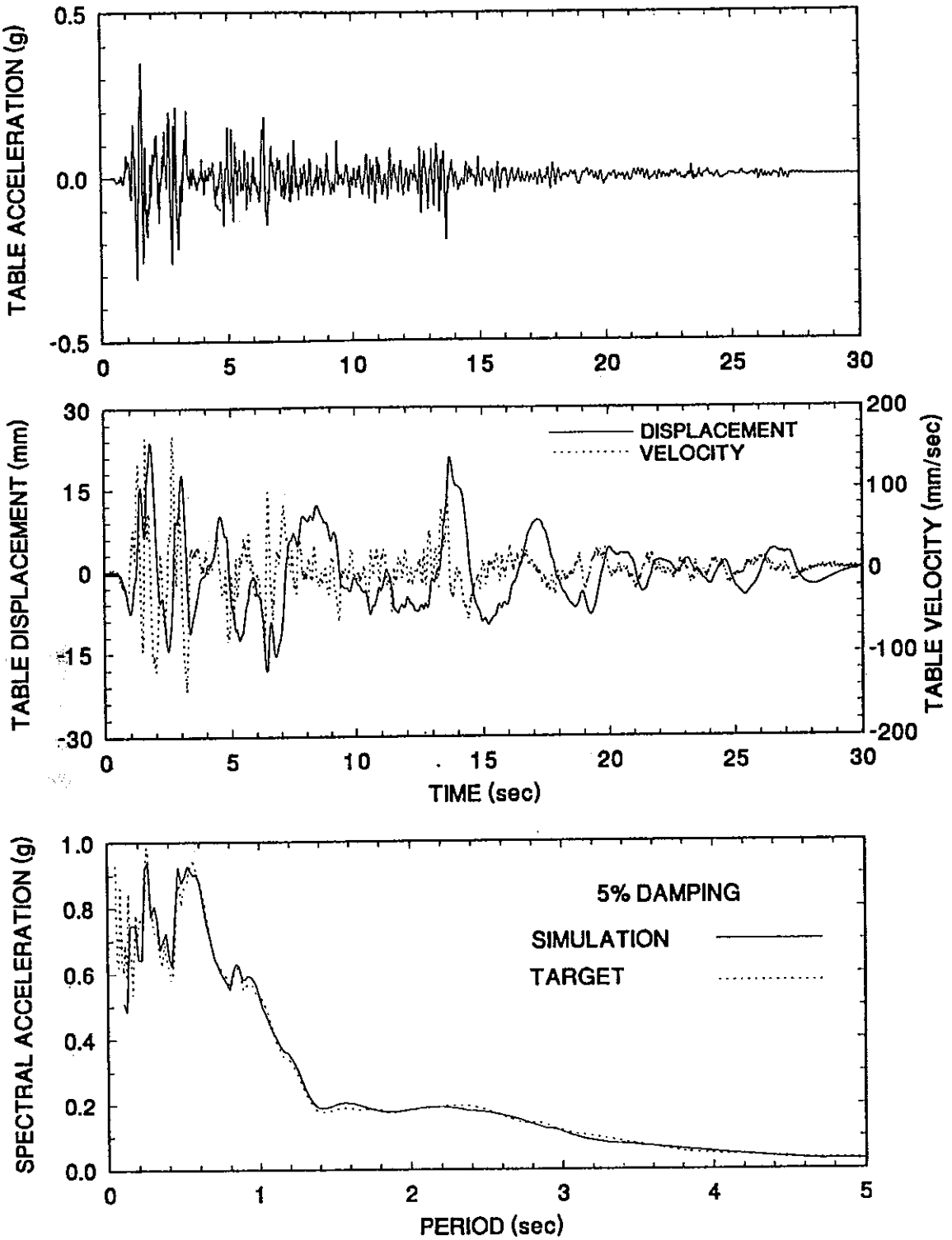

Figure 4-10 **Time Histories of Displacement, Velocity and Acceleration and Acceleration Response Spectrum of Shaking Table Motion Excited with El Centro S00E 100% Motion.**

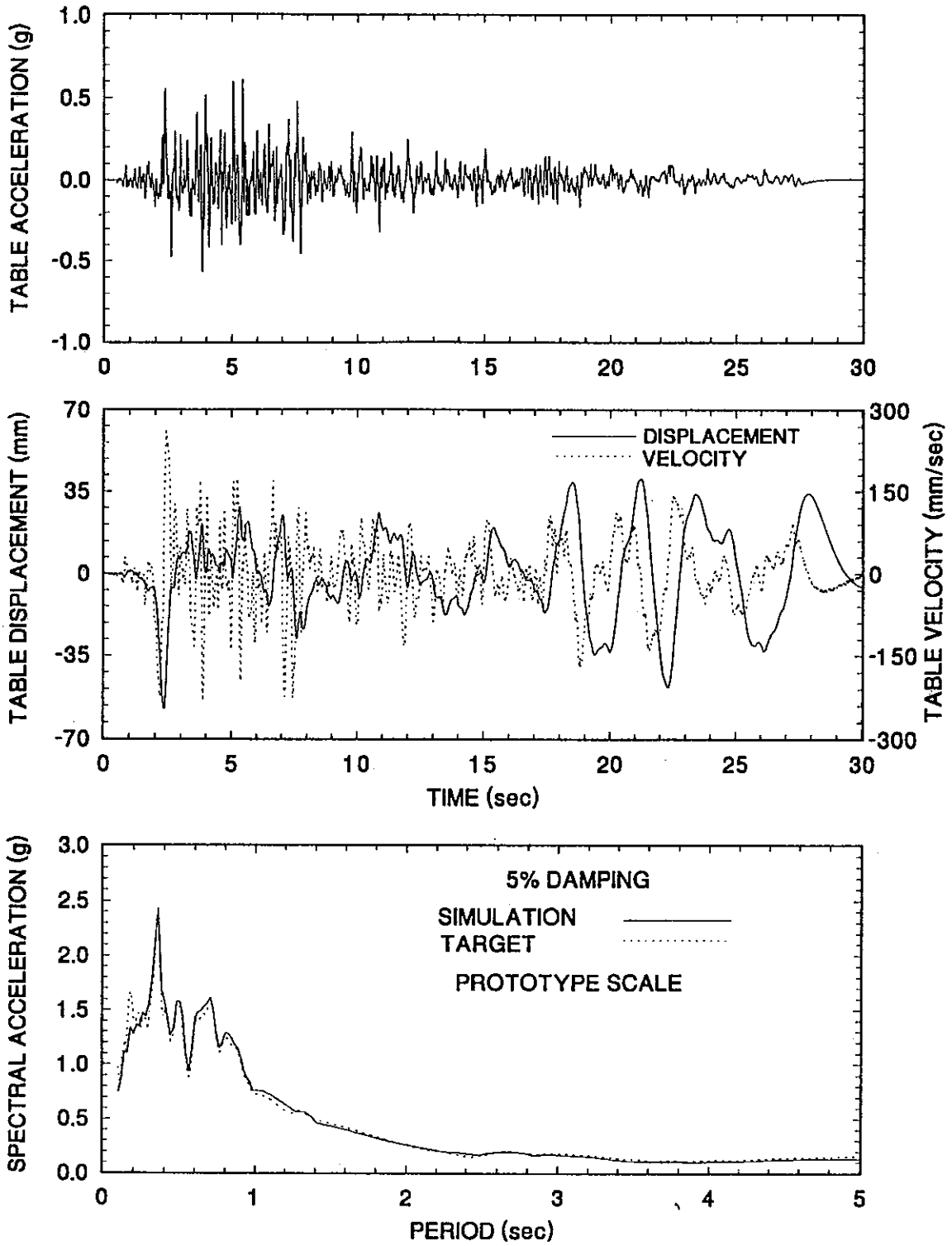

Figure 4-11 **Time Histories of Displacement, Velocity and Acceleration and Acceleration Response Spectrum of Shaking Table Motion Excited with Taft N21E 400% Motion.**

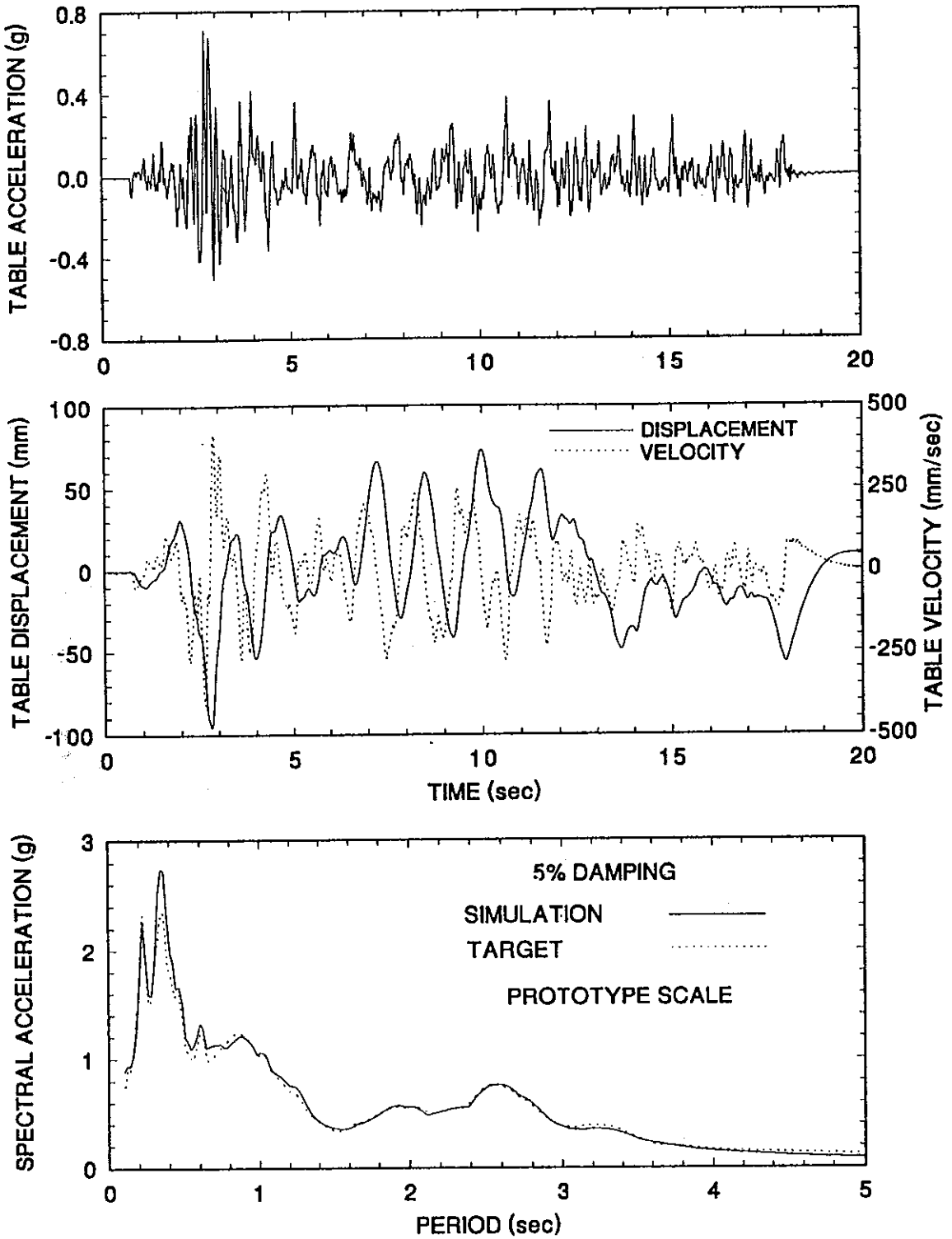

Figure 4-12 **Time Histories of Displacement, Velocity and Acceleration and Acceleration Response Spectrum of Shaking Table Motion Excited with Hachinohe N-S 300% Motion.**

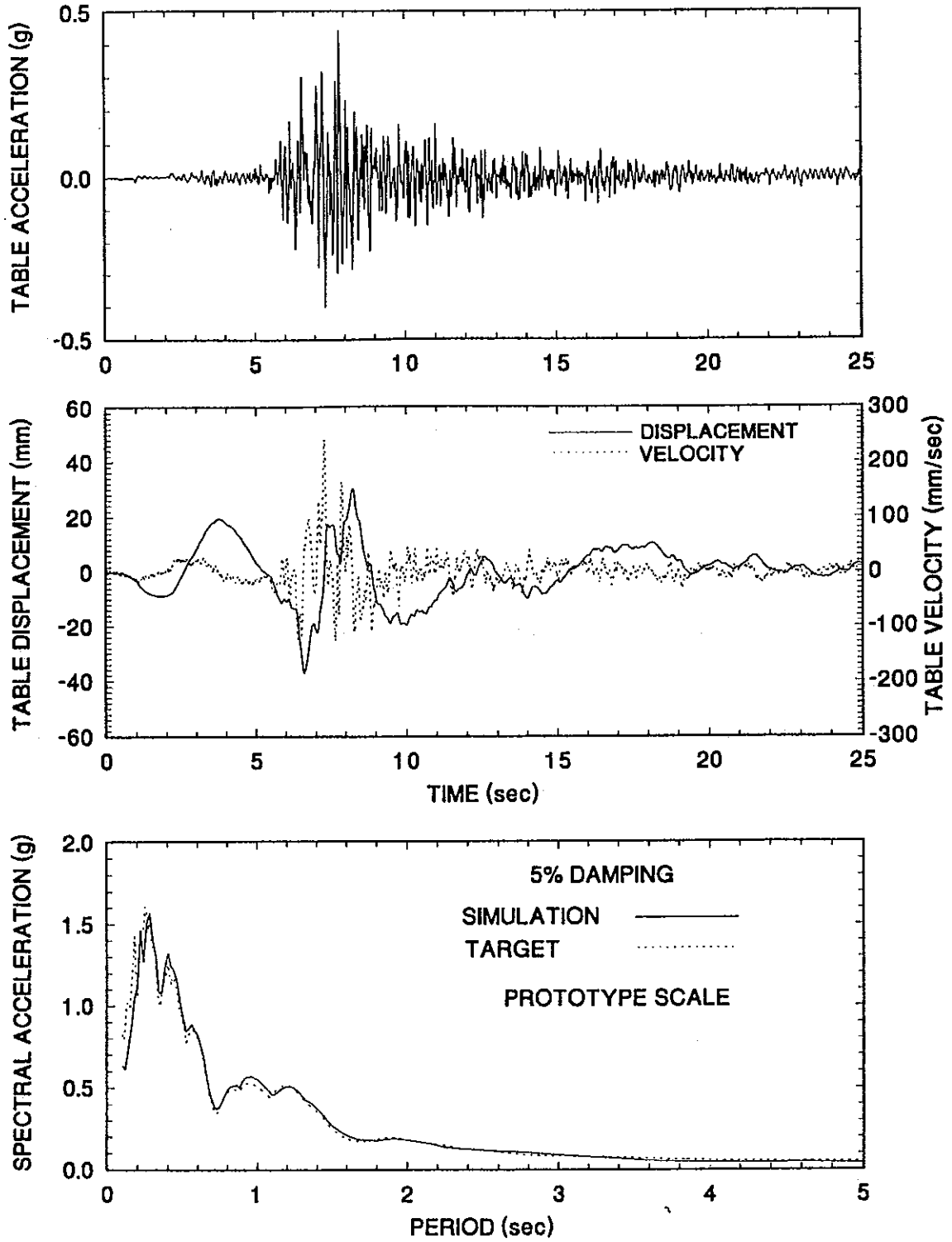

Figure 4-13 **Time Histories of Displacement, Velocity and Acceleration and Acceleration Response Spectrum of Shaking Table Motion Excited with Miyagiken Oki E-W 300% Motion.**

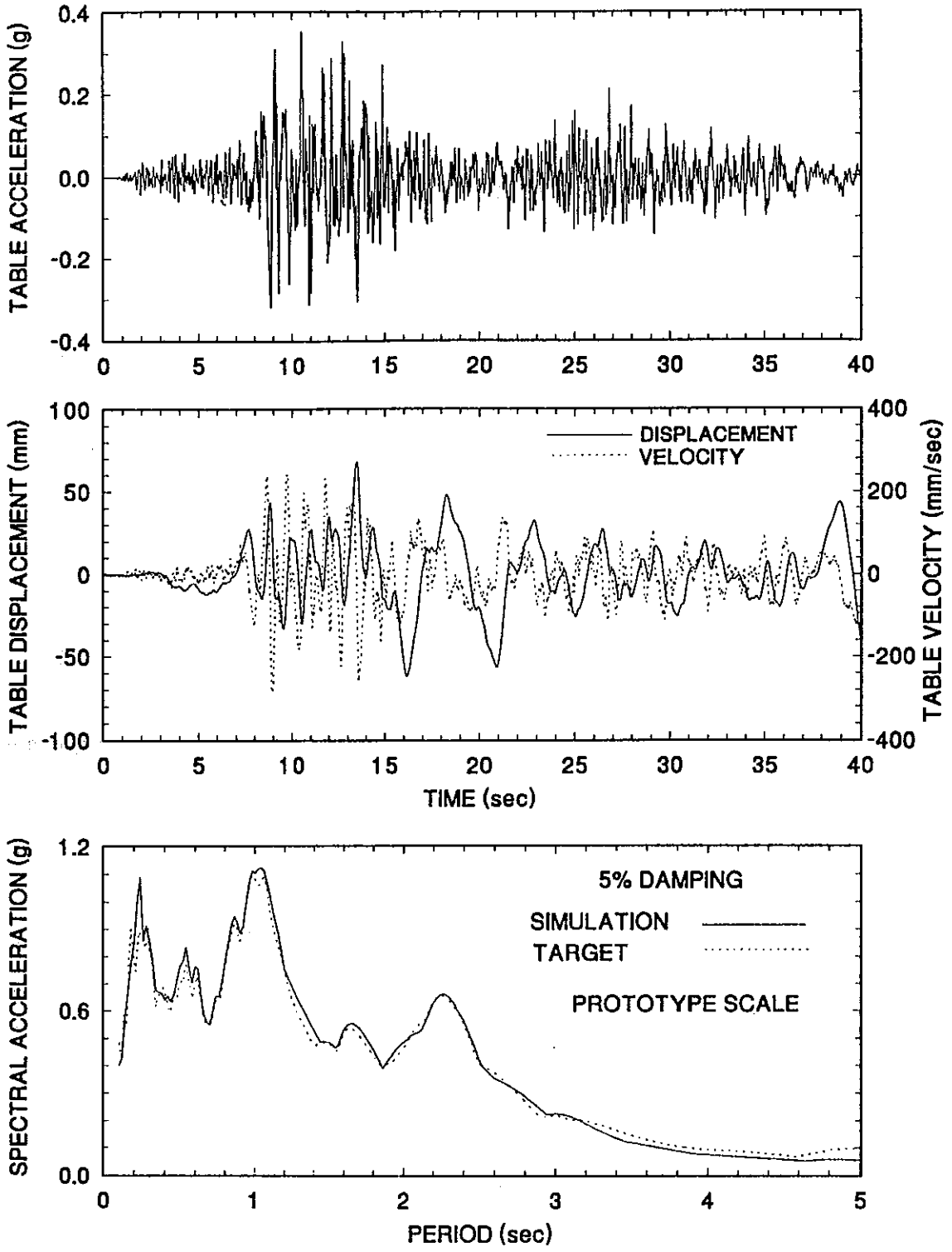

Figure 4-14 **Time Histories of Displacement, Velocity and Acceleration and Acceleration Response Spectrum of Shaking Table Motion Excited with Akita N-S 200% Motion.**

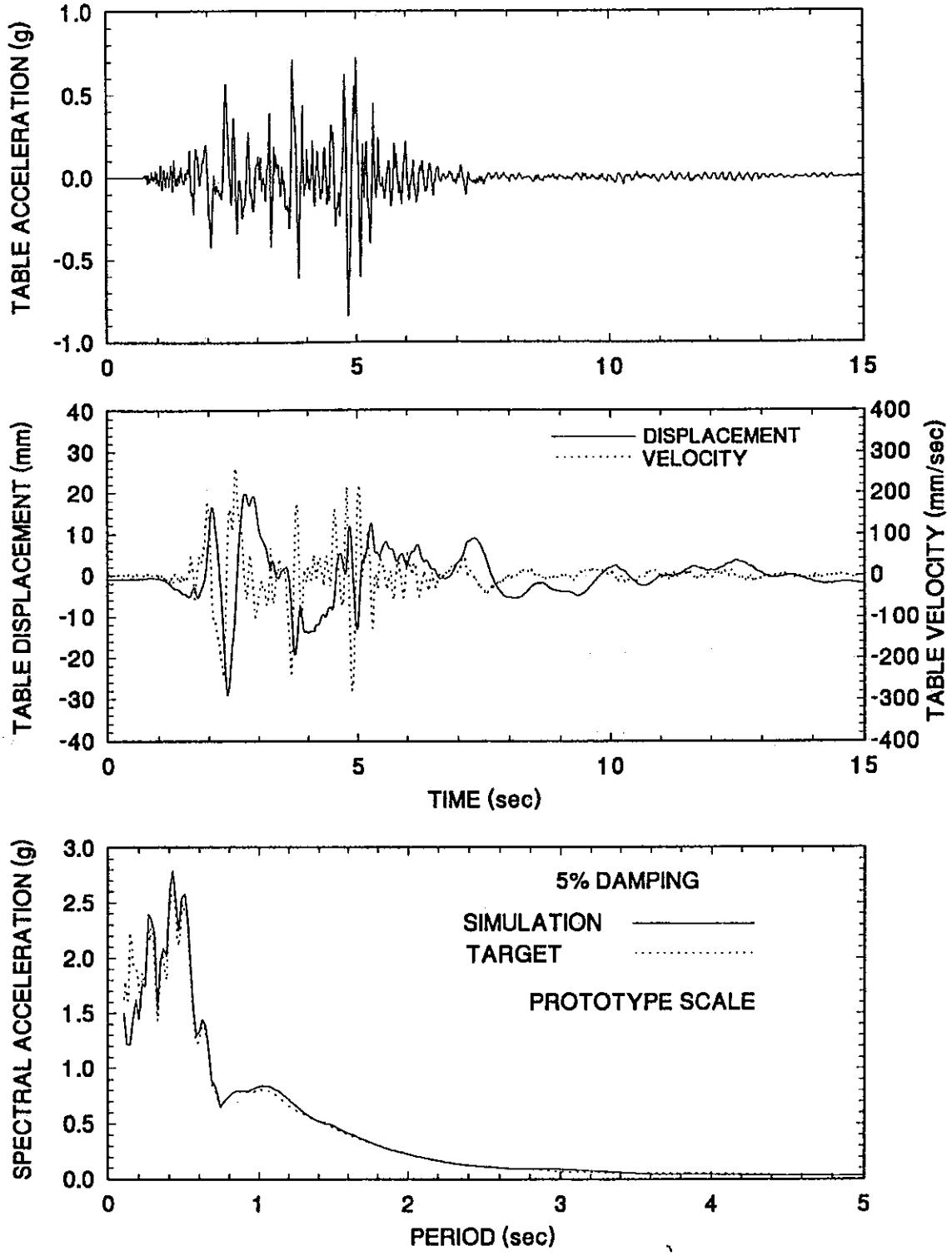

Figure 4-15 **Time Histories of Displacement, Velocity and Acceleration and Acceleration Response Spectrum of Shaking Table Motion Excited with Pacoima S74W 100% Motion.**

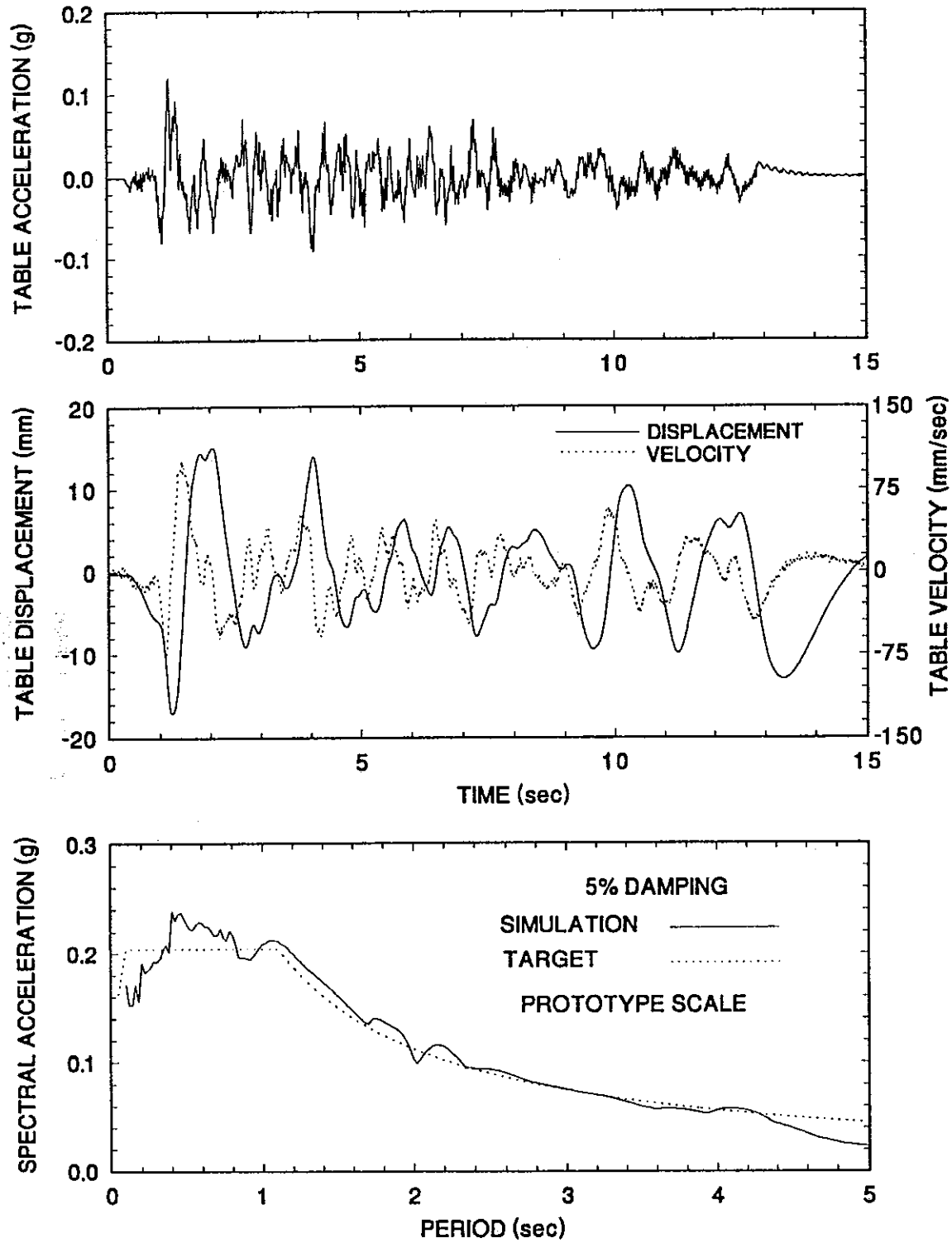

Figure 4-18 **Time Histories of Displacement, Velocity and Acceleration and Acceleration Response Spectrum of Shaking Table Motion Excited with JP. Level 1 G.C.1 100% Motion.**

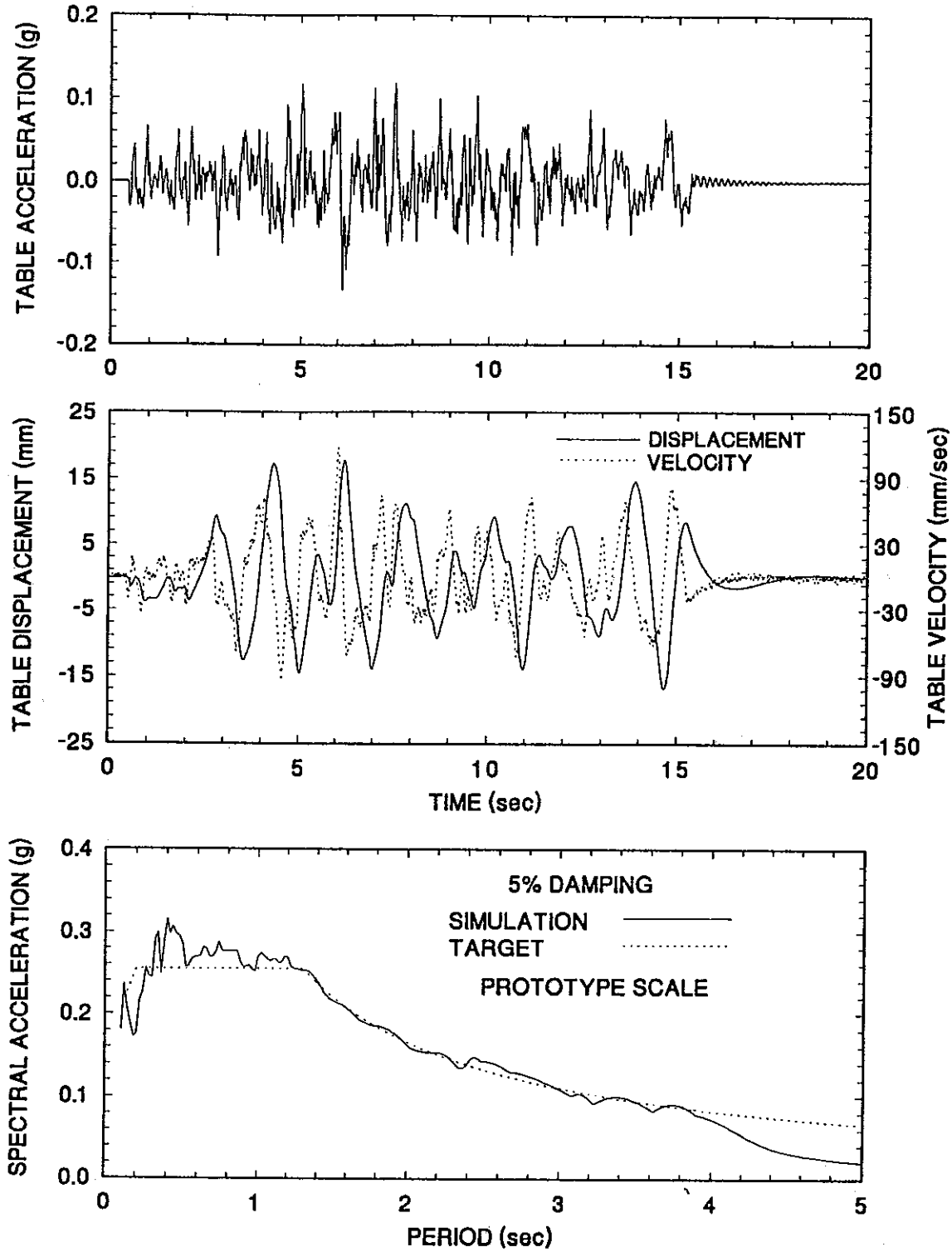

Figure 4-19 **Time Histories of Displacement, Velocity and Acceleration and Acceleration Response Spectrum of Shaking Table Motion Excited with JP. Level 1 G.C.2 100% Motion.**

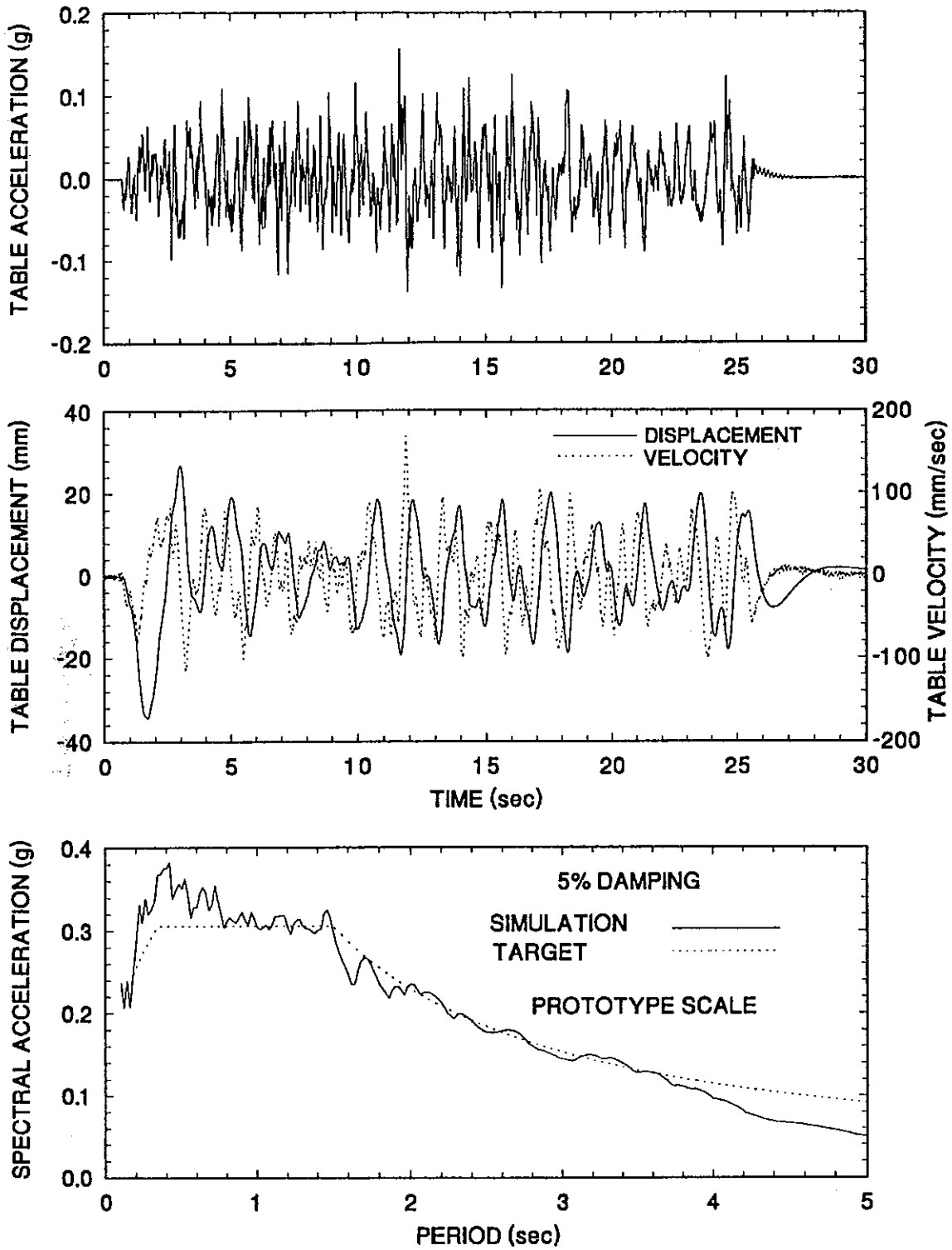

Figure 4-20 **Time Histories of Displacement, Velocity and Acceleration and Acceleration Response Spectrum of Shaking Table Motion Excited with JP. Level 1 G.C.3 100% Motion.**

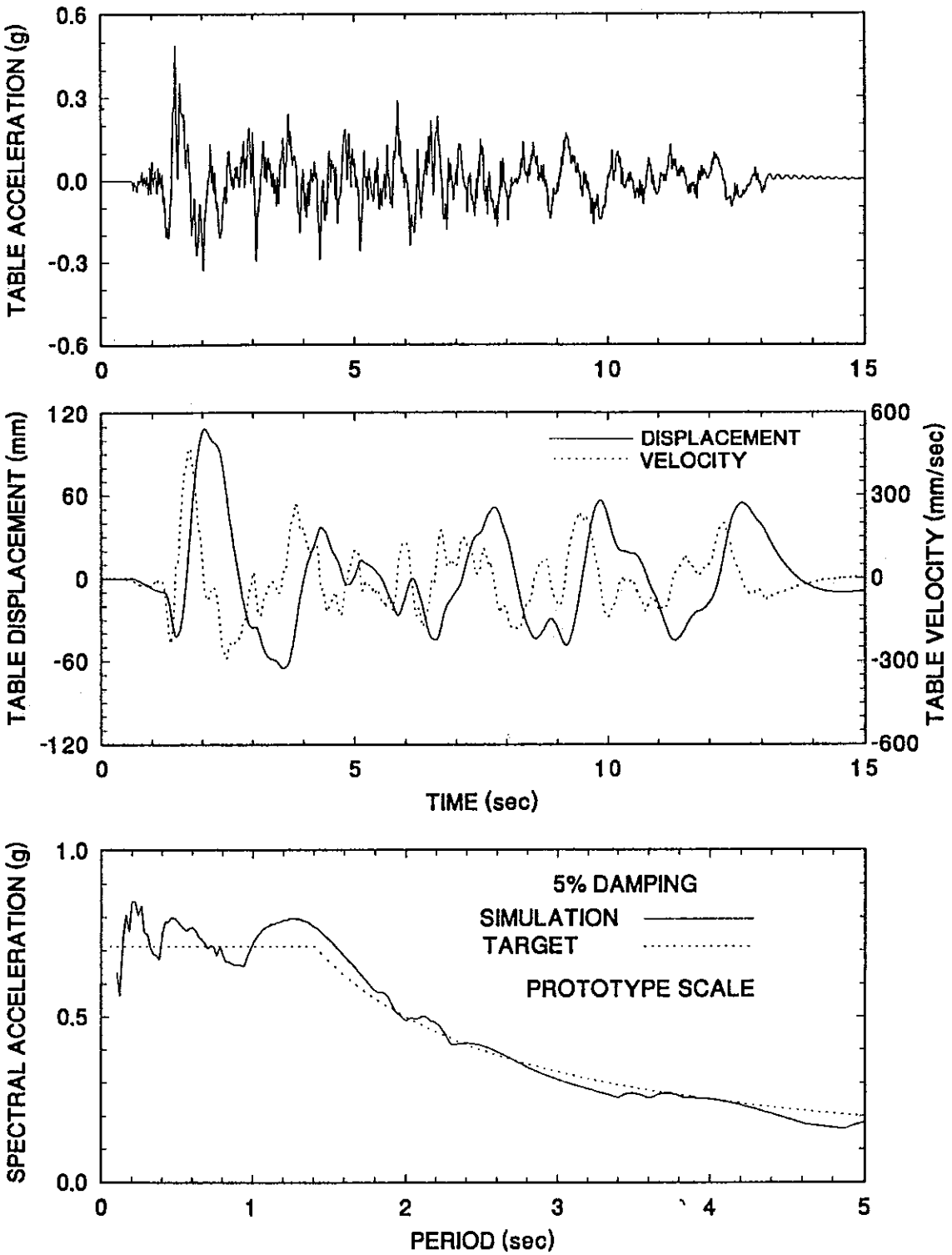

Figure 4-21 **Time Histories of Displacement, Velocity and Acceleration and Acceleration Response Spectrum of Shaking Table Motion Excited with JP. Level 2 G.C.1 100% Motion.**

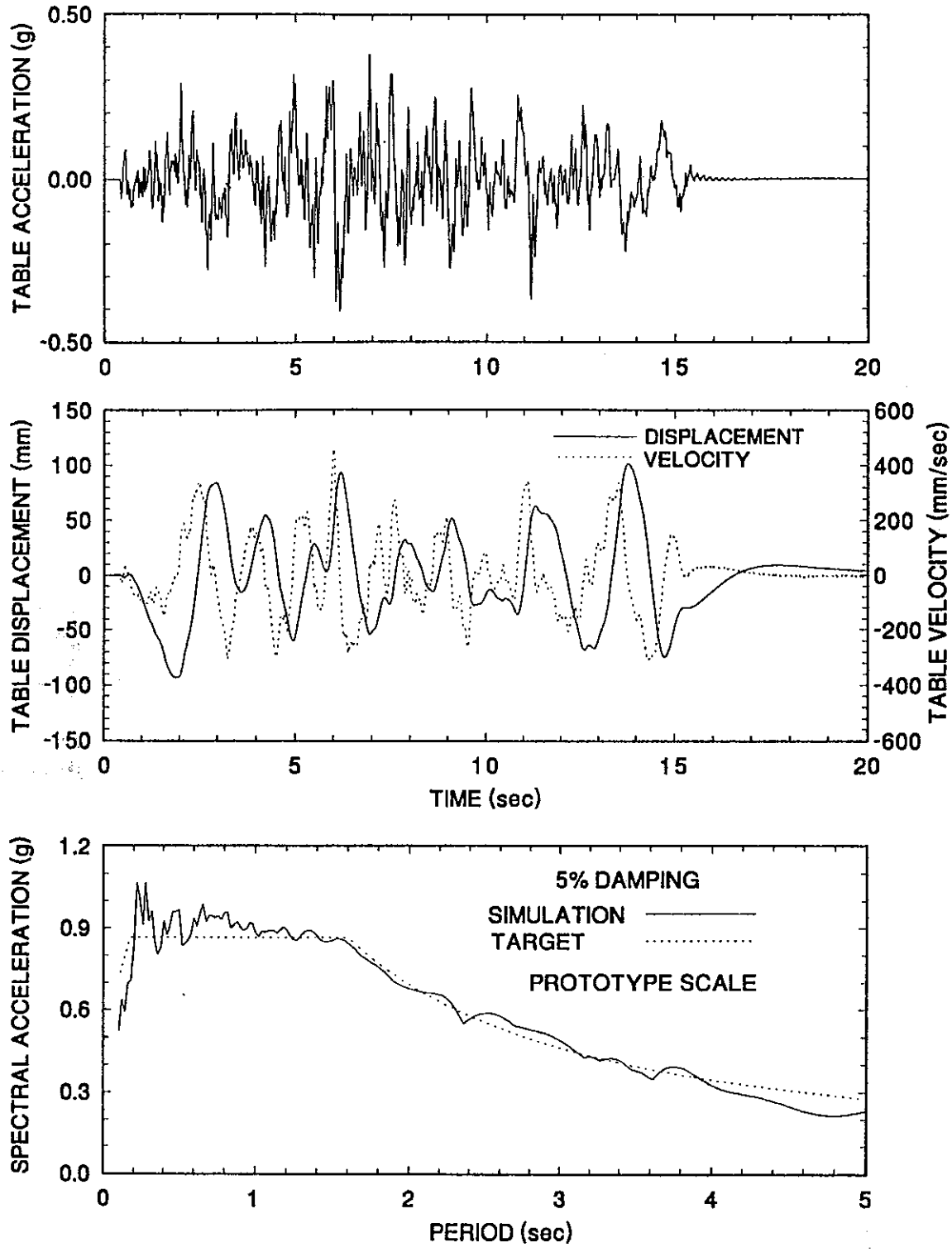

Figure 4-22 **Time Histories of Displacement, Velocity and Acceleration and Acceleration Response Spectrum of Shaking Table Motion Excited with JP. Level 2 G.C.2 100% Motion.**

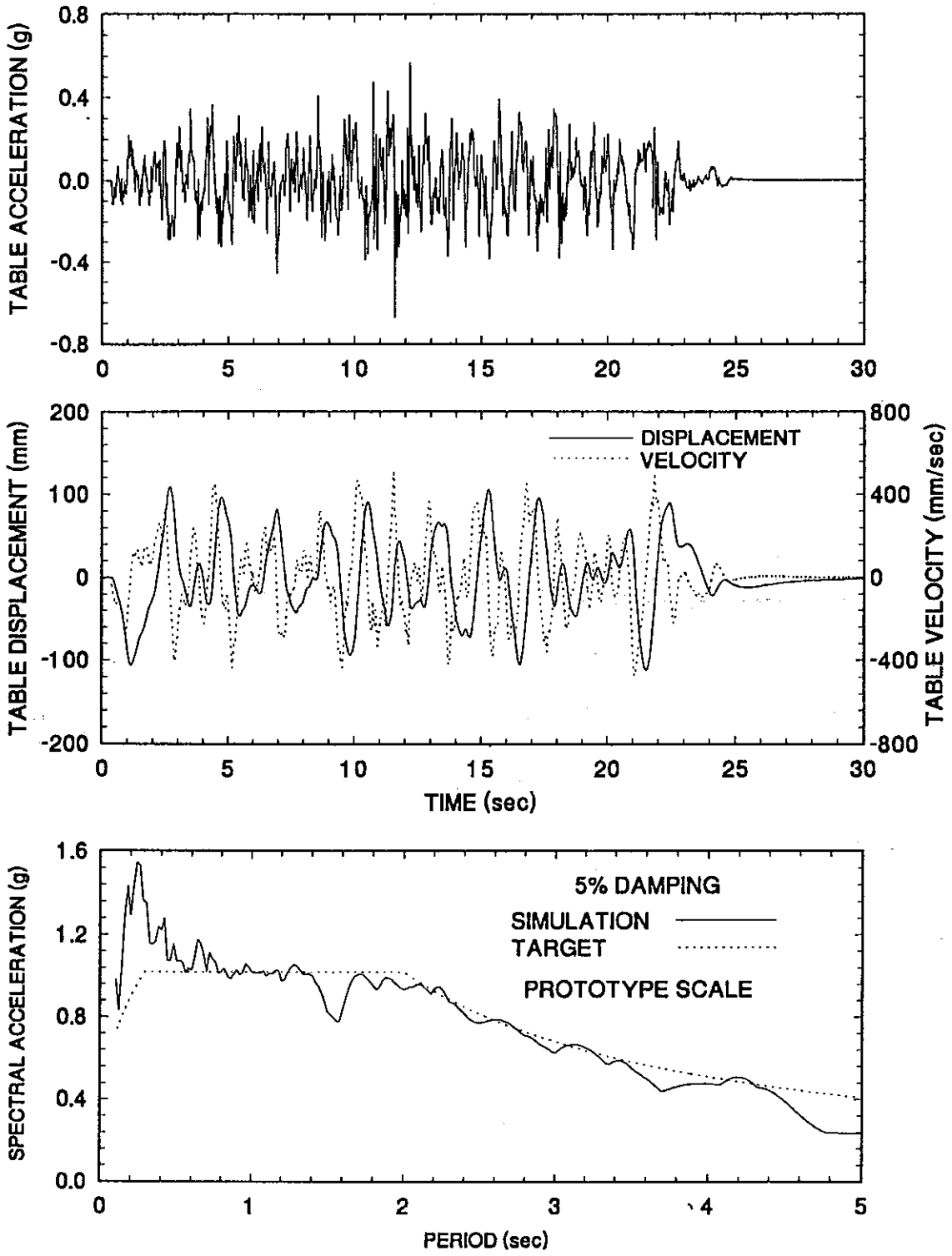

Figure 4-23 **Time Histories of Displacement, Velocity and Acceleration and Acceleration Response Spectrum of Shaking Table Motion Excited with JP. Level 2 G.C.3 100% Motion.**

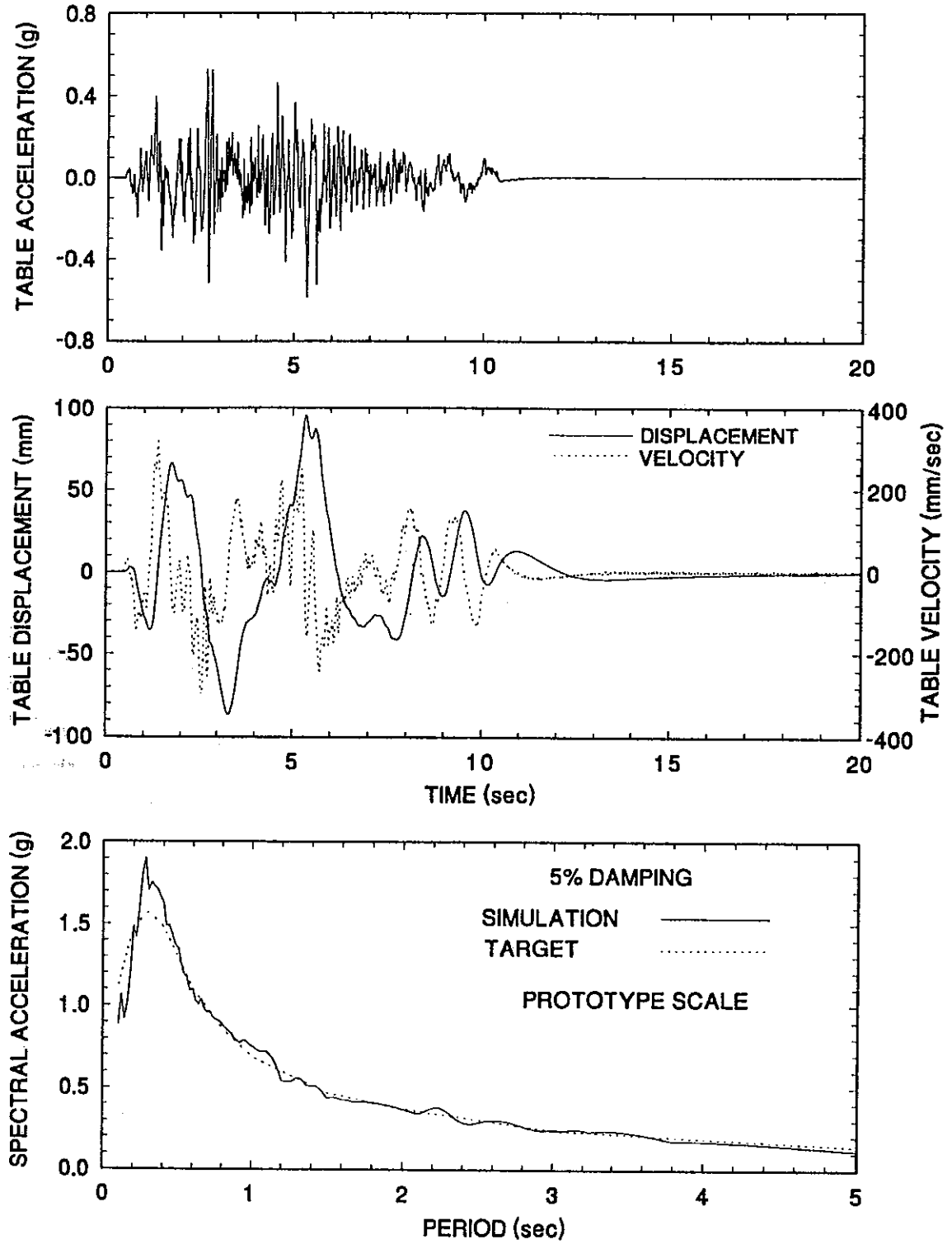

Figure 4-24 **Time Histories of Displacement, Velocity and Acceleration and Acceleration Response Spectrum of Shaking Table Motion Excited with CalTrans Rock No.3 0.6g 100% Motion.**

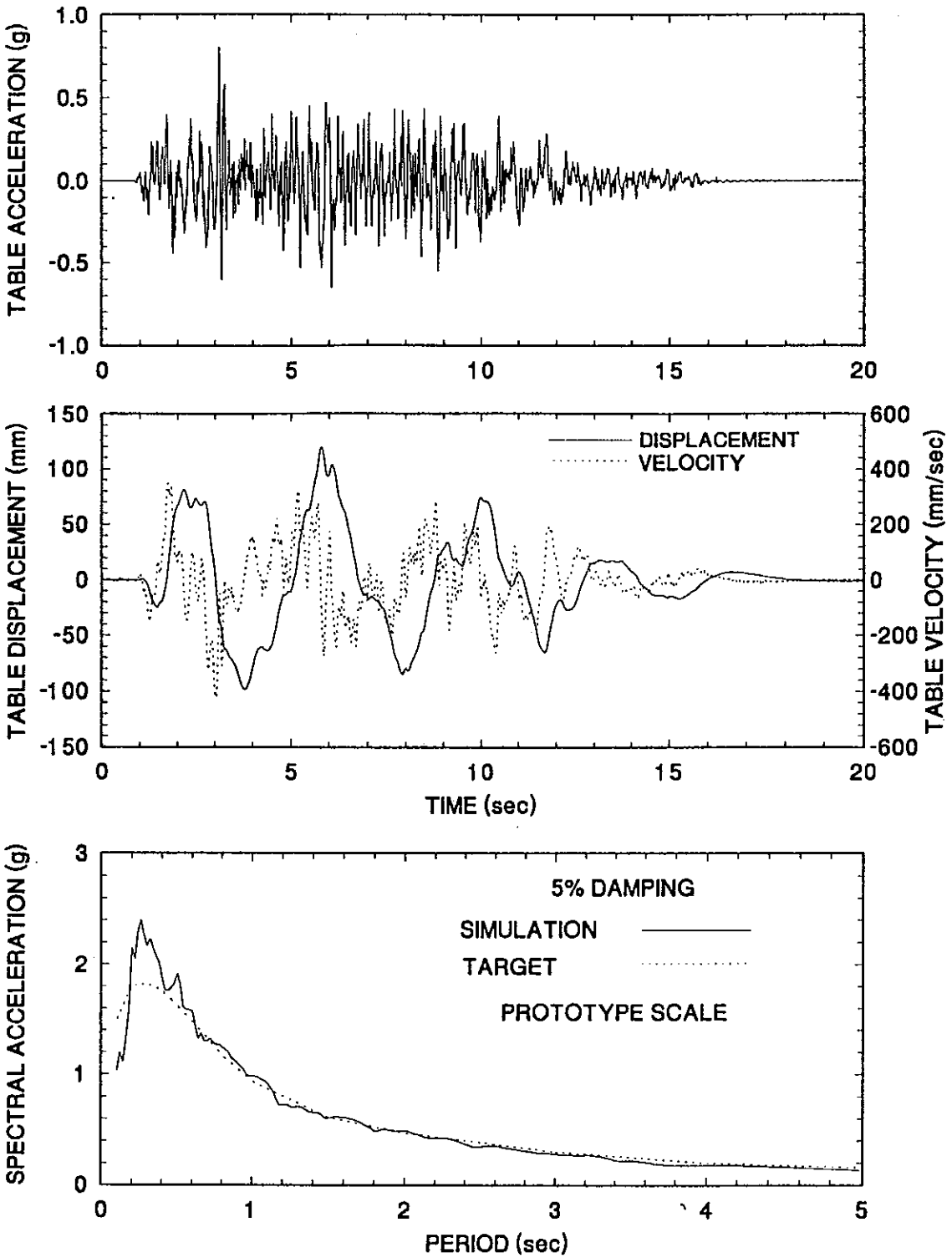

Figure 4-25 **Time Histories of Displacement, Velocity and Acceleration and Acceleration Response Spectrum of Shaking Table Motion Excited with CalTrans 10'-80' Alluvium No.3 0.6g 100% Motion.**

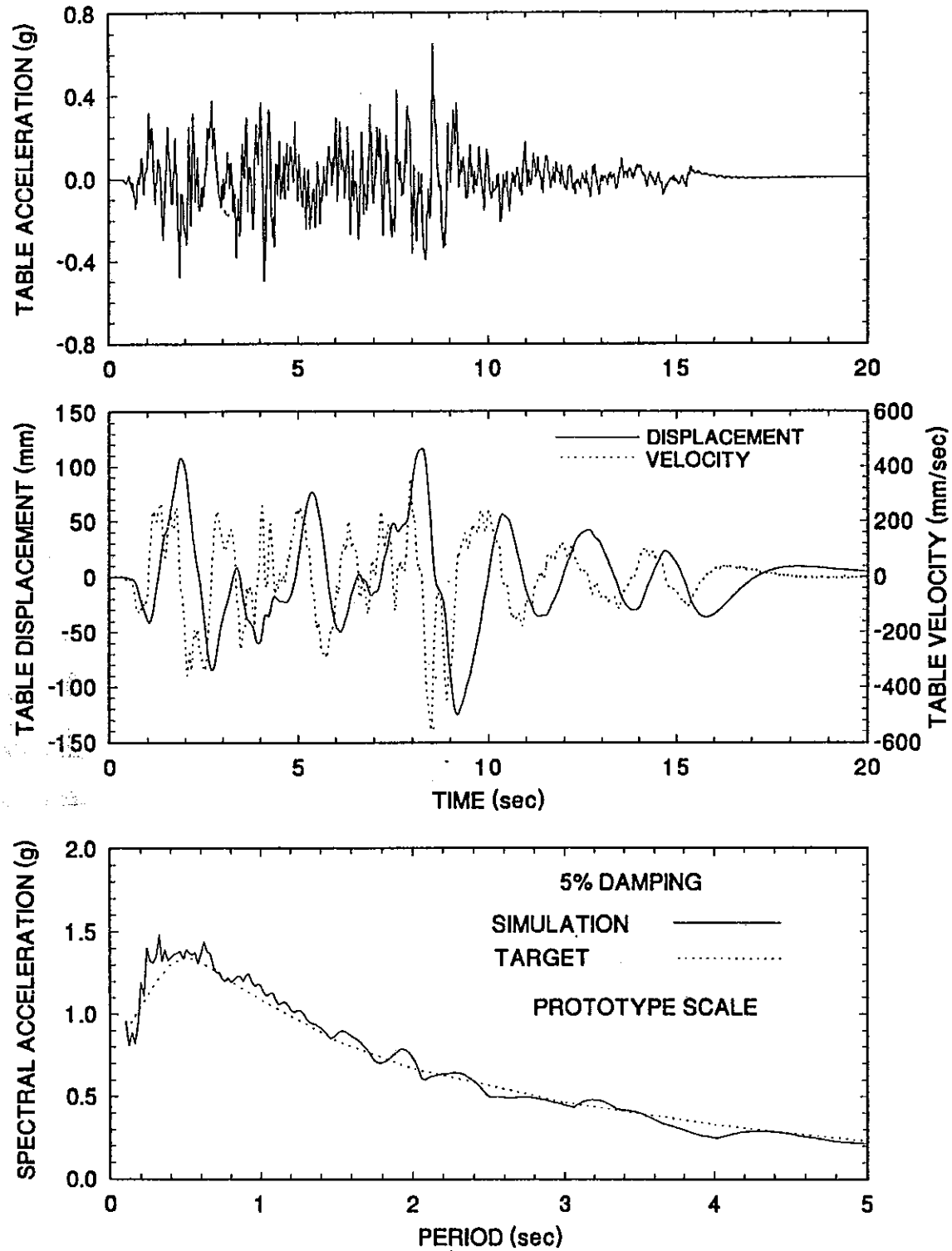

Figure 4-26 **Time Histories of Displacement, Velocity and Acceleration and Acceleration Response Spectrum of Shaking Table Motion Excited with CalTrans 80'-150' Alluvium No.2 0.6g 100% Motion.**

SECTION 5

EARTHQUAKE SIMULATOR TEST RESULTS

5.1 Results for Non-isolated Bridge

Testing of the non-isolated bridge (see Figure 4-5, configuration 1 and Figure 4-6) was conducted with only horizontal excitation. The experimental results for the bridge in its non-isolated configuration are summarized in Table 5-I. For each test the peak values of the table motion in the horizontal direction are given. The displacement and acceleration were directly measured whereas the velocity was determined by numerical differentiation of the displacement record. The peak pier drift is given as a percentage of the pier height which was 1290.3mm. This is the length of the column excluding the stiffeners at the ends (see Figure 4-1). The peak shear force is given as a fraction of the axial load carried by the pier (71.5 kN each pier).

5.2 Results for Isolated Bridge

Tables 5-II list the earthquake simulation tests and model conditions in the tests of the isolated bridge. The excitation in these tables is identified with a percentage figure which represents a scaling factor on the acceleration, velocity and displacement of the actual record. For example, the figure 200% denotes a motion scaled up by a factor of two in comparison to the actual record.

Table 5-III presents a summary of the experimental results of the isolated bridge. The tables include the following results:

(a) Displacement of bearings located at the south pier (see Figures 4-2 to 4-4). The transducers monitoring the south bearing displacement were continuously monitored and not initialized prior to each test. Thus, the instruments recorded correctly the initial and permanent bearing displacements. Figure 5-1 shows an example of bearing displacement time history. The initial displacement is the permanent displacement in the previous test and the initial displacement in the current test.

Table 5-I Summary of Experimental Results of Non-Isolated Bridge

TEST No.	EXCITATION	PEAK TABLE MOTION			DECK ACCEL.	PIER SHEAR / AXIAL LOAD		PIER DRIFT RATIO (%)	
		DISP. (mm)	VEL. (mm/sec)	ACCEL. (g)	(g)	SOUTH	NORTH	SOUTH	NORTH
FRUN05	EL CENTRO S00E 25%	5.8	40.0	0.095	0.25	0.266	0.271	N/A	0.381
FRUN06	TAFT N21E 50%	7.0	32.7	0.069	0.21	0.230	0.234	N/A	0.315
FRUN07	TAFT N21E 75%	10.5	47.7	0.102	0.25	0.273	0.278	N/A	0.385
FRUN08	JP LEVEL 1 G.C.1 100%	16.6	96.0	0.109	0.21	0.231	0.222	N/A	0.346
FRUN09	JP LEVEL 1 G.C.2 100%	17.3	113.6	0.110	0.26	0.280	0.269	N/A	0.414
FRUN10	JP LEVEL 1 G.C.3 100%	33.7	158.3	0.130	0.33	0.353	0.354	N/A	0.623
FRUN11	AKITA N-S 75%	25.1	108.4	0.138	0.26	0.284	0.283	N/A	0.474
FRUN12	HACHINOHE N-S 50%	15.8	66.0	0.103	0.18	0.200	0.198	N/A	0.311
FRUN13	MIYAGIKEN OKI E-W 75%	8.0	38.0	0.080	0.22	0.242	0.235	N/A	0.384
FRUN14	MEXICO N90W 100%	51.7	303.1	0.169	0.26	0.286	0.284	N/A	0.522
FRUN15	JP LEVEL 2 G.C.1 25%	26.7	114.1	0.104	0.17	0.189	0.181	N/A	0.301
FRUN16	JP LEVEL 2 G.C.2 25%	25.0	109.8	0.098	0.21	0.232	0.225	N/A	0.365
FRUN17	JP LEVEL 2 G.C.3 25%	27.6	116.6	0.117	0.26	0.285	0.283	N/A	0.497
FRUN18	PACOIMA S74W 13%	4.0	36.4	0.103	0.2	0.221	0.214	N/A	0.346
FRUN19	PACOIMA S16E 13%	10.4	63.9	0.095	0.17	0.187	0.186	N/A	0.275
FRUN20	CALTRANS R3 0.6g 20%	23.5	124.8	0.101	0.22	0.227	0.234	N/A	0.389
FRUN21	CALTRANS S3 0.6g 20%	32.1	102.4	0.112	0.31	0.320	0.345	N/A	0.565
FRUN22	CALTRANS A2 0.6g 20%	47.2	128.3	0.104	0.27	0.278	0.298	N/A	0.475

(b) Maximum travel of bearings located at the North pier. The transducers monitoring the North bearing displacements were initialized prior to each test so that the initial displacement appeared always as zero. Thus, only the maximum travel (MAX.-INIT. in Figure 5-1) could be accurately obtained and not the initial and permanent displacements.

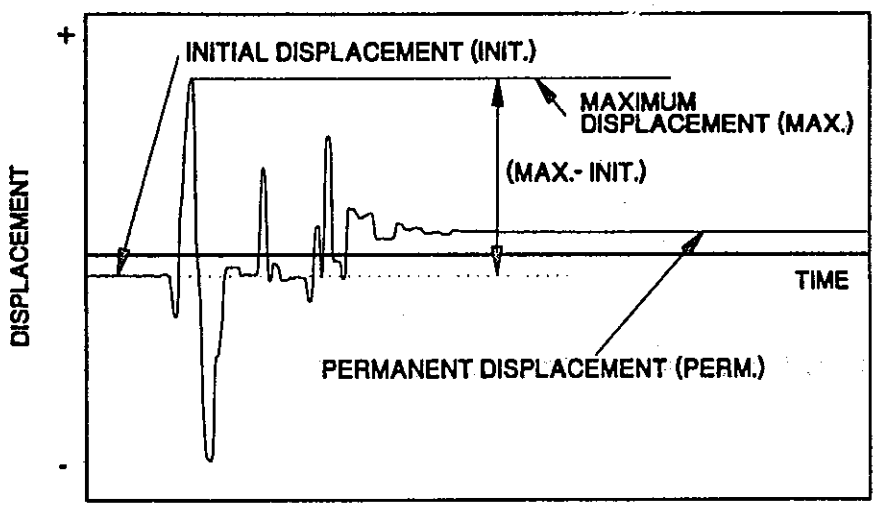

Figure 5-1 Example of Bearing Displacement History.

(c) Isolation system shear force normalized by the carried weight (143 kN for total shear force and 71.5 kN for shear force at each pier). The isolation system force at each pier location was obtained from the sum of the recorded friction forces and forces in the restoring force/damping devices. For example, the isolation system force at the south pier location, V_S , was obtained from

$$V_S = F_{fs} + F_{ts} \tag{5-1}$$

where F_{fs} is the friction force in the two sliding bearings on top of the south pier and F_{ts} is the force in the restoring force/damping device. A similar equation is

valid for the isolation system force at the north pier location, V_N. The total isolation system force, V, was then derived from

$$V = V_S + V_N \tag{5-2}$$

Equations (5-1) and (5-2) were used to obtain time histories of forces V_S, V_N and V, from which the peak values were extracted and included in Table 5-III.

It should be noted that for a rigid deck the isolation system force could be directly obtained from the deck acceleration measurement :

$$V = \frac{W_d a_d}{g} \tag{5-3}$$

where W_d = 143 kN and a_d is the recorded deck acceleration. However, the deck had some flexibility which caused amplification of the recorded deck acceleration. When Equation (5-3) was used, the loops of isolation system force (as obtained from the deck acceleration) versus bearing displacement were wavy. Since the recorded loops of friction force versus displacement did not exhibit a similar wavy form, it was concluded that the recorded acceleration of the deck contained additional components caused by the deck's flexibility.

An example of the errors which may be introduced by the use of the deck acceleration is presented in Figure 5-2. The graphs compare the recorded deck acceleration to the measured isolation system force in three tests. For an ideal case (infinitely rigid deck) the relation between the two quantities should have been a straight line. In reality it is not. The deviation from the straight line increases with increasing strength of excitation as a result of amplification of acceleration due to the deck flexibility and measurement errors due to pier top rotation.

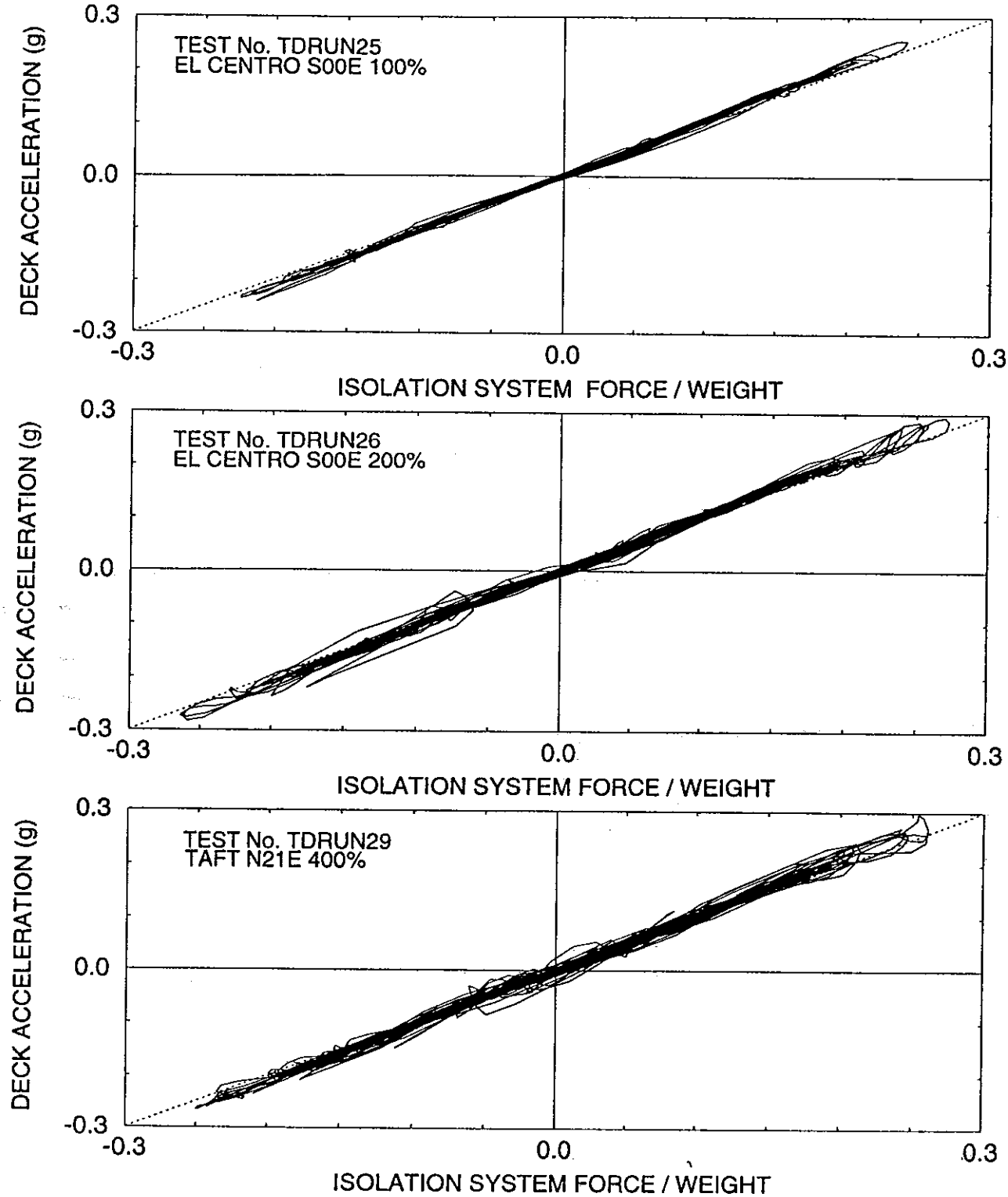

Figure 5-2 Comparison of Deck Acceleration to Isolation System Shear Force in Tests of Model with Flexible Piers.

(d) Device force normalized by the deck weight carried by each pier (71.5 kN). This is the force in each of two restoring force/damping devices. This force was measured directly from load cells placed at the side of the devices which was connected to the deck. This setup was chosen to minimize any errors in the measurements of the force that could be introduced from the acceleration of the load cell (acceleration at the top of piers is higher than the acceleration experienced by the deck of the bridge).

(e) Device displacement. The peak values of displacement of the devices at the south and north piers are reported. There displacements are not identical to the bearings displacements. The minor difference between the two (see Table 5-III) is due to some small flexibility of the mounting arrangements of the restoring force/damping devices to the deck of the bridge.

(f) Pier acceleration. The peak accelerations of the top of the south and north piers are reported.

(g) Deck horizontal acceleration.

(h) Pier shear force normalized by axial load. Each column was instrumented with strain gages to measure the shear force. The reported quantity is the sum of the shear forces in the two columns of each pier divided by the axial load on each pier (143/2=71.5 kN). The pier shear force is, in general, different than the isolation system shear force. The two forces differ by the inertia force of the accelerating part of the pier between the sliding interface and the location of the strain gages. The pier shear force in the case of stiff piers could not be measured and is not reported in the tables. It should be noted that in the case of stiff piers the columns were braced (see Figures 4-1, 4-5 and 4-8), so that the force measured by the strain gage load cells of the columns represented only part of the total pier shear force.

(i) Pier drift ratio. This is the displacement of the top of the pier relative to the shake table, divided by the length of the column (1290.3 mm).

During testing of the model bridge in its isolated condition it was observed that the overhangs of the shake table extension, which supported the piers (see Figure 4-1), underwent significant vertical motion even when only horizontal table motion was imposed. The two overhangs did not move vertically in unison. Rather, the motion of the two overhangs was anti-symmetric with the two sides moving with different amplitude and content in frequency. It was concluded that this vertical motion of the overhangs was the combined result of table-structure interaction, vertical flexibility of the overhangs and differences in the vertical stiffness of the overhangs (it was later found that on one side of the concrete table extension the reinforcement was misplaced).

The implications of this phenomenon were to increase the severity of the testing. In effect, in all tests the piers experienced out-of-phase vertical input at their bases. This caused changes in the vertical load carried by the sliding bearings, which in turn affected the friction force of the bearings. This explains the differences in the isolation system shear force, pier acceleration and pier shear force and drift between the south and north piers (see Table 5-III). Furthermore, it explains the mildly wavy nature of the recorded force versus displacement loops of the isolation system (see Appendix A).

Table 5-II Eartquake Simulation Tests and Model Conditions in Tests with Sliding Bearings and Fluid Restoring Force/Damping Devices

TEST No.	EXCITATION	PEAK TABLE MOTION			PIER CONDITION		BEARING MATERIAL		BEARING PRESSURE (MPa)		FRICTIONAL PROPERTIES		COMMENTS
		DIS. (mm)	VEL. (mm/s)	ACC. (g)	SOUTH	NORTH	SOUTH	NORTH	SOUTH	NORTH	fmax	fmin	
TDRUN01	EL CENTRO S00E 100%	24.0	163.9	0.376	STIFF	STIFF	T1	T1	5.0	5.0	0.14	0.06	
TDRUN02	EL CENTRO S00E 200%	48.3	319.8	0.639	STIFF	STIFF	T1	T1	5.0	5.0	0.14	0.06	
TDRUN03	JP LEVEL 1 G.C.1 100%	17.2	106.7	0.119	STIFF	STIFF	T1	T1	5.0	5.0	0.14	0.06	
TDRUN04	JP LEVEL 1 G.C.2 100%	17.5	111.8	0.131	STIFF	STIFF	T1	T1	5.0	5.0	0.14	0.06	
TDRUN05	JP LEVEL 1 G.C.3 100%	34.4	169.4	0.172	STIFF	STIFF	T1	T1	5.0	5.0	0.14	0.06	
TDRUN06	JP LEVEL 2 G.C.1 100%	109.1	482.8	0.490	STIFF	STIFF	T1	T1	5.0	5.0	0.14	0.06	
TDRUN07	JP LEVEL 2 G.C.2 100%	101.9	448.3	0.504	STIFF	STIFF	T1	T1	5.0	5.0	0.14	0.06	
TDRUN08	JP LEVEL 2 G.C.3 100%	112.2	502.9	0.475	STIFF	STIFF	T1	T1	5.0	5.0	0.14	0.06	
TDRUN09	TAFT N21E 200%	28.6	134.6	0.271	STIFF	STIFF	T1	T1	5.0	5.0	0.14	0.06	
TDRUN10	TAFT N21E 400%	57.5	264.8	0.554	STIFF	STIFF	T1	T1	5.0	5.0	0.14	0.06	
TDRUN11	TAFT N21E 600%	86.1	416.8	0.865	STIFF	STIFF	T1	T1	5.0	5.0	0.14	0.06	
TDRUN12	HACHINOHE N-S 100%	32.4	139.0	0.244	STIFF	STIFF	T1	T1	5.0	5.0	0.14	0.06	
TDRUN13	HACHINOHE N-S 200%	64.6	274.1	0.445	STIFF	STIFF	T1	T1	5.0	5.0	0.14	0.06	
TDRUN14	HACHINOHE N-S 300%	96.9	412.8	0.638	STIFF	STIFF	T1	T1	5.0	5.0	0.14	0.06	
TDRUN15	PACOIMA S74W 100%	29.5	272.8	0.824	STIFF	STIFF	T1	T1	5.0	5.0	0.14	0.06	
TDRUN16	CALTRANS R3 0.6g 100%	96.0	307.5	0.674	STIFF	STIFF	T1	T1	5.0	5.0	0.14	0.06	
TDRUN17	CALTRANS S3 0.6g 100%	119.9	431.3	0.911	STIFF	STIFF	T1	T1	5.0	5.0	0.14	0.06	
TDRUN18	CALTRANS A2 0.6g 100%	125.9	554.8	0.625	STIFF	STIFF	T1	T1	5.0	5.0	0.14	0.06	
TDRUN19	MEXICO N90W 100%	52.7	310.2	0.178	STIFF	STIFF	T1	T1	5.0	5.0	0.14	0.06	
TDRUN20	MEXICO N90W 120%	63.3	376.5	0.220	STIFF	STIFF	T1	T1	5.0	5.0	0.14	0.06	
TDRUN21	PACOIMA S16E 75%	61.3	363.6	0.629	STIFF	STIFF	T1	T1	5.0	5.0	0.14	0.06	
TDRUN22	PACOIMA S16E 85%	69.2	411.5	0.717	STIFF	STIFF	T1	T1	5.0	5.0	0.14	0.06	
TDRUN23	TAFT N21E H+V 400%	57.7	269.2	0.534	STIFF	STIFF	T1	T1	5.0	5.0	0.14	0.06	
TDRUN24	EL CENTRO S00E H+V 200%	48.1	317.4	0.648	STIFF	STIFF	T1	T1	5.0	5.0	0.14	0.06	
TDRUN25	EL CENTRO S00E 100%	24.0	156.1	0.259	FLEXIBLE	FLEXIBLE	T1	T1	5.0	5.0	0.14	0.06	
TDRUN26	EL CENTRO S00E 200%	47.6	308.5	0.577	FLEXIBLE	FLEXIBLE	T1	T1	5.0	5.0	0.14	0.06	

Table 5-II Cont'd

TEST No.	EXCITATION	PEAK TABLE MOTION			PIER CONDITION		BEARING MATERIAL		BEARING PRESSURE (MPa)		FRICTIONAL PROPERTIES		COMMENTS
		DIS. (mm)	VEL. (mm/s)	ACC. (g)	SOUTH	NORTH	SOUTH	NORTH	SOUTH	NORTH	fmax	fmin	
TDRUN27	EL CENTRO S00E 250%	59.3	389.3	0.746	FLEXIBLE	FLEXIBLE	T1	T1	5.0	5.0	0.14	0.06	
TDRUN28	TAFT N21E 200%	28.8	131.6	0.283	FLEXIBLE	FLEXIBLE	T1	T1	5.0	5.0	0.14	0.06	
TDRUN29	TAFT N21E 400%	57.6	268.0	0.564	FLEXIBLE	FLEXIBLE	T1	T1	5.0	5.0	0.14	0.06	
TDRUN30	TAFT N21E 500%	71.8	335.7	0.713	FLEXIBLE	FLEXIBLE	T1	T1	5.0	5.0	0.14	0.06	
TDRUN31	HACHINOHE N-S 200%	64.1	277.7	0.424	FLEXIBLE	FLEXIBLE	T1	T1	5.0	5.0	0.14	0.06	
TDRUN32	HACHINOHE N-S 300%	96.0	412.1	0.608	FLEXIBLE	FLEXIBLE	T1	T1	5.0	5.0	0.14	0.06	
TDRUN33	PACOIMA S74W 100%	29.5	252.7	0.862	FLEXIBLE	FLEXIBLE	T1	T1	5.0	5.0	0.14	0.06	
TDRUN34	CALTRANS R3 0.6g 100%	96.9	305.4	0.609	FLEXIBLE	FLEXIBLE	T1	T1	5.0	5.0	0.14	0.06	
TDRUN35	CALTRANS S3 0.6g 100%	119.4	416.9	0.652	FLEXIBLE	FLEXIBLE	T1	T1	5.0	5.0	0.14	0.06	
TDRUN36	CALTRANS A2 0.6g 100%	125.6	553.7	0.506	FLEXIBLE	FLEXIBLE	T1	T1	5.0	5.0	0.14	0.06	
TDRUN37	JP LEVEL 1 G.C.1 100%	17.3	102.9	0.100	FLEXIBLE	FLEXIBLE	T1	T1	5.0	5.0	0.14	0.06	
TDRUN38	JP LEVEL 1 G.C.2 100%	17.8	109.8	0.108	FLEXIBLE	FLEXIBLE	T1	T1	5.0	5.0	0.14	0.06	
TDRUN39	JP LEVEL 1 G.C.3 100%	34.3	163.0	0.111	FLEXIBLE	FLEXIBLE	T1	T1	5.0	5.0	0.14	0.06	
TDRUN40	JP LEVEL 2 G.C.1 75%	81.8	357.8	0.280	FLEXIBLE	FLEXIBLE	T1	T1	5.0	5.0	0.14	0.06	
TDRUN41	JP LEVEL 2 G.C.1 100%	109.3	474.1	0.390	FLEXIBLE	FLEXIBLE	T1	T1	5.0	5.0	0.14	0.06	
TDRUN42	JP LEVEL 2 G.C.2 100%	101.9	446.4	0.405	FLEXIBLE	FLEXIBLE	T1	T1	5.0	5.0	0.14	0.06	
TDRUN43	JP LEVEL 2 G.C.3 100%	112.3	498.4	0.422	FLEXIBLE	FLEXIBLE	T1	T1	5.0	5.0	0.14	0.06	
TDRUN44	PACOIMA S16E 50%	41.2	246.9	0.383	FLEXIBLE	FLEXIBLE	T1	T1	5.0	5.0	0.14	0.06	
TDRUN45	PACOIMA S16E 75%	61.0	366.6	0.556	FLEXIBLE	FLEXIBLE	T1	T1	5.0	5.0	0.14	0.06	
TDRUN46	MEXICO N90W 100%	52.8	309.1	0.184	FLEXIBLE	FLEXIBLE	T1	T1	5.0	5.0	0.14	0.06	
TDRUN47	MEXICO N90W 120%	63.3	375.1	0.221	FLEXIBLE	FLEXIBLE	T1	T1	5.0	5.0	0.14	0.06	
TDRUN48	AKITA N-S 100%	34.2	146.7	0.168	FLEXIBLE	FLEXIBLE	T1	T1	5.0	5.0	0.14	0.06	
TDRUN49	AKITA N-S 200%	68.3	295.2	0.330	FLEXIBLE	FLEXIBLE	T1	T1	5.0	5.0	0.14	0.06	
TDRUN50	MIYAGIKENOKI E-W 100%	12.4	73.9	0.122	FLEXIBLE	FLEXIBLE	T1	T1	5.0	5.0	0.14	0.06	
TDRUN51	MIYAGIKENOKI E-W 200%	24.8	144.5	0.248	FLEXIBLE	FLEXIBLE	T1	T1	5.0	5.0	0.14	0.06	
TDRUN52	MIYAGIKENOKI E-W 400%	49.3	302.5	0.543	FLEXIBLE	FLEXIBLE	T1	T1	5.0	5.0	0.14	0.06	

Table 5-II Cont'd

TEST No.	EXCITATION	PEAK TABLE MOTION			PIER CONDITION		BEARING MATERIAL		BEARING PRESSURE (MPa)		FRICTIONAL PROPERTIES		COMMENTS
		DIS. (mm)	VEL. (mm/s)	ACC. (g)	SOUTH	NORTH	SOUTH	NORTH	SOUTH	NORTH	fmax	fmin	
TDRUN53	MIYAGIKENOKI E-W 600%	73.5	460.9	0.914	FLEXIBLE	FLEXIBLE	T1	T1	5.0	5.0	0.14	0.06	
TDRUN54	TAFT N21E H+V 400%	57.7	269.9	0.544	FLEXIBLE	FLEXIBLE	T1	T1	5.0	5.0	0.14	0.06	
TDRUN55	EL CENTRO S00E H+V 200%	47.3	312.6	0.580	FLEXIBLE	FLEXIBLE	T1	T1	5.0	5.0	0.14	0.06	

Table 5-III Summary of Experimental Results of Isolated Bridge with Sliding Bearings and Fluid Restoring Force/Damping Devices

TEST No.	BEARING DISPLACEMENT (mm)				ISOLATION SYSTEM SHEAR / WEIGHT			DECK ACC. (g)	PIER ACC. (g)		PIER DRIFT (%)		PIER SHEAR / AXIAL LOAD		DEVICE DISPLACEMENT (mm)		DEVICE FORCE / DECK WEIGHT	
	SOUTH			NORTH														
	INIT.	MAX.	PERM.	MAX.-INIT.	SOUTH	NORTH	TOTAL		SOUTH	NORTH	SOUTH	NORTH	SOUTH	NORTH	SOUTH	NORTH	SOUTH	NORTH
TDRUN01	0.0	-7.3	-0.1	7.2	0.240	0.233	0.227	0.274	0.454	0.524	N/A	0.06	N/A	N/A	7.1	6.8	0.078	0.082
TDRUN02	-0.1	25.8	0.0	25.8	0.269	0.281	0.272	0.320	0.933	1.024	N/A	0.08	N/A	N/A	25.7	25.3	0.112	0.102
TDRUN03	0.0	-0.4	0.0	0.5	0.142	0.138	0.139	0.153	0.167	0.156	N/A	0.03	N/A	N/A	0.3	0.4	0.050	0.042
TDRUN04	0.0	0.9	0.1	0.9	0.168	0.156	0.162	0.183	0.220	0.234	N/A	0.04	N/A	N/A	0.8	0.9	0.059	0.058
TDRUN05	0.1	2.2	-0.1	2.1	0.177	0.180	0.179	0.204	0.298	0.271	N/A	0.04	N/A	N/A	2.1	1.8	0.065	0.070
TDRUN06	-0.1	-23.6	-0.2	23.5	0.253	0.247	0.245	0.292	0.575	0.544	N/A	0.06	N/A	N/A	23.3	23.3	0.098	0.094
TDRUN07	-0.1	43.1	0.2	42.8	0.299	0.316	0.304	0.372	0.642	0.597	N/A	0.07	N/A	N/A	42.9	42.3	0.142	0.128
TDRUN08	0.2	37.4	0.0	36.8	0.279	0.291	0.284	0.333	0.791	0.760	N/A	0.08	N/A	N/A	37.0	36.1	0.118	0.121
TDRUN09	0.0	5.5	0.0	5.3	0.211	0.210	0.207	0.256	0.458	0.548	N/A	0.05	N/A	N/A	5.3	5.2	0.072	0.086
TDRUN10	0.0	18.1	-0.1	17.9	0.247	0.256	0.240	0.303	0.908	0.997	N/A	0.07	N/A	N/A	17.8	17.2	0.099	0.101
TDRUN11	-0.1	-36.4	-0.3	36.4	0.318	0.332	0.295	0.351	1.336	1.471	N/A	0.09	N/A	N/A	36.1	35.8	0.131	0.129
TDRUN12	-0.3	-3.2	-0.0	3.4	0.179	0.206	0.189	0.234	0.345	0.417	N/A	0.05	N/A	N/A	3.1	3.1	0.080	0.074
TDRUN13	-0.1	-22.0	-0.2	21.9	0.265	0.252	0.252	0.307	0.692	0.717	N/A	0.07	N/A	N/A	21.8	21.3	0.087	0.103
TDRUN14	-0.2	-44.7	-0.6	44.2	0.352	0.310	0.325	0.380	0.963	0.922	N/A	0.08	N/A	N/A	44.1	43.5	0.124	0.152
TDRUN15	-0.6	-21.9	-0.2	21.2	0.262	0.270	0.254	0.304	0.952	1.219	N/A	0.07	N/A	N/A	21.3	20.9	0.133	0.116
TDRUN16	-0.2	21.9	-0.3	21.8	0.243	0.261	0.252	0.288	0.722	0.859	N/A	0.06	N/A	N/A	21.7	21.4	0.109	0.101
TDRUN17	-0.3	33.1	-0.1	33.2	0.276	0.281	0.278	0.326	0.994	1.054	N/A	0.09	N/A	N/A	32.9	32.5	0.145	0.122
TDRUN18	-0.1	-33.1	-0.1	32.8	0.280	0.290	0.279	0.356	0.817	1.032	N/A	0.08	N/A	N/A	32.5	32.2	0.105	0.122
TDRUN19	-0.1	-2.4	-0.3	2.3	0.151	0.163	0.156	0.181	0.195	0.192	N/A	0.03	N/A	N/A	2.1	1.8	0.059	0.064
TDRUN20	-0.3	-12.2	0.0	11.8	0.208	0.216	0.209	0.252	0.315	0.292	N/A	0.04	N/A	N/A	11.8	11.5	0.093	0.081
TDRUN21	0.0	-32.6	-0.1	32.6	0.281	0.269	0.269	0.330	0.823	0.658	N/A	0.06	N/A	N/A	32.4	32.1	0.100	0.123
TDRUN22	-0.1	-44.6	-0.1	44.4	0.321	0.292	0.300	0.372	0.961	0.811	N/A	0.07	N/A	N/A	44.2	44.1	0.120	0.143
TDRUN23	-0.1	18.6	-0.1	18.3	0.254	0.298	0.268	0.316	0.937	0.845	N/A	0.07	N/A	N/A	18.34	18.3	0.102	0.097
TDRUN24	-0.1	27.0	0.0	26.9	0.252	0.282	0.262	0.318	0.947	0.920	N/A	0.09	N/A	N/A	26.8	26.2	0.115	0.104
TDRUN25	0.0	10.9	0.1	10.5	0.229	0.249	0.228	0.257	1.008	1.002	N/A	0.40	0.268	0.325	11.7	10.9	0.093	0.089
TDRUN26	0.1	25.4	0.1	24.3	0.258	0.284	0.262	0.295	1.525	1.880	N/A	0.42	0.320	0.340	25.6	23.9	0.104	0.109

Table 5-III Cont'd

TEST No.	BEARING DISPLACEMENT (mm)				ISOLATION SYSTEM SHEAR / WEIGHT			DECK ACC. (g)	PIER ACC. (g)		PIER DRIFT (%)		PIER SHEAR / AXIAL LOAD		DEVICE DISPLACEMENT (mm)		DEVICE FORCE / DECK WEIGHT	
	SOUTH			NORTH														
	INIT.	MAX.	PERM.	MAX.-INIT.	SOUTH	NORTH	TOTAL		SOUTH	NORTH	SOUTH	NORTH	SOUTH	NORTH	SOUTH	NORTH	SOUTH	NORTH
TDRUN27	0.1	35.2	0.1	34.3	0.274	0.306	0.283	0.319	1.654	2.023	N/A	0.46	0.335	0.365	35.7	34.1	0.126	0.122
TDRUN28	0.1	8.6	0.1	8.1	0.207	0.241	0.218	0.242	0.737	0.698	N/A	0.37	0.244	0.289	9.2	8.2	0.079	0.082
TDRUN29	0.1	20.5	0.1	19.7	0.244	0.278	0.255	0.297	1.371	1.216	N/A	0.43	0.299	0.340	20.9	20.3	0.096	0.101
TDRUN30	0.1	-36.3	0.2	37.2	0.281	0.293	0.268	0.313	1.582	1.405	N/A	0.46	0.351	0.370	37.6	37.8	0.127	0.134
TDRUN31	0.2	-31.6	0.1	32.4	0.280	0.262	0.271	0.328	0.791	0.825	N/A	0.46	0.357	0.341	32.6	33.1	0.126	0.130
TDRUN32	0.1	-43.3	0.1	44.0	0.318	0.301	0.310	0.371	1.165	1.101	N/A	0.53	0.402	0.399	44.5	44.9	0.150	0.164
TDRUN33	0.2	-35.6	-0.4	36.1	0.271	0.267	0.267	0.333	1.245	1.191	N/A	0.48	0.344	0.348	36.5	36.7	0.118	0.125
TDRUN34	-0.4	23.6	0.1	23.2	0.249	0.297	0.271	0.295	0.858	0.809	N/A	0.43	0.314	0.354	24.6	23.1	0.118	0.116
TDRUN35	0.1	42.4	0.1	41.3	0.281	0.331	0.303	0.342	1.349	1.444	N/A	0.48	0.320	0.406	42.6	40.5	0.151	0.132
TDRUN36	0.1	-40.2	0.2	40.8	0.299	0.290	0.294	0.378	1.257	1.266	N/A	0.54	0.403	0.392	41.0	41.5	0.139	0.153
TDRUN37	0.2	2.5	0.1	2.3	0.170	0.180	0.173	0.193	0.283	0.228	N/A	0.27	0.203	0.216	3.5	2.6	0.072	0.071
TDRUN38	0.1	3.7	0.1	3.7	0.193	0.189	0.187	0.207	0.405	0.369	N/A	0.30	0.224	0.226	4.3	3.9	0.077	0.077
TDRUN39	0.1	6.5	0.0	5.9	0.197	0.211	0.195	0.212	0.408	0.399	N/A	0.32	0.228	0.253	7.1	6.2	0.072	0.077
TDRUN40	0.0	-25.3	0.1	25.8	0.252	0.269	0.251	0.294	0.657	0.556	N/A	0.41	0.294	0.333	26.2	26.6	0.097	0.105
TDRUN41	0.1	-43.6	0.0	44.2	0.289	0.310	0.298	0.372	1.079	0.966	N/A	0.55	0.356	0.444	45.2	46.1	0.130	0.140
TDRUN42	0.0	52.7	0.1	52.0	0.386	0.385	0.364	0.446	1.186	1.123	N/A	0.58	0.414	0.469	52.3	51.6	0.310	0.302 @
TDRUN43	0.1	45.8	0.4	44.7	0.289	0.304	0.295	0.362	1.151	1.204	N/A	0.56	0.364	0.451	46.4	44.3	0.161	0.139
TDRUN44	0.4	-20.2	0.5	20.9	0.250	0.253	0.251	0.304	0.555	0.605	N/A	0.43	0.310	0.320	21.6	21.7	0.091	0.106
TDRUN45	0.5	-49.8	0.4	50.8	0.313	0.320	0.316	0.392	1.081	1.173	N/A	0.58	0.421	0.428	51.5	51.7	0.141	0.165
TDRUN46	0.5	-6.5	0.4	7.1	0.214	0.203	0.209	0.233	0.379	0.381	N/A	0.33	0.246	0.252	7.7	7.8	0.069	0.082
TDRUN47	0.4	-16.7	0.4	17.3	0.228	0.244	0.236	0.269	0.507	0.453	N/A	0.38	0.267	0.303	18.1	18.2	0.088	0.089
TDRUN48	0.4	5.2	0.5	4.2	0.193	0.198	0.190	0.214	0.458	0.461	N/A	0.31	0.220	0.240	5.7	4.9	0.072	0.076
TDRUN49	0.5	30.1	0.5	29.0	0.262	0.277	0.268	0.308	0.853	0.862	N/A	0.47	0.336	0.365	30.4	29.4	0.116	0.110
TDRUN50	0.5	0.9	0.5	0.2	0.142	0.141	0.142	0.155	0.153	0.119	N/A	0.22	0.154	0.169	1.1	0.8	0.062	0.061
TDRUN51	0.5	3.1	0.5	2.0	0.181	0.174	0.178	0.188	0.319	0.242	N/A	0.28	0.202	0.213	3.1	2.3	0.066	0.068
TDRUN52	0.5	22.2	0.4	20.8	0.246	0.272	0.257	0.285	1.141	1.049	N/A	0.40	0.269	0.319	22.2	21.2	0.105	0.094

@ DISPLACEMENT CAPACITY OF RESTORING FORCE/DAMPING DEVICE EXCEEDED

Table 5-III Cont'd

TEST No.	BEARING DISPLACEMENT (mm)				ISOLATION SYSTEM SHEAR / WEIGHT			DECK ACC. (g)	PIER ACC. (g)		PIER DRIFT (%)		PIER SHEAR / AXIAL LOAD		DEVICE DISPLACEMENT (mm)		DEVICE FORCE / DECK WEIGHT	
	SOUTH			NORTH														
	INIT.	MAX.	PERM.	MAX.-INIT.	SOUTH	NORTH	TOTAL		SOUTH	NORTH	SOUTH	NORTH	SOUTH	NORTH	SOUTH	NORTH	SOUTH	NORTH
TDRUN53	0.5	-33.9	0.4	34.9	0.308	0.289	0.299	0.325	1.485	0.659	N/A	0.46	0.320	0.354	35.3	35.7	0.123	0.142
TDRUN54	0.5	20.6	0.5	19.3	0.282	0.318	0.299	0.312	1.281	0.554	N/A	0.48	0.326	0.377	20.6	19.5	0.113	0.102
TDRUN55	0.5	26.0	0.5	24.7	0.273	0.295	0.278	0.319	1.683	0.952	N/A	0.44	0.328	0.332	25.8	24.4	0.121	0.112

SECTION 6

INTERPRETATION OF EXPERIMENTAL RESULTS

6.1 Behavior of Isolation System in Weak Seismic Excitation

The sliding bearings (type T1, unfilled PTFE) delivered a coefficient of friction at high velocity of sliding f_{max}= 0.14. The isolation system has been designed for optimum performance in strong earthquake excitation. Therefore, it may be argued that this system might be ineffective in weak seismic excitations, such as the Japanese Level 1 motions. Figure 6-1 compares the recorded hysteresis loops in the piers of the non-isolated and isolated bridges (case of flexible piers) for the Japanese Level 1 motions. It is evident that the isolated bridge response is significantly less sensitive to the frequency content of the input than that of the non-isolated. Furthermore, drift and shear force in the piers of the isolated bridge are less so that inelastic pier behavior does not occur.

In another comparison of test results under weak excitation, Figure 6-2 shows the response of the isolated and non-isolated bridges in the Miyagiken Oki E-W motion. The isolated bridge is subjected to the actual earthquake motion (recorded table PGA=0.122g). The isolation system undergoes a very small, only 0.4 mm, displacement. Nevertheless, it effectively limits the transmission of force to the substructure, resulting in a pier shear force of 0.17 times the weight and pier drift ratio of 0.22%. The non-isolated bridge, which is subjected to 75% of the Miyagiken Oki E-W motion, develops a pier shear force equal to 0.24 times the weight and pier drift ratio equal to 0.38%. Thus, the isolated bridge experiences substructure forces and drifts which are about one half of those of the non-isolated bridge in a weak excitation.

The behavior of the isolation system may be explained as follows. In seismic excitation the isolation system provides resistance to motion at the bearing level for isolation system force F_I up to the limit

$$F_I = 2F_o + f_{min}W_d \tag{6-1}$$

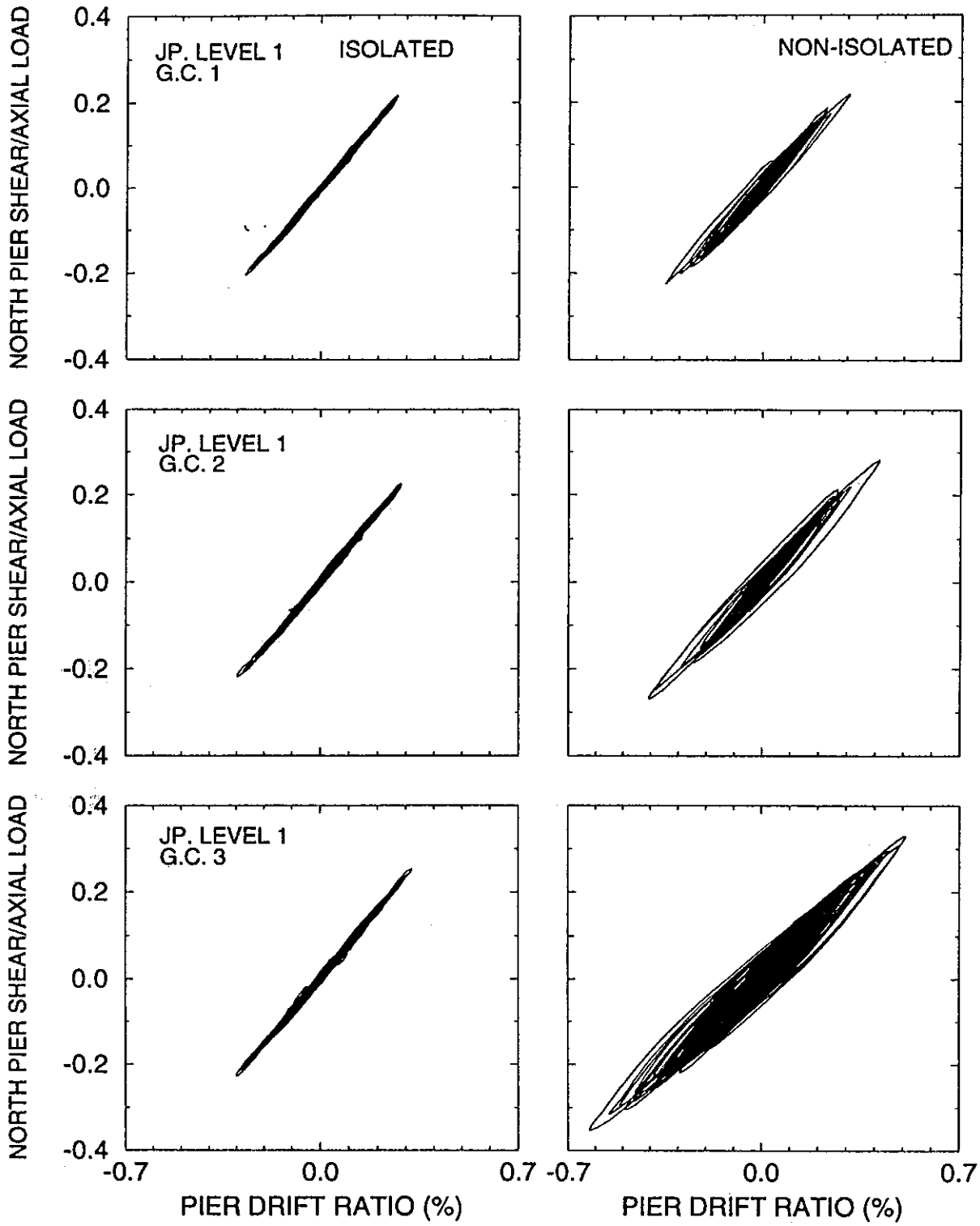

Figure 6-1 Comparison of Pier Response of Non-Isolated and Isolated Bridge Recorded in the Japanese Level 1 Motions.

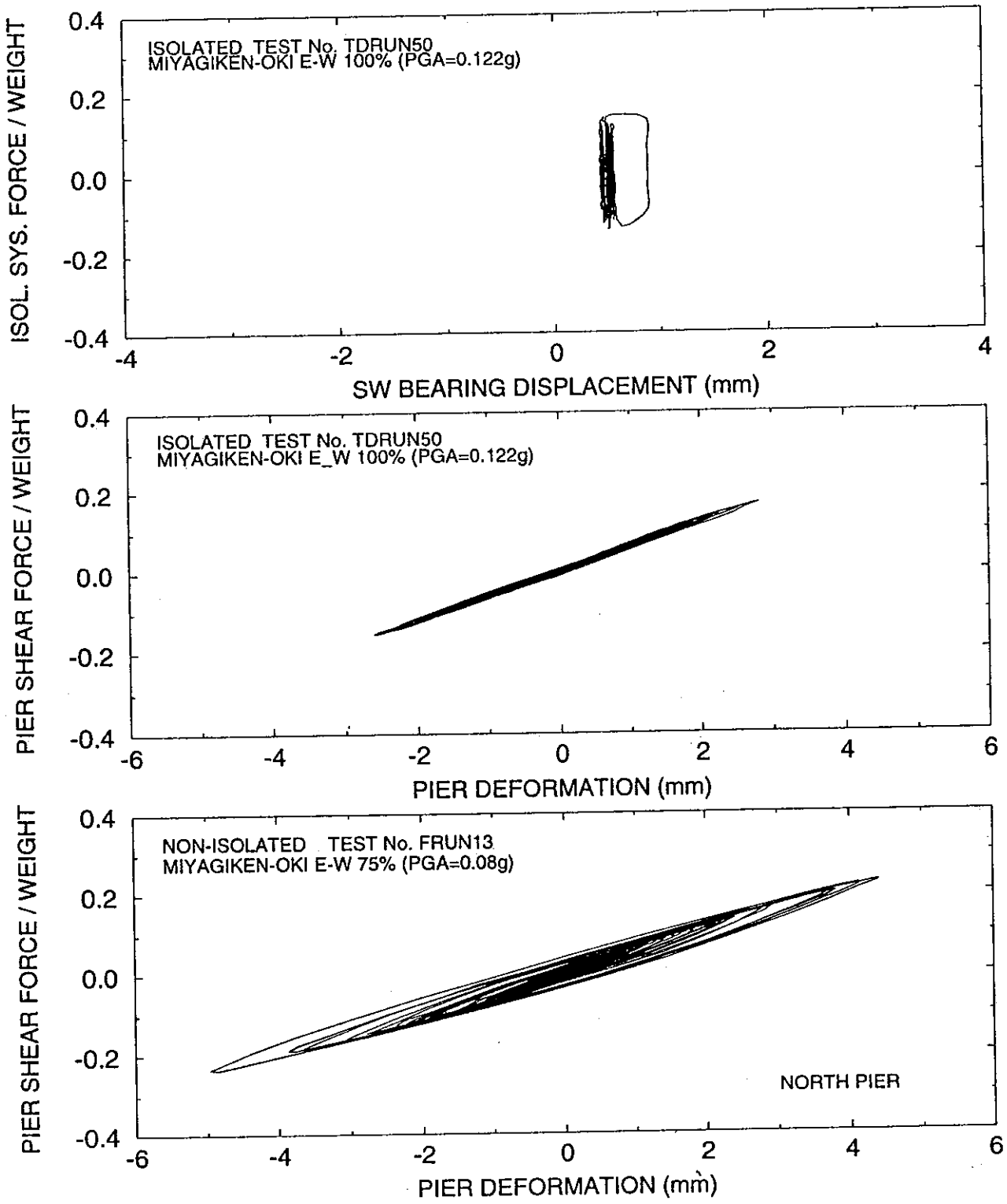

Figure 6-2 **Comparison of Response of Isolated and Non-Isolated Bridge in the Weak Miyagiken Oki E-W Motion.**

where F_o is the preload in one of the two restoring force/damping devices and W_d is the deck weight. Note that the frictional resistance is described by the coefficient f_{min} which is much less than f_{max}, the value at large sliding velocity. For the tested system F_1= 0.126 W_d. To reach this level of force at the isolation system it would require a ground acceleration of 0.126 g for infinitely stiff piers, or about 0.05 g for flexible piers (based on an average amplification factor of 2.5 - see Table 5-I). Thus, the system is activated even in weak seismic excitation.

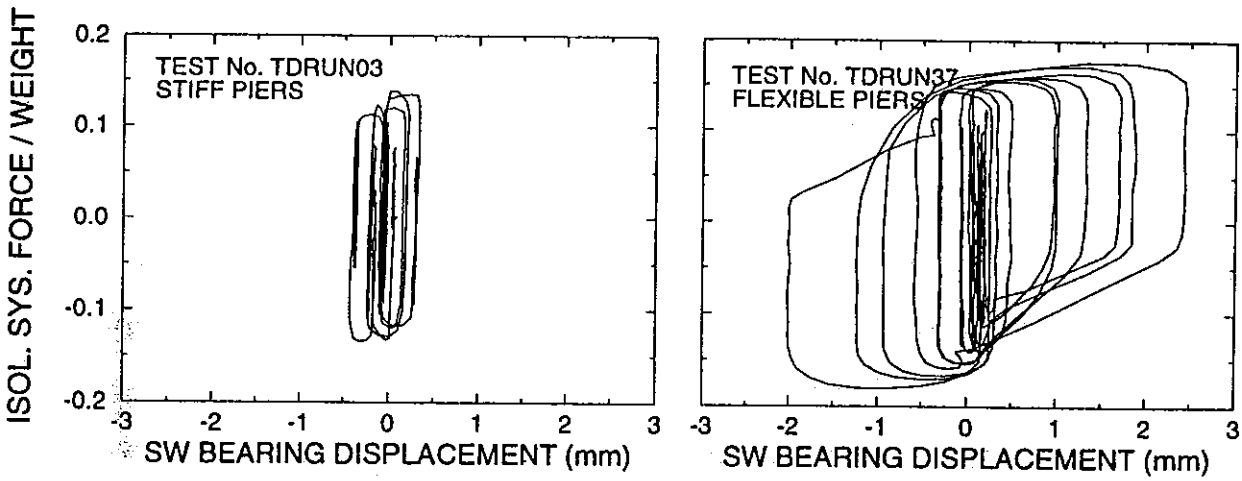

Figure 6-3 Comparison of Isolated System Force-Displacement Loops of Bridge with Stiff and with Flexible Piers in the Japanese Level 1, Ground Condition 1 Motion.

An example demonstrating this behavior is presented in Figure 6-3. The figure shows the isolation system force-displacement loops in the Japanese level 1, ground condition 1 motion, which has peak ground acceleration equal to about 0.1g (see Table 5-II). In the case of stiff piers, the ground acceleration is amplified to a sufficient level to induce some small amount of sliding. As seen in Figure 6-3 the peak force in the isolation system is about equal to 0.14 W_d. In the case of flexible piers, the ground acceleration is amplified and reaches at the pier top a value of 0.228g, which is significantly more than the critical value (0.126g) needed for sliding to initiate. The result is more sliding

displacement than the case of stiff piers. The peak force is $0.18W_d$ as compared to $0.14W_d$ in the case of stiff piers. The difference is primarily the result of higher friction force due to higher velocity of sliding in the case of flexible piers.

6.2 Behavior of Isolation System in Strong Seismic Excitation

A comparison of the response of the isolated bridge to that of the non-isolated bridge for the case of flexible piers is presented in Figure 6-4. The benefits of seismic isolation are evident. The response of the isolated bridge is maintained at a peak deck acceleration between 0.15 to 0.43g, and a peak pier shear force between 0.15 and 0.45 W_p (W_p=axial load carried by pier) for all tests. It should be noted that the input had peak acceleration between 0.1 and nearly 1g, with significantly varying content in frequency.

The tested isolated bridge remained elastic (theoretical yield limit equal to $0.5W_d$) while bearing displacements were maintained at less than about 50 mm (or 200 mm in prototype scale). In two tests No. TDRUN42 and TDRUN45, with excitation being the Japanese Level 2 Ground Condition 2 and Pacoima S16E signals, the displacements reached the maximum stroke of the devices (50 mm). In the first test the displacements demand exceeded by a small amount the capacity, whereas in the second test the displacement just reached the capacity. The difference between the two cases may be seen in the isolation system force loops, which are shown in Figure 6-5. This difference amounts a small sudden increase in the isolation system force due to impact of the piston head on the bottom of the cylinder of the restoring force/damping devices.

Figure 6-6 compares the response of the isolated bridge with stiff piers to that of the bridge with flexible piers in selected earthquakes. The bearing displacements in the bridge with flexible piers are systematically larger than those of the bridge with stiff piers. The same is true for the pier acceleration. Actually, the pier acceleration is always larger than the table acceleration. The amplification of the table acceleration in the piers is an expected phenomenon and it is related to the pier flexibility.

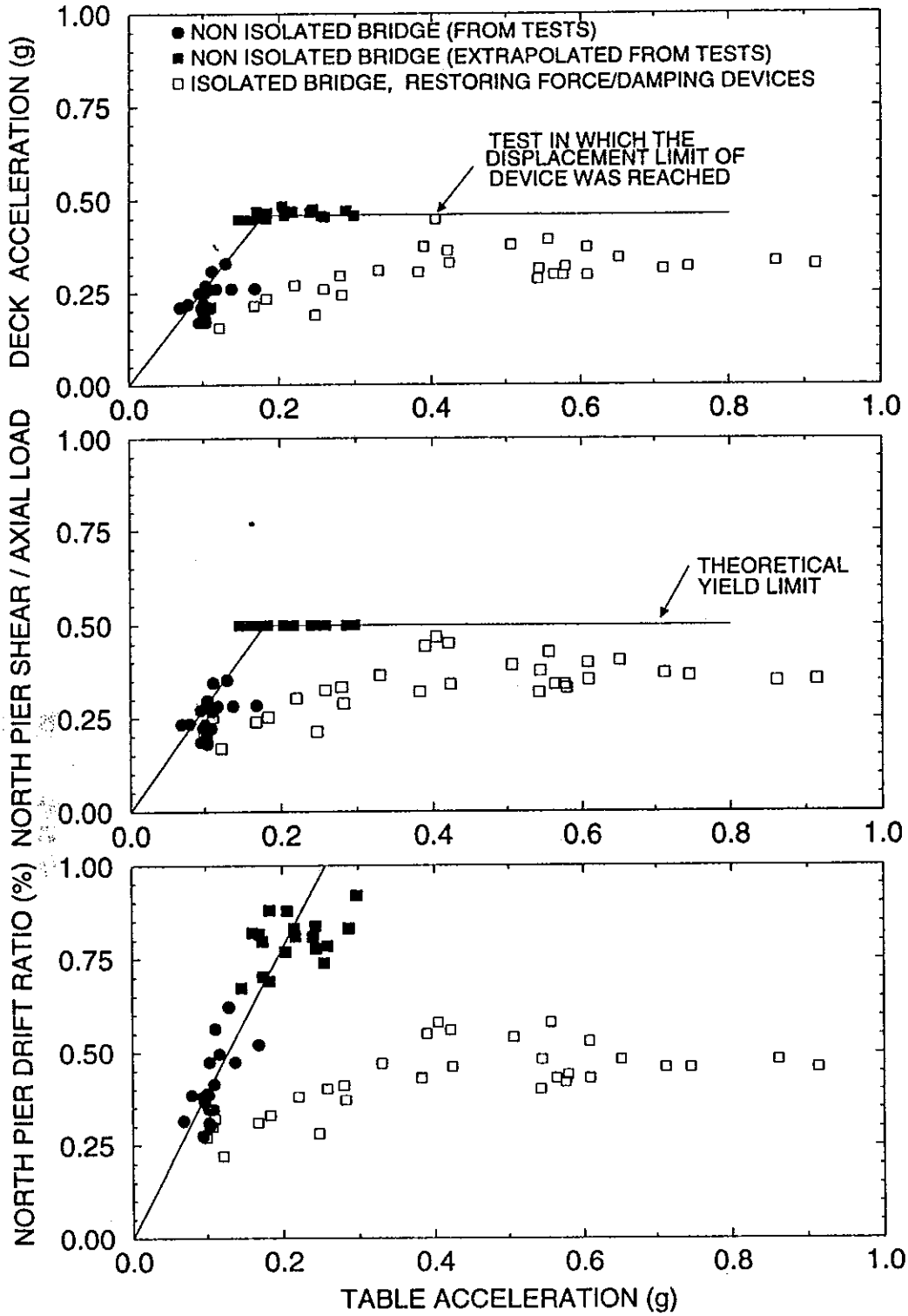

Figure 6-4 **Comparison of Response of Non-Isolated and Isolated Bridges. Case of Bridge with Flexible Piers.**

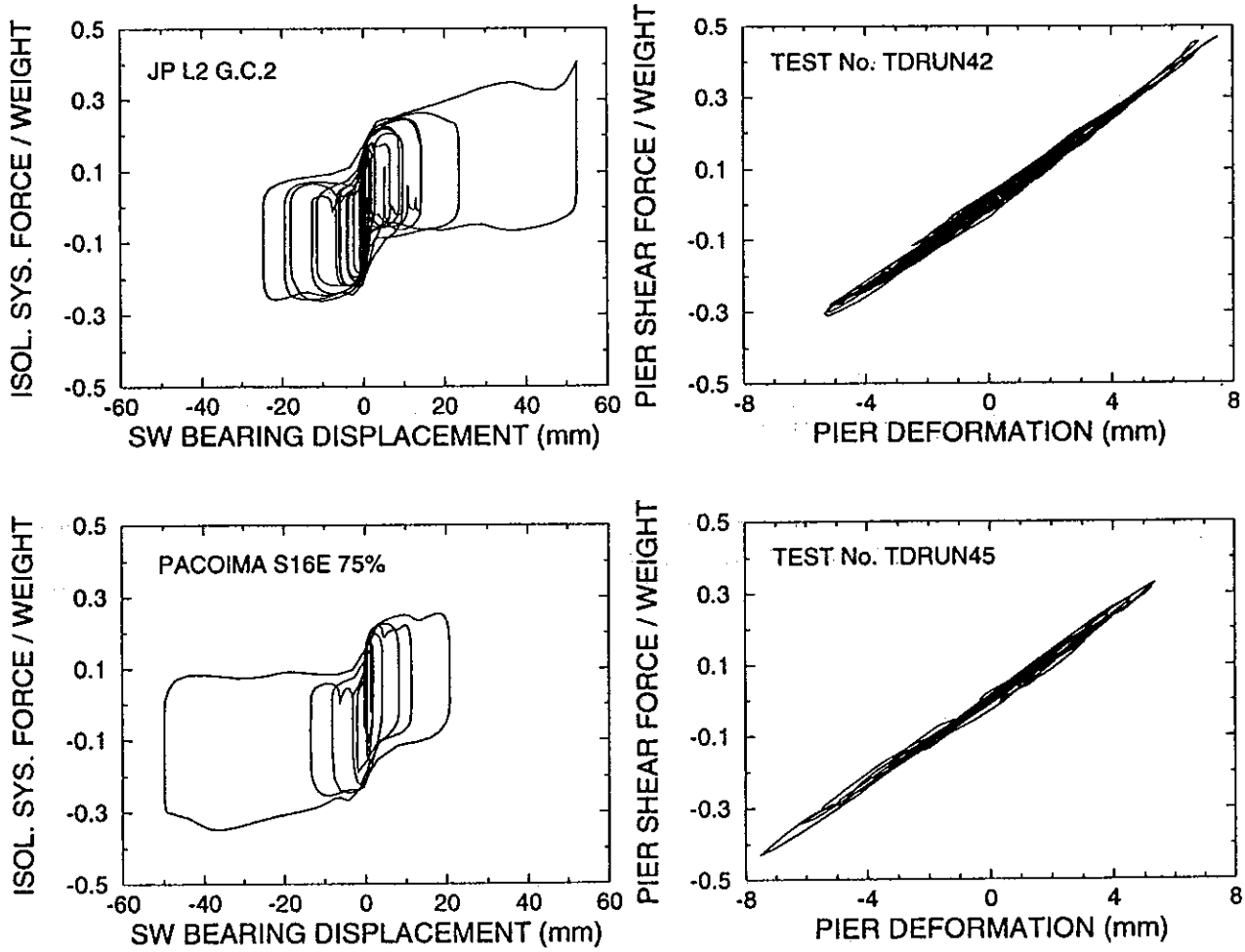

Figure 6-5 **Force-Displacement Loops of the Isolation System and Pier in Tests in which the Displacement Reached or Exceeded the Capacity of the Fluid Restoring Force/Damping Devices.**

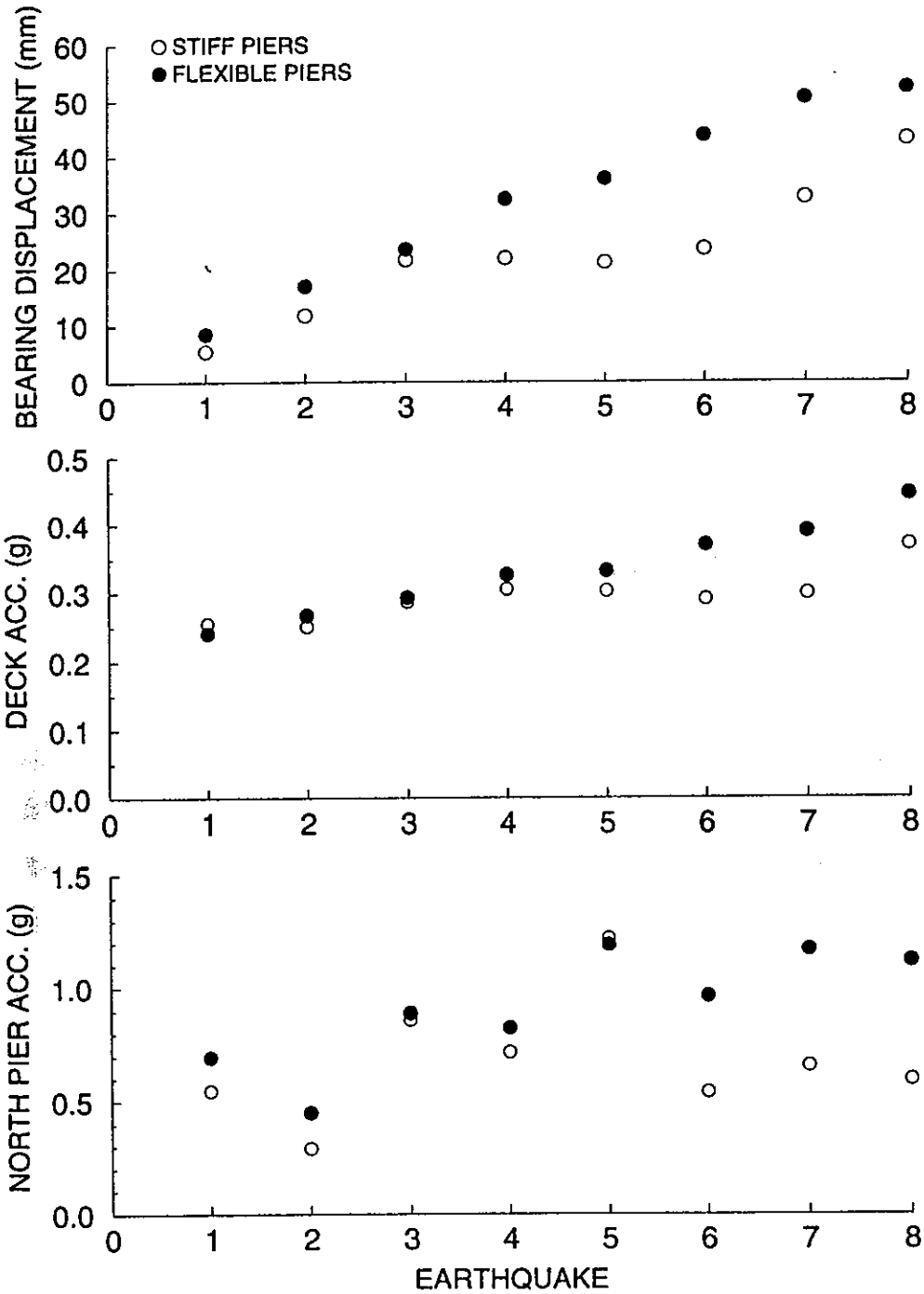

1 TAFT N21E 200% ; 2 MEXICO N90W 120% ; 3 CALTRANS ROCK 0.6g 100% ;
4 HACHINOHE N-S 200% ; 5 PACOIMA S74W 100% ; 6 JP. LEVEL 2 G.C.1 100% ;
7 PACOIMA S16E 75% ; 8 JP. LEVEL 2 G.C. 8 100%

Figure 6-6 Comparison of Response of Isolated Bridge with Stiff and Flexible Piers.

The effects of increasing intensity of seismic excitation on the response of the isolated bridge are illustrated in Figures 6-7 to 6-8, which depict the response of the isolated bridge with flexible piers and stiff piers respectively as a function of increasing intensity of earthquake input. The intensity of the excitation is represented by the peak table velocity, which is regarded as a better single measure of intensity of input than the peak table acceleration. This is because the response of isolated structures is primarily influenced by the amplitude and frequency content of the velocity domain of the response spectrum of the input. It may be observed that the acceleration and force responses of the isolated bridge are only marginally affected by the intensity of the input. Rather, we observe a noticeable effect of input intensity on the bearing displacement. However, the bearing displacement is always less than the table displacement (typically less than or about equal to half the table displacement, see Figures 6-7 and 6-8).

The experimental results demonstrated that, for the tested bridge, it was possible to restrict the isolation system displacement to within 200 mm in prototype scale and maintain elastic behavior of the piers provided that the piers are designed for a lateral force between 0.3 and 0.45 times the carried weight. On this we note that piers of isolated bridges in Japan are designed for seismic coefficient of at least 0.3 to avoid very flexible structures (CERC 1992). This minimum value of 0.3 includes the effect of inelastic pier behavior, that is reduction by factor $1/\sqrt{2\mu-1}$, where μ is the pier allowable ductility factor.

A different way of demonstrating the effectiveness of seismic isolation is by comparing the peak accelerations above and below the isolation bearings. The information used in this case is the one typically obtained from instrumented isolated bridges. A comparison of these accelerations for the tested bridge is provided in Figure 6-9. The comparison demonstrates the effectiveness of isolation in strong excitation. However, in weak excitation the acceleration above the bearings is nearly the same as the acceleration below the bearings. One may casually conclude that the isolation system was ineffective in weak excitation. However, the system performed better than the comparable non-isolated bridge in weak excitation (see Figures 6-1 and 6-2). Thus, the best way of demonstrating

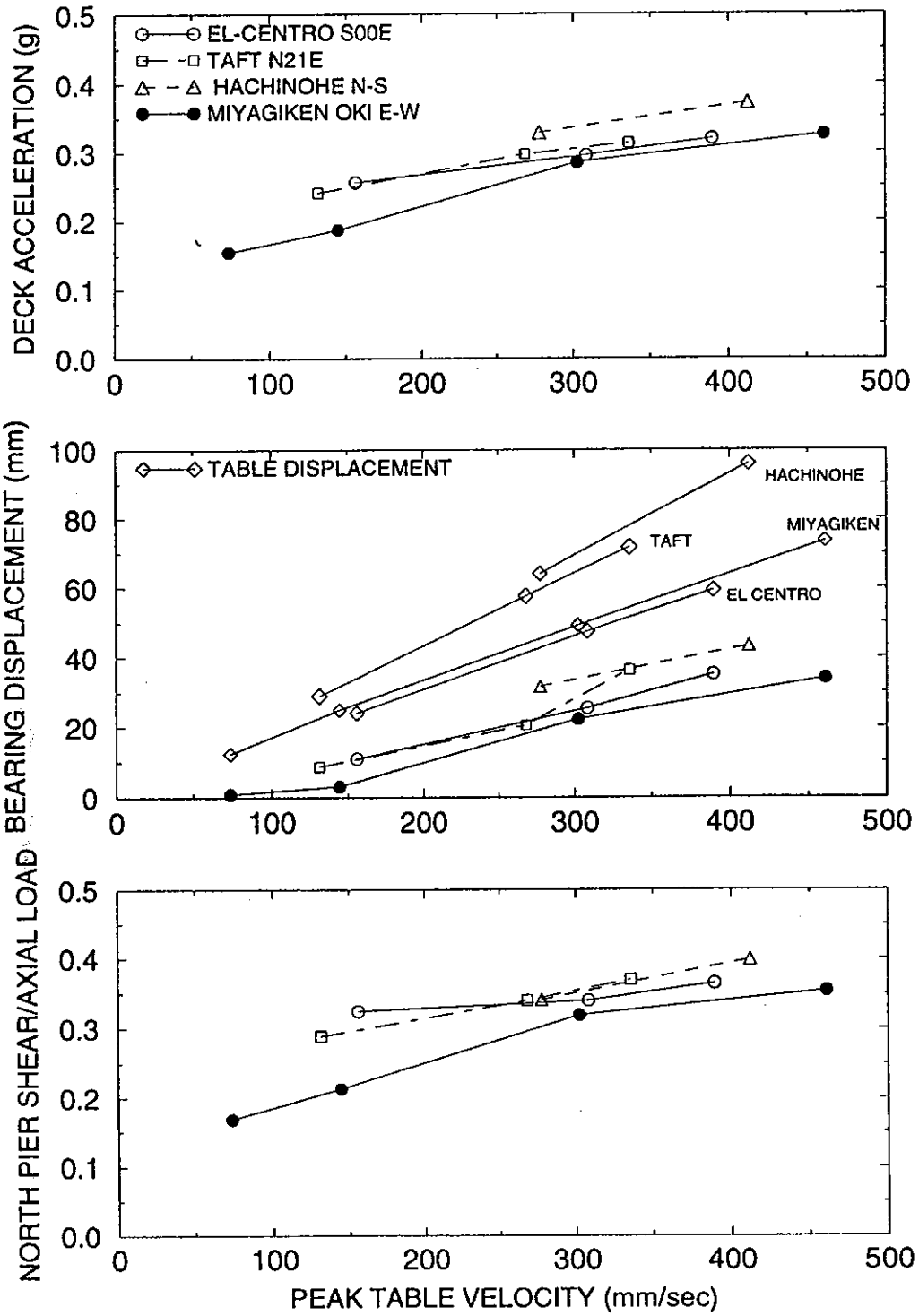

Figure 6-7 **Response of Isolated Bridge with Flexible Piers under Increasing Intensity of Input (Represented by Peak Table Velocity).**

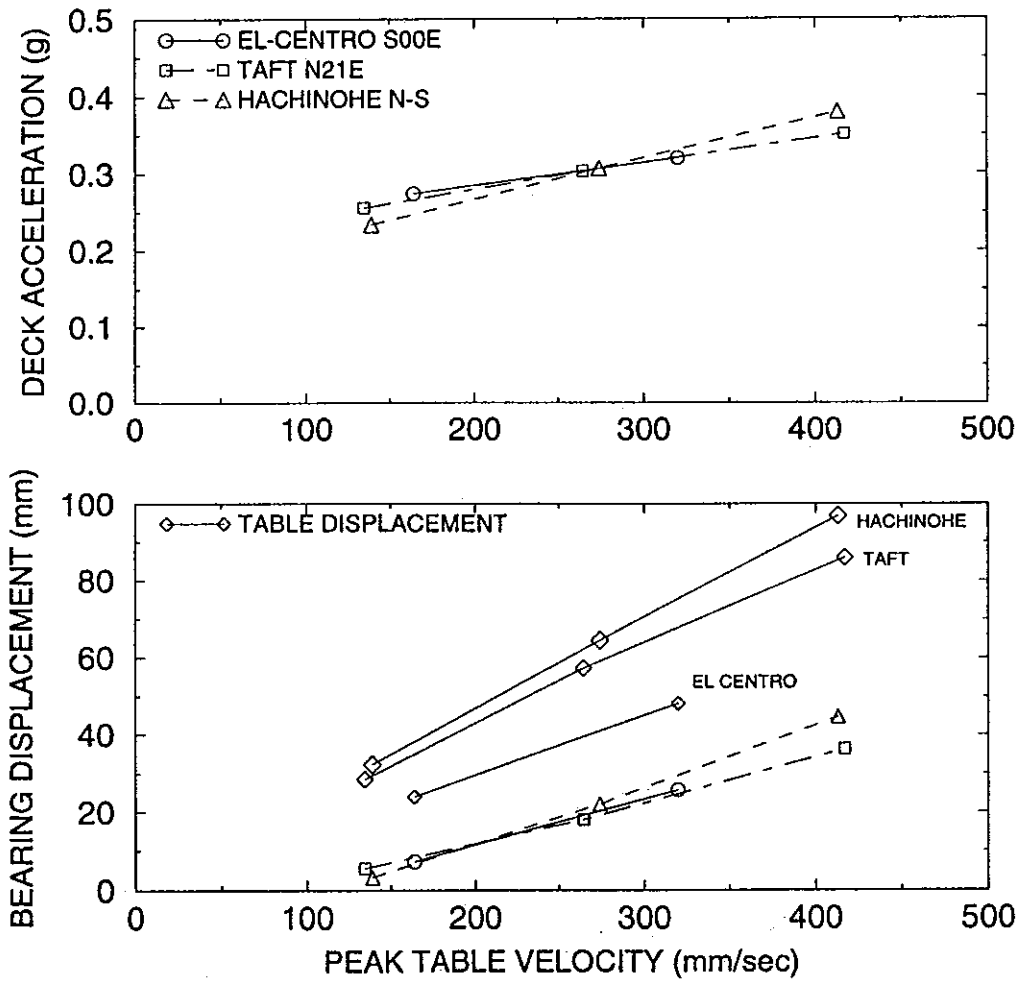

Figure 6-8 Response of Isolated Bridge with Stiff Piers under Increasing Intensity of Input (Represented by Peak Table Velocity).

effectiveness is by comparison to the case of the bridge without seismic isolation. One such comparison, in which the isolated bridge nearly reached the displacement capacity, is shown in Figure 6-10. Even under this extreme condition, the isolated bridge develops substructure forces and drifts which are comparable to those of the non-isolated bridge, except that the input motion is five times stronger.

Another similar comparison is presented in Figure 6-11. The isolated bridge undergoes nearly the same response as the non-isolated bridge, except that the input is about eight times stronger.

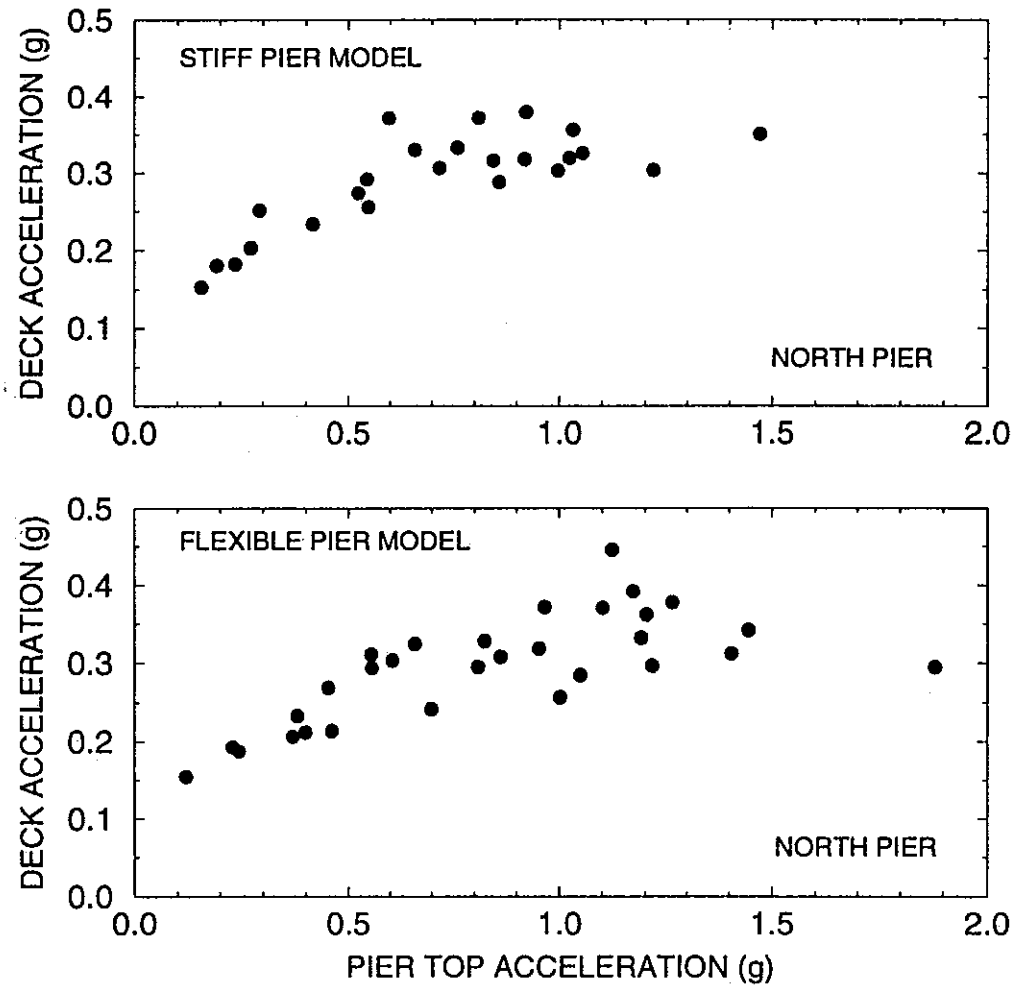

Figure 6-9 **Comparison of Deck Acceleration (Acceleration above Bearings) to Pier Top Acceleration (Acceleration below Bearings).**

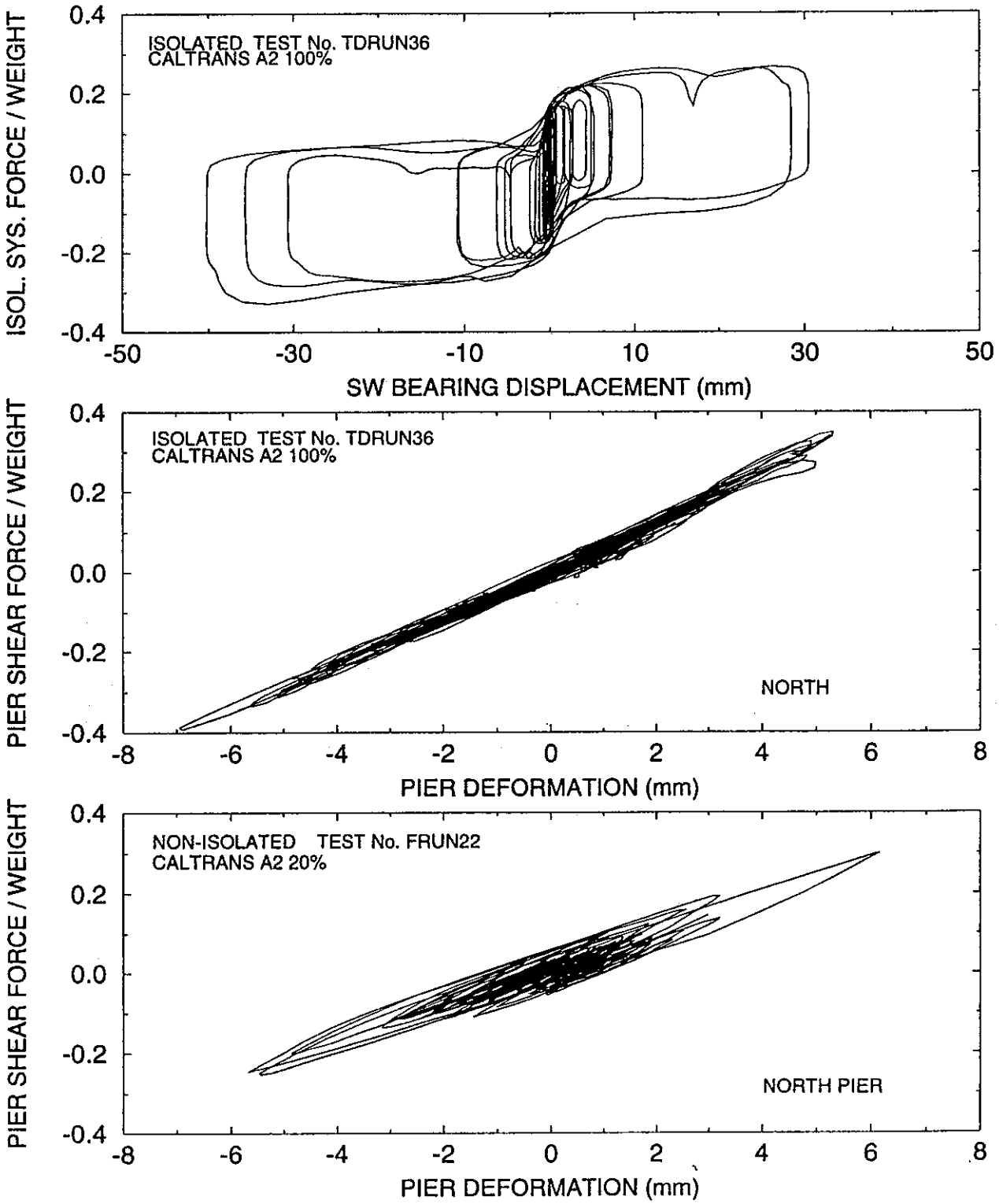

Figure 6-10 **Comparison of Non-Isolated and Isolated Bridge Response. Note that Displacement of Isolated Bridge Nearly Reaches Capacity. Responses are Nearly the Same for Input Being Five Times Stronger in the Isolated Case.**

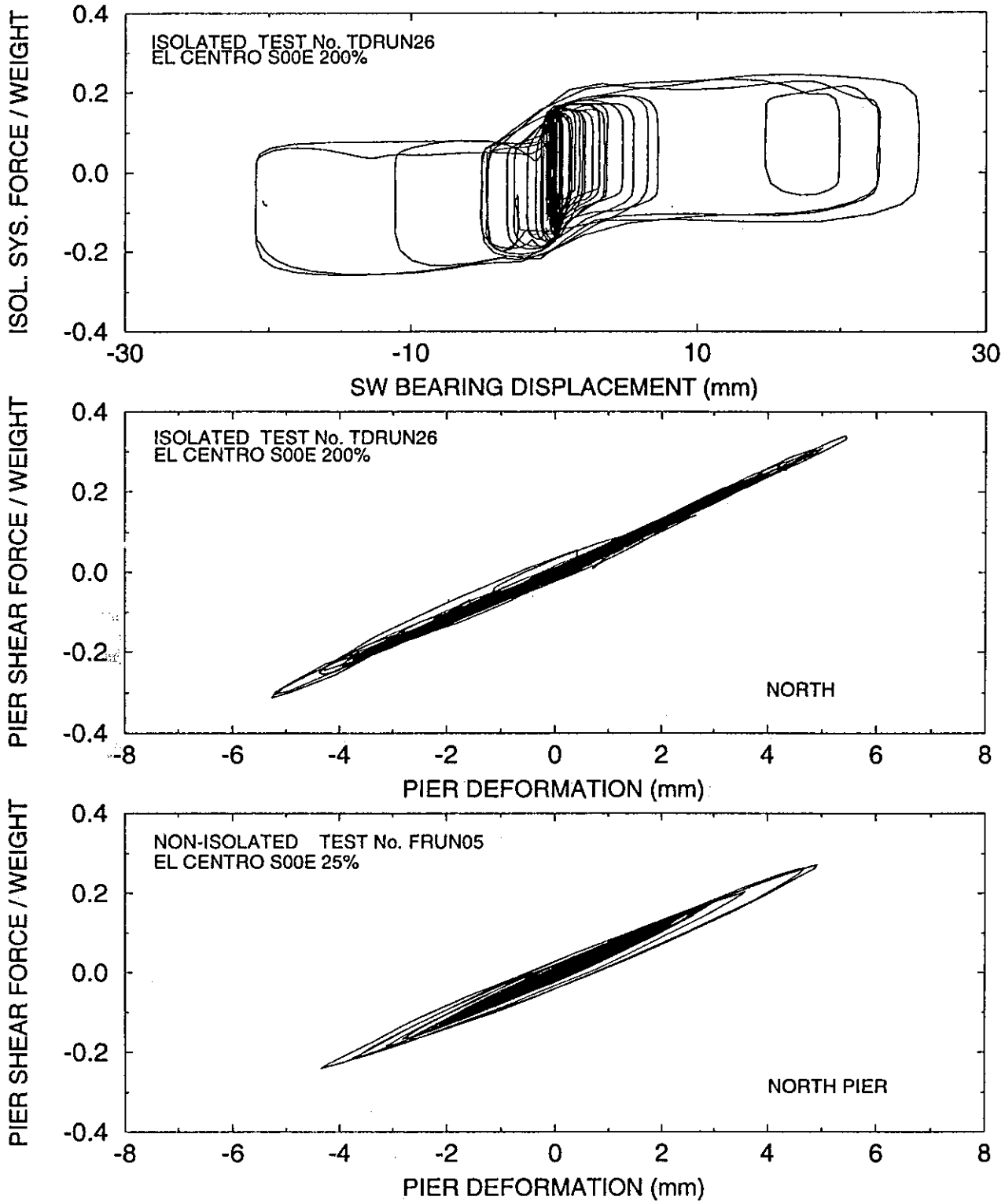

Figure 6-11 **Comparison of Non-Isolated and Isolated Bridge Response in the El Centro S00E Motion. Responses are Nearly the Same for Input Being Eight Times Stronger in the Isolated Case.**

6.3 Effect of Vertical Ground Motion

Tests were conducted with only horizontal and with combined horizontal-vertical input. Even when only horizontal input was applied, the overhangs of the shake table (see Figure 4-1) underwent significant vertical motion. As seen in Figure 6-12, the vertical accelerations at the north and south piers in the case of only horizontal input were out-of-phase with peak values about equal to 1/3 the peak horizontal table acceleration. In the case of combined horizontal-vertical input, the pier vertical accelerations were either out-of-phase or in-phase with peak values between 1/2 and 2/3 of the peak horizontal table acceleration.

Despite the severity of vertical input in the combined horizontal-vertical input, the response of the isolated bridge was only marginally affected. For example, Figures 6-13 and 6-14 compare the responses of the system to the Taft 400% and El Centro 200% motions, respectively. Other than the wavy form of the loops in the case of combined horizontal-vertical input, the vertical motion had either minor or no effect on the peak response of the tested system.

6.4 Permanent Displacements

The permanent displacements were recorded in all tests and are listed in Table 5-III. The initial displacement (that is, the permanent at the start of each experiment) was monitored in all tests. The bridge was never recentered prior to conducting a test. It may be observed in the result of Table 5-III that the permanent displacements are very small. The maximum recorded permanent displacement is 0.6 mm, a value within the range of connection tolerances and instrument errors. Practically, the permanent displacements were zero. Of course, this was expected since the isolation system was designed with sufficient preload to prevent the occurrence of permanent displacements.

The 1991 AASHTO, Section 12.2 requires that isolation systems are configured to have sufficient restoring force. Specifically, AASHTO requires that the lateral force at the design displacement is at least 0.025 W_d (W_d=supported weight) greater than the lateral force at 50 percent of the design displacement. This definition of sufficient restoring force

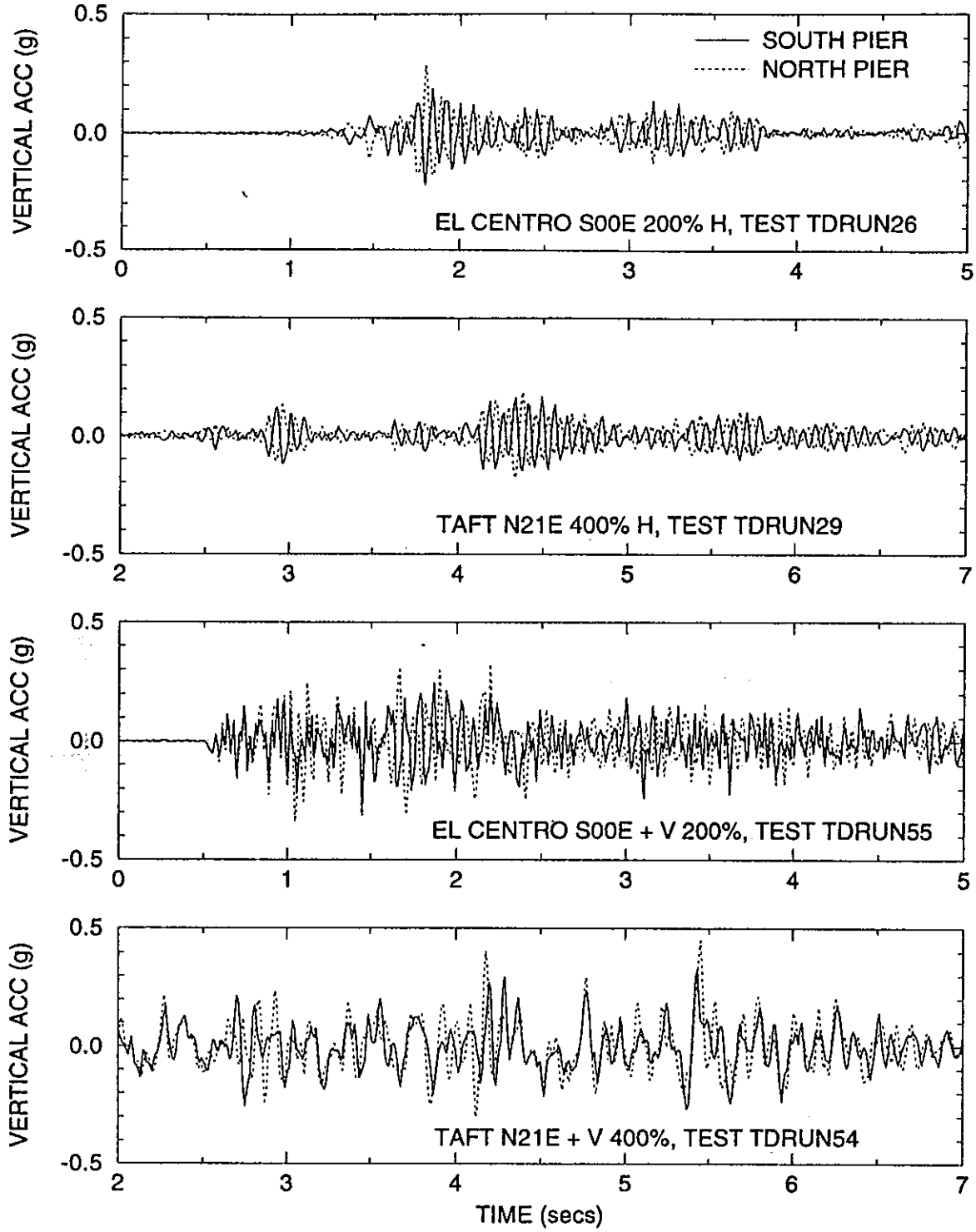

Figure 6-12 Recorded Vertical Acceleration at the Base of Piers in Tests with only Horizontal and with Combined Horizontal-Vertical Excitation.

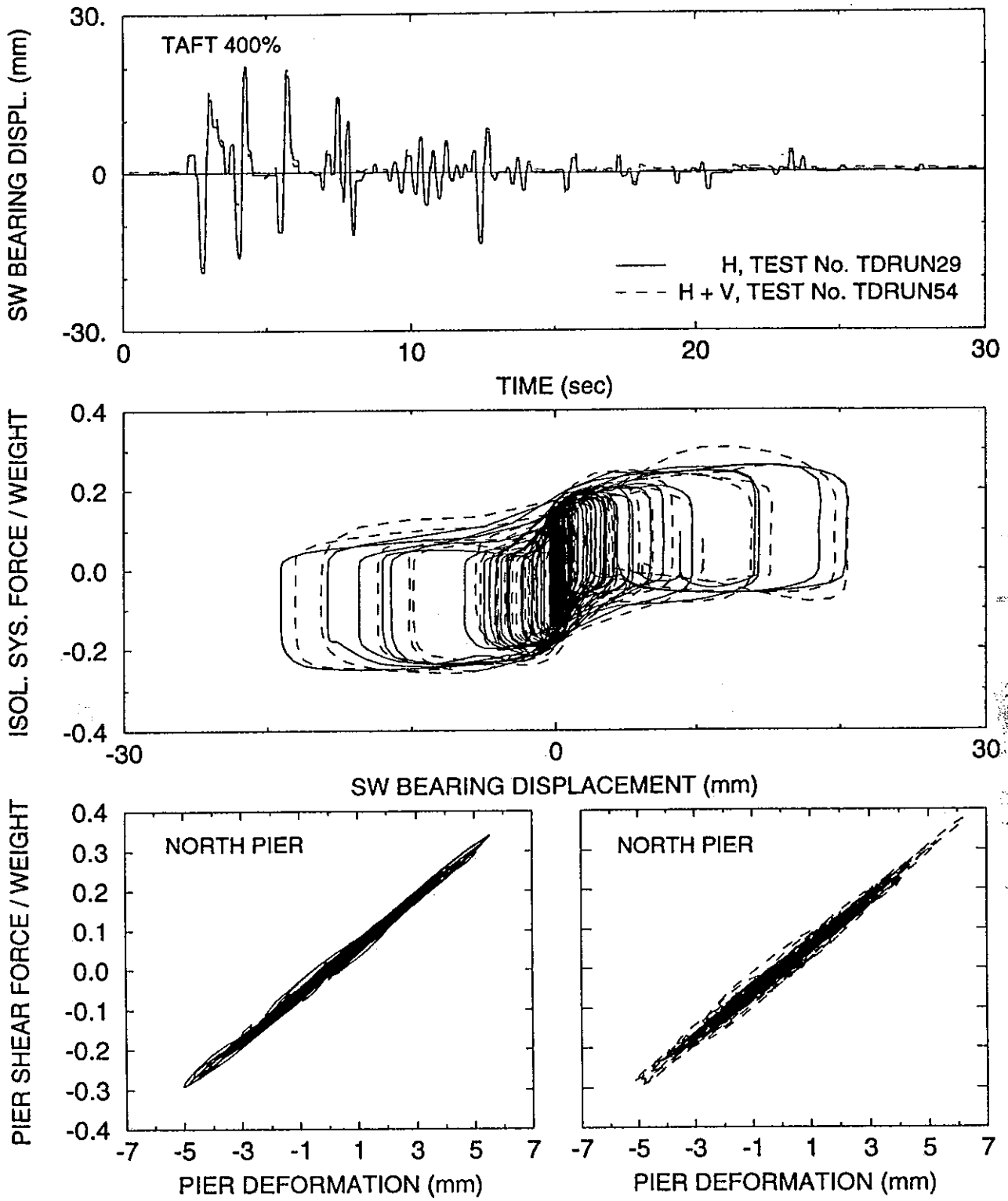

Figure 6-13 Effect of Vertical Ground Motion on Response of System Subjected to Taft 400% Input.

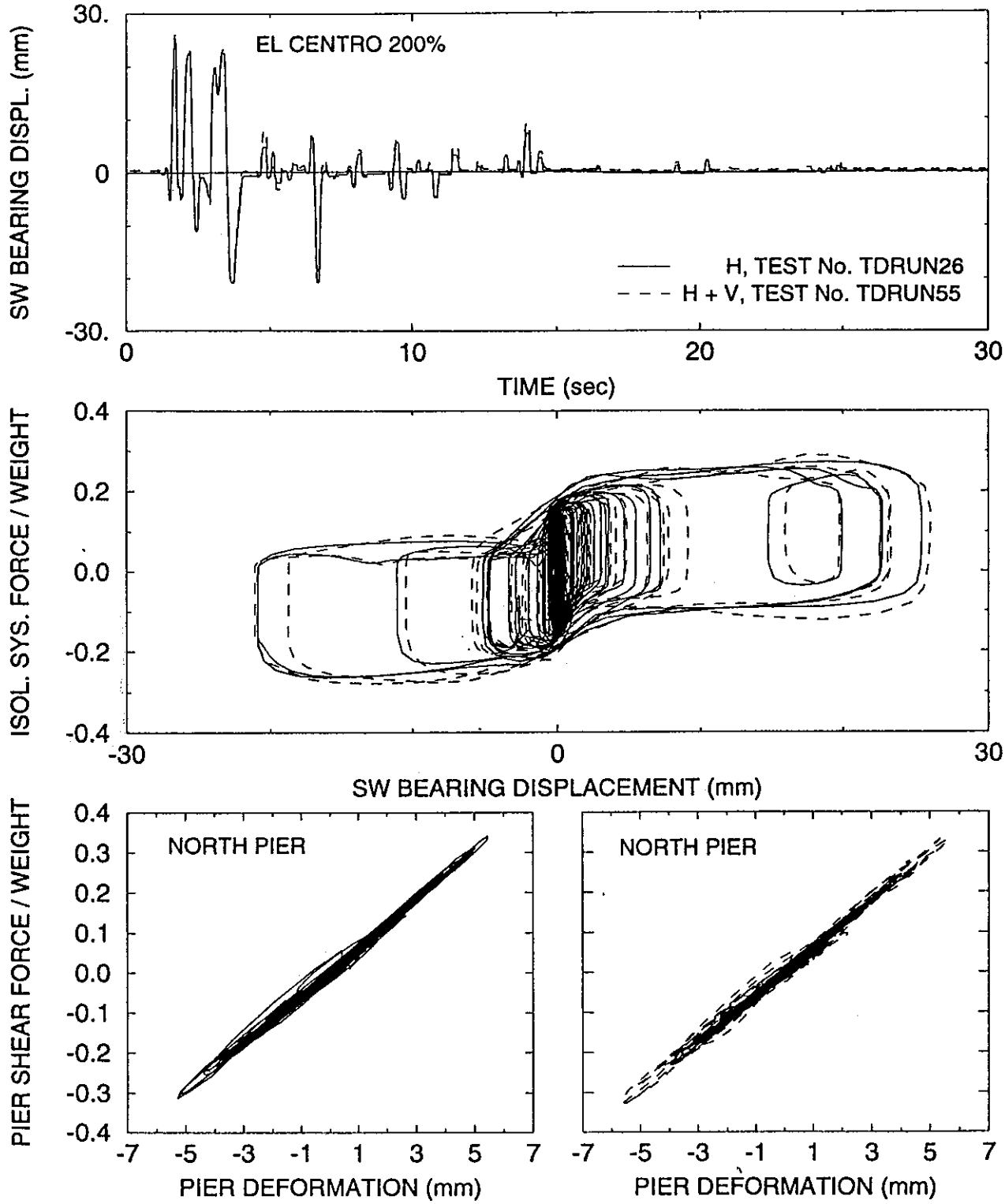

Figure 6-14 Effect of Vertical Ground Motion on Response of System Subjected to El Centro 200% Input.

by AASHTO is based on the assumption of spring-like restoring force, that is restoring force which is proportional to the displacement. However, a device with preload may provide restoring force which is independent of displacement. As demonstrated by the tests reported herein, such designs provide sufficient restoring force for recentering the bridge and eliminating permanent displacements.

We conclude that the AASHTO requirements for minimum restoring force are not generally valid. In addition to the case of preload which is not covered by the AASHTO specifications, Tsopelas, 1994 addressed the issue of the relation between restoring force and characteristic strength of isolation systems. It appears that Section 12.2 of the 1991 AASHTO requires a revision.

SECTION 7

ANALYTICAL PREDICTION OF RESPONSE

7.1 Introduction

Analytical techniques for predicting the dynamic response of sliding isolation systems are available (Mokha 1988, 1990b and 1991; Constantinou 1990a, 1990b, 1991a 1991b and 1993, Tsopelas 1994). These analytical techniques are employed herein in the prediction of the response of the tested bridge model. The analytical model accounts for the pier flexibility, pier top rotation, vertical motion effects on the properties of the sliding bearings, and characteristics of the restoring force/damping devices.

7.2 Analytical Model

Figure 7-1 shows the analytical model in the case of the bridge with flexible piers. The degrees of freedom are selected to be the deck displacement with respect to the table, U_d, the pier displacements with respect to the table, U_{p1} and U_{p2}, and the pier rotations, ϕ_{p1} and ϕ_{p2}.

Each pier is modeled by a beam element of length L_i, moment of inertia I_i and modulus of elasticity E_i (i=1 or 2). The beam element is fixed to the table and connected at its top to a rigid block of height h, mass m_{pi} and mass moment of inertia about the center of mass (C.M.) I_{pi}. The center of mass is located at distance h_i from the bottom of the block. This block represents the pier top.

Free body diagrams of the deck and pier tops of the bridge model are shown in Figure 7-2. It should be noted that it was assumed that there is no transfer of moment between the deck and the supporting pier top. In reality, there is transfer of moment due to the rotational stiffness of the supporting disc of the sliding bearings. The equations of motion are derived by consideration of dynamic equilibrium of the deck and piers in the horizontal direction and of the piers in the rotational direction :

$$m_d(\ddot{U}_d + \ddot{U}_g) + F_{b1} + F_{b2} = 0 \qquad (7\text{-}1)$$

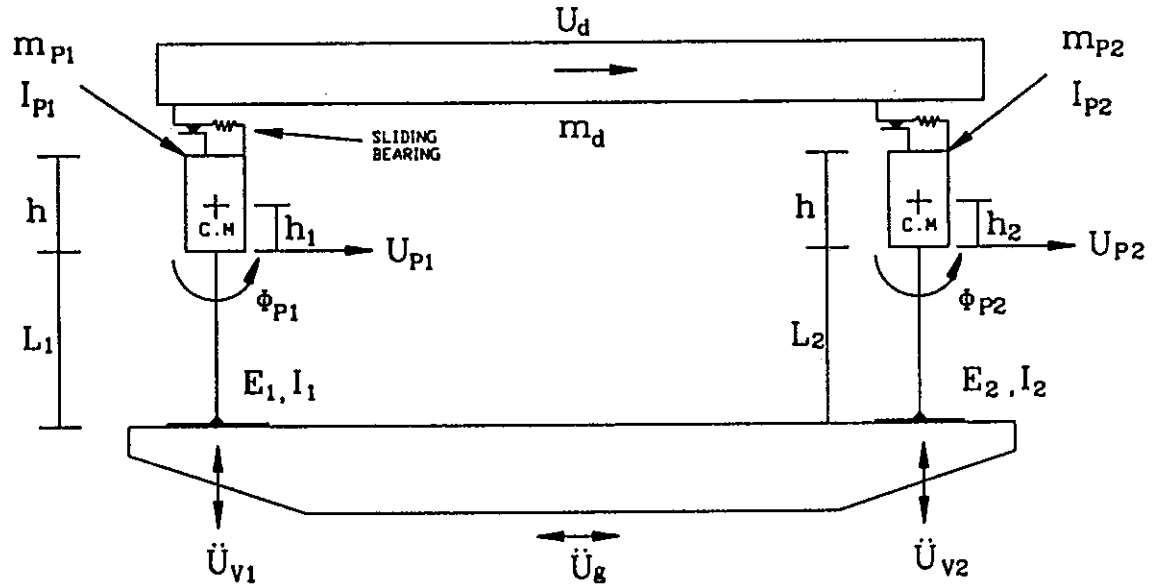

Figure 7-1 Longitudinal Direction Model of Isolated Bridge.

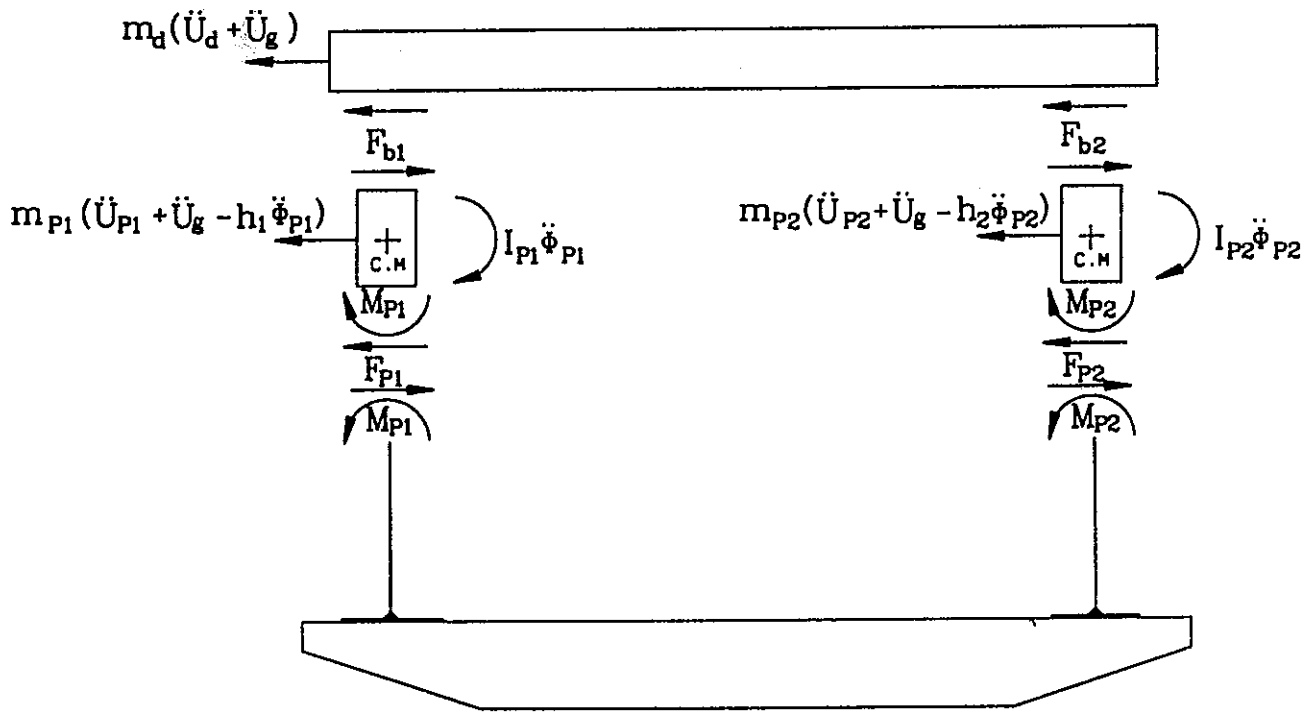

Figure 7-2 Free Body Diagram of Bridge Model.

$$m_{p1}(\ddot{U}_{p1}+\ddot{U}_g-h_1\ddot{\phi}_{p1})+F_{p1}-F_{b1}=0 \tag{7-2}$$

$$m_{p2}(\ddot{U}_{p2}+\ddot{U}_g-h_2\ddot{\phi}_{p2})+F_{p2}-F_{b2}=0 \tag{7-3}$$

$$I_{p1}\ddot{\phi}_{p1}+M_{p1}+F_{p1}h_1+F_{b1}(h-h_1)=0 \tag{7-4}$$

$$I_{p2}\ddot{\phi}_{p2}+M_{p2}+F_{p2}h_2+F_{b2}(h-h_2)=0 \tag{7-5}$$

where $\ddot{U}_g$ is the horizontal table (ground) acceleration, F_{b1} and F_{b2} are the lateral forces in the isolation system (sliding bearings and restoring force/damping devices), and F_{pi} and M_{pi} are the lateral force and bending moment at the connection of the pier top to the end of the column:

$$\begin{Bmatrix} F_{pi} \\ M_{pi} \end{Bmatrix} = E_i I_i \begin{bmatrix} \frac{12}{L_i^3} & \frac{6}{L_i^2} \\ \frac{6}{L_i^2} & \frac{4}{L_i} \end{bmatrix} \begin{Bmatrix} U_{pi} \\ \phi_{pi} \end{Bmatrix} + \begin{bmatrix} C_{pi}^1 & 0 \\ 0 & C_{pi}^2 \end{bmatrix} \begin{Bmatrix} \dot{U}_{pi} \\ \dot{\phi}_{pi} \end{Bmatrix} \tag{7-6}$$

The first part of Equation (7-6) describes the elastic forces, whereas the second part is used to account for linear viscous energy dissipation in the piers.

Forces F_{bi} (i=1,2) include a component from friction in the sliding bearings and a component from the restoring force/damping devices. These forces are described as follows:

$$F_{bi}=\mu_i(\dot{U}_{bi})W_i^*Z_i+F_{ti} \tag{7-7}$$

where μ_i = coefficient of sliding friction at pier i, W_i^* = normal load on two sliding interfaces at pier i and F_{ti} = force from the restoring force/damping device at pier i. Furthermore, U_{bi} is the bearing displacement at pier i:

$$U_{bi}=U_d-U_{pi}+h\phi_{pi} \tag{7-8}$$

The coefficient of sliding friction follows the relation (Constantinou 1990a, see also Section 3)

$$\mu_i=f_{\max i}-(f_{\max i}-f_{\min i})\exp(-a_i|\dot{U}_{bi}|) \tag{7-9}$$

with parameters f_{maxi}, f_{mini} and a_i (i =1,2) listed in Table 3-I. The normal load, W_i^*, is given by

$$W_i^* = W_i\left(1+\frac{\ddot{U}_{vi}}{g}\right) \tag{7-10}$$

where W_i = weight carried by pier i and $\ddot{U}_{vi}$ is the table (ground) vertical acceleration of pier i. Furthermore, variable Z_i in Equation (7-7) satisfies the following equation (Constantinou 1990a):

$$Y_i\dot{Z}_i + \gamma|\dot{U}_{bi}|Z_i|Z_i| + \beta\dot{U}_{bi}Z_i^2 - \dot{U}_{bi} = 0 \tag{7-11}$$

In this equation, Y_i= "yield" displacement (=0.25 mm) and β and γ = parameters satisfying the condition $\beta+\gamma=1$.

7.3 Analytical Model for Fluid Restoring Force/Damping Devices

The force in a restoring force/damping device consists of a preload, the restoring force, the friction force at the seal and the fluid damping force. Section 3.3 presents a discussion on the origin of the components and Figure 3-7 illustrates these components. The four components may be mathematically expressed as follows:

$$F_t = F_o[1-\exp(-\delta|u|)]sgn(u) + K_o u + [F_{\min} + \zeta K_o|u|]Z_t + F_d sgn(\dot{u}) \tag{7-12}$$

$$F_d = \begin{cases} F_1(\dot{u}) & \text{when } u\dot{u} > 0 \\ F_2(\dot{u}) & \text{when } u\dot{u} < 0 \end{cases} \tag{7-13}$$

in which F_o is the preload, K_o is the stiffness, $F_{\min}$ is the seal friction at zero displacement and F_d is the fluid damping force, which is dependent on velocity and direction of motion. Furthermore, Z_t is a hysteretic variable governed by an equation identical to Equation 7-11, u is the device displacement and $\dot{u}$ is the device velocity (actually displacement and velocity of one end of the device with respect to the other end).

The term $\zeta K_o|u|$ accounts for increased friction in the seal as a result of increased internal pressure during stroking. The seal typically consists of very soft material that cold flows under the internal pressure to seal microscopic surface finish patterns. Thus as pressure increases during stroking, so does friction. Herein we use a linearly increasing friction force based on the experimental results. Furthermore, we selected a linear restoring force ($K_o u$) as an acceptable approximation to the actual condition, which has a

mild nonlinear behavior. The physical origin of this nonlinearity has been explained in Section 3.3.

The preload term should, for ideal conditions, be represented by a term $F_o sgn(u)$. In reality, the stiffness of the device is not infinitely large at zero displacement. Rather, it is dependent on the velocity of motion of the piston rod. This behavior is accounted for in the model by the exponential term for the preload $F_p = F_o[1 - \exp(-\delta|u|)]sgn(u)$, in which δ is a function of velocity. The experimental results suggest an exponential form for variable δ :

$$\delta = \delta_o \exp(-\delta_1 |\dot{u}|) \tag{7-14}$$

It is easily shown that the slope dF_p/du at zero displacement is equal to $F_o\delta$. It is, thus, only dependent on velocity.

The damping force is accounted for by the dual term of Equation 7-13. This difference in behavior is due to the utilization of lower orifice area when stroke increases than when it decreases. Approximate expressions for the damping forces F_1 and F_2 are

$$F_j = F_{\max j}[1 - \exp(-\varepsilon_j |\dot{u}|)] \quad , j = 1, 2 \tag{7-15}$$

This expression was found to be appropriate for the tested device and for velocity up to about 500 mm/sec. A limitation of this expression is that it predicts constant damping force at large velocities, which is apparently incorrect. An alternative expression, which could account for the actual behavior at velocities beyond the range of testing, is

$$\underset{j=1,2}{F_j} = \begin{cases} C_{j1}|\dot{u}| & \text{when } |\dot{u}| \le \dot{u}_1 \\ C_{j1}\dot{u}_1 + C_{j2}(|\dot{u}| - \dot{u}_1)^{a_j} & \text{when } |\dot{u}| > \dot{u}_1 \end{cases} \tag{7-16}$$

with $\dot{u}_1$ equal to about 50 mm/sec and a_j equal to about 0.3.

The various parameters in the model of Equations 7-12 to 7-15 are illustrated in Figure 7-3. The values of the parameters for the tested device are given in Table 7-I. Figure 7-4 compares the predictions of the calibrated model of Equations 7-12 to 7-15 to experimental results. The tests consisted of static and dynamic sinusoidal tests at specified

frequency and amplitude. It may be seen that the model is capable of representing the behavior of the device with very good accuracy.

Table 7-I Parameters in Calibrated Model of Fluid Restoring Force/Damping Device

Parameter	Value
F_o (kN)	4.72
F_{min} (kN)	0.20
F_{max1} (kN)	4.50
F_{max2} (kN)	2.90
K_o (kN/mm)	0.095
δ_o (mm^{-1})	1.78
δ_1 (sec/mm)	0.00385
ε_1 (sec/mm)	0.007
ε_2 (sec/mm)	0.005
ζ (-)	0.0618

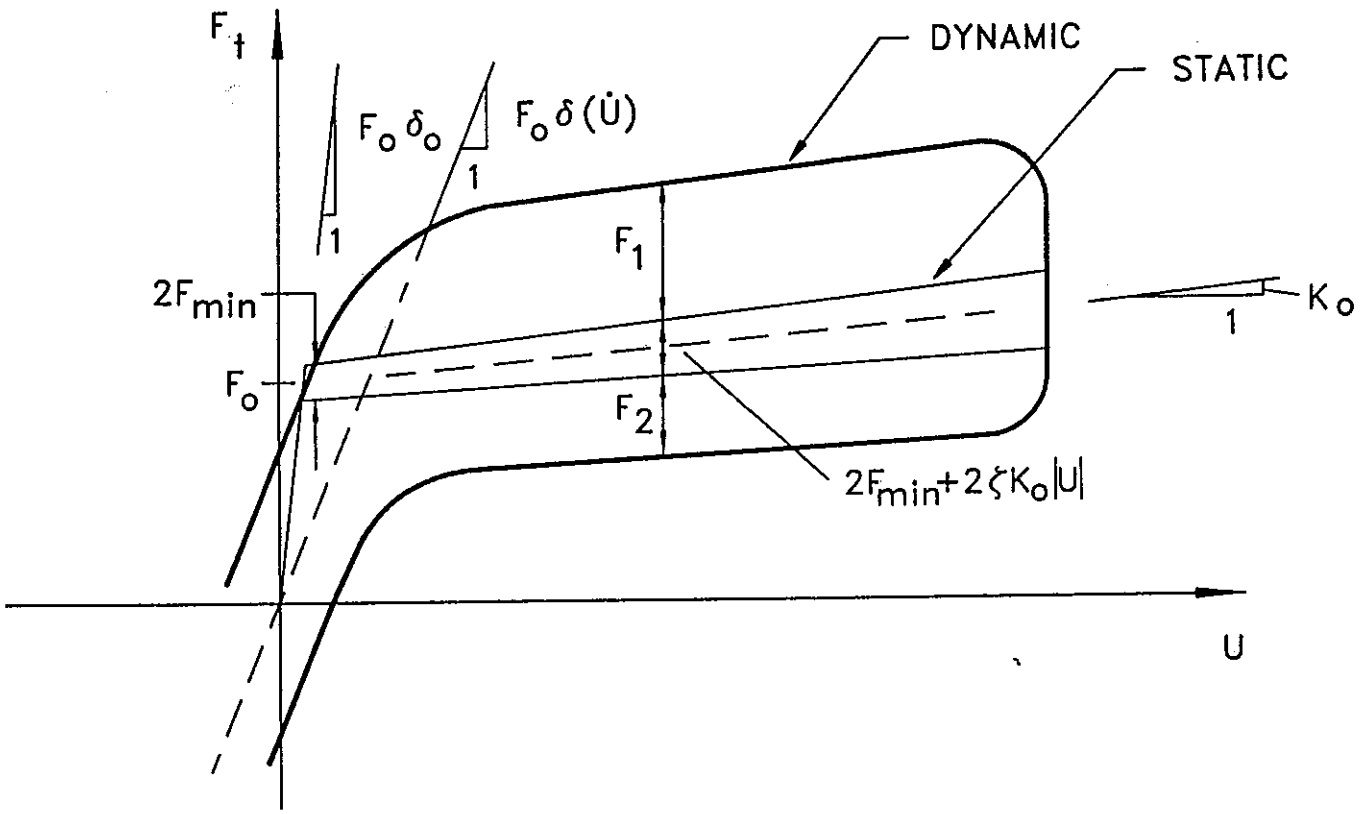

Figure 7-3 Definition of Terms in Model of Fluid Restoring Force/Damping Device.

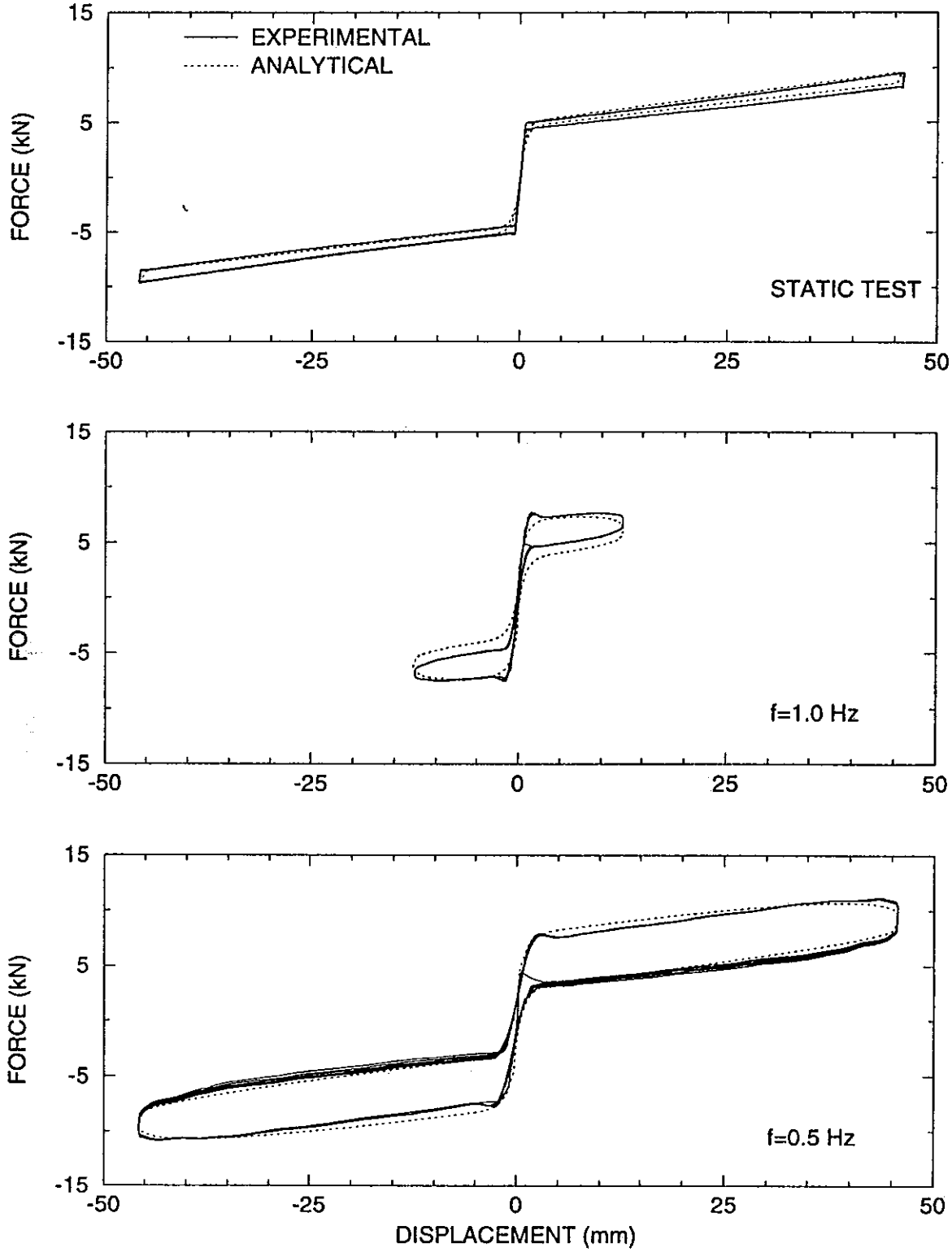

Figure 7-4 Comparison of Experimental and Analytical Force-Displacement Loops of Fluid Restoring Force/Damping Device.

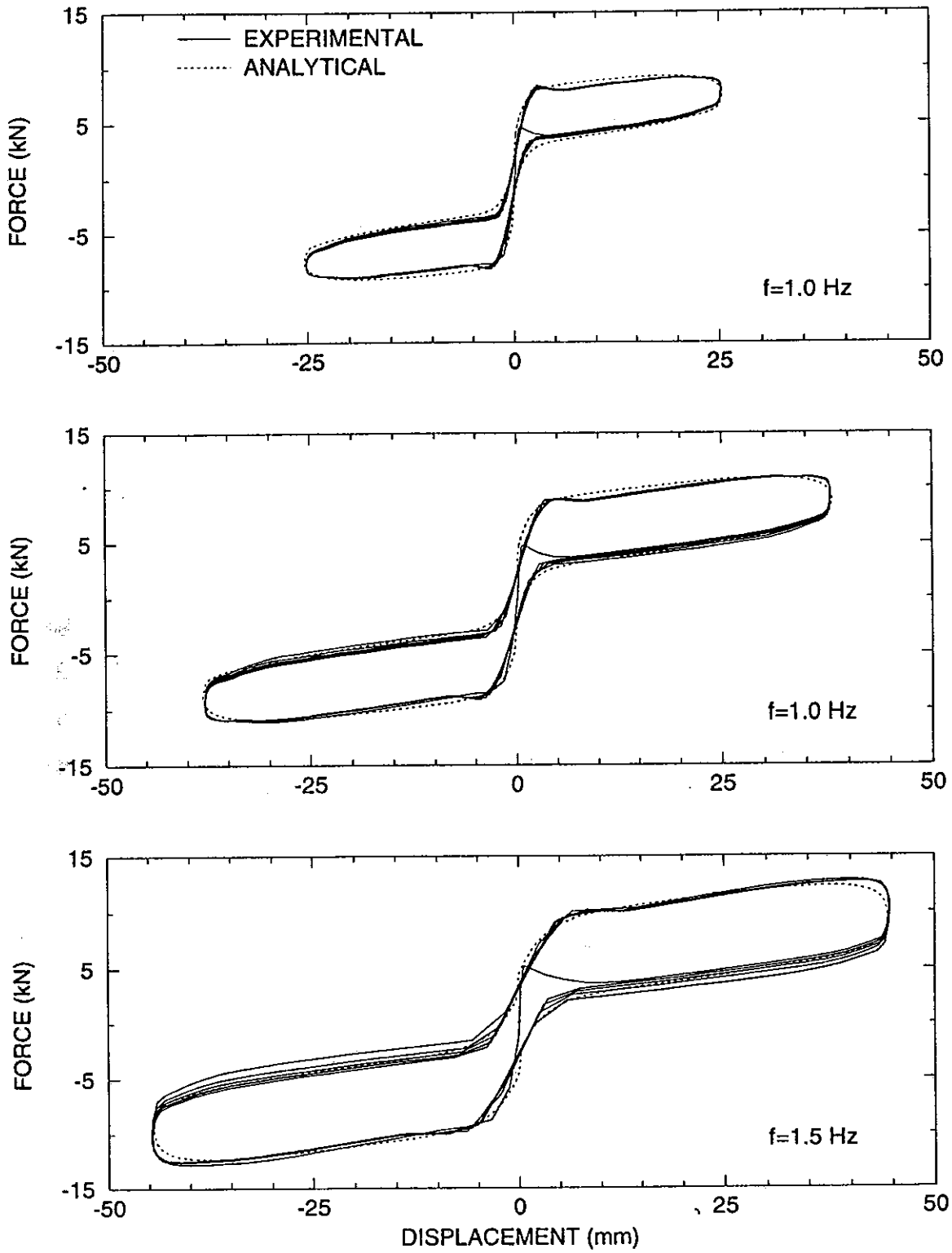

Figure 7-4 Continued.

7.4 Comparison of Analytical and Experimental Results

The equation of motion of the isolated bridge model are Equations (7-1) to (7-11) with force F_{ti} described by Equations (7-12) to (7-15) and $u = U_{bi}$. Thus, we assume that the device displacement is equal to the sliding bearing displacement. This is not exact since the height of installation of the device was slightly different than that of the sliding bearings and the bracing assembly of the device exhibited some limited flexibility.

Solution of the governing Equations (7-1) through (7-15) was obtained by first reducing the equations to a system of first order differential equations and then numerically integrating the system by using an adaptive integration scheme with truncation error control (Gear 1971). The initial conditions were specified to be zero due to the fact that permanent displacement did not occur.

The data used in the analytical model were : deck weight $m_d g$ = 143 kN, pier weight $m_{pi} g$ = 8.9 kN, $L_1 = L_2$ = 1600 mm, $h_1 = h_2$ = 98 mm, h = 413 mm, $I_{p1} = I_{p2}$ = 38.22 kN s^2 mm, $E_1 = E_2$ = 200000 MPa, $I_1 = I_2$ = 3.022x10^{-5} m^4 (2 AISC tubes Ts 6x6x5/16). Based on these data the fundamental period of each pier, in its cantilever position, was calculated to be 0.092s. This is in close agreement with the experimentally determined value of 0.096s. The second mode of the cantilever pier had a calculated frequency of 102 Hz. This frequency could neither be detected in the tests nor have any significance in the analysis.

Damping in the piers was described by the second term in Equation (7-6). The fact that the calculated second frequency of the cantilever pier is much larger than the first frequency indicates that the second mode of the pier may be neglected. Accordingly, constant C^2_{pi} in Equation (7-6) was set equal to zero and constant C^1_{pi} was assigned a value equal to 0.0062 kNs/mm. Based on this value, the damping ratio in the fundamental mode of the cantilever pier was calculated to be 5% of critical. This is consisted with the experimental data.

Comparisons of analytical and experimental results are presented in Figures 7-5 to 7-9 in the case of tests with only horizontal excitation. The analysis was based on Equations (7-1) to (7-15) but with $\ddot{U}_{vi}$ set equal to zero (vertical acceleration effects were neglected). Evidently, the analytical results are in very good agreement with the experimental results.

Figures 7-10 and 7-11 compare experimental and analytical results in the tests with combined horizontal-vertical El Centro 200% and Taft 400% inputs. The analysis accounted for the vertical acceleration effects. Again the two sets of results appear to be in good agreement.

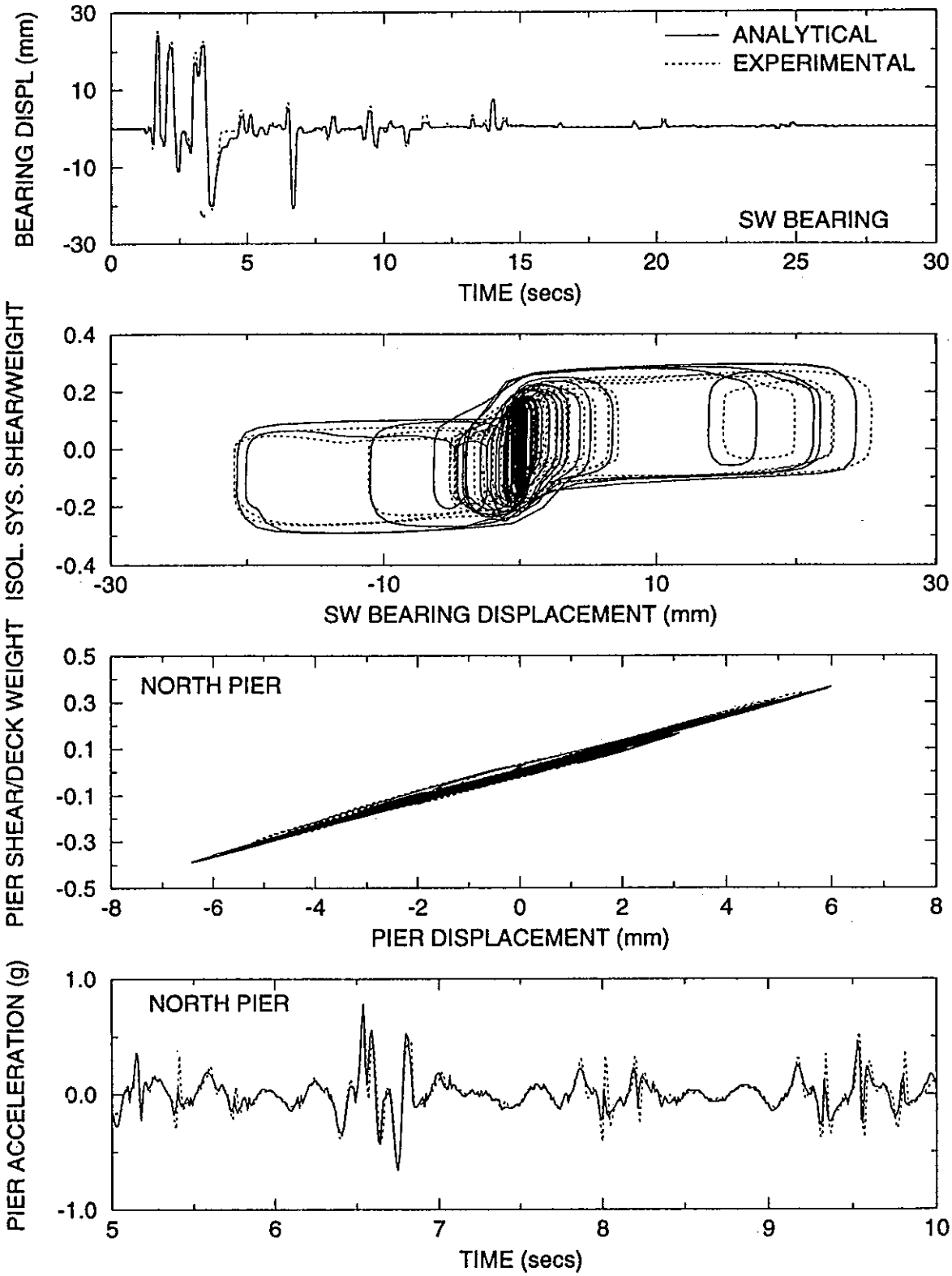

Figure 7-5 **Comparison of Experimental and Analytical Results in Test with El Centro S00E 200% Input (Test No.TDRUN26). Analysis Performed without the Effect of Vertical Pier Acceleration ($\ddot{U}_{vi}$=0).**

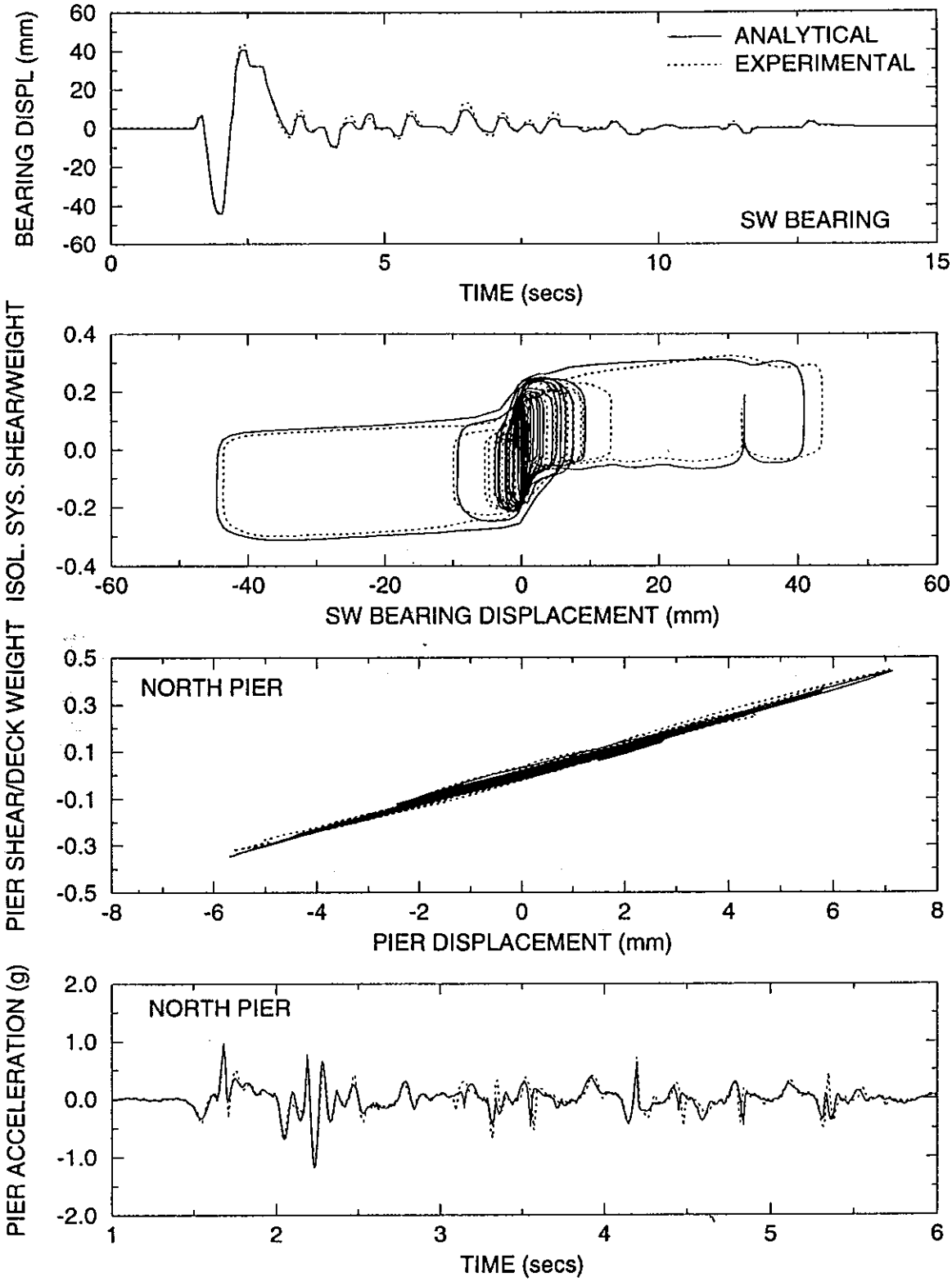

Figure 7-6 **Comparison of Experimental and Analytical Results in Test with Japanese Level 2 G.C. 1 100% Input (Test No.TDRUN41). Analysis Performed without the Effect of Vertical Pier Acceleration ($\ddot{U}_{vi}$=0).**

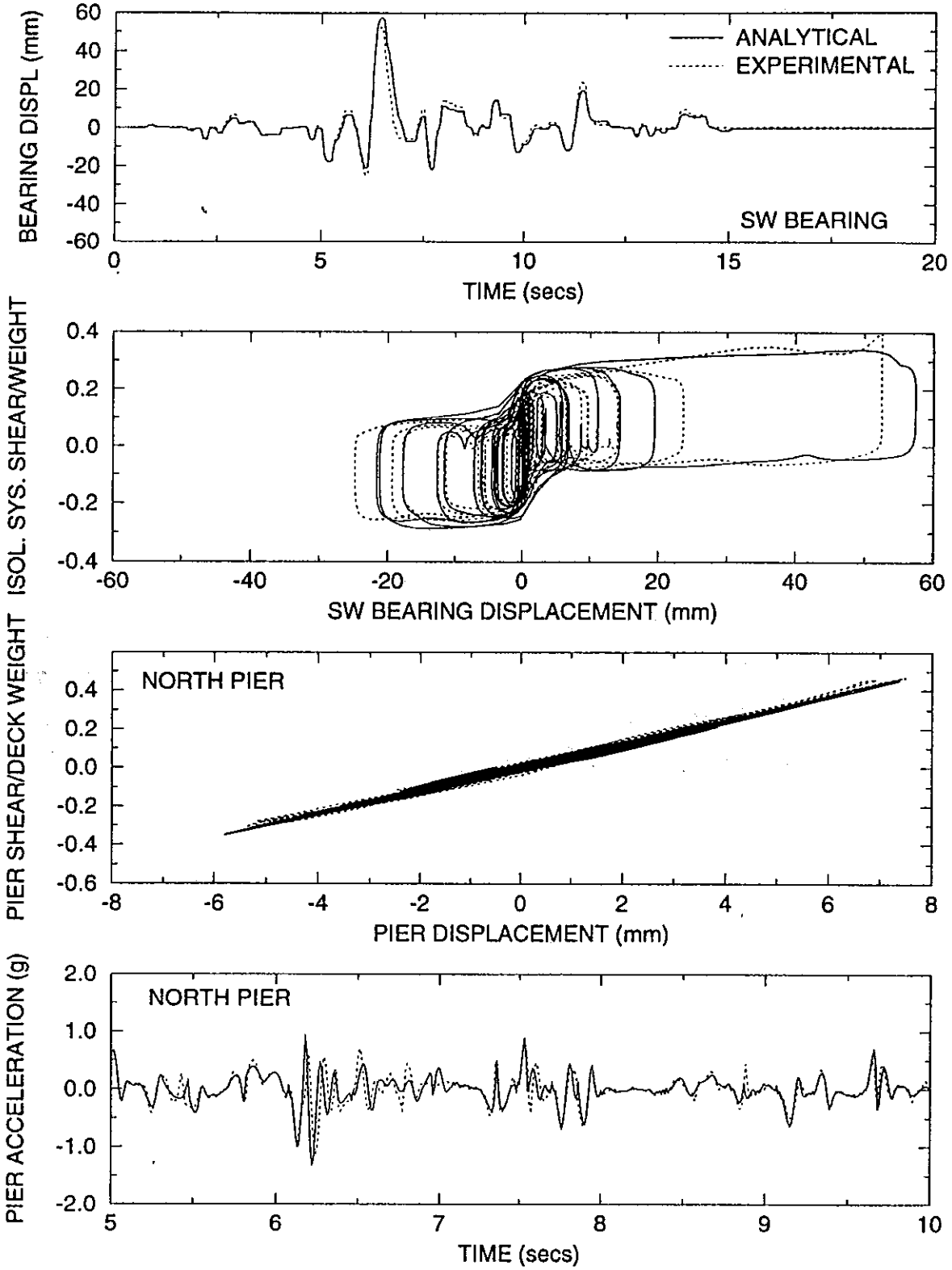

Figure 7-7 **Comparison of Experimental and Analytical Results in Test with Japanese Level 2 G.C. 2 100% Input (Test No.TDRUN42). Analysis Performed without the Effect of Vertical Pier Acceleration ($\ddot{U}_{vi}$=0).**

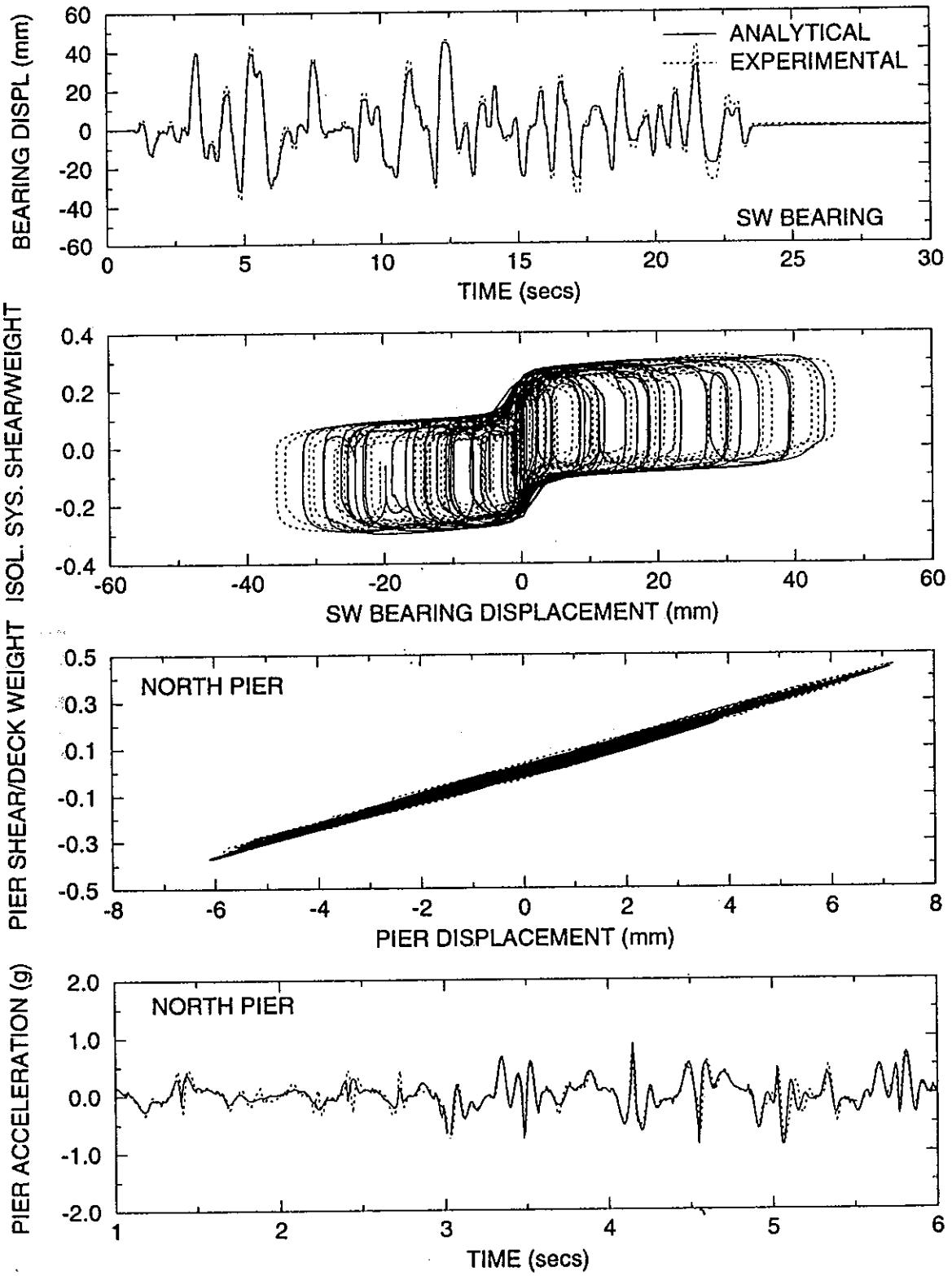

Figure 7-8 **Comparison of Experimental and Analytical Results in Test with Japanese Level 2 G.C.3 100% Input (Test No.TDRUN43). Analysis Performed without the Effect of Vertical Pier Acceleration ($\ddot{U}_{vi}$=0).**

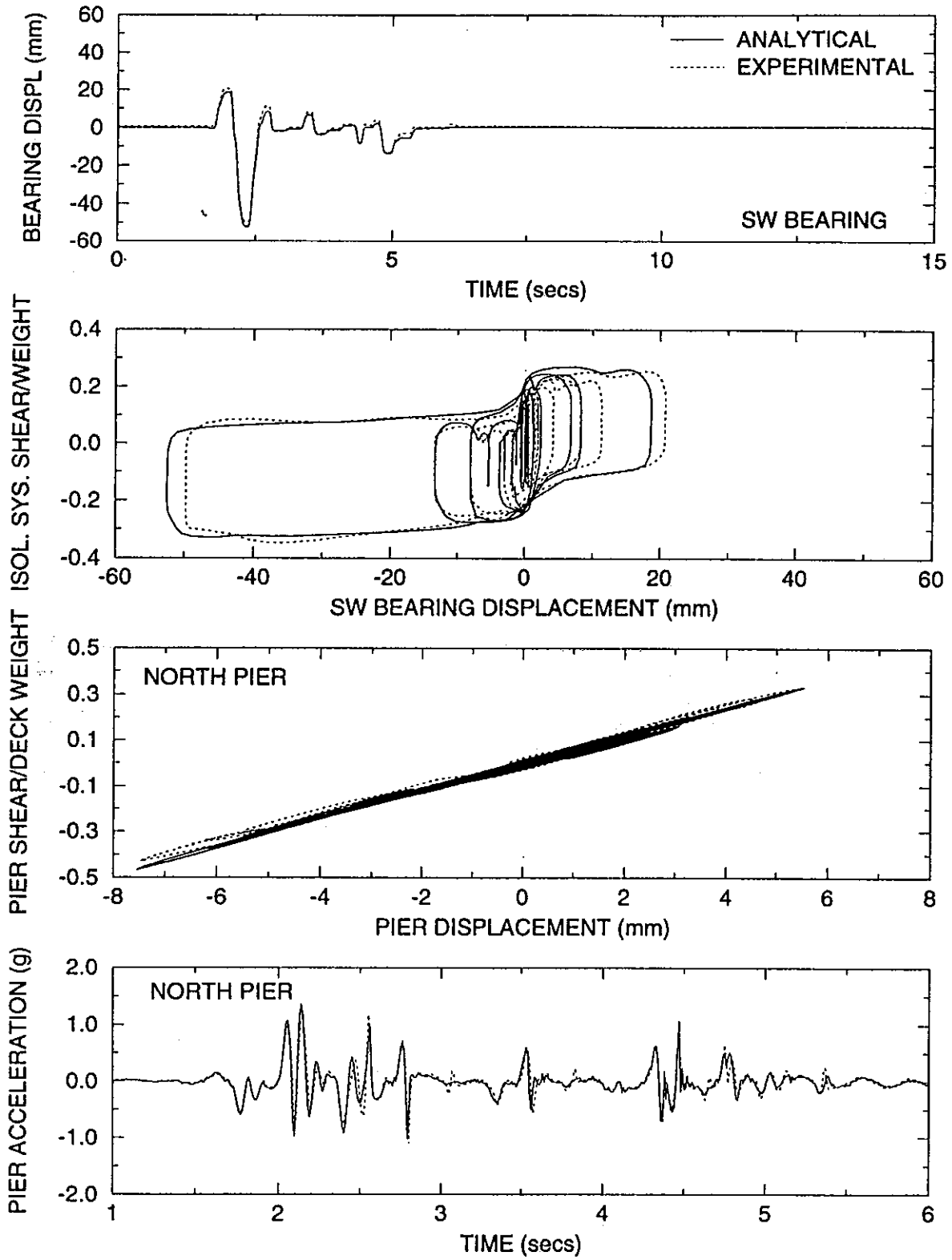

Figure 7-9 **Comparison of Experimental and Analytical Results in Test with Pacoima S16E 75% Input (Test No.TDRUN45). Analysis Performed without the Effect of Vertical Pier Acceleration ($\ddot{U}_{vi}$=0).**

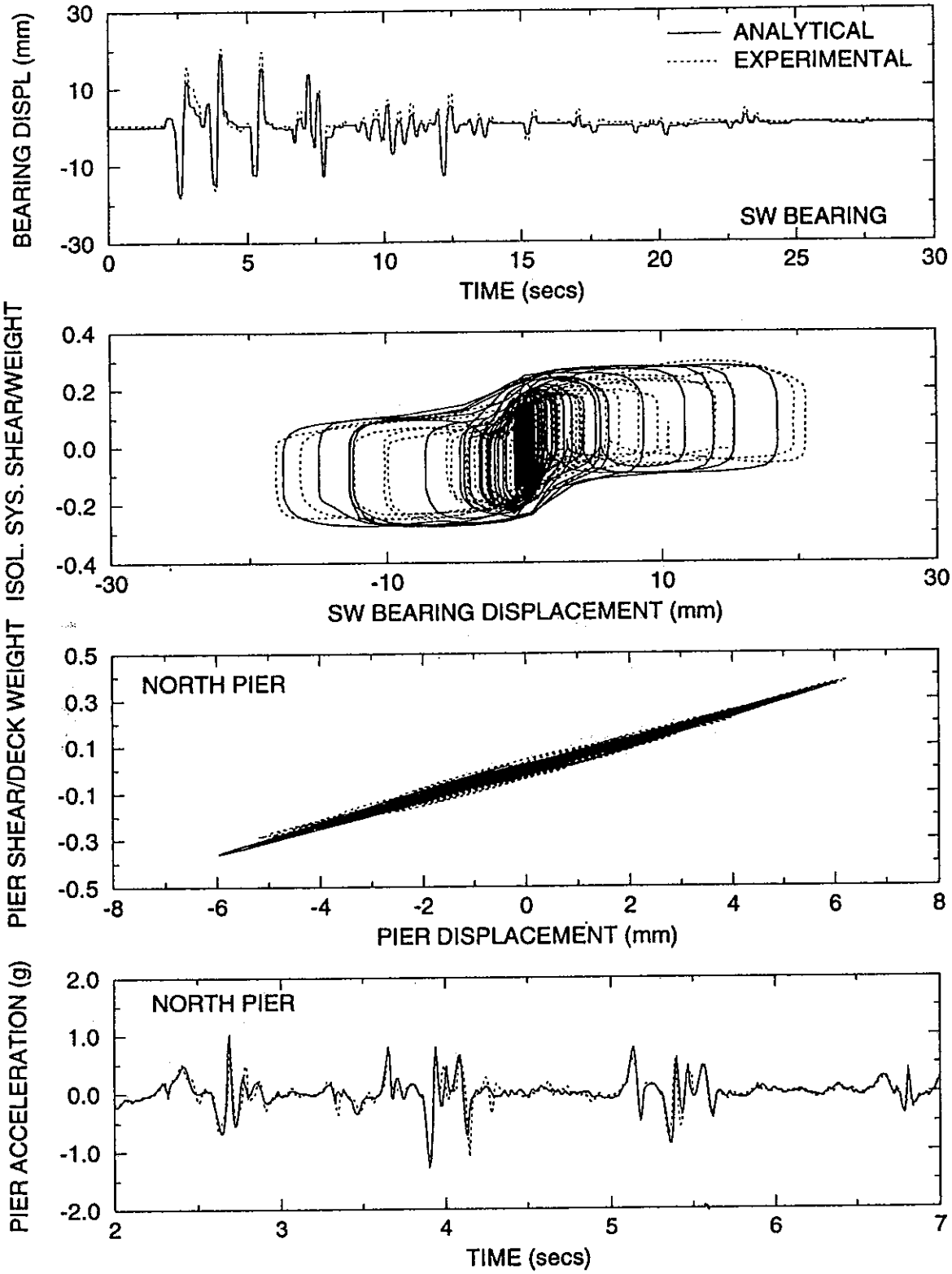

Figure 7-10 **Comparison of Experimental and Analytical Results in Test with Taft N21E plus Vertical 400% Input (Test No.TDRUN54). Analysis Performed with the Effects of Vertical Pier Acceleration.**

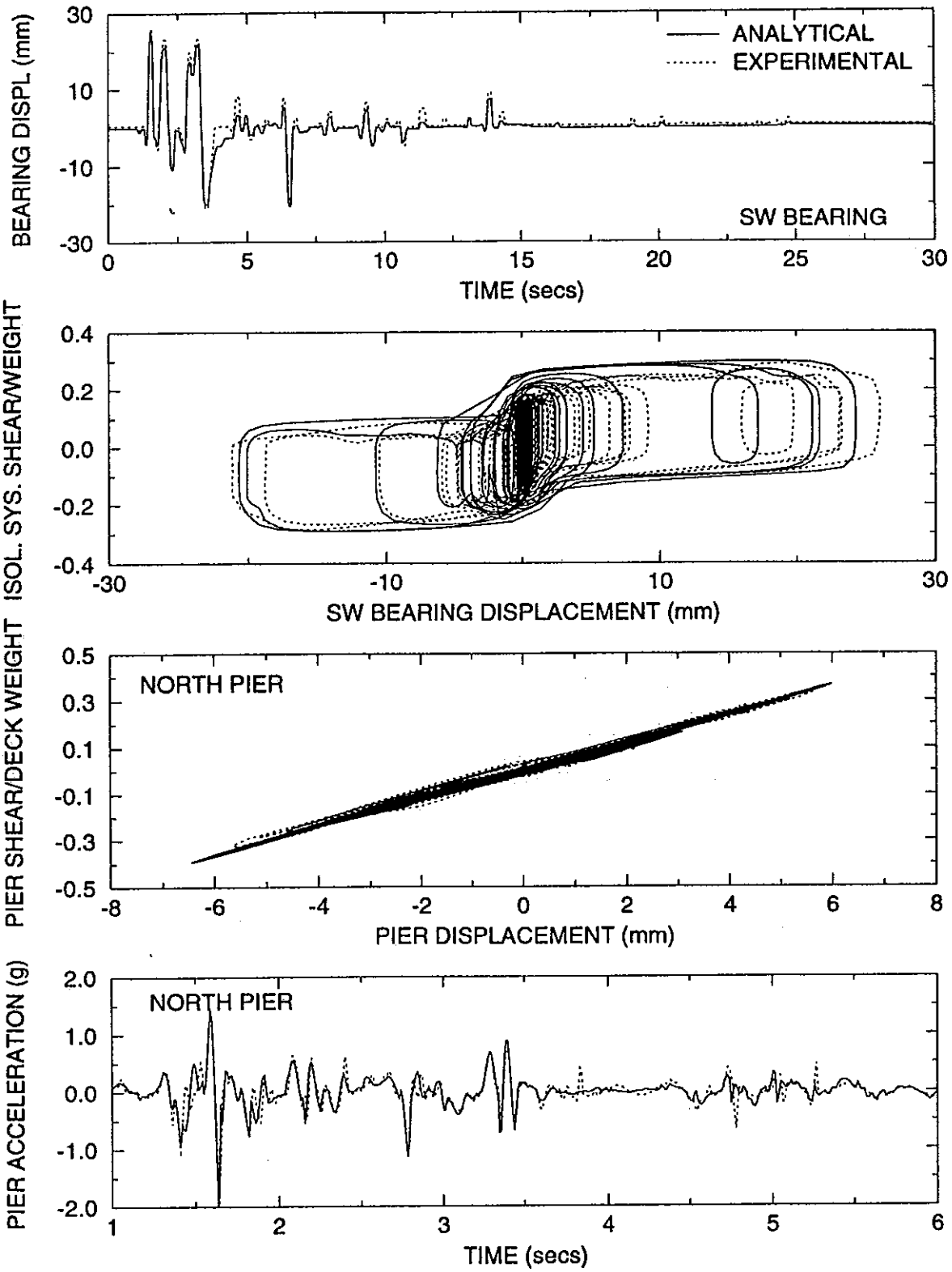

Figure 7-11 Comparison of Experimental and Analytical Results in Test with El Centro S00E plus Vertical 200% Input (Test No.TDRUN55). Analysis Performed with the Effects of Vertical Pier Acceleration.

SECTION 8

CONCLUSIONS

This report presented an experimental study of the seismic response of an isolated bridge and a comparison of its response to that of a comparable non-isolated bridge. The isolation system consisted of sliding bearings and fluid restoring force/damping devices. The fluid devices were pressurized to develop preload. That is, the devices resisted motion by the combination of a constant force, the preload, a weak restoring force and a viscous damping force. The preload was selected to be just larger than the minimum friction force in the bearings, so that permanent displacements did not occur.

The conclusions of the study are :

(1) While the tested isolation system was designed for strong seismic excitation, it also performed well in weak seismic excitation. Specifically, the isolated bridge performed better than the comparable non-isolated bridge in terms of the substructure response and insensitivity to the frequency content of the input.

(2) In strong seismic excitations the tested isolation system performed in accordance with its design. That is, displacements were maintained at less than 200 mm in prototype scale and the isolation system force was restricted to values below 0.33 times the deck weight. Only in one test with input being the Japanese level 2, ground condition 2 motion, the displacement exceeded 200 mm and forces reached nearly 0.40 times the deck weight.

(3) The vertical ground motion had minor effects on the peak response of the tested system.

(4) Permanent displacements in the tested system were practically zero (maximum recorded value was 2.4 mm in prototype scale). The development of permanent displacements was prevented by the preload in the fluid devices, which was selected to just exceed the minimum friction force in the isolation system.

(5) The preload of the fluid devices alone was sufficient to prevent the occurrence of any permanent displacements. That is, the spring force of the devices (due to fluid

compression) was not necessary for preventing the development of permanent displacements. Nevertheless, the 1991 AASHTO would have classified a system with only preload as one which lacks restoring force capability and , thus, penalize the system. It is clear that the AASHTO procedures are not generally valid.

(6) An analytical model has been presented for the fluid restoring force/damping devices, which is capable of describing their behavior with good accuracy. Analyses of the dynamic response of the tested isolated bridge showed very good agreement of experimental and analytical results.

SECTION 9

REFERENCES

American Association of State Highway and Transportation Officials-AASHTO (1991). "Guide Specifications for Seismic Isolation Design." Washington, D.C.

Buckle, I.G. and Mayes, R.L. (1990). "Seismic Isolation History, Application, and Performance - A World View." Earthquake Spectra, 6(2), 161-201.

Civil Engineering Research Center-CERC (1992). "Temporary Manual of Design Method for Base-Isolated Highway Bridges." Japan (in Japanese).

Constantinou, M.C., Mokha, A. and Reinhorn, A.M. (1990a). "Teflon Bearings in Base Isolation II: Modeling." J. Stuct. Engrg., ASCE, 116(2), 455-474.

Constantinou, M.C., Mokha, A. and Reinhorn, A.M. (1990b). "Experimental and Analytical Study of a Combined Sliding Disc Bearing and Helical Steel Spring Isolation System." NCEER-90-0019, Nat. Ctr. for Earthquake Engrg. Res., State Univ. of New York, Buffalo, NY.

Constantinou, M.C., Kartoum, A., Reinhorn, A.M. and Bradford, P. (1991a). "Experimental and Theoretical Study of a Sliding Isolation System for Bridges." Report No. NCEER-91-0027, Nat. Ctr. for Earthquake Engrg. Res., State Univ. of New York, Buffalo, NY.

Constantinou, M.C., Mokha, A. and Reinhorn, A.M. (1991b). "Study of Sliding Bearing and Helical-Steel-Spring Isolation System." J. Struct. Engrg., ASCE, 117(4), 1257-1275.

Constantinou, M.C. (1992). "NCEER-Taisei Research on Sliding Isolation Systems for Bridges." NCEER Bulletin, Nat. Ctr. for Earthquake Engrg. Res., State Univ. of New York, Buffalo, NY, 6(3), 1-4.

Constantinou, M.C., Tsopelas, P., Kim, Y-S., and Okamoto, S. (1993). "NCEER-TAISEI Corporation Research Program on Sliding Seismic Isolation Systems for Bridges-Experimental and Analytical Study of Friction Pendulum System (FPS)." Report No. NCEER 93-0020. Nat. Ctr. for Earthquake Engrg. Res., State Univ. of New York, Buffalo, NY.

Eisenberg J.M., Melentyev, A.M., Smirov, V.I. and Nemykin, A.N. (1992). "Applications of Seismic Isolation in the USSR." Proc. 10th WCEE, Madrid, Spain, 4,2039-2046.

Gates, J.H. (1979). "Factors Considered in the Development of the California Seismic Design Criteria for Bridges." Proc. Workshop on Earthquake Resistance of Highway Bridges, Applied Technology Council, Palo Alto, Calif., 141-162.

Gear, C.W. (1971). "The Automatic Integration of Ordinary Differential Equations." Numer. Math., Commun. of ACM, 14(3), 176-190.

Grenier, A. (1991). "Seismic Protection of Bridges by the Viscoelastic Technique." Proc. 3rd World Congress on Joint Sealing and Bearing Systems for Concrete Structures, Vol. 2, 1205-1224, Toronto, Canada.

International Conference of Building Officials ICBO (1991). "Uniform Building Code, Earthquake Regulations for Seismic-Isolated Structures." Whittier, Calif.

Kartoum, A., Constantinou, M.C. and Reinhorn, A.M. (1992). "Sliding Isolation System for Bridges: Analytical Study." Earthquake Spectra, 8(3), 345-372.

Kawamura, S., Kitazawa, K., Hisano, M. and Nagashima, I. (1988). "Study of a Sliding-Type Base Isolation System. System Composition and Element Properties." Proceedings of 9th World Conference on Earthquake Engineering, Tokyo-Kyoto, Vol. V, 735-740.

Kawashima, K., Hasegawa, K. and Nagashima, H. (1991). "A Perspective of Menshin Design for Highway Bridges in Japan." First US-Japan Workshop on Earthquake Protective Systems for Bridges, Buffalo, NY, September.

Kelly, J.M., Buckle, I.G., and Tsai, H-C. (1986). "Earthquake Simulator Testing of a Base-Isolated Bridge Deck." Report No. UCB/EERC-85/09, Earthquake Engrg. Res. Ctr., Univ. of California, Berkeley, Calif., Jan.

Kelly, J. (1993). "State-of-the-Art and State-of-the-Practice in Base Isolation." ATC-17-1 Seminar on Seismic Isolation, Passive Energy Dissipation and Active Control, San Francisco, CA, March.

Marioni, A. (1991). "Antiseismic Devices for Bridges in Italy." Proc. 3rd World Congress on Joint Sealing and Bearing Systems for Concrete Structures, Vol. 2, 1263- 1280, Toronto, Canada.

Martelli, A., Parducci, A. and Forni, M. (1993). "State-of-the-Art on Development and Application of Seismic Isolation and Other Innovative Seismic Design Techniques in Italy." ATC-17-1 Seminar on Seismic Isolation, Passive Energy Dissipation and Active Control, San Francisco, CA, March.

Mayes, R.L., Jones, L.R. and Buckle, I.G., (1990). "Impediments to the Implementation of Seismic Isolation." Earthquake Spectra, 6(2), 283-296.

Medeot, R. (1991). "The Evolution of Aseismic Devices for Bridges in Italy." 3rd World Congress on Joint Sealing and Bearing Systems for Concrete Structures, Vol. 2 of Preprints, 1295-1320, Toronto, Canada.

Mokha, A., Constantinou, M.C., and Reinhorn, A.M. (1988). "Teflon Bearings in Aseismic Base Isolation. Experimental Studies and Mathematical Modeling." Report No. NCEER- 88-0038, Nat. Ctr. for Earthquake Engrg. Res., State Univ. of New York, Buffalo, NY.

Mokha, A., Constantinou, M.C. and Reinhorn, A.M. (1990a). "Teflon Bearings in Base Isolation. I: Testing." J. Struct. Engrg., ASCE, 116(2), 438-454.

Mokha, A., Constantinou, M.C. and Reinhorn, A.M. (1990b). "Experimental Study and Analytical Prediction of Earthquake Response of a Sliding Isolation System with a Spherical Surface." Report No. NCEER-90-0020, Nat. Ctr. for Earthquake Engrg. Res., State Univ. of New York, Buffalo, NY.

Mokha, A., Constantinou, M.C., Reinhorn, A.M., and Zayas, V. (1991). "Experimental Study of Friction Pendulum Isolation System." J. Struct. Engrg., ASCE, 117(4), 1201- 1217.

Palfalvi, B., Amin, A., Mokha, A., Fatehi, H. and Lee, P. (1993). "Implementation Issues in Seismic Isolation Retrofit of Government Buildings." ATC-17-1 Seminar on Seismic Isolation, Passive Energy Dissipation and Active Control, San Francisco, CA, March.

Sabnis, G.M., Harris, H.G., White, R.N. and Mirza, M.S. (1983). "Structural Modeling and Experimental Techniques." Prentice-Hall, Inc., Englewood Cliffs, N.J.

Soong, T.T. and Constantinou, M.C. (1992). "Base Isolation and Active Control Technology Case Studies in the U.S.A." Proc. IDNDR Intl. Symp. on Earthq. Disaster Reduction Technol.-30th Anniv. of IISEE, Tsukuba, Japan, 455-469.

Tsopelas, P., Okamoto, S., Constantinou, M.C., Ozaki, D., and Fujii, S. (1994). "NCEER-TAISEI Corporation Research Program on Sliding Seismic Isolation Systems for Bridges-Experimental and Analytical Study of Systems Consisting of Sliding Bearings, Rubber Restoring Force Devices and Fluid Dampers." Report No. NCEER 94-0002, Nat. Ctr. for Earthquake Engrg. Res., State Univ. of New York, Buffalo, NY.

Zayas, V., Low, S.S and Mahin, S.A. (1987). "The FPS Earthquake Resisting System, Experimental Report." Report No. UCB/ EERC-87/01, Earthquake Engineering Research Center, University of California, Berkeley, Calif., June.

APPENDIX A

EXPERIMENTAL RESULTS

This Appendix contains experimental results of the tested bridge model in the non-isolated and the isolated configuration with either two stiff or two flexible piers. In the case of the non-isolated bridge (test No. FRUN05 to FRUN22), the recorded time history of the deck displacement with respect to the table and the loops of the shear force versus deformation of the north pier are presented. In the case of the isolated bridge with stiff piers (tests No TDRUN01 to TDRUN24), the recorded SW bearing displacement history and the loops of isolation system force versus SW bearing displacement are presented. The isolation system force was obtained as the sum of the forces recorded by the four load cells supporting the sliding bearings and the forces in the two load cells of the fluid restoring force/damping devices. In the case of the isolated bridge with flexible piers (tests No. TDRUN25 to TDRUN55), the recorded SW bearing displacement history, the loops of isolation system force versus SW bearing displacement and the loops of shear force versus deformation of the north pier are presented. The test number and excitation are identified at the top of each page.

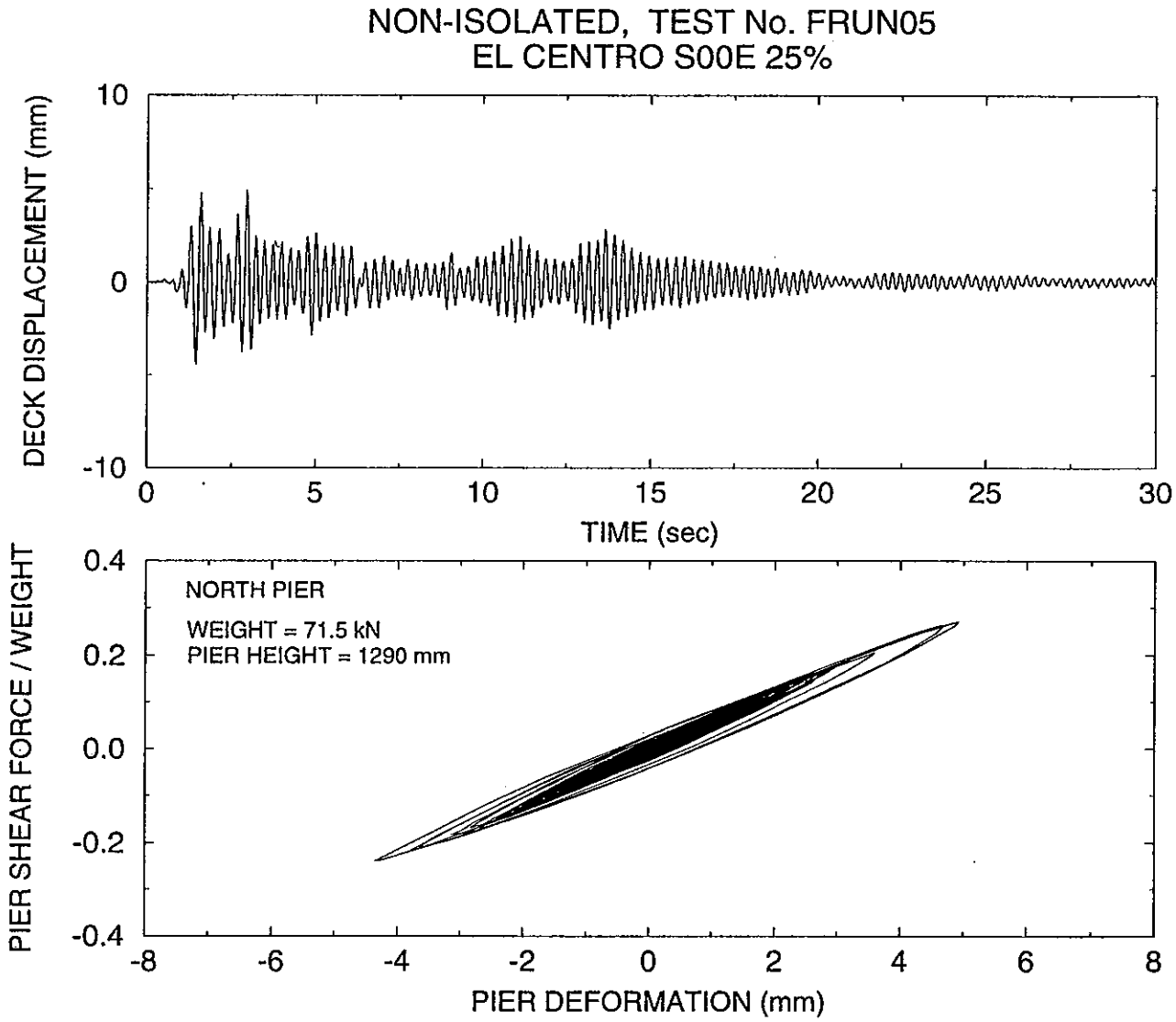
NON-ISOLATED, TEST No. FRUN05
EL CENTRO S00E 25%
DECK DISPLACEMENT (mm)
10
0
-10
0
5
10
15
20
25
30
TIME (sec)
PIER SHEAR FORCE / WEIGHT
NORTH PIER
WEIGHT = 71.5 kN
PIER HEIGHT = 1290 mm
0.4
0.2
0.0
-0.2
-0.4
-8
-6
-4
-2
0
2
4
6
8
PIER DEFORMATION (mm)

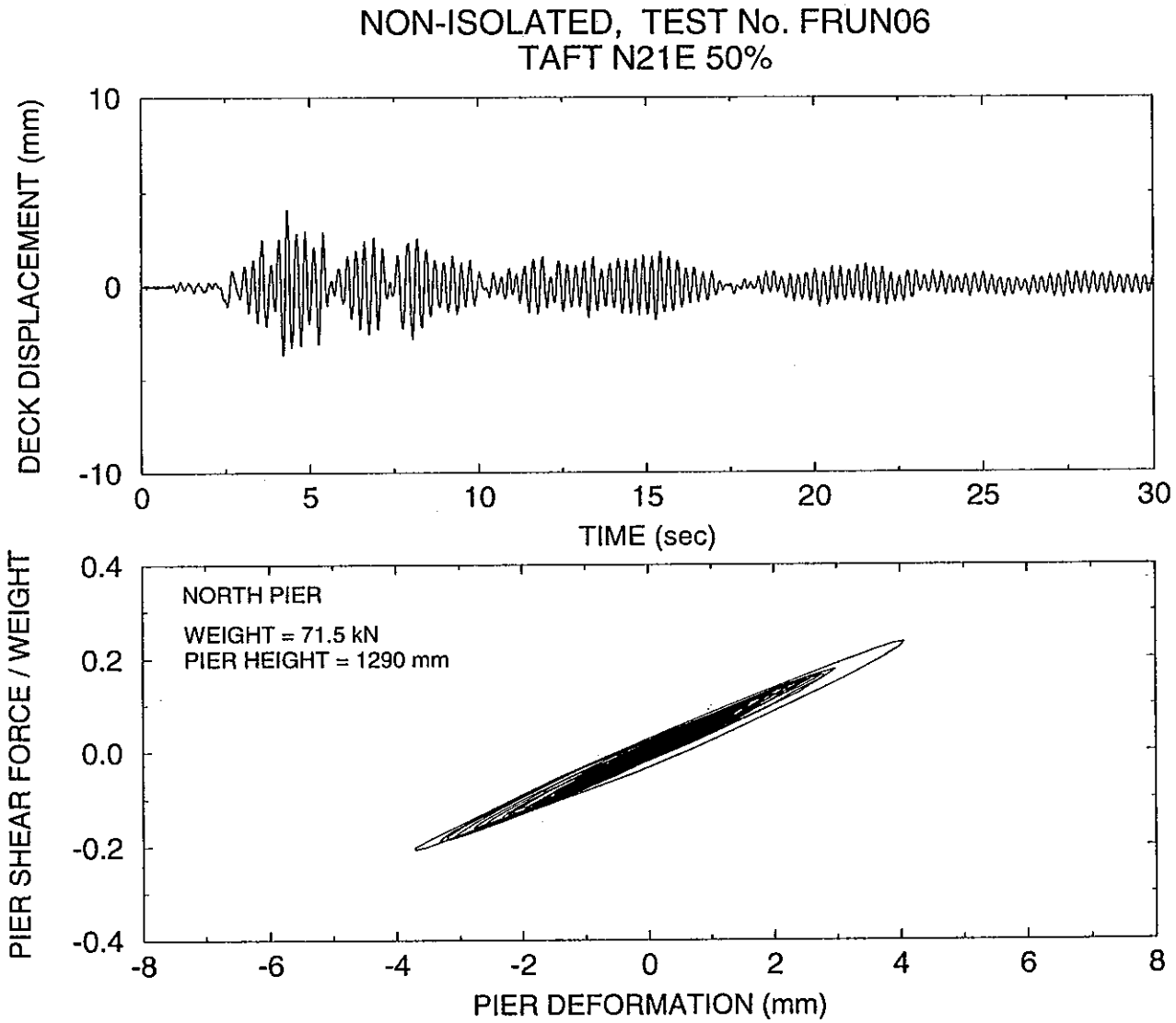
NON-ISOLATED, TEST No. FRUN06
TAFT N21E 50%
DECK DISPLACEMENT (mm)
10
0
-10
0
5
10
15
20
25
30
TIME (sec)
PIER SHEAR FORCE / WEIGHT
0.4
0.2
0.0
-0.2
-0.4
NORTH PIER
WEIGHT = 71.5 kN
PIER HEIGHT = 1290 mm
-8
-6
-4
-2
0
2
4
6
8
PIER DEFORMATION (mm)

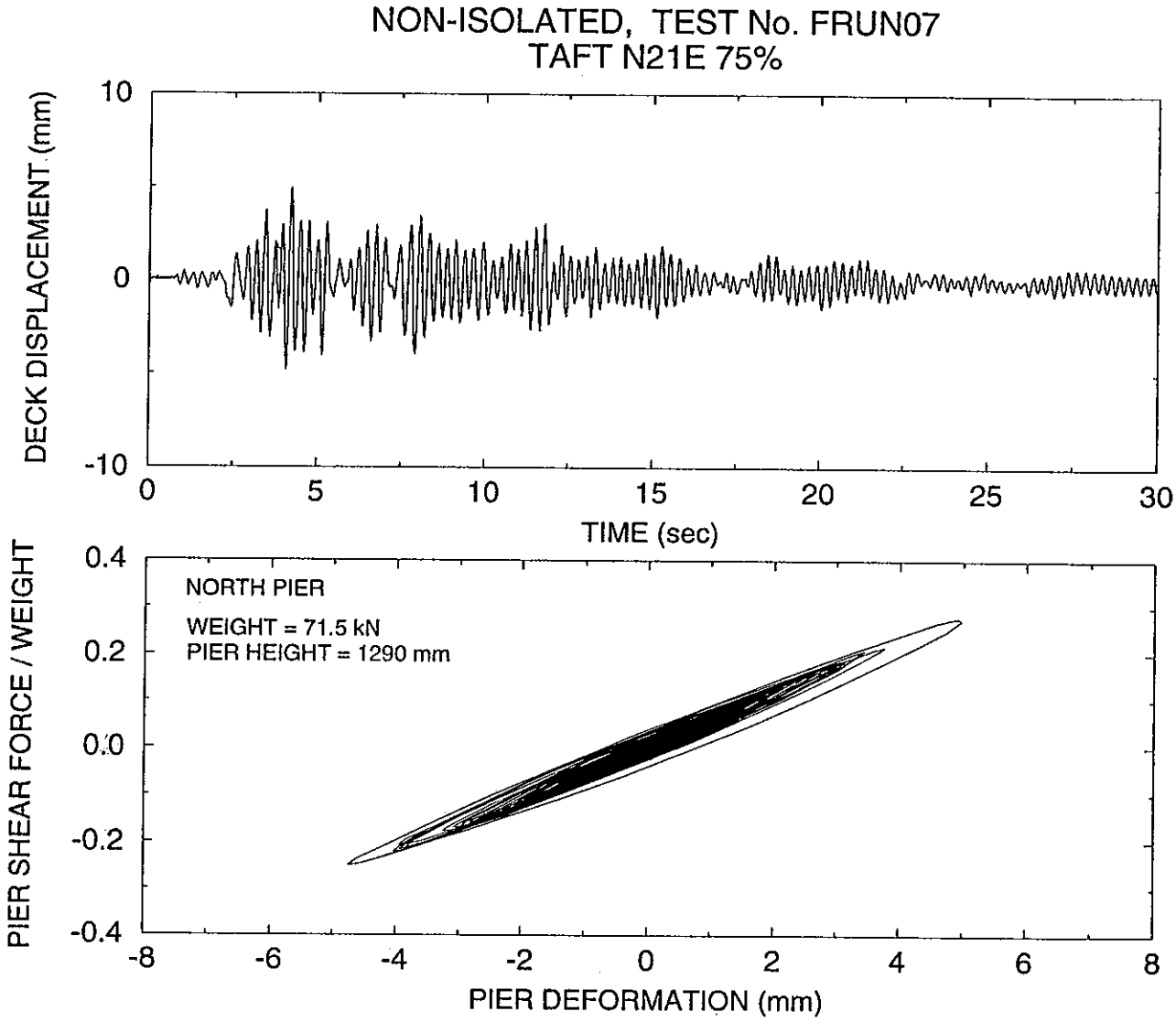
NON-ISOLATED, TEST No. FRUN07
TAFT N21E 75%
DECK DISPLACEMENT (mm)
10
0
-10
0
5
10
15
20
25
30
TIME (sec)
PIER SHEAR FORCE / WEIGHT
NORTH PIER
WEIGHT = 71.5 kN
PIER HEIGHT = 1290 mm
0.4
0.2
0.0
-0.2
-0.4
-8
-6
-4
-2
0
2
4
6
8
PIER DEFORMATION (mm)

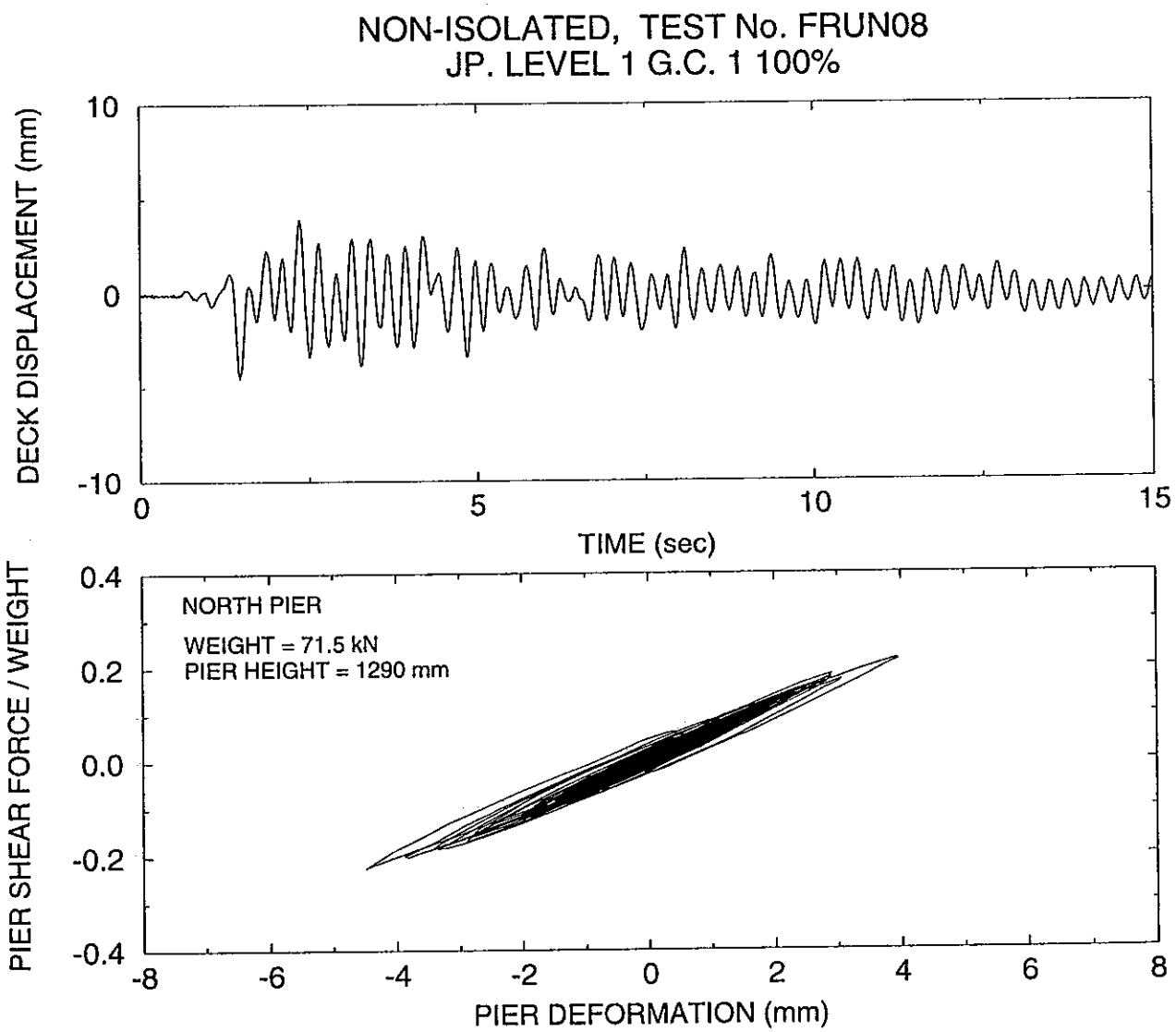
NON-ISOLATED, TEST No. FRUN08
JP. LEVEL 1 G.C. 1 100%
DECK DISPLACEMENT (mm)
10
0
-10
0
5
10
15
TIME (sec)
PIER SHEAR FORCE / WEIGHT
NORTH PIER
WEIGHT = 71.5 kN
PIER HEIGHT = 1290 mm
0.4
0.2
0.0
-0.2
-0.4
-8
-6
-4
-2
0
2
4
6
8
PIER DEFORMATION (mm)

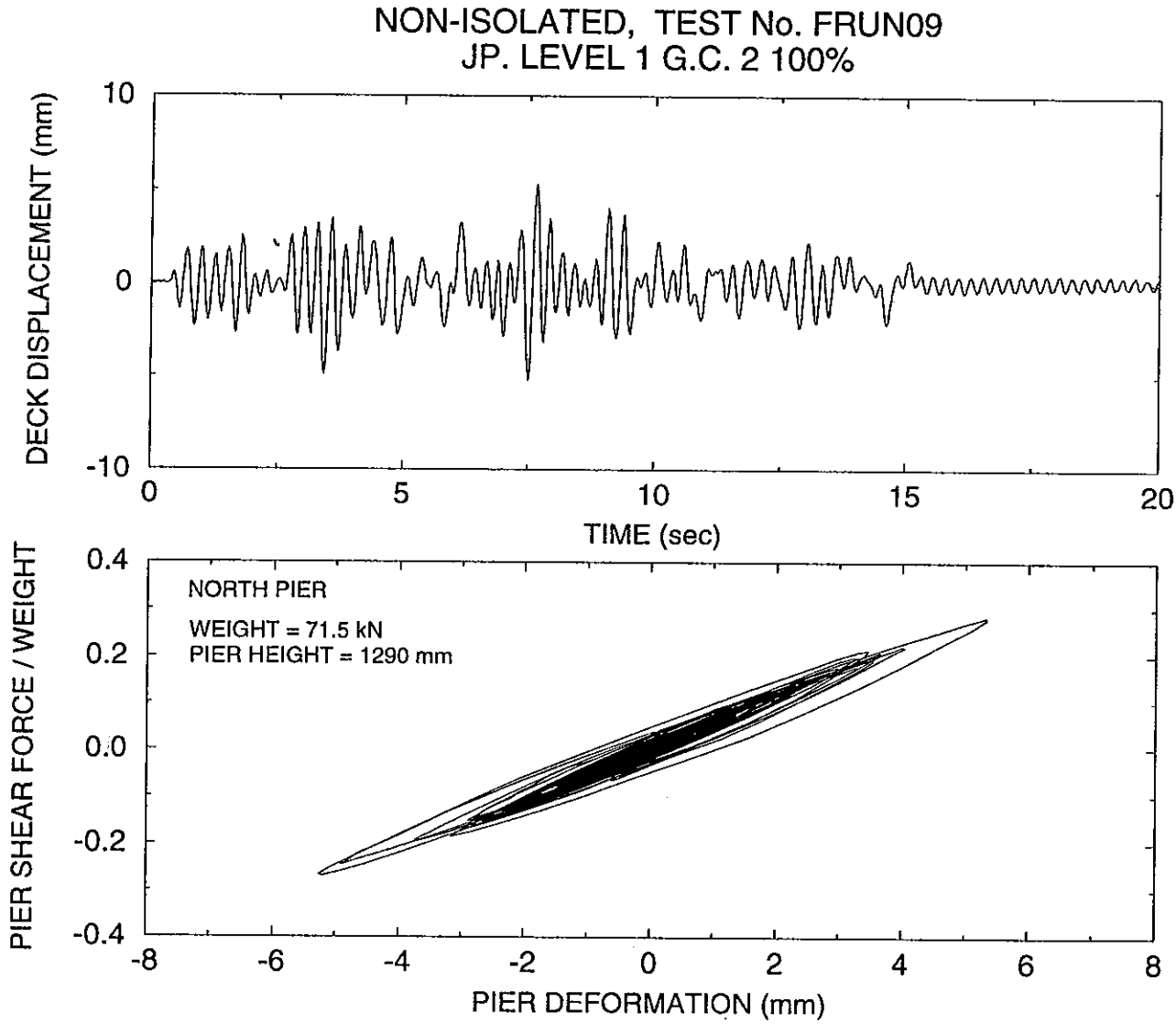
NON-ISOLATED, TEST No. FRUN09
JP. LEVEL 1 G.C. 2 100%
DECK DISPLACEMENT (mm)
10
0
-10
0
5
10
15
20
TIME (sec)
PIER SHEAR FORCE / WEIGHT
NORTH PIER
WEIGHT = 71.5 kN
PIER HEIGHT = 1290 mm
0.4
0.2
0.0
-0.2
-0.4
-8
-6
-4
-2
0
2
4
6
8
PIER DEFORMATION (mm)

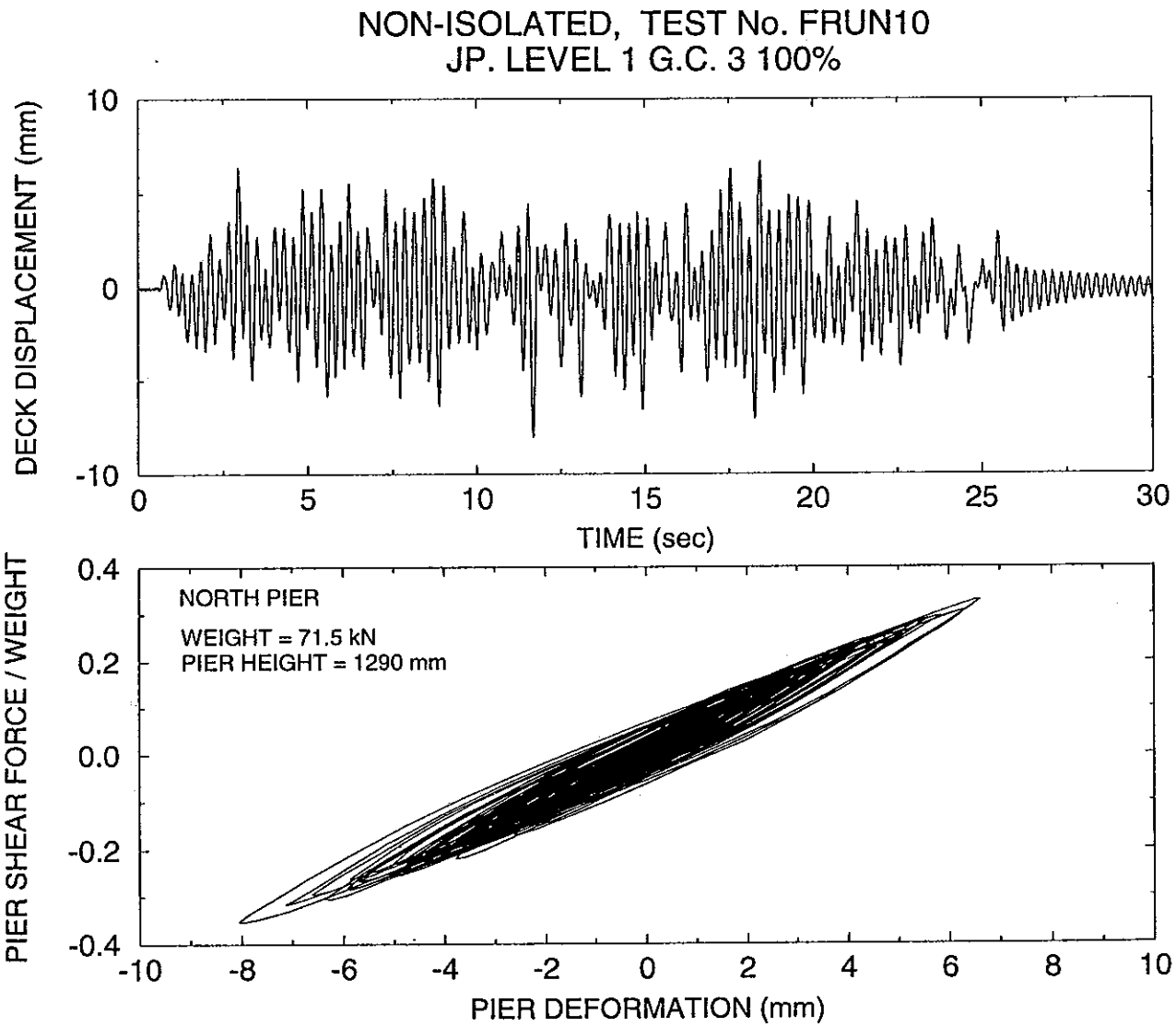
NON-ISOLATED, TEST No. FRUN10
JP. LEVEL 1 G.C. 3 100%
DECK DISPLACEMENT (mm)
10
0
-10
0
5
10
15
20
25
30
TIME (sec)
PIER SHEAR FORCE / WEIGHT
NORTH PIER
WEIGHT = 71.5 kN
PIER HEIGHT = 1290 mm
0.4
0.2
0.0
-0.2
-0.4
-10
-8
-6
-4
-2
0
2
4
6
8
10
PIER DEFORMATION (mm)

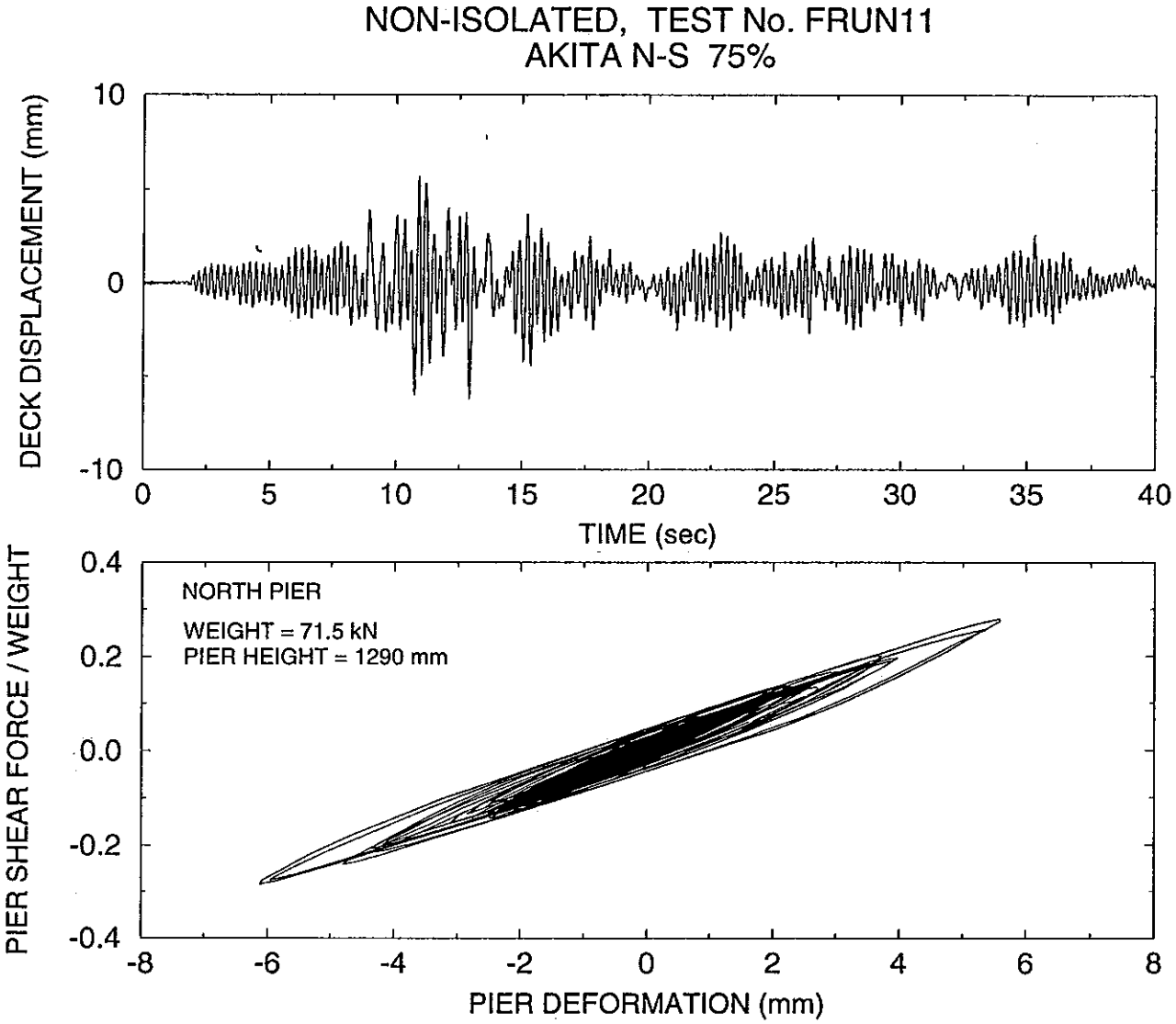
NON-ISOLATED, TEST No. FRUN11
AKITA N-S 75%
DECK DISPLACEMENT (mm)
10
0
-10
0
5
10
15
20
25
30
35
40
TIME (sec)
PIER SHEAR FORCE / WEIGHT
NORTH PIER
WEIGHT = 71.5 kN
PIER HEIGHT = 1290 mm
0.4
0.2
0.0
-0.2
-0.4
-8
-6
-4
-2
0
2
4
6
8
PIER DEFORMATION (mm)

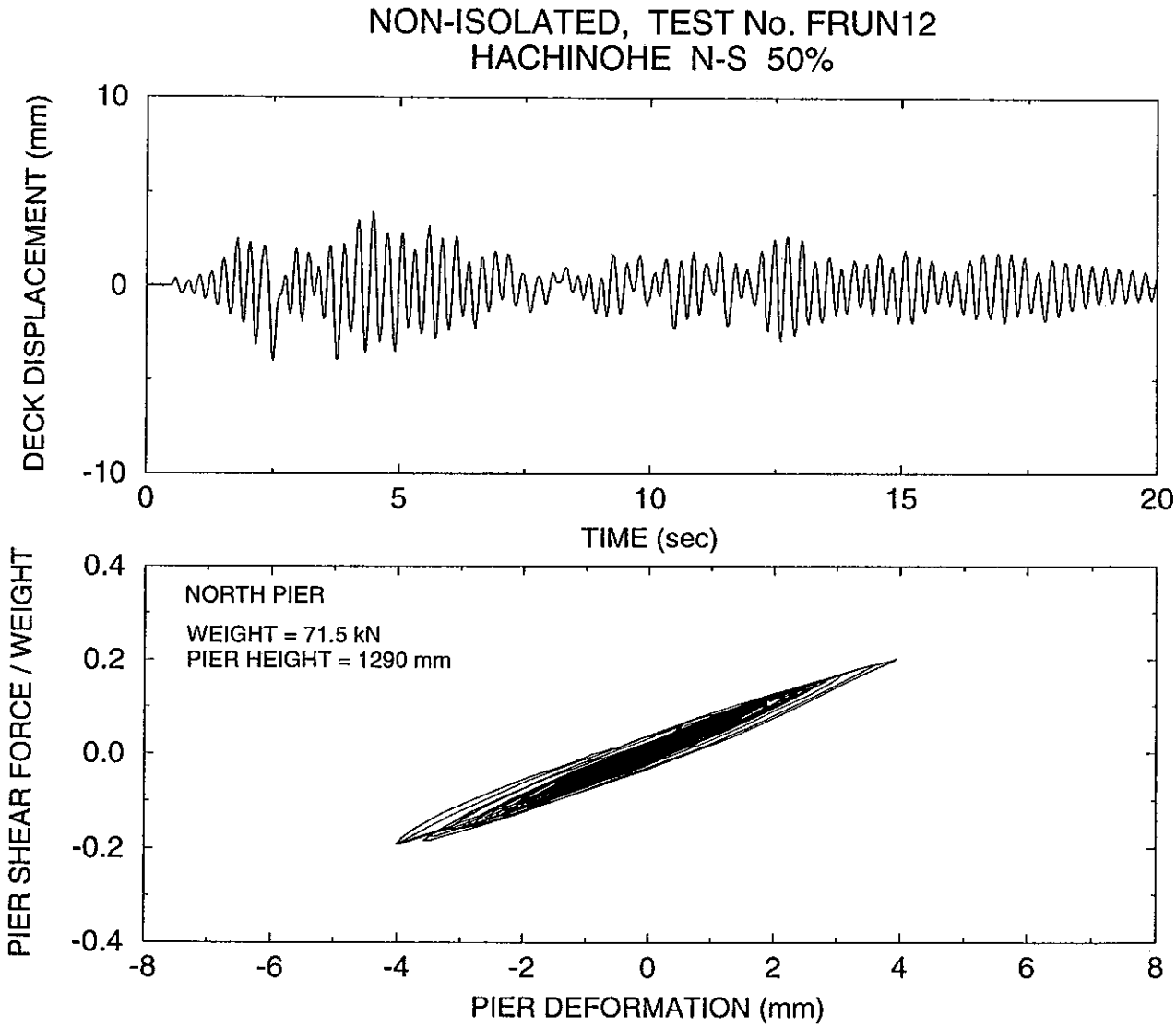
NON-ISOLATED, TEST No. FRUN12
HACHINOHE N-S 50%
DECK DISPLACEMENT (mm)
10
0
-10
0
5
10
15
20
TIME (sec)
PIER SHEAR FORCE / WEIGHT
0.4
0.2
0.0
-0.2
-0.4
NORTH PIER
WEIGHT = 71.5 kN
PIER HEIGHT = 1290 mm
-8
-6
-4
-2
0
2
4
6
8
PIER DEFORMATION (mm)

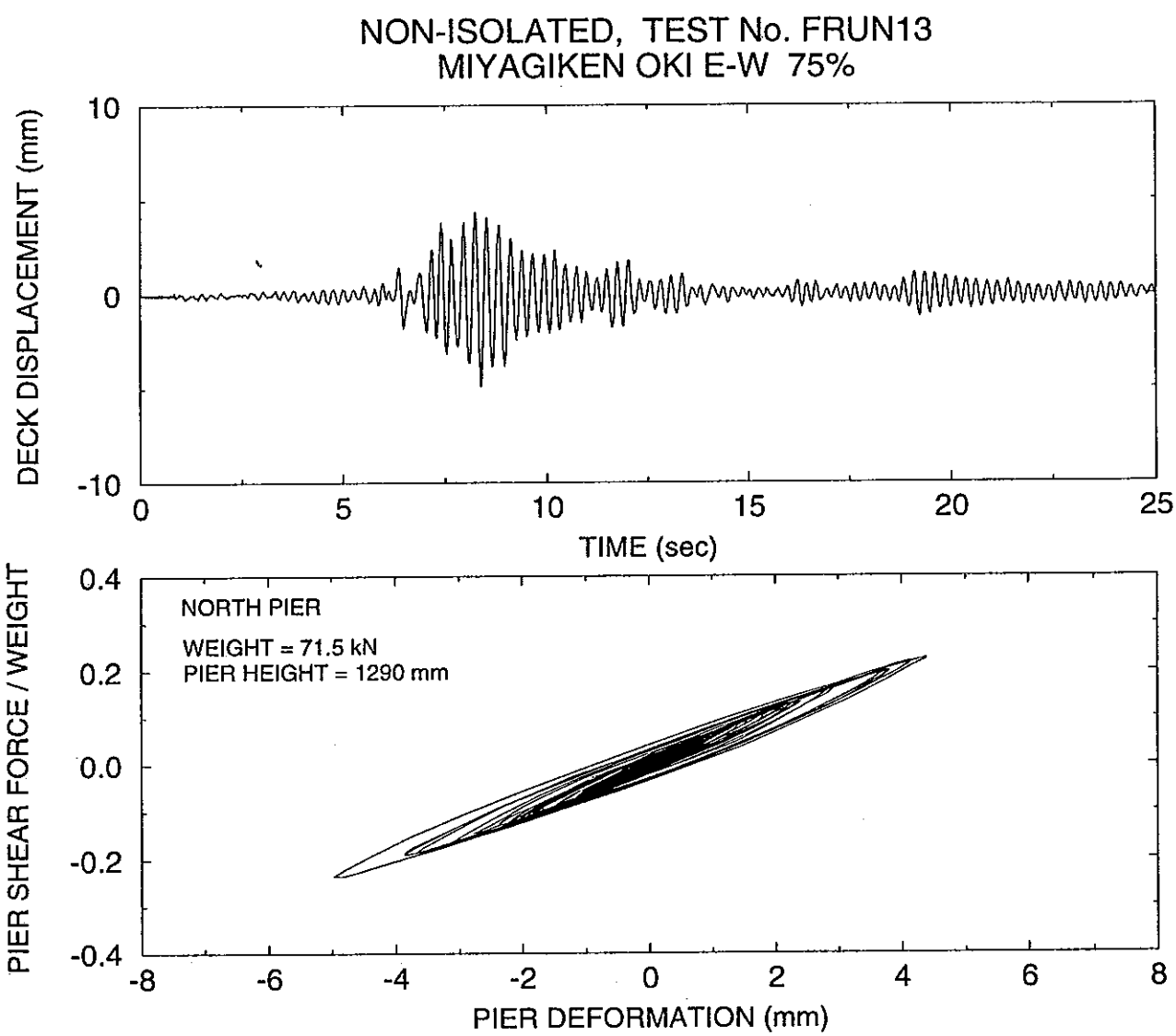
NON-ISOLATED, TEST No. FRUN13
MIYAGIKEN OKI E-W 75%
DECK DISPLACEMENT (mm)
10
0
-10
0
5
10
15
20
25
TIME (sec)
PIER SHEAR FORCE / WEIGHT
0.4
0.2
0.0
-0.2
-0.4
NORTH PIER
WEIGHT = 71.5 kN
PIER HEIGHT = 1290 mm
-8
-6
-4
-2
0
2
4
6
8
PIER DEFORMATION (mm)

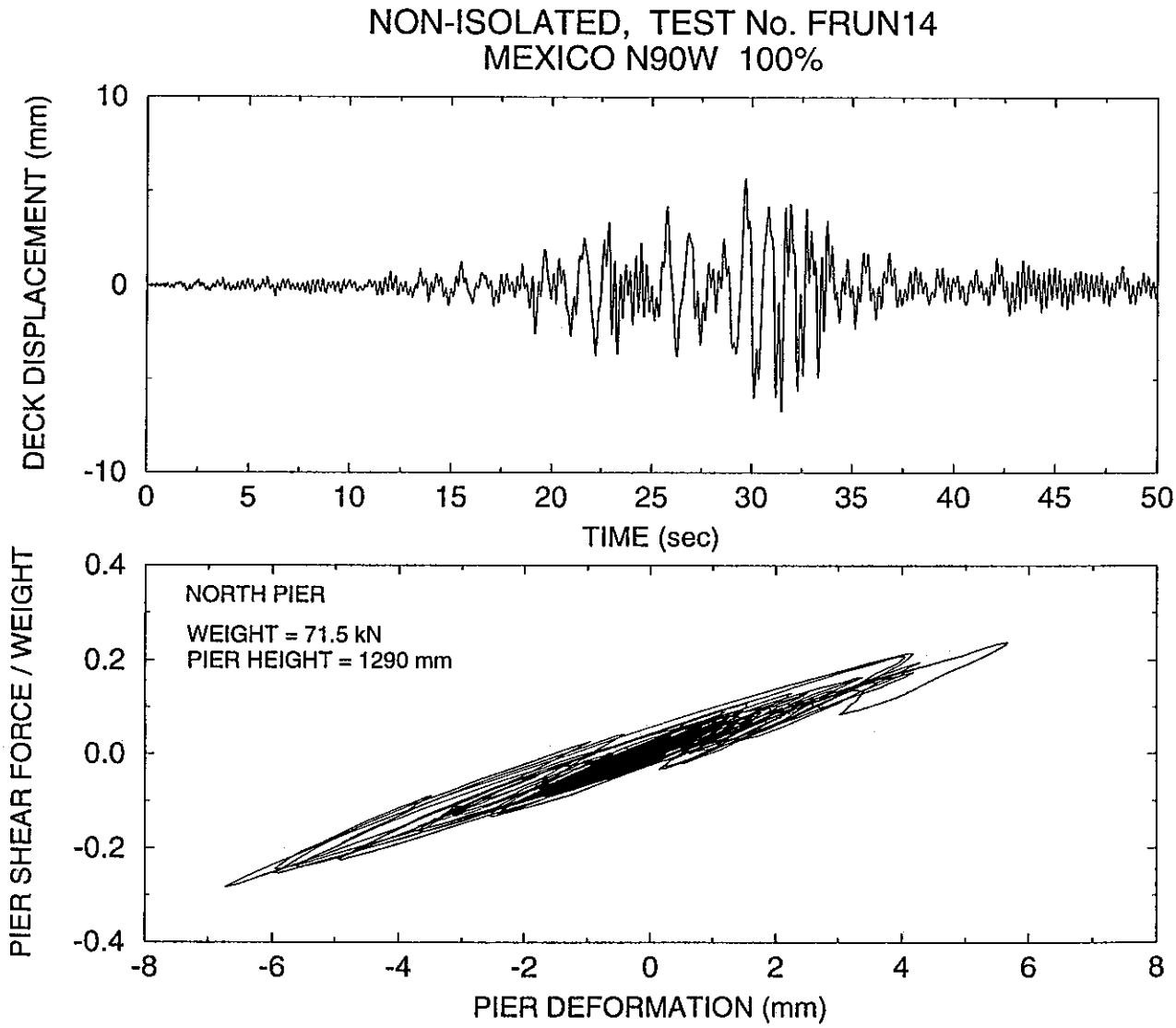
NON-ISOLATED, TEST No. FRUN14
MEXICO N90W 100%
DECK DISPLACEMENT (mm)
10
0
-10
0
5
10
15
20
25
30
35
40
45
50
TIME (sec)
PIER SHEAR FORCE / WEIGHT
NORTH PIER
WEIGHT = 71.5 kN
PIER HEIGHT = 1290 mm
0.4
0.2
0.0
-0.2
-0.4
-8
-6
-4
-2
0
2
4
6
8
PIER DEFORMATION (mm)

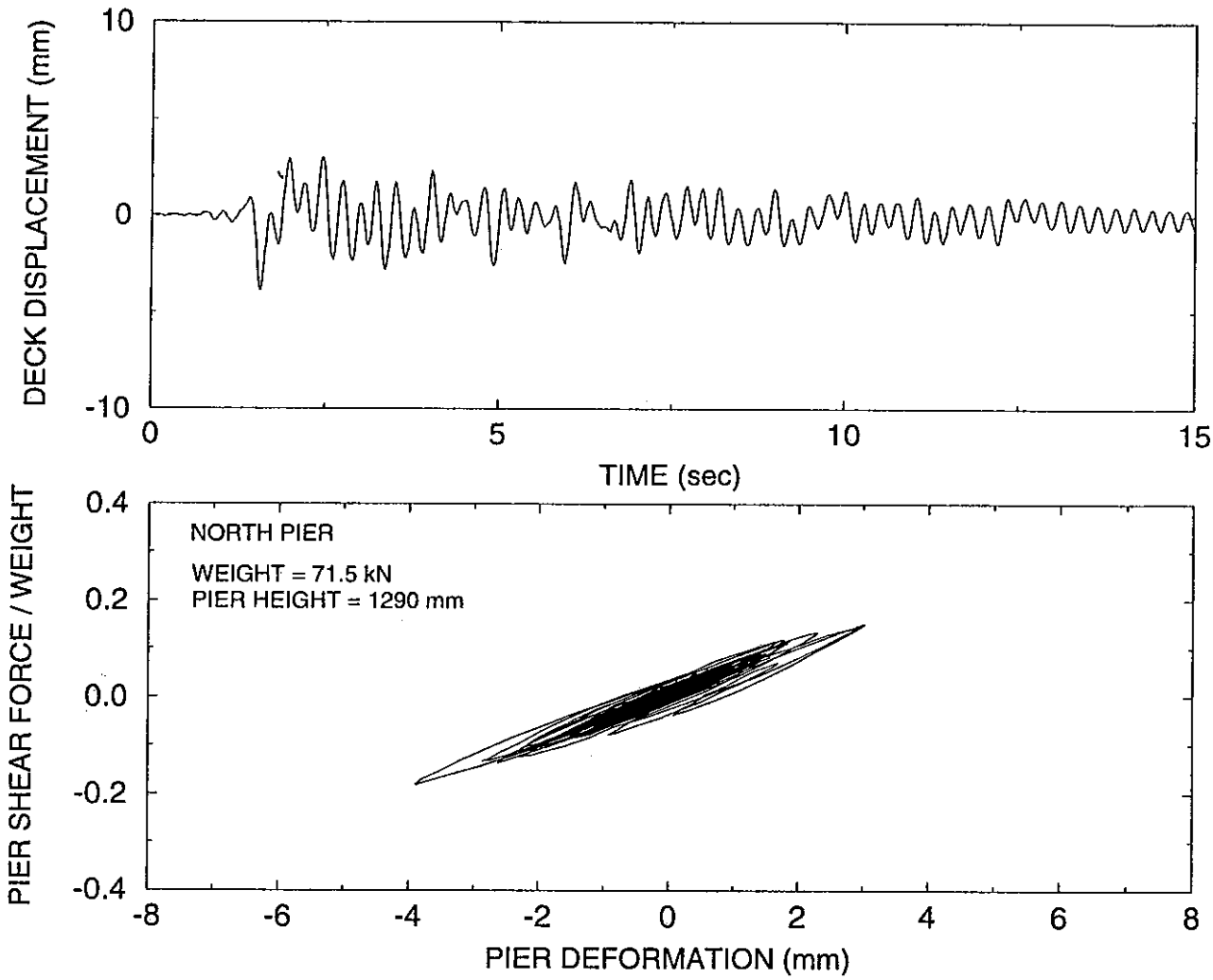
NON-ISOLATED, TEST No. FRUN15
JP. LEVEL 2 G.C. 1 25%
DECK DISPLACEMENT (mm)
10
0
-10
0
5
10
15
TIME (sec)
PIER SHEAR FORCE / WEIGHT
0.4
0.2
0.0
-0.2
-0.4
NORTH PIER
WEIGHT = 71.5 kN
PIER HEIGHT = 1290 mm
-8
-6
-4
-2
0
2
4
6
8
PIER DEFORMATION (mm)

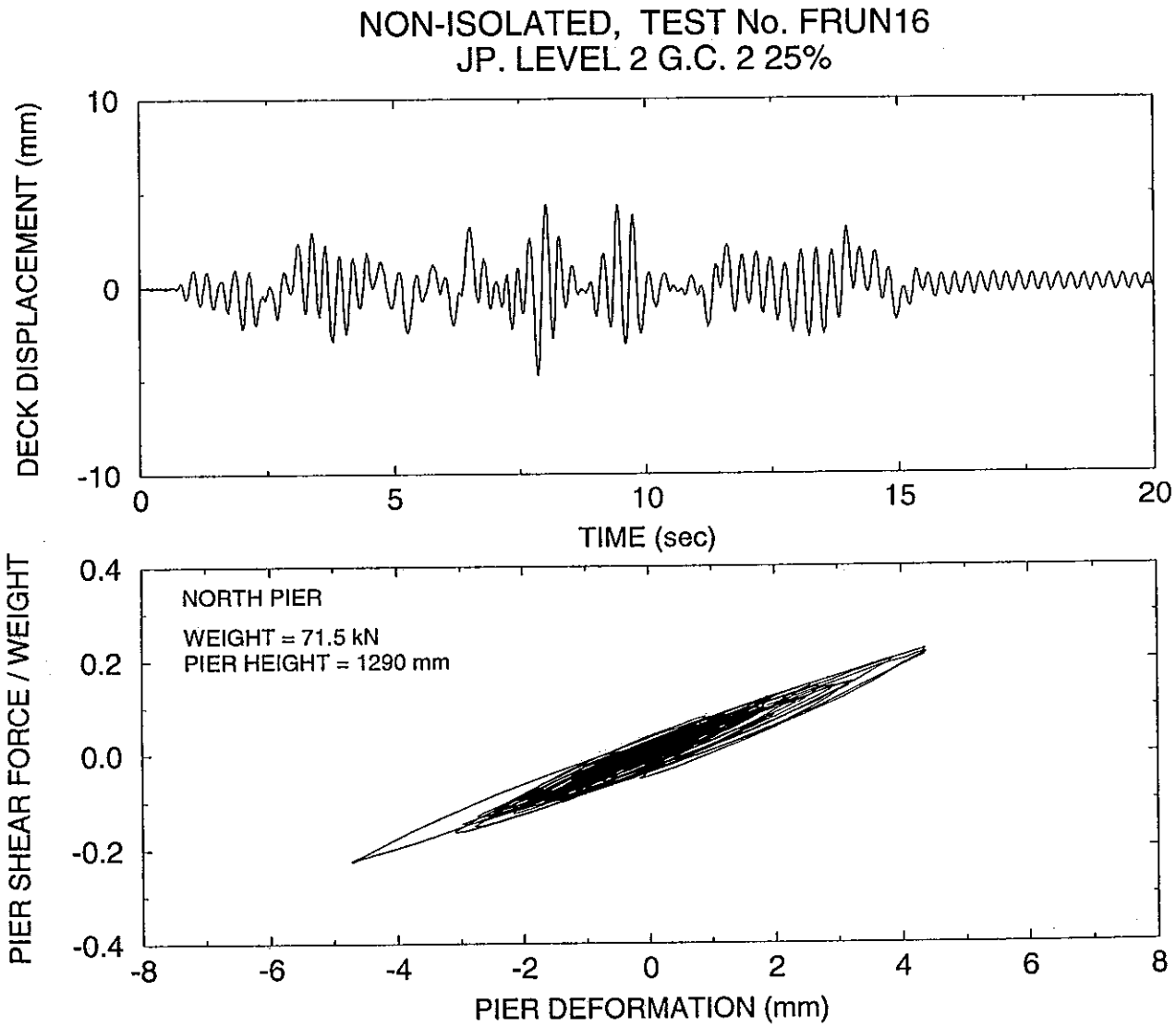
NON-ISOLATED, TEST No. FRUN16
JP. LEVEL 2 G.C. 2 25%
DECK DISPLACEMENT (mm)
10
0
-10
0
5
10
15
20
TIME (sec)
PIER SHEAR FORCE / WEIGHT
0.4
0.2
0.0
-0.2
-0.4
NORTH PIER
WEIGHT = 71.5 kN
PIER HEIGHT = 1290 mm
-8
-6
-4
-2
0
2
4
6
8
PIER DEFORMATION (mm)

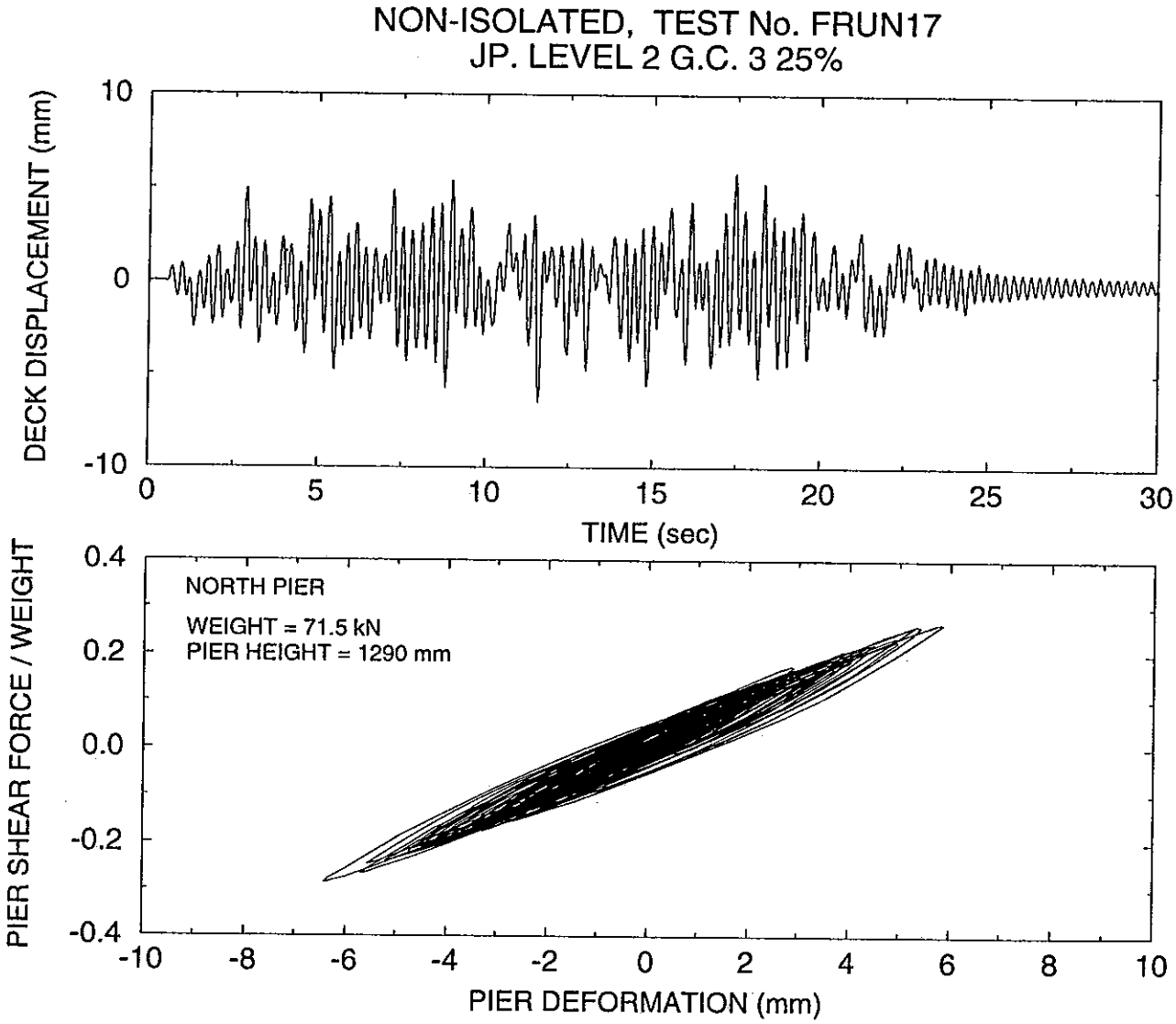
NON-ISOLATED, TEST No. FRUN17
JP. LEVEL 2 G.C. 3 25%
DECK DISPLACEMENT (mm)
10
0
-10
0
5
10
15
20
25
30
TIME (sec)
PIER SHEAR FORCE / WEIGHT
0.4
0.2
0.0
-0.2
-0.4
NORTH PIER
WEIGHT = 71.5 kN
PIER HEIGHT = 1290 mm
-10
-8
-6
-4
-2
0
2
4
6
8
10
PIER DEFORMATION (mm)

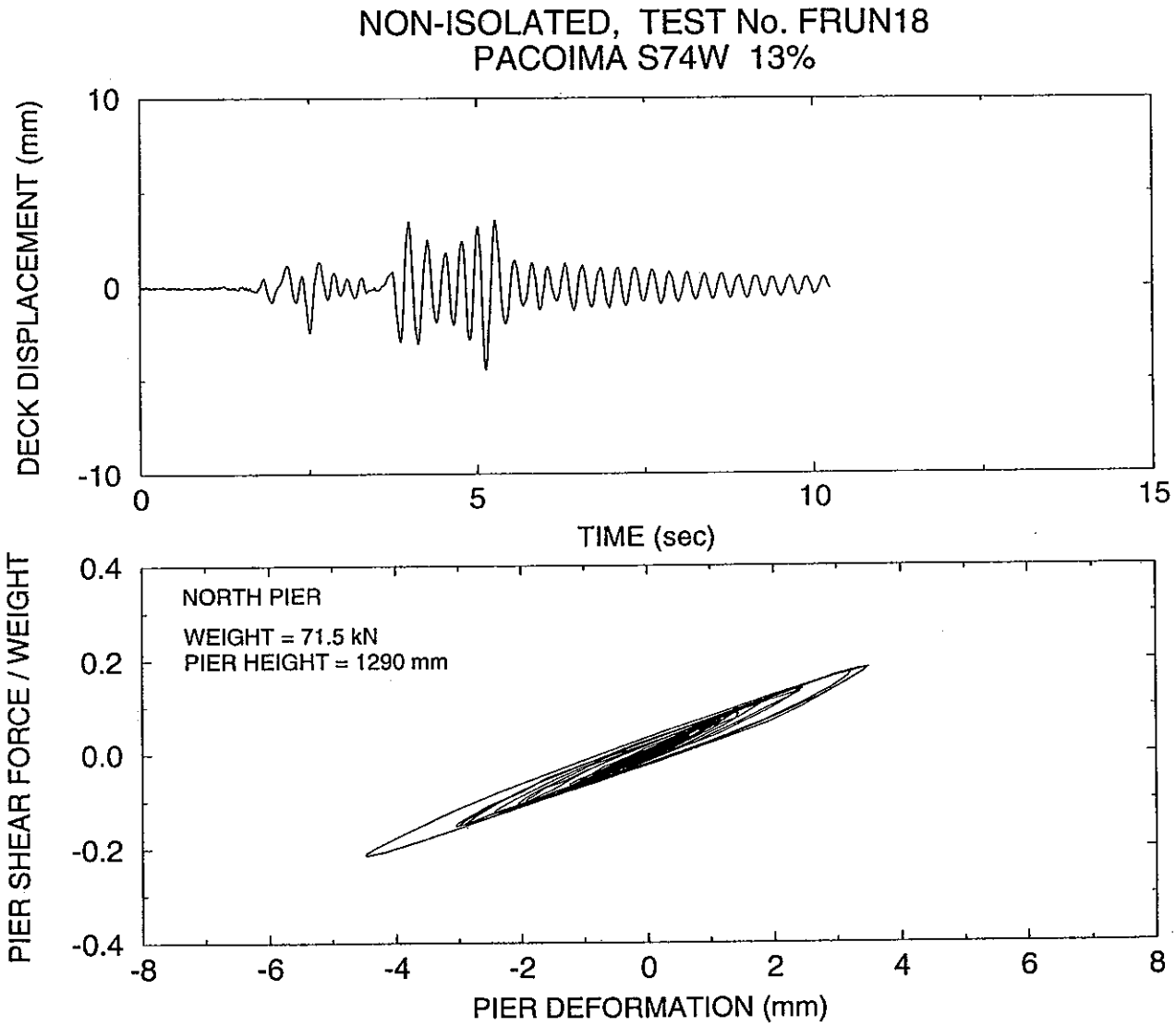
NON-ISOLATED, TEST No. FRUN18
PACOIMA S74W 13%
DECK DISPLACEMENT (mm)
10
0
-10
0
5
10
15
TIME (sec)
PIER SHEAR FORCE / WEIGHT
0.4
0.2
0.0
-0.2
-0.4
NORTH PIER
WEIGHT = 71.5 kN
PIER HEIGHT = 1290 mm
-8
-6
-4
-2
0
2
4
6
8
PIER DEFORMATION (mm)

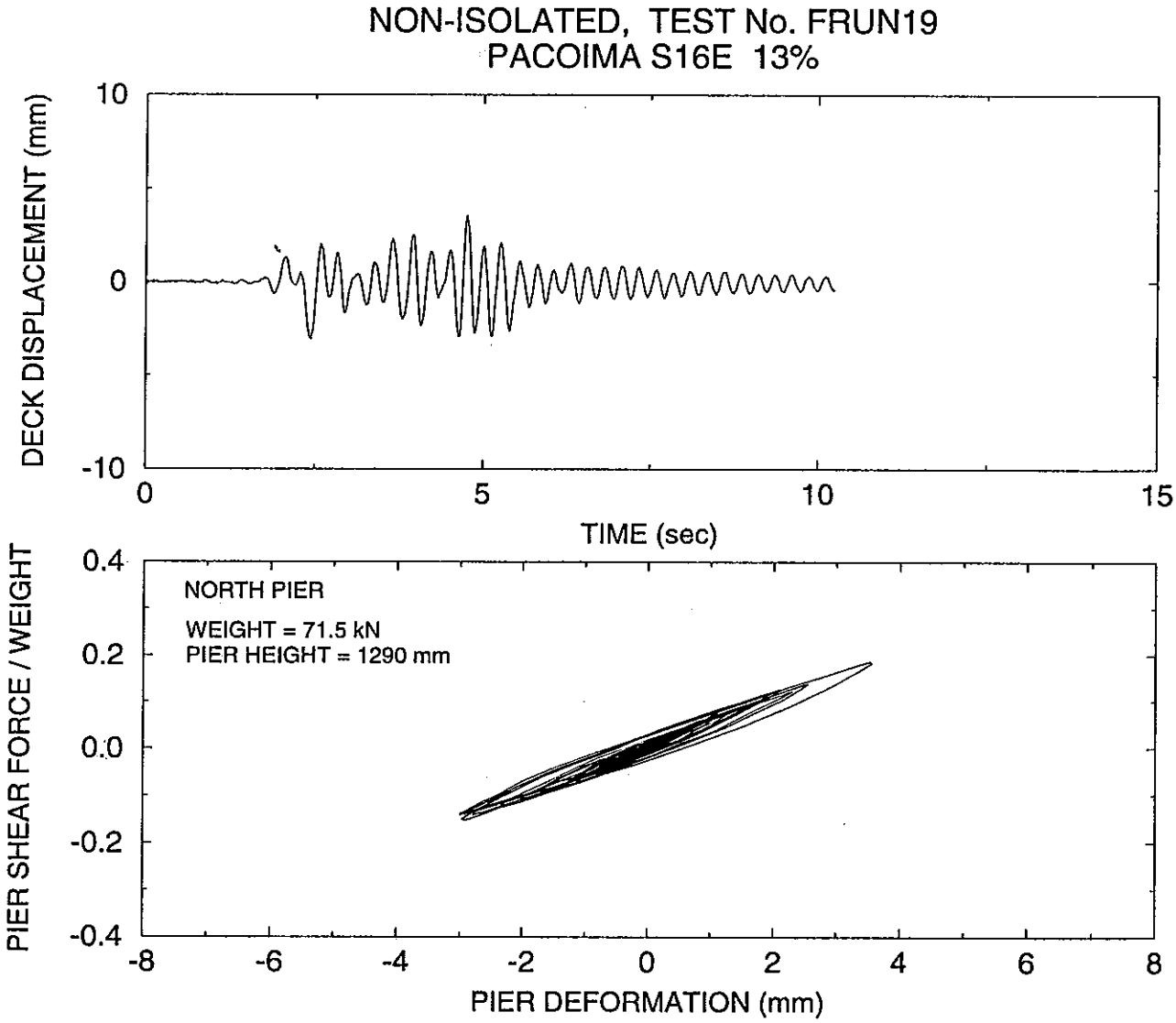
NON-ISOLATED, TEST No. FRUN19
PACOIMA S16E 13%
DECK DISPLACEMENT (mm)
10
0
-10
0
5
10
15
TIME (sec)
PIER SHEAR FORCE / WEIGHT
NORTH PIER
WEIGHT = 71.5 kN
PIER HEIGHT = 1290 mm
0.4
0.2
0.0
-0.2
-0.4
-8
-6
-4
-2
0
2
4
6
8
PIER DEFORMATION (mm)

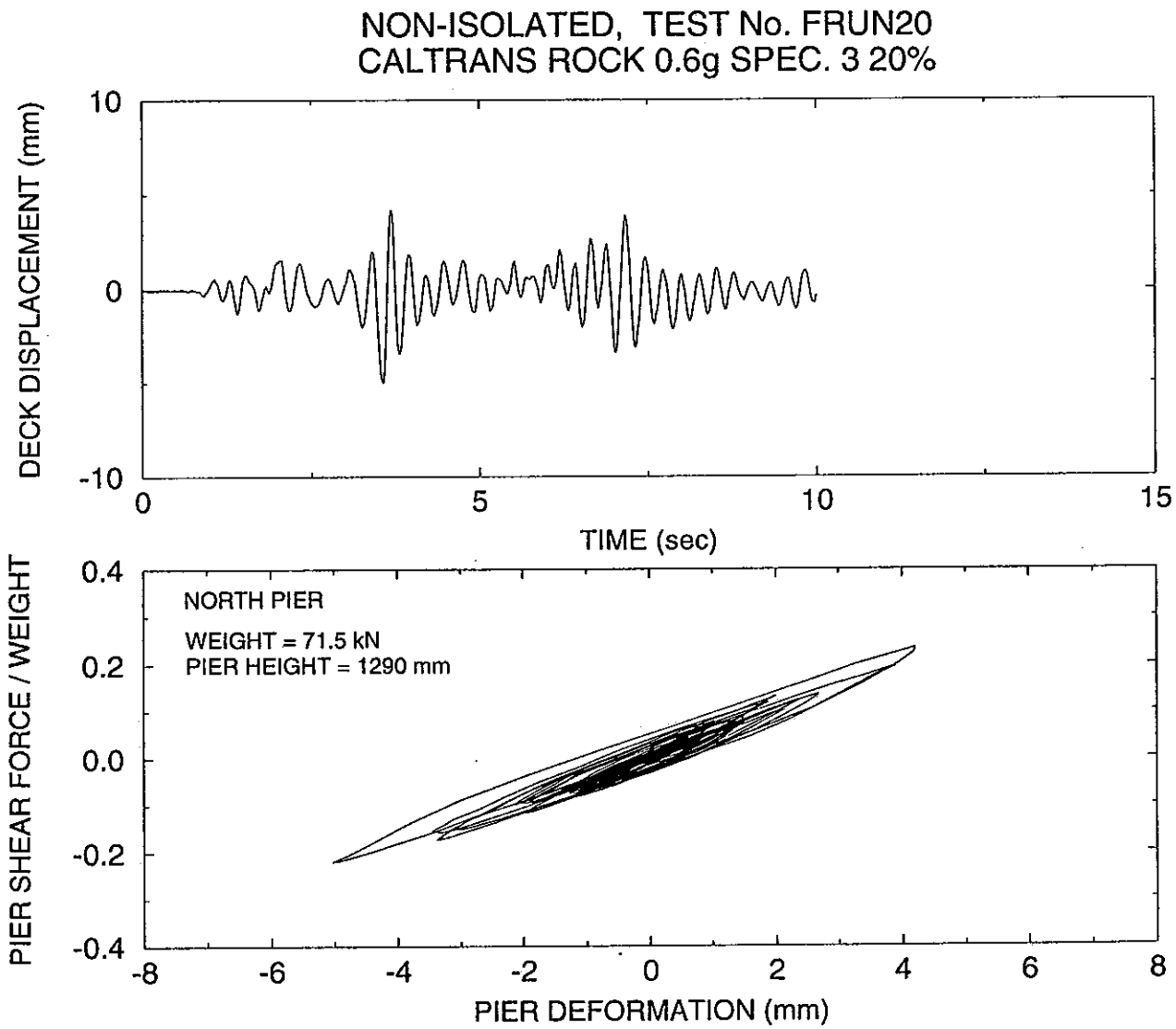
NON-ISOLATED, TEST No. FRUN20
CALTRANS ROCK 0.6g SPEC. 3 20%
DECK DISPLACEMENT (mm)
10
0
-10
0
5
10
15
TIME (sec)
PIER SHEAR FORCE / WEIGHT
0.4
0.2
0.0
-0.2
-0.4
NORTH PIER
WEIGHT = 71.5 kN
PIER HEIGHT = 1290 mm
-8
-6
-4
-2
0
2
4
6
8
PIER DEFORMATION (mm)

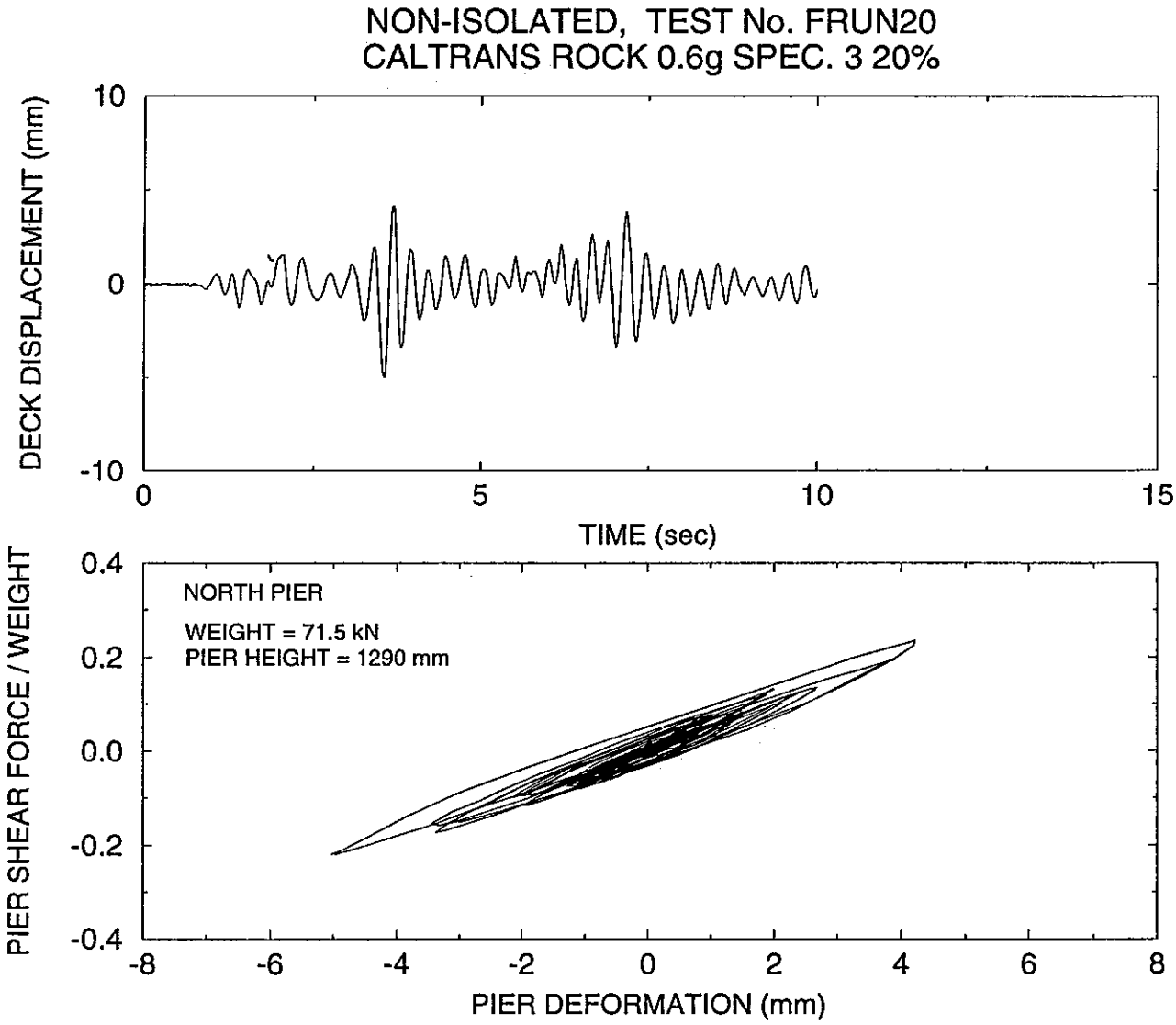
NON-ISOLATED, TEST No. FRUN20
CALTRANS ROCK 0.6g SPEC. 3 20%
DECK DISPLACEMENT (mm)
10
0
-10
0
5
10
15
TIME (sec)
PIER SHEAR FORCE / WEIGHT
0.4
0.2
0.0
-0.2
-0.4
NORTH PIER
WEIGHT = 71.5 kN
PIER HEIGHT = 1290 mm
-8
-6
-4
-2
0
2
4
6
8
PIER DEFORMATION (mm)

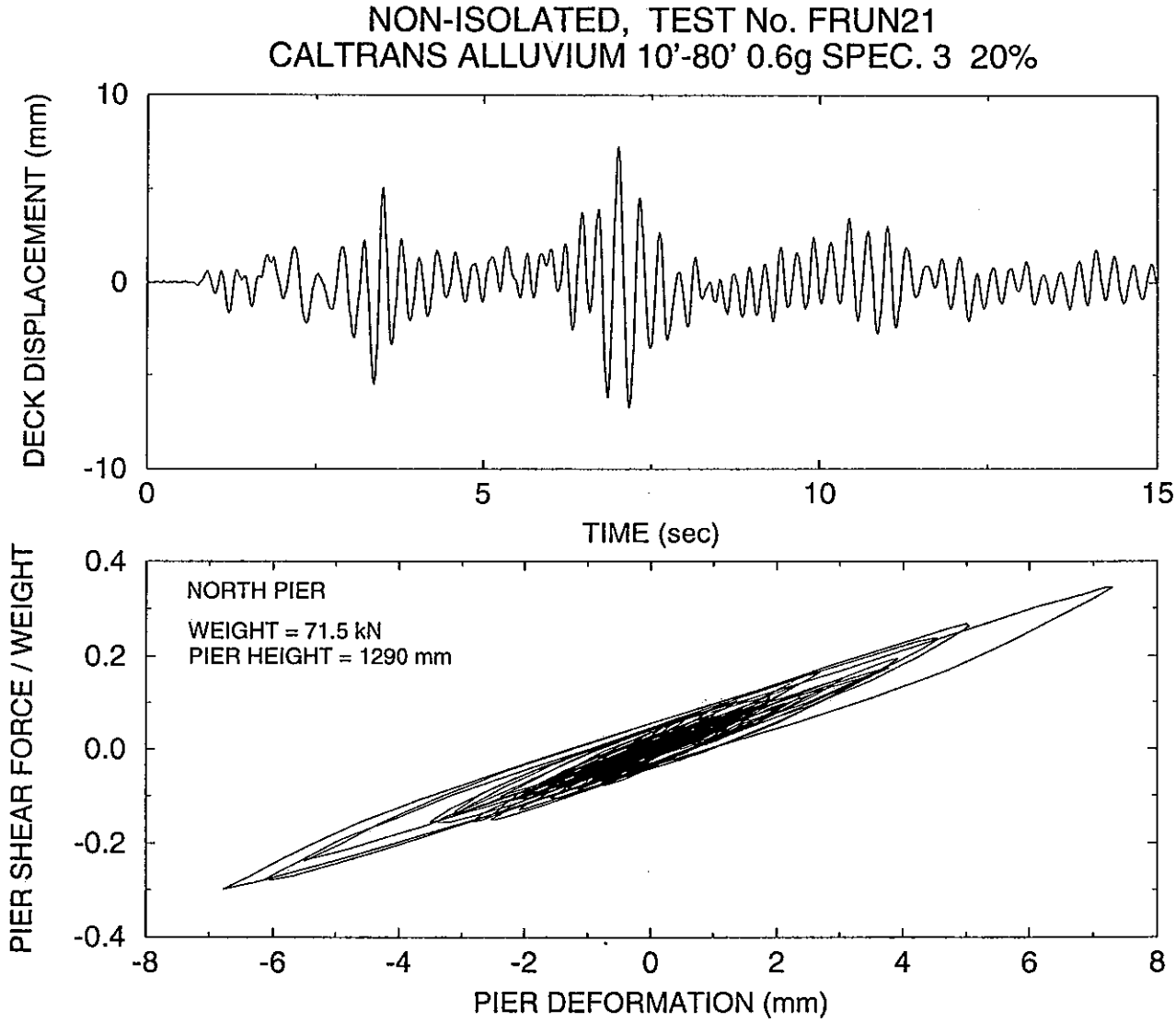
NON-ISOLATED, TEST No. FRUN21
CALTRANS ALLUVIUM 10'-80' 0.6g SPEC. 3 20%
DECK DISPLACEMENT (mm)
10
0
-10
0
5
10
15
TIME (sec)
PIER SHEAR FORCE / WEIGHT
NORTH PIER
WEIGHT = 71.5 kN
PIER HEIGHT = 1290 mm
0.4
0.2
0.0
-0.2
-0.4
-8
-6
-4
-2
0
2
4
6
8
PIER DEFORMATION (mm)

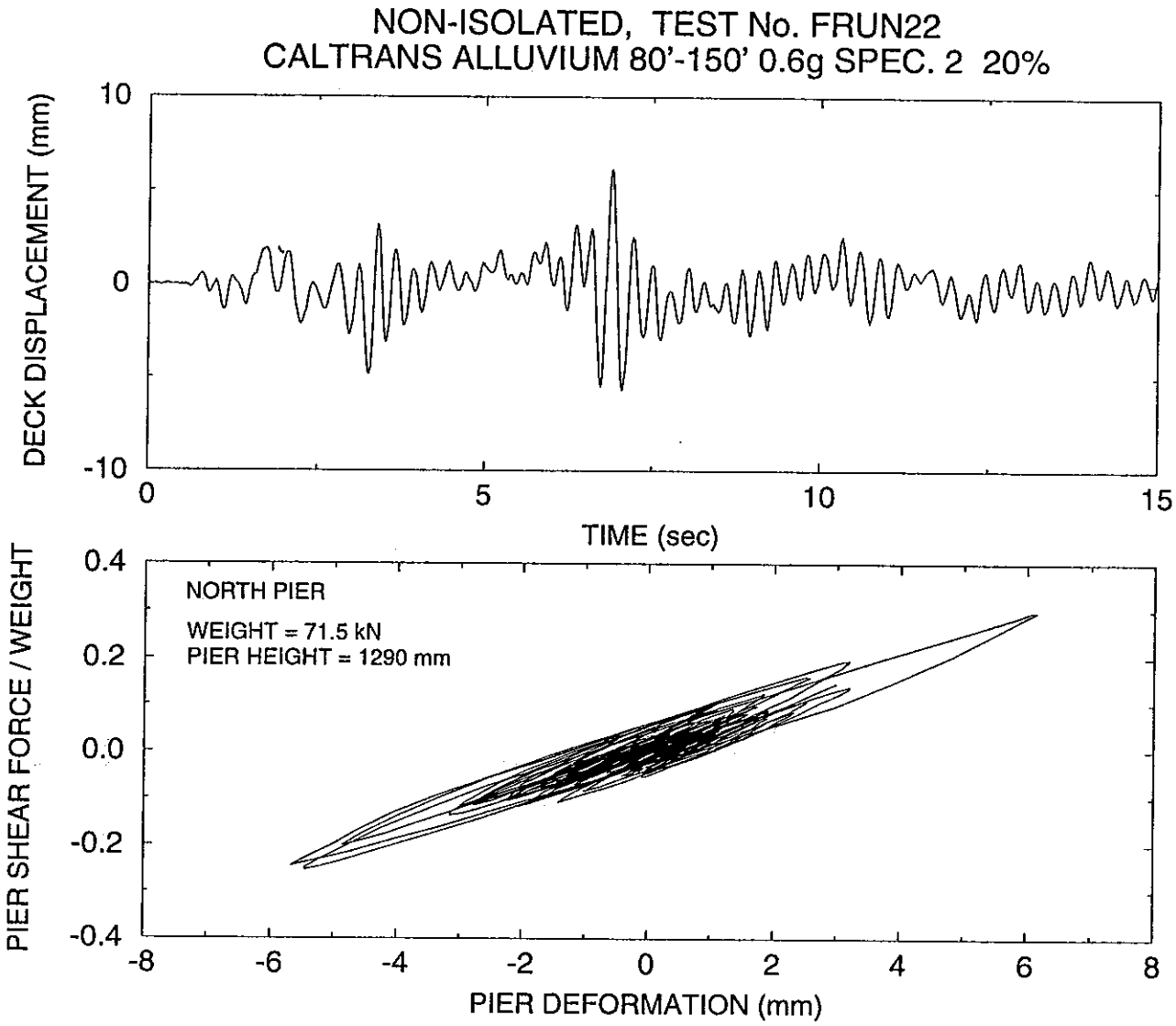
NON-ISOLATED, TEST No. FRUN22
CALTRANS ALLUVIUM 80'-150' 0.6g SPEC. 2 20%
DECK DISPLACEMENT (mm)
10
0
-10
0
5
10
15
TIME (sec)
PIER SHEAR FORCE / WEIGHT
0.4
0.2
0.0
-0.2
-0.4
NORTH PIER
WEIGHT = 71.5 kN
PIER HEIGHT = 1290 mm
-8
-6
-4
-2
0
2
4
6
8
PIER DEFORMATION (mm)

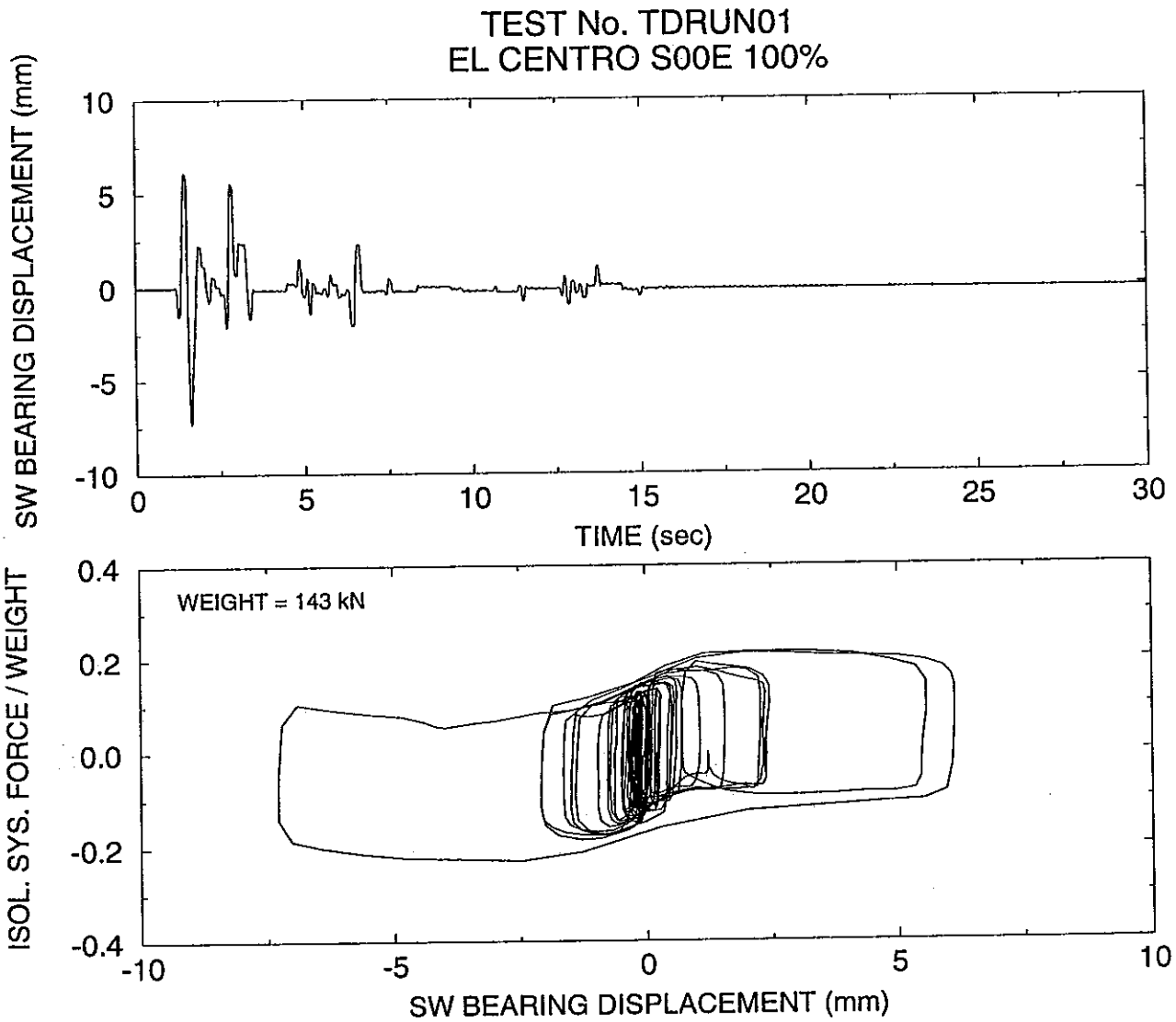
TEST No. TDRUN01
EL CENTRO S00E 100%
SW BEARING DISPLACEMENT (mm)
10
5
0
-5
-10
0
5
10
15
20
25
30
TIME (sec)
ISOL. SYS. FORCE / WEIGHT
WEIGHT = 143 kN
0.4
0.2
0.0
-0.2
-0.4
-10
-5
0
5
10
SW BEARING DISPLACEMENT (mm)

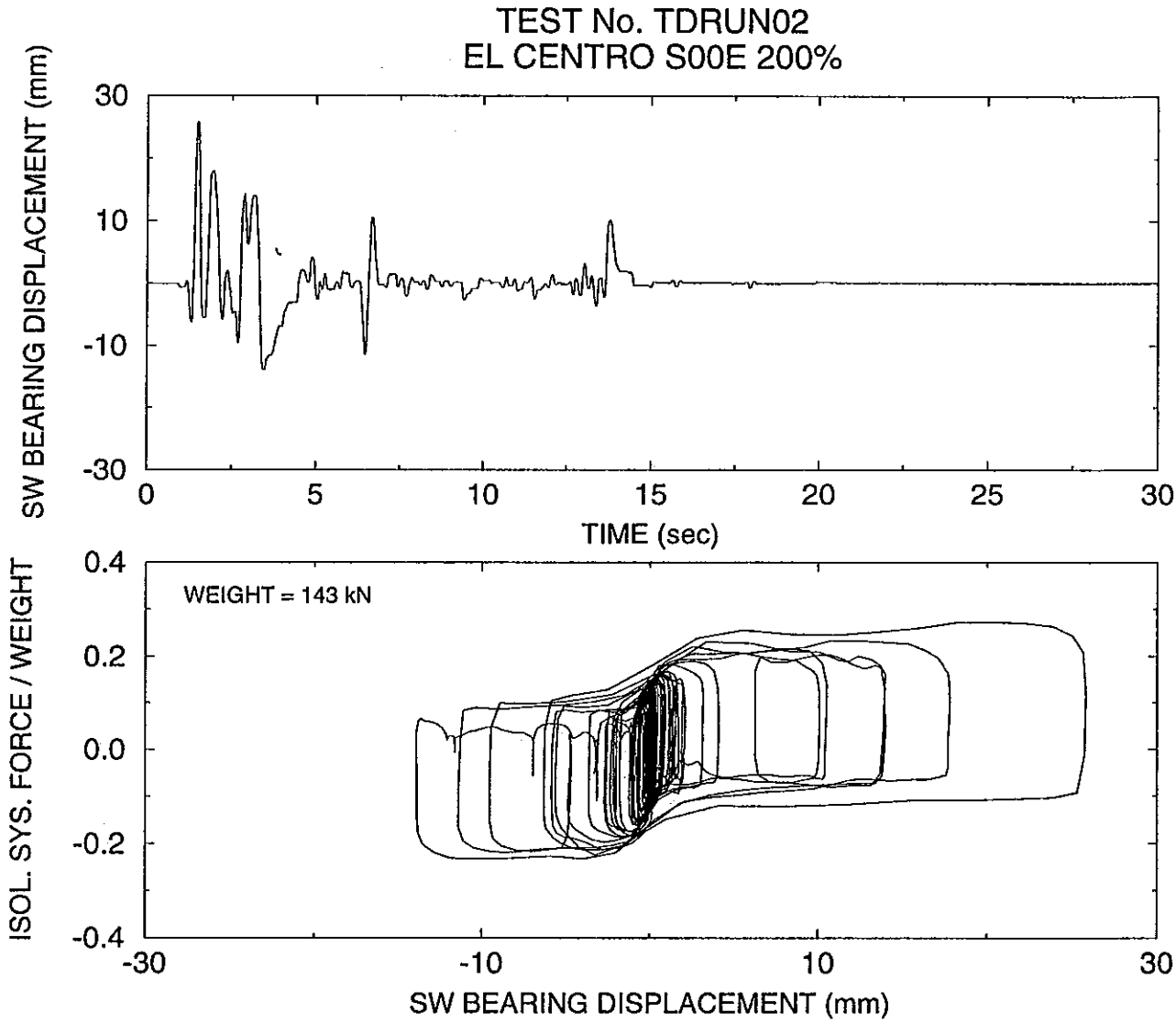
TEST No. TDRUN02
EL CENTRO S00E 200%
SW BEARING DISPLACEMENT (mm)
30
10
-10
-30
0
5
10
15
20
25
30
TIME (sec)
ISOL. SYS. FORCE / WEIGHT
WEIGHT = 143 kN
0.4
0.2
0.0
-0.2
-0.4
-30
-10
10
30
SW BEARING DISPLACEMENT (mm)

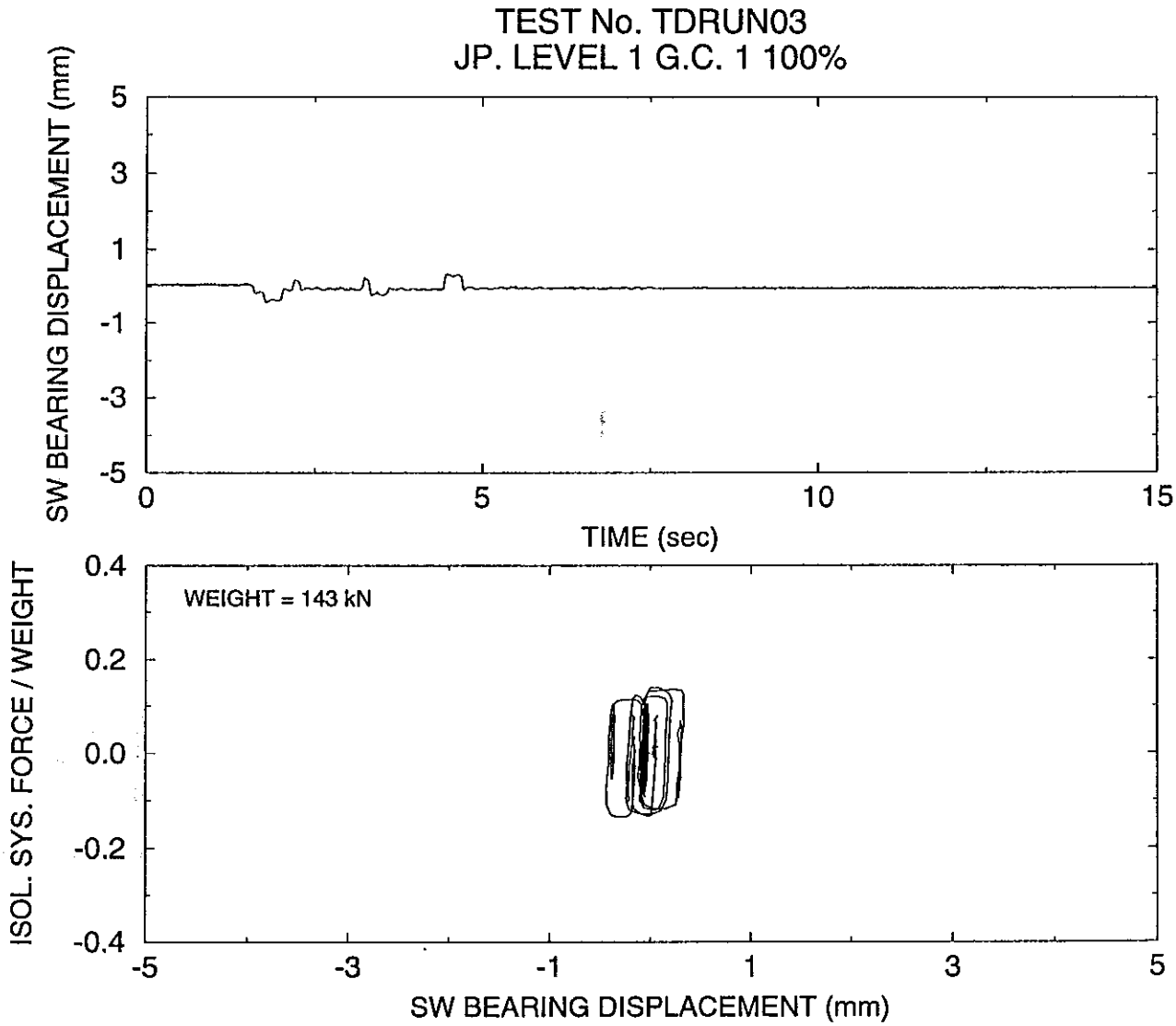
TEST No. TDRUN03
JP. LEVEL 1 G.C. 1 100%
SW BEARING DISPLACEMENT (mm)
5
3
1
-1
-3
-5
0
5
10
15
TIME (sec)
ISOL. SYS. FORCE / WEIGHT
0.4
0.2
0.0
-0.2
-0.4
WEIGHT = 143 kN
-5
-3
-1
1
3
5
SW BEARING DISPLACEMENT (mm)

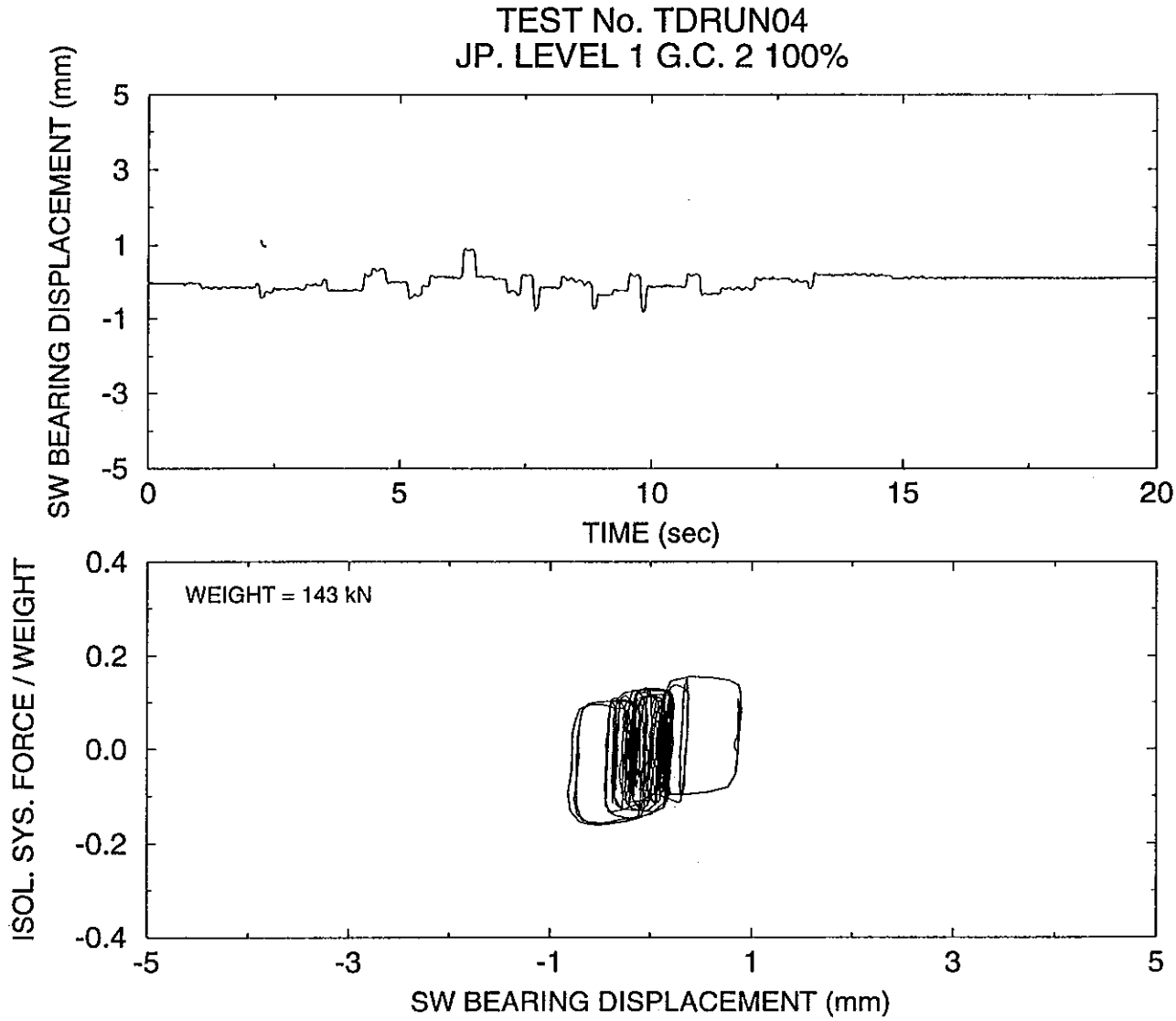
TEST No. TDRUN04
JP. LEVEL 1 G.C. 2 100%
SW BEARING DISPLACEMENT (mm)
5
3
1
-1
-3
-5
0
5
10
15
20
TIME (sec)
ISOL. SYS. FORCE / WEIGHT
WEIGHT = 143 kN
0.4
0.2
0.0
-0.2
-0.4
-5
-3
-1
1
3
5
SW BEARING DISPLACEMENT (mm)

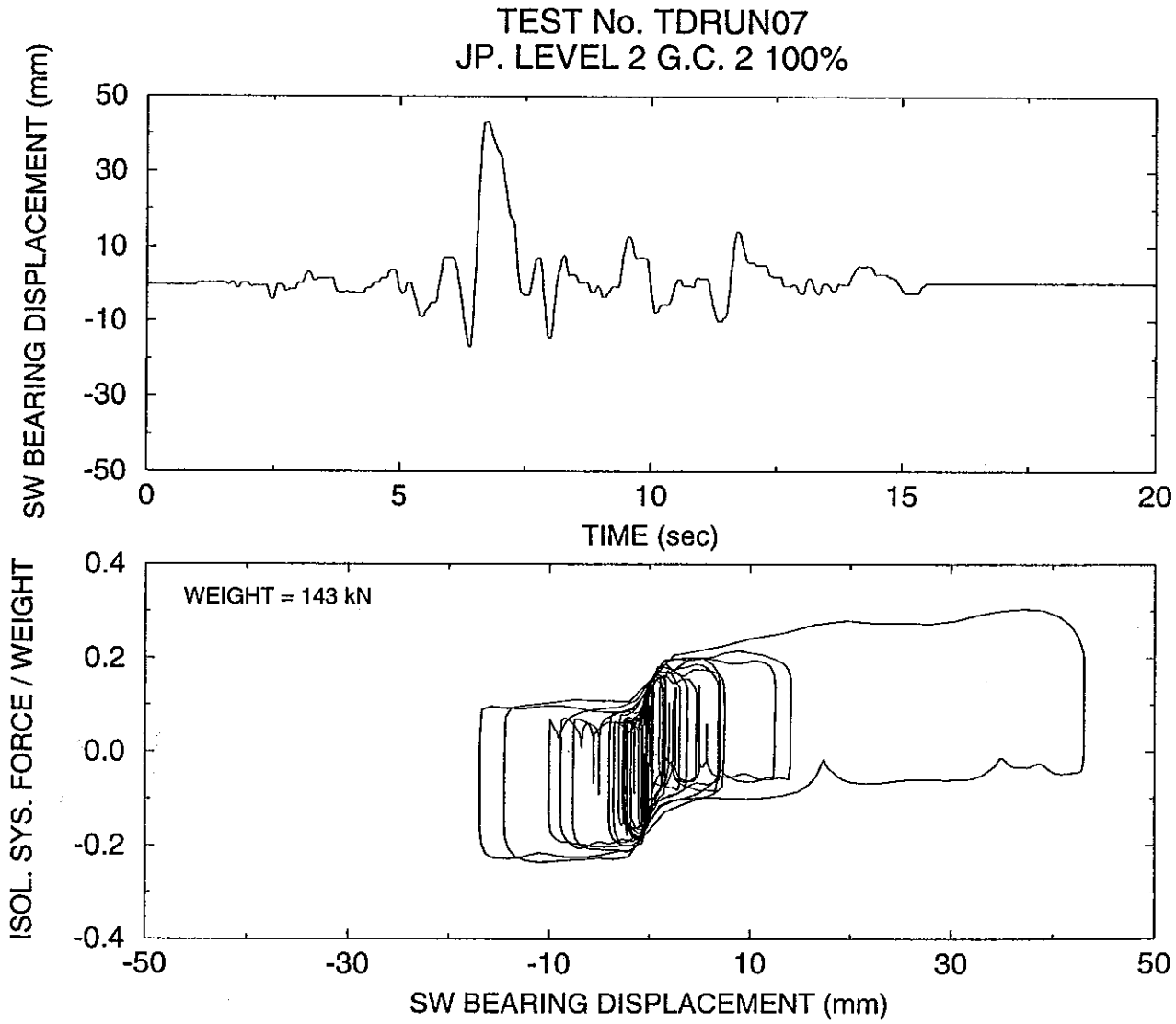
TEST No. TDRUN07
JP. LEVEL 2 G.C. 2 100%
SW BEARING DISPLACEMENT (mm)
50
30
10
-10
-30
-50
0
5
10
15
20
TIME (sec)
ISOL. SYS. FORCE / WEIGHT
WEIGHT = 143 kN
0.4
0.2
0.0
-0.2
-0.4
-50
-30
-10
10
30
50
SW BEARING DISPLACEMENT (mm)

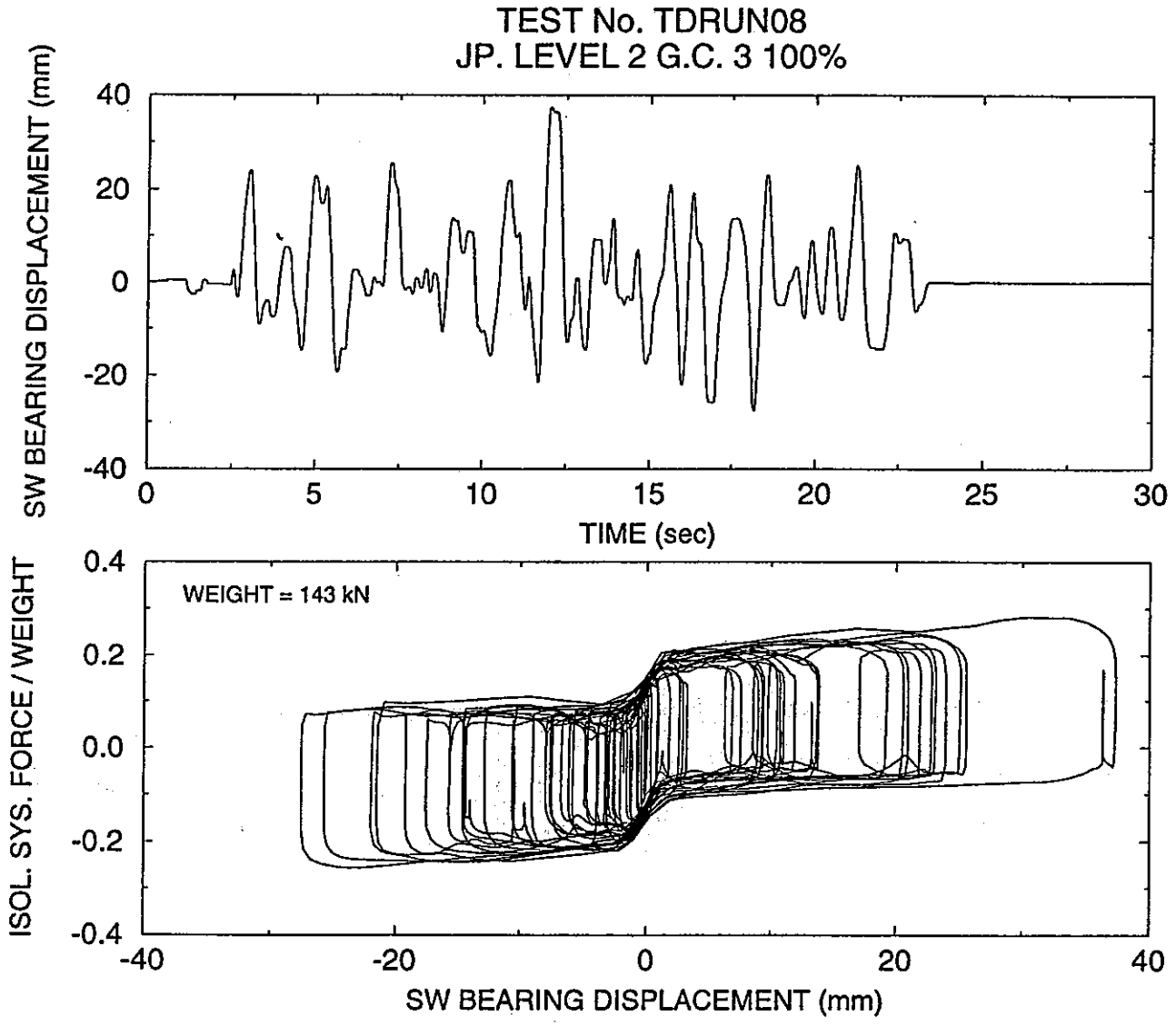
TEST No. TDRUN08
JP. LEVEL 2 G.C. 3 100%
SW BEARING DISPLACEMENT (mm)
40
20
0
-20
-40
0
5
10
15
20
25
30
TIME (sec)
ISOL. SYS. FORCE / WEIGHT
WEIGHT = 143 kN
0.4
0.2
0.0
-0.2
-0.4
-40
-20
0
20
40
SW BEARING DISPLACEMENT (mm)

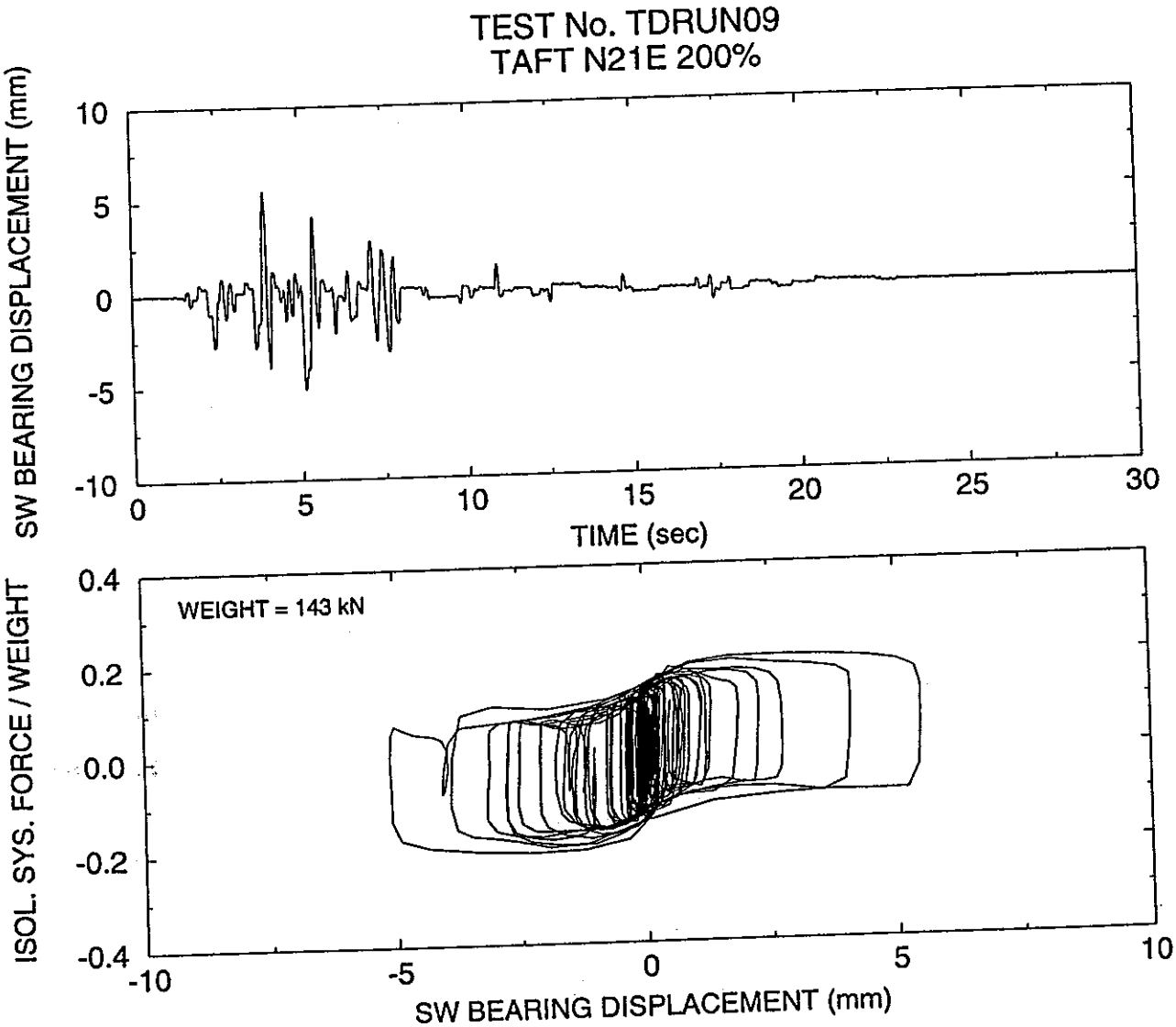
TEST No. TDRUN09
TAFT N21E 200%
SW BEARING DISPLACEMENT (mm)
10
5
0
-5
-10
0
5
10
15
20
25
30
TIME (sec)
ISOL. SYS. FORCE / WEIGHT
WEIGHT = 143 kN
0.4
0.2
0.0
-0.2
-0.4
-10
-5
0
5
10
SW BEARING DISPLACEMENT (mm)

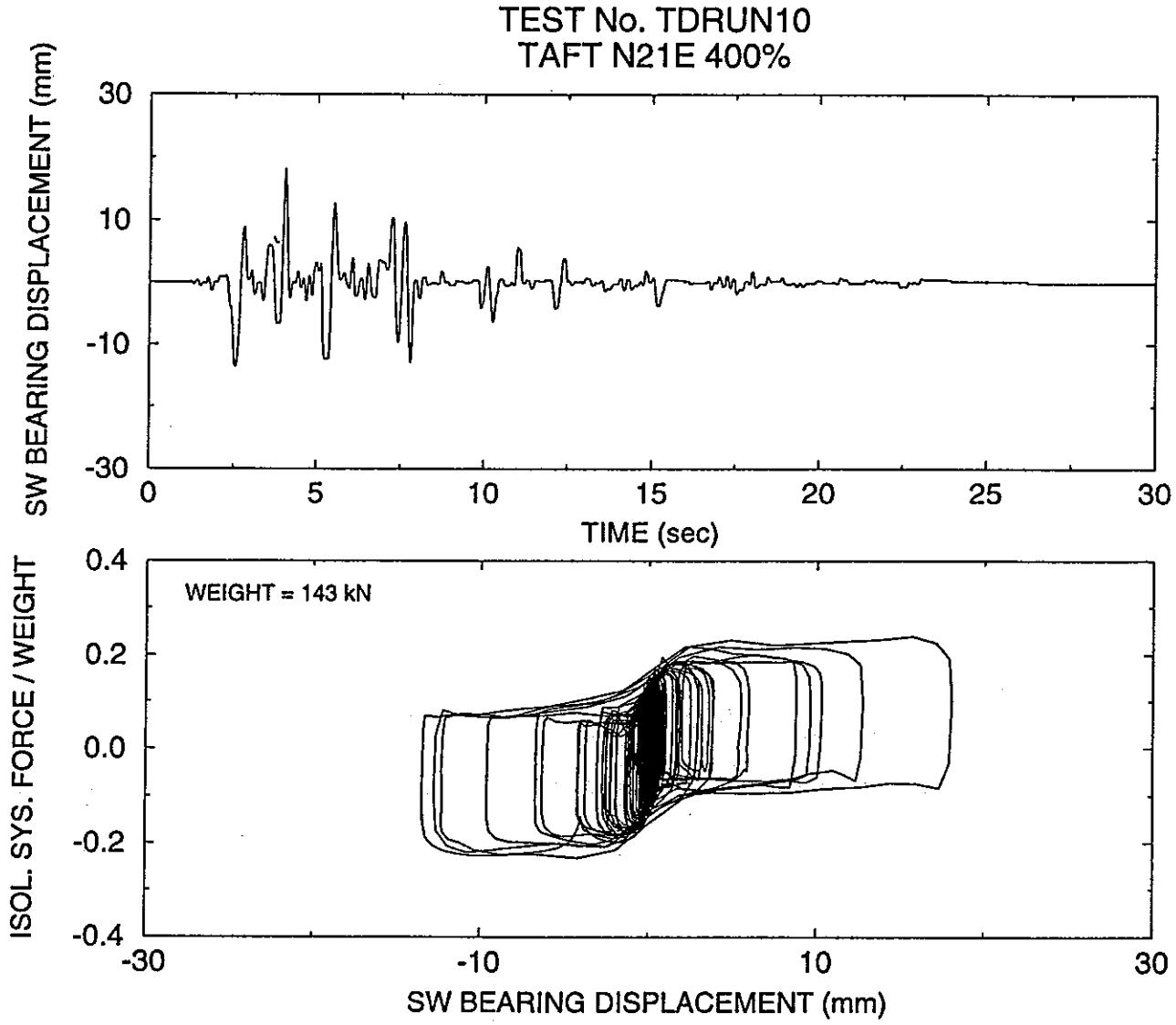
TEST No. TDRUN10
TAFT N21E 400%
SW BEARING DISPLACEMENT (mm)
30
10
-10
-30
0
5
10
15
20
25
30
TIME (sec)
ISOL. SYS. FORCE / WEIGHT
WEIGHT = 143 kN
0.4
0.2
0.0
-0.2
-0.4
-30
-10
10
30
SW BEARING DISPLACEMENT (mm)

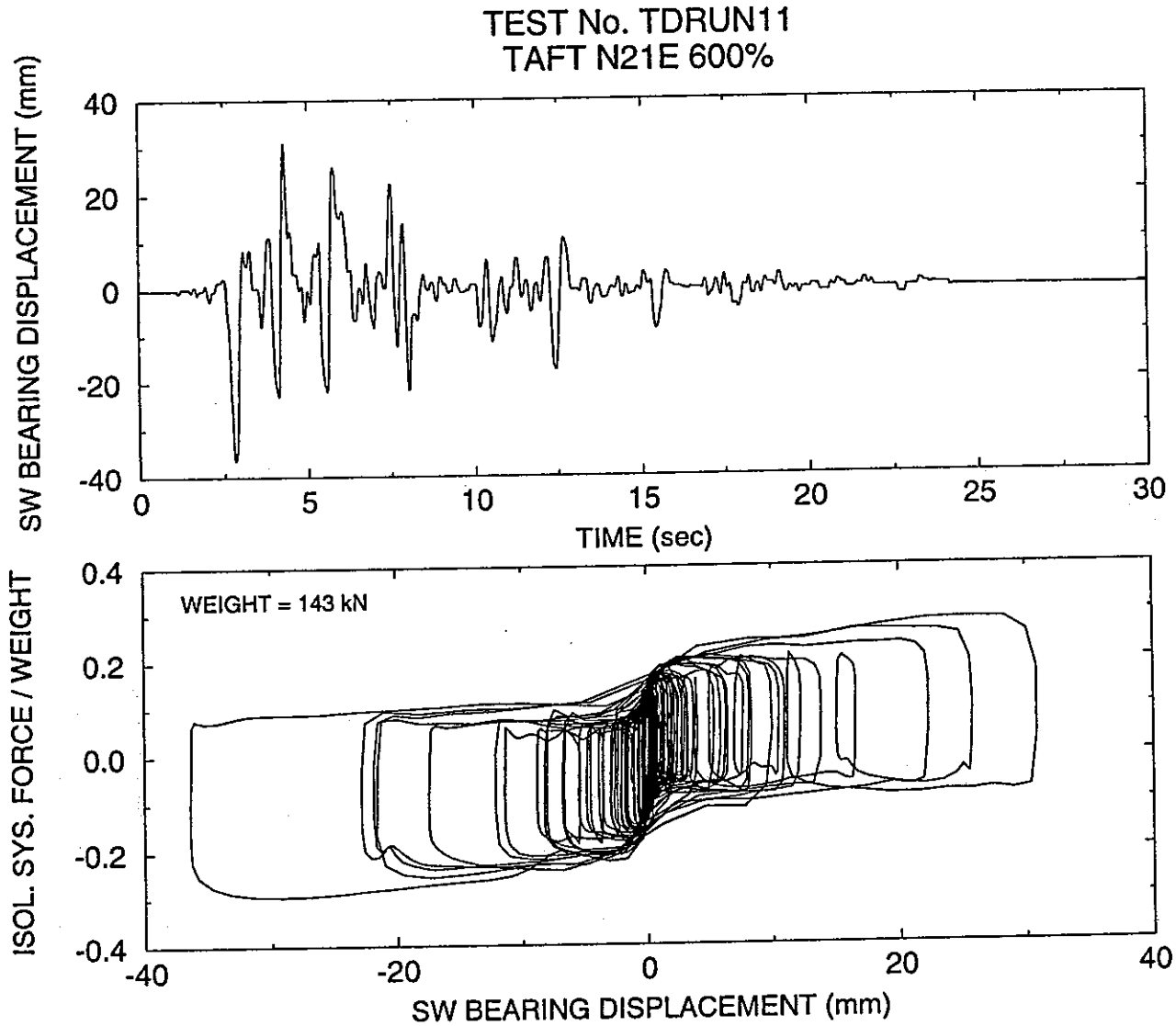
TEST No. TDRUN11
TAFT N21E 600%
SW BEARING DISPLACEMENT (mm)
40
20
0
-20
-40
0
5
10
15
20
25
30
TIME (sec)
ISOL. SYS. FORCE / WEIGHT
WEIGHT = 143 kN
0.4
0.2
0.0
-0.2
-0.4
-40
-20
0
20
40
SW BEARING DISPLACEMENT (mm)

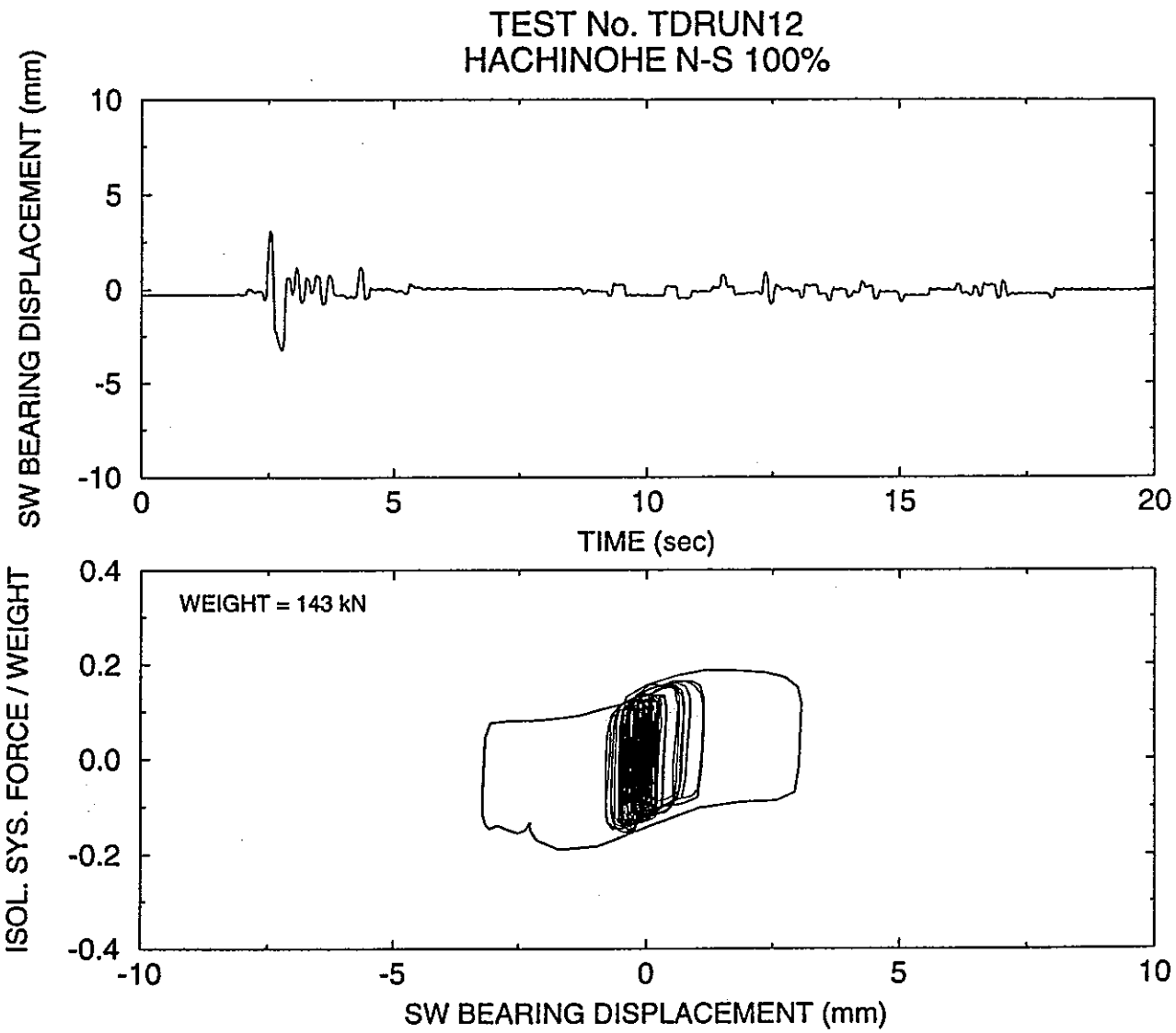
TEST No. TDRUN12
HACHINOHE N-S 100%
SW BEARING DISPLACEMENT (mm)
10
5
0
-5
-10
0
5
10
15
20
TIME (sec)
ISOL. SYS. FORCE / WEIGHT
WEIGHT = 143 kN
0.4
0.2
0.0
-0.2
-0.4
-10
-5
0
5
10
SW BEARING DISPLACEMENT (mm)

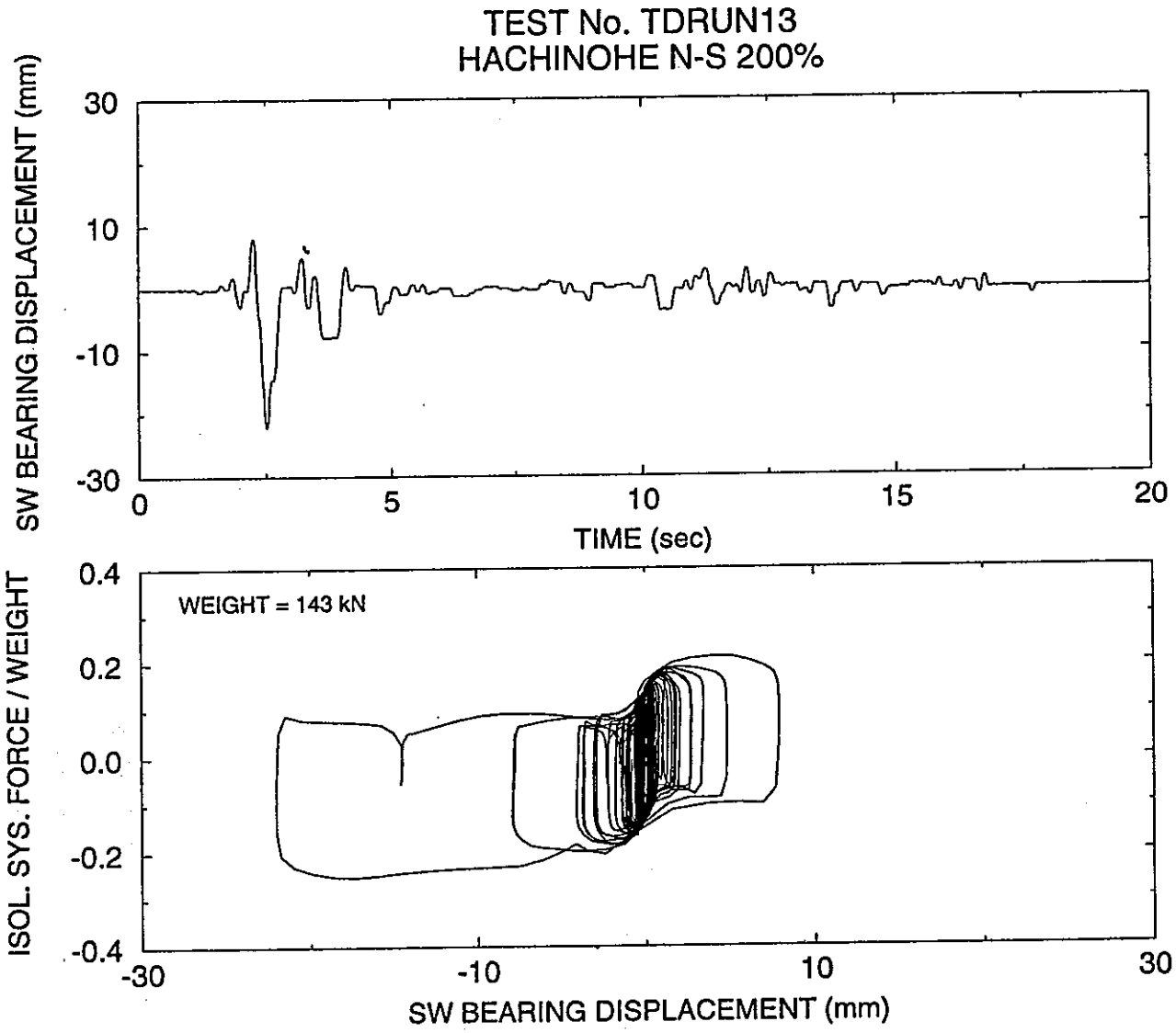
TEST No. TDRUN13
HACHINOHE N-S 200%
SW BEARING DISPLACEMENT (mm)
30
10
-10
-30
0
5
10
15
20
TIME (sec)
ISOL. SYS. FORCE / WEIGHT
WEIGHT = 143 kN
0.4
0.2
0.0
-0.2
-0.4
-30
-10
10
30
SW BEARING DISPLACEMENT (mm)

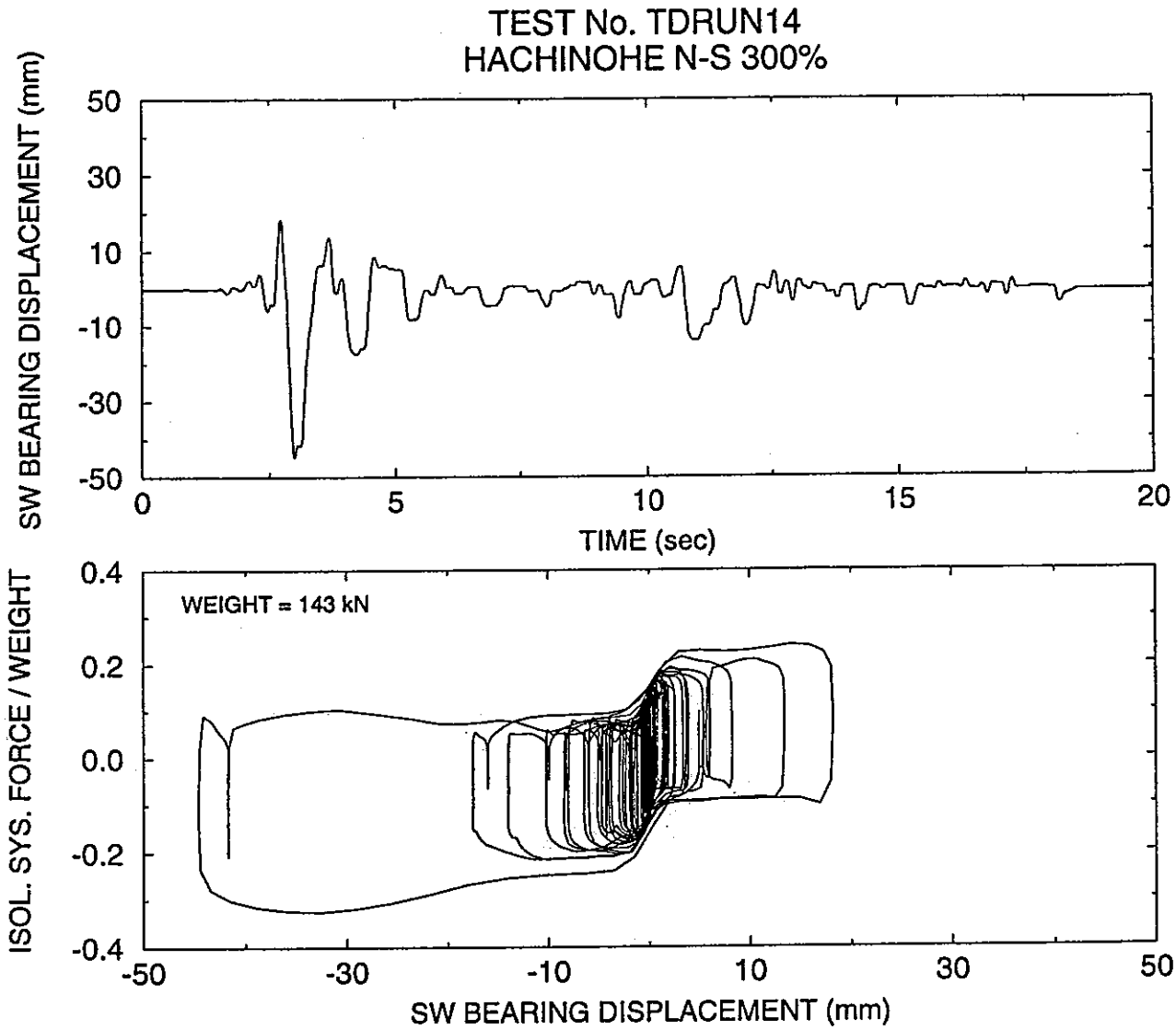
TEST No. TDRUN14
HACHINOHE N-S 300%
SW BEARING DISPLACEMENT (mm)
50
30
10
-10
-30
-50
0
5
10
15
20
TIME (sec)
ISOL. SYS. FORCE / WEIGHT
WEIGHT = 143 kN
0.4
0.2
0.0
-0.2
-0.4
-50
-30
-10
10
30
50
SW BEARING DISPLACEMENT (mm)

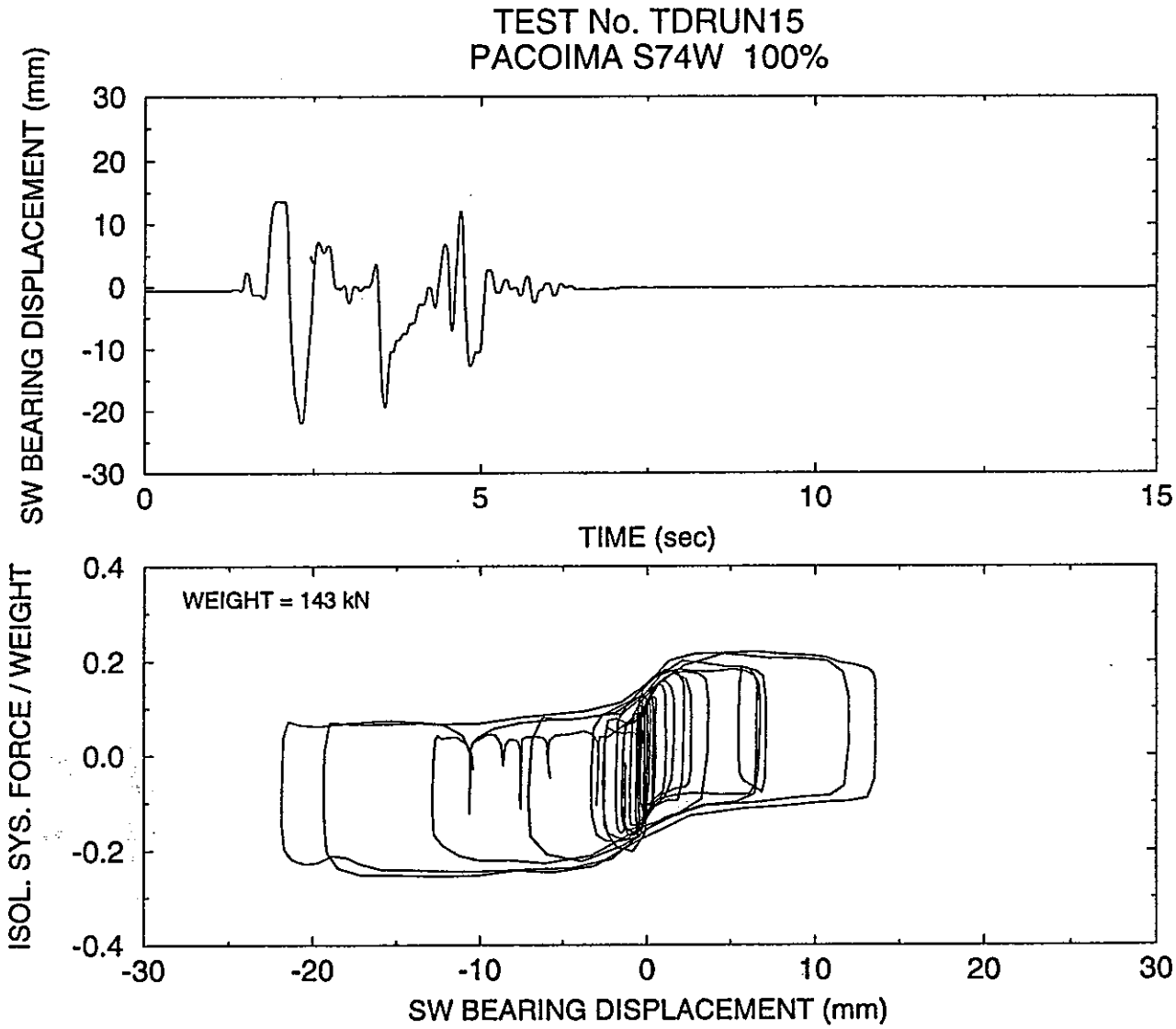
TEST No. TDRUN15
PACOIMA S74W 100%
SW BEARING DISPLACEMENT (mm)
30
20
10
0
-10
-20
-30
0
5
10
15
TIME (sec)
ISOL. SYS. FORCE / WEIGHT
WEIGHT = 143 kN
0.4
0.2
0.0
-0.2
-0.4
-30
-20
-10
0
10
20
30
SW BEARING DISPLACEMENT (mm)

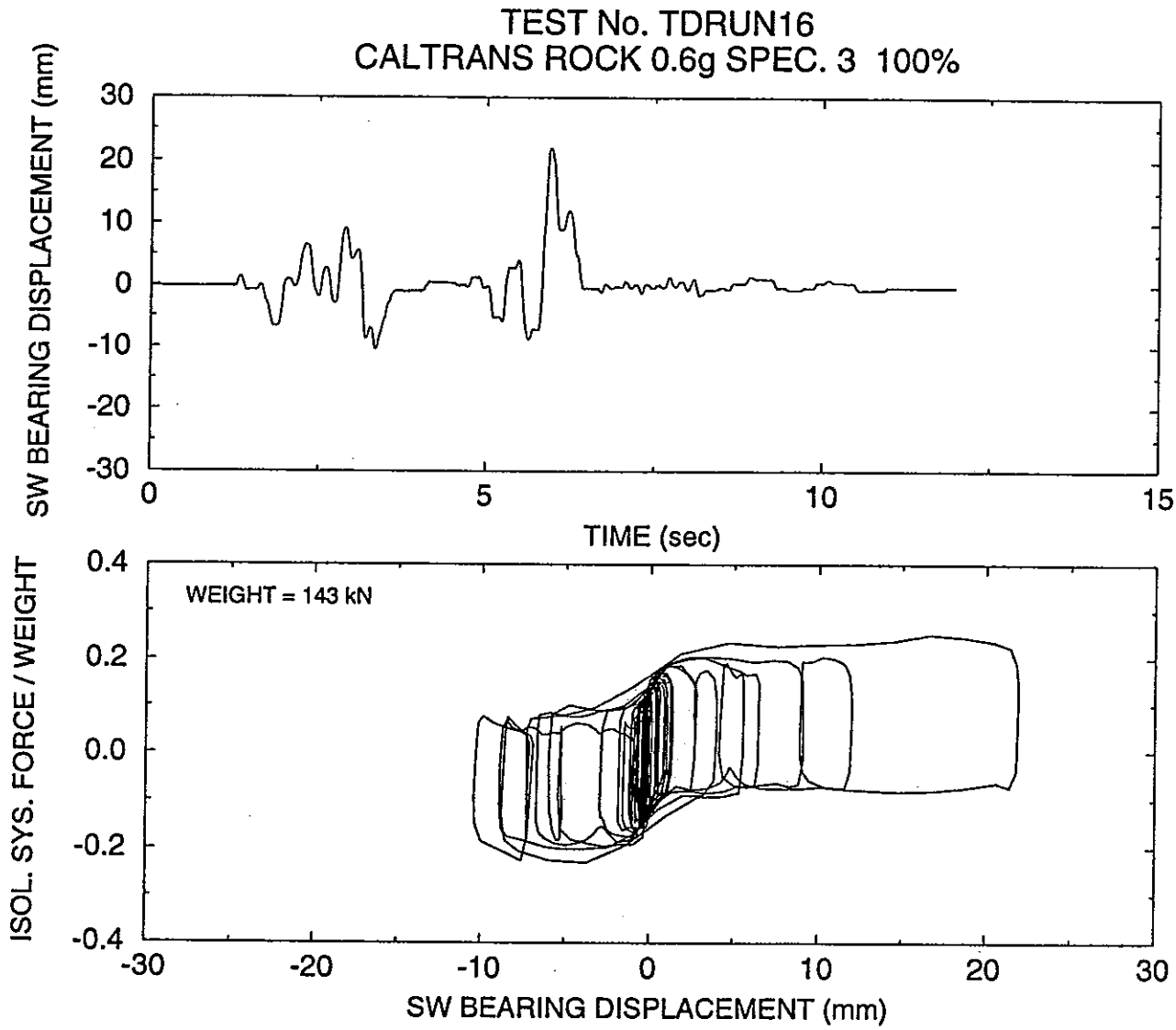
TEST No. TDRUN16
CALTRANS ROCK 0.6g SPEC. 3 100%
SW BEARING DISPLACEMENT (mm)
30
20
10
0
-10
-20
-30
0
5
10
15
TIME (sec)
ISOL. SYS. FORCE / WEIGHT
WEIGHT = 143 kN
0.4
0.2
0.0
-0.2
-0.4
-30
-20
-10
0
10
20
30
SW BEARING DISPLACEMENT (mm)

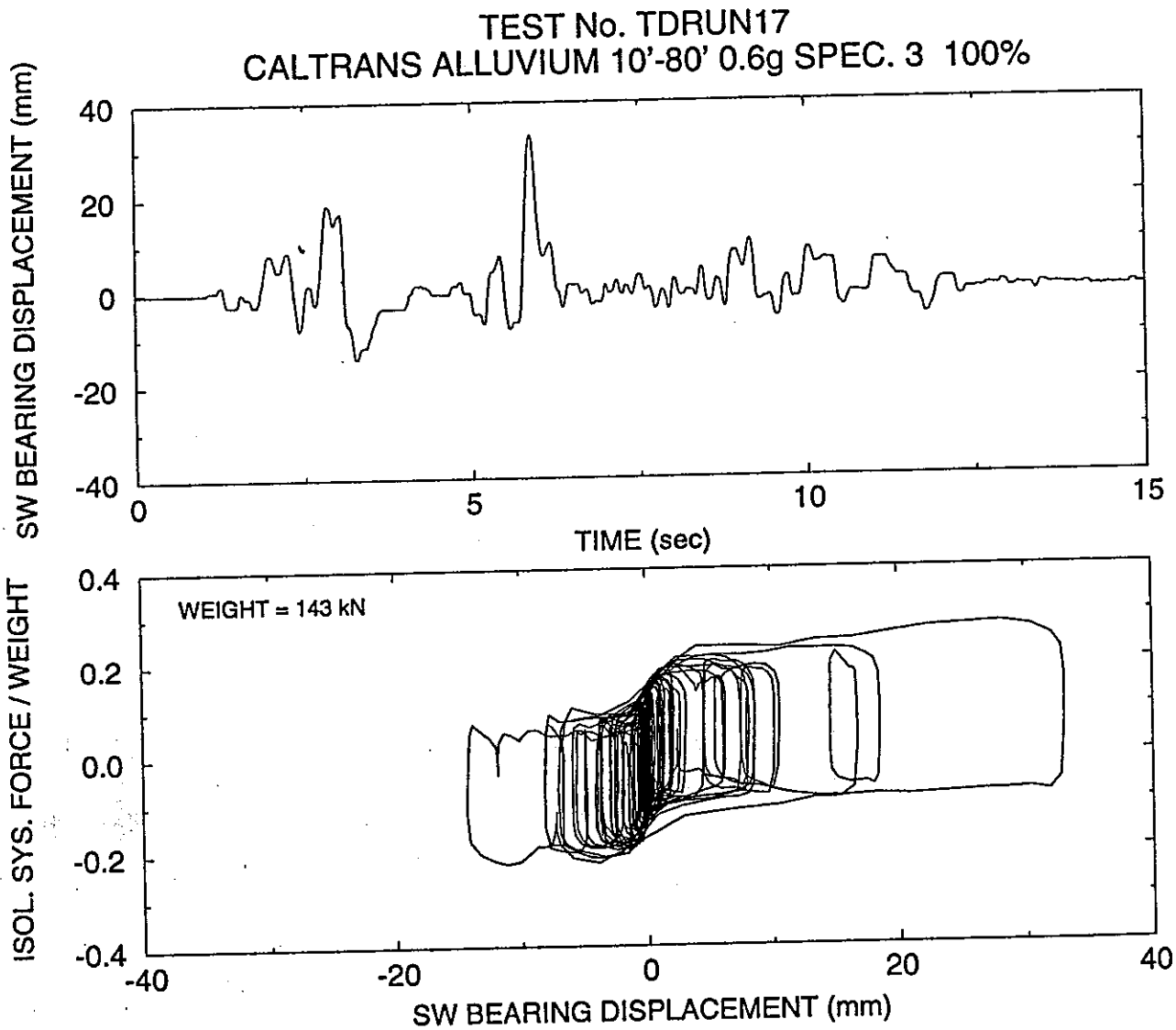
TEST No. TDRUN17
CALTRANS ALLUVIUM 10'-80' 0.6g SPEC. 3 100%
SW BEARING DISPLACEMENT (mm)
40
20
0
-20
-40
0
5
10
15
TIME (sec)
ISOL. SYS. FORCE / WEIGHT
WEIGHT = 143 kN
0.4
0.2
0.0
-0.2
-0.4
-40
-20
0
20
40
SW BEARING DISPLACEMENT (mm)

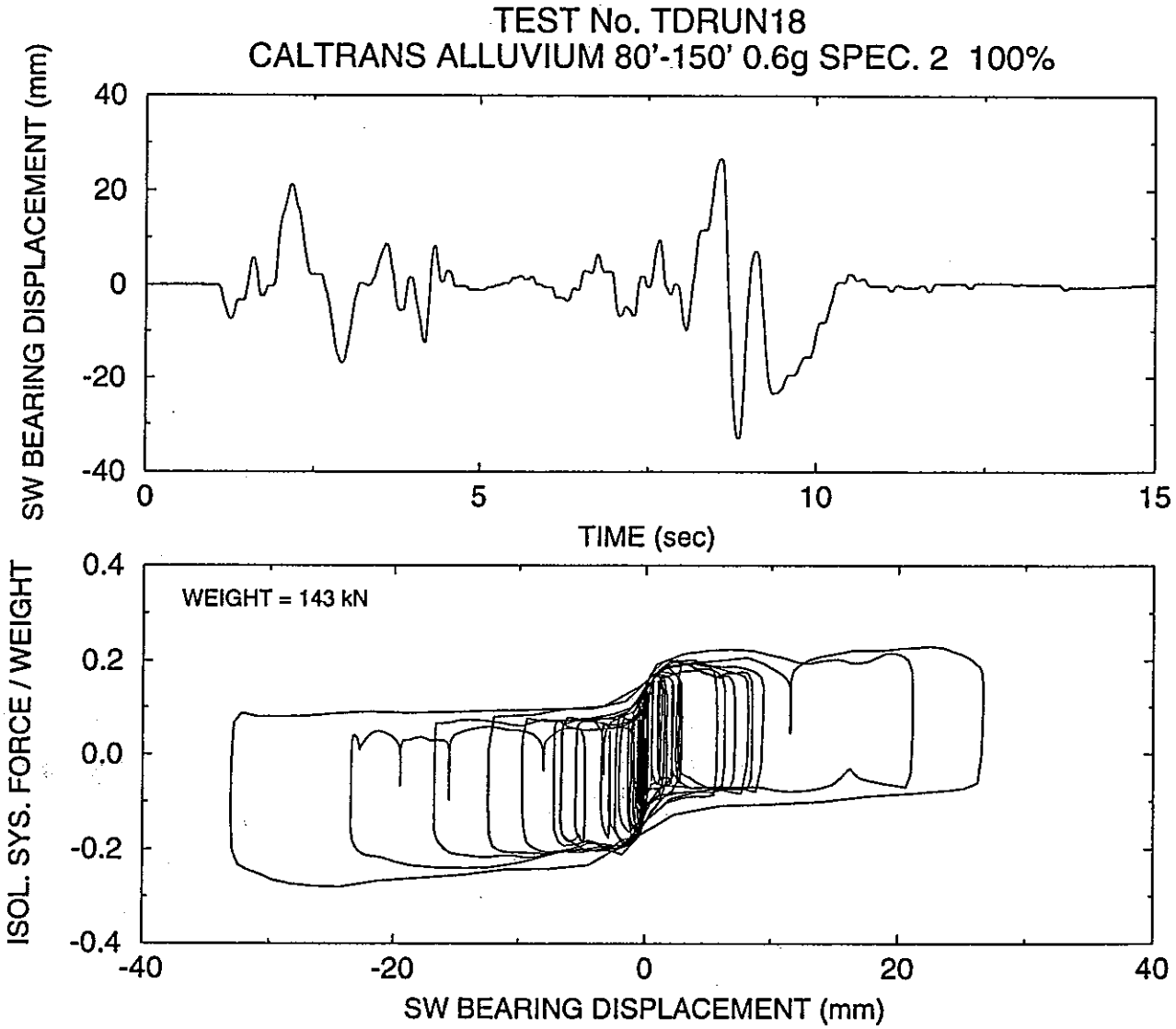
TEST No. TDRUN18
CALTRANS ALLUVIUM 80'-150' 0.6g SPEC. 2 100%
SW BEARING DISPLACEMENT (mm)
40
20
0
-20
-40
0
5
10
15
TIME (sec)
ISOL. SYS. FORCE / WEIGHT
WEIGHT = 143 kN
0.4
0.2
0.0
-0.2
-0.4
-40
-20
0
20
40
SW BEARING DISPLACEMENT (mm)

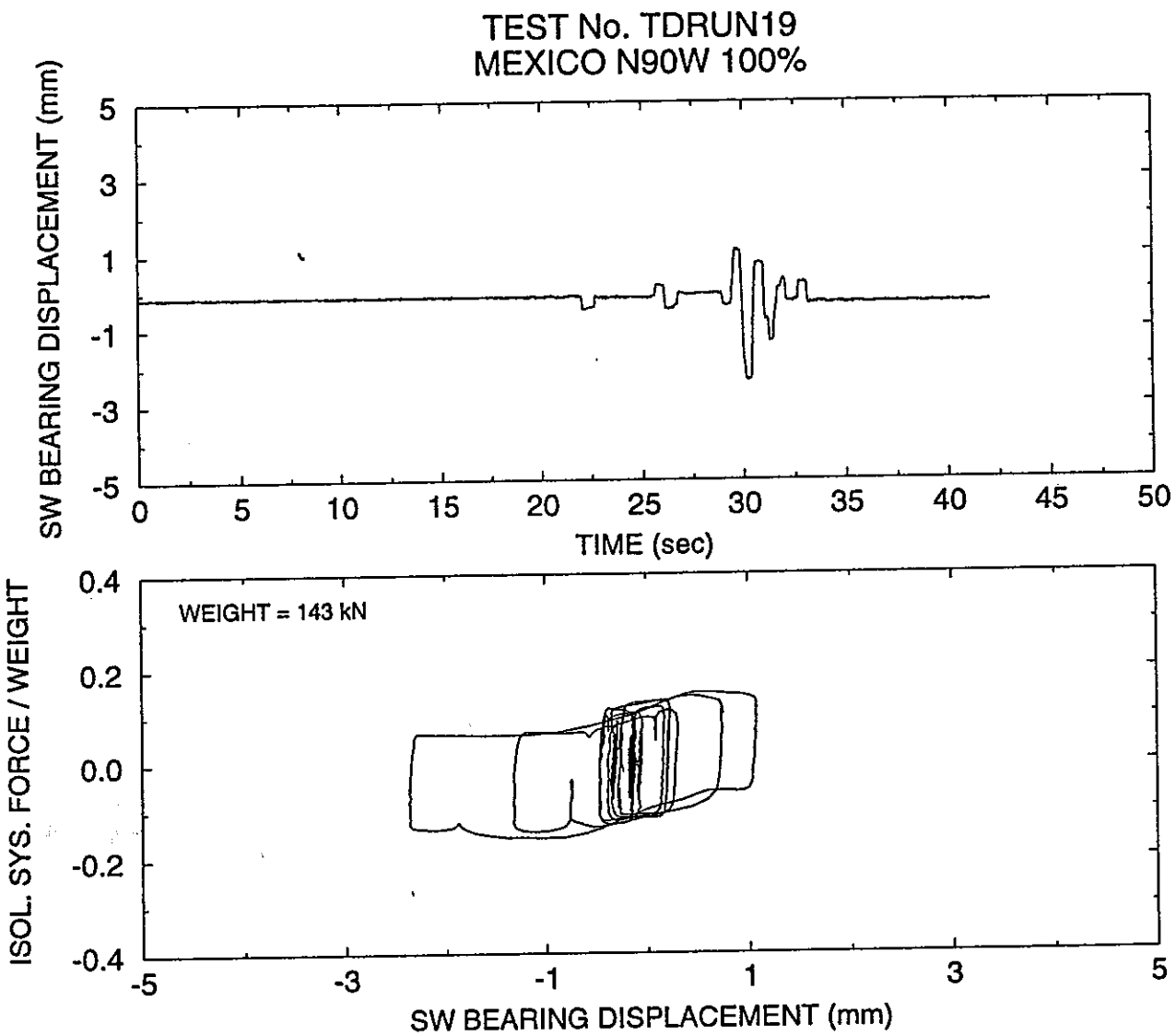
TEST No. TDRUN19
MEXICO N90W 100%
SW BEARING DISPLACEMENT (mm)
5
3
1
-1
-3
-5
0
5
10
15
20
25
30
35
40
45
50
TIME (sec)
ISOL. SYS. FORCE / WEIGHT
WEIGHT = 143 kN
0.4
0.2
0.0
-0.2
-0.4
-5
-3
-1
1
3
5
SW BEARING DISPLACEMENT (mm)

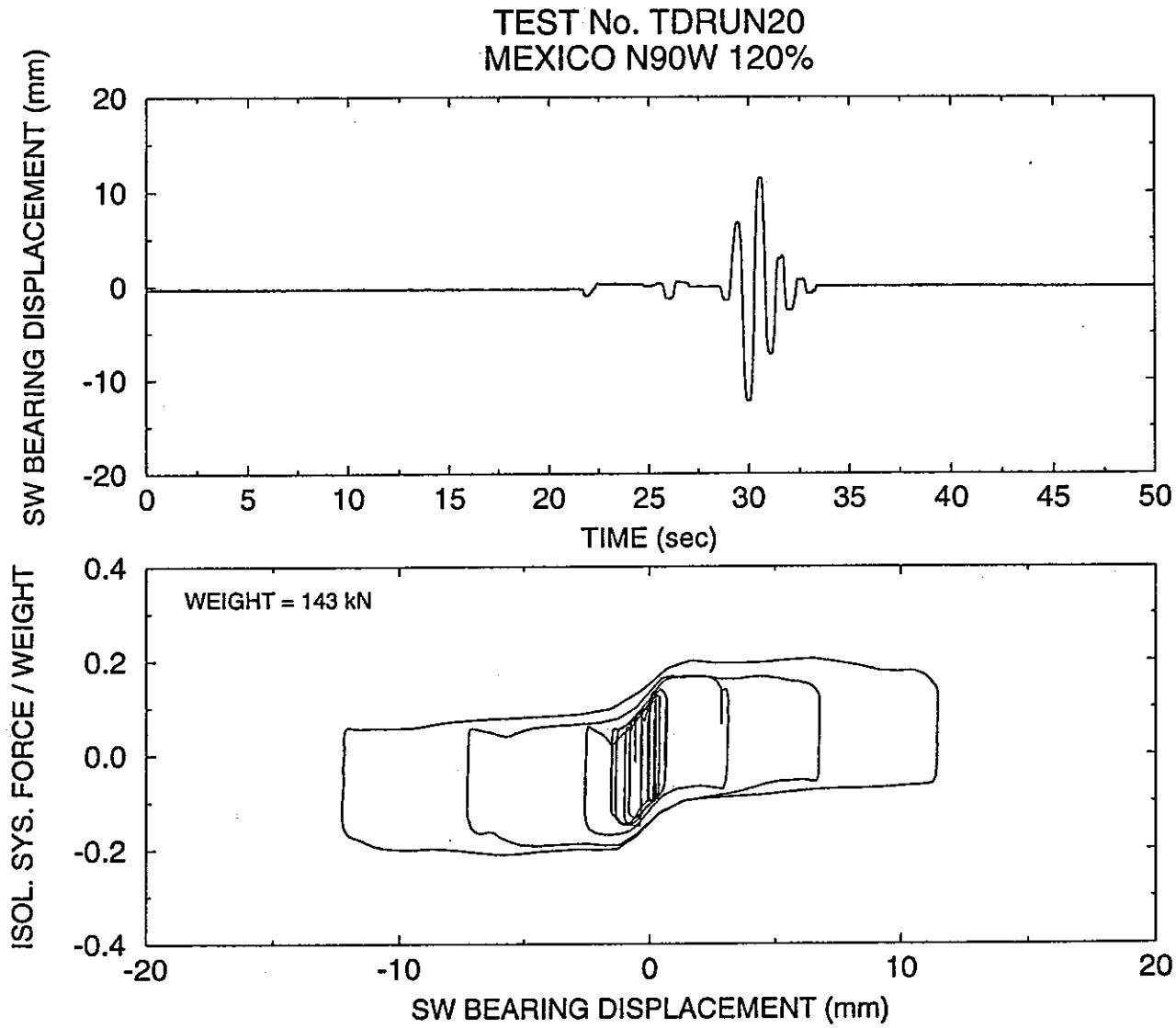
TEST No. TDRUN20
MEXICO N90W 120%
SW BEARING DISPLACEMENT (mm)
20
10
0
-10
-20
0
5
10
15
20
25
30
35
40
45
50
TIME (sec)
ISOL. SYS. FORCE / WEIGHT
WEIGHT = 143 kN
0.4
0.2
0.0
-0.2
-0.4
-20
-10
0
10
20
SW BEARING DISPLACEMENT (mm)

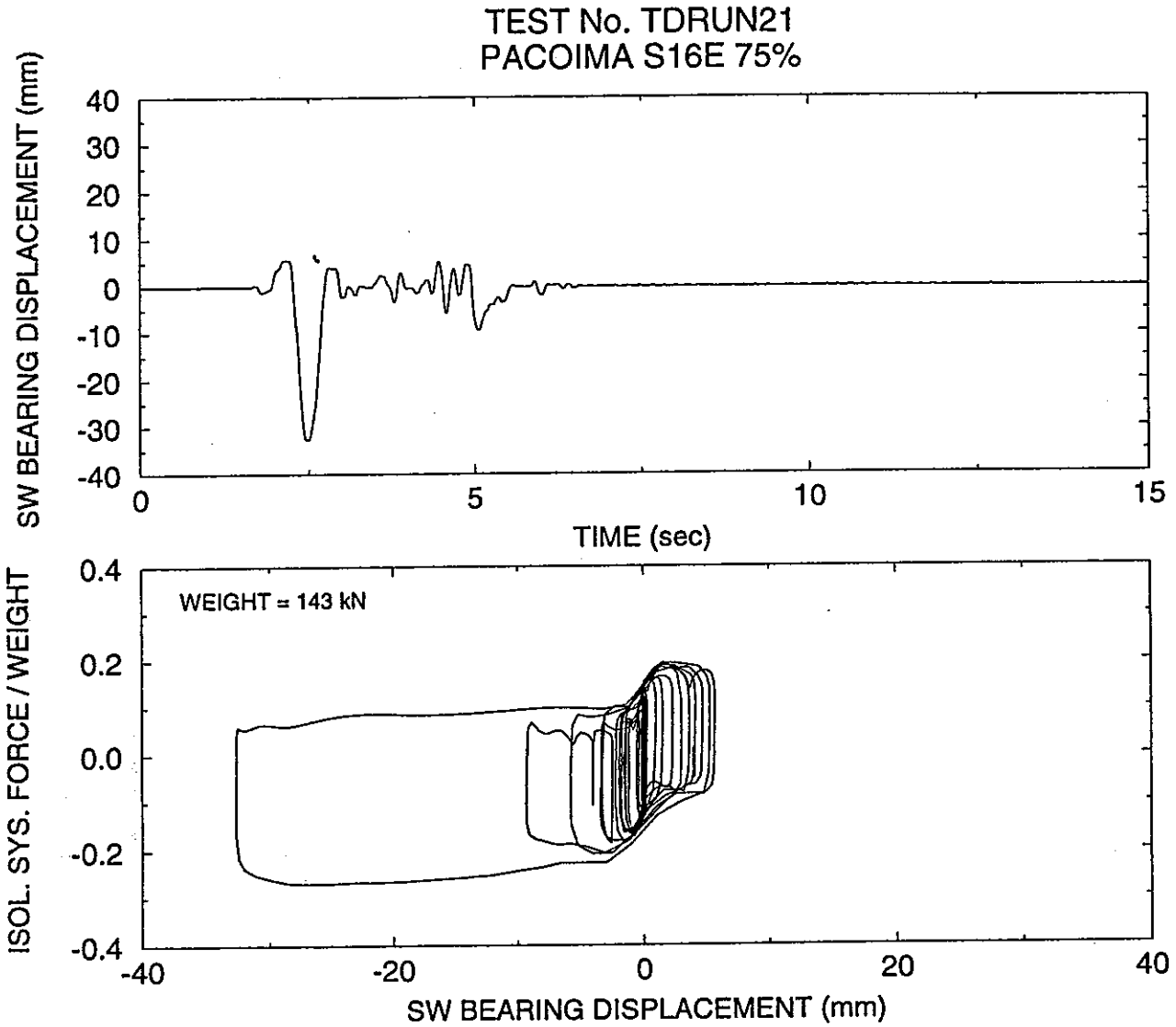
TEST No. TDRUN21
PACOIMA S16E 75%
SW BEARING DISPLACEMENT (mm)
40
30
20
10
0
-10
-20
-30
-40
0
5
10
15
TIME (sec)
ISOL. SYS. FORCE / WEIGHT
WEIGHT = 143 kN
0.4
0.2
0.0
-0.2
-0.4
-40
-20
0
20
40
SW BEARING DISPLACEMENT (mm)

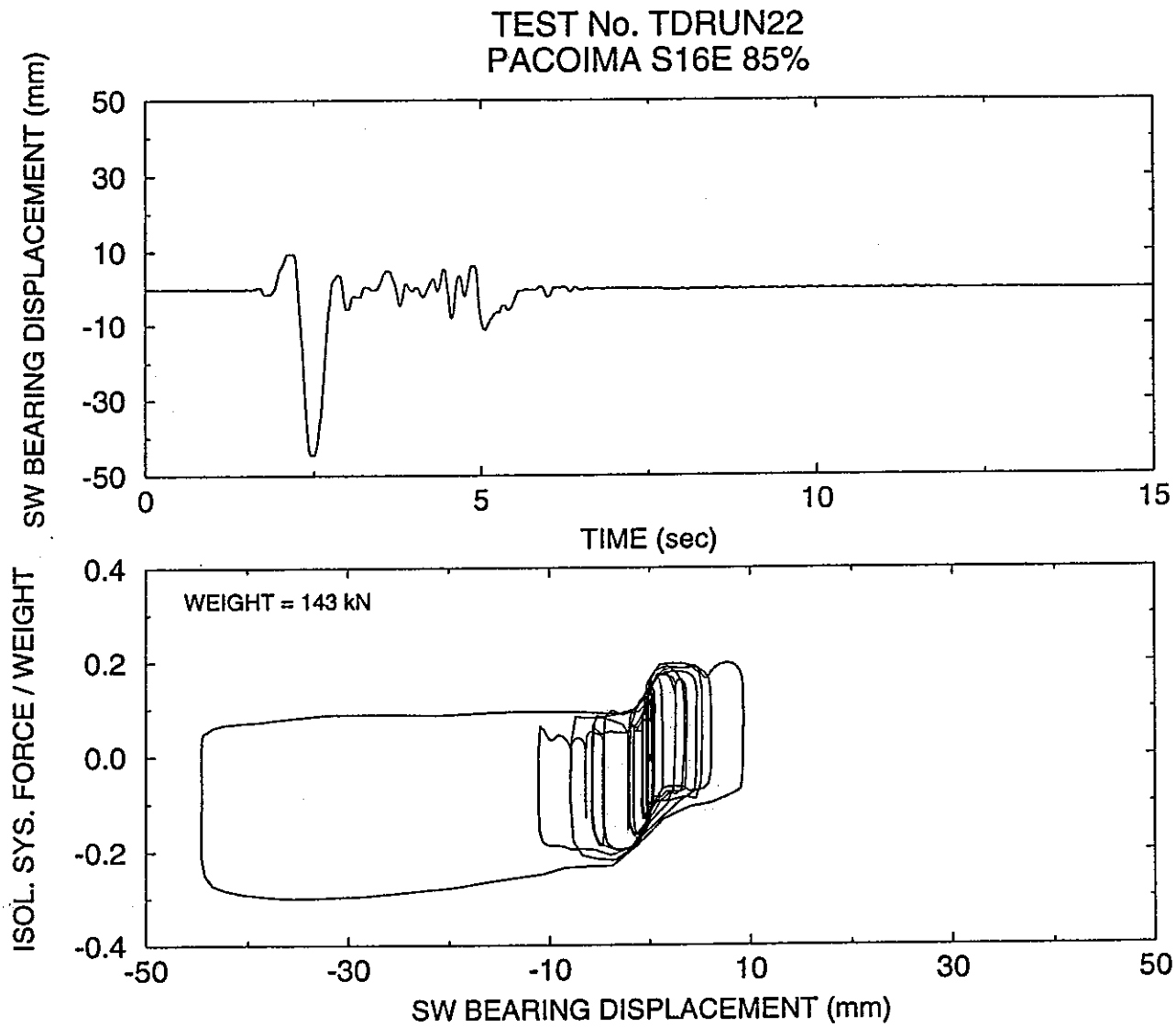
TEST No. TDRUN22
PACOIMA S16E 85%
SW BEARING DISPLACEMENT (mm)
50
30
10
-10
-30
-50
0
5
10
15
TIME (sec)
ISOL. SYS. FORCE / WEIGHT
WEIGHT = 143 kN
0.4
0.2
0.0
-0.2
-0.4
-50
-30
-10
10
30
50
SW BEARING DISPLACEMENT (mm)

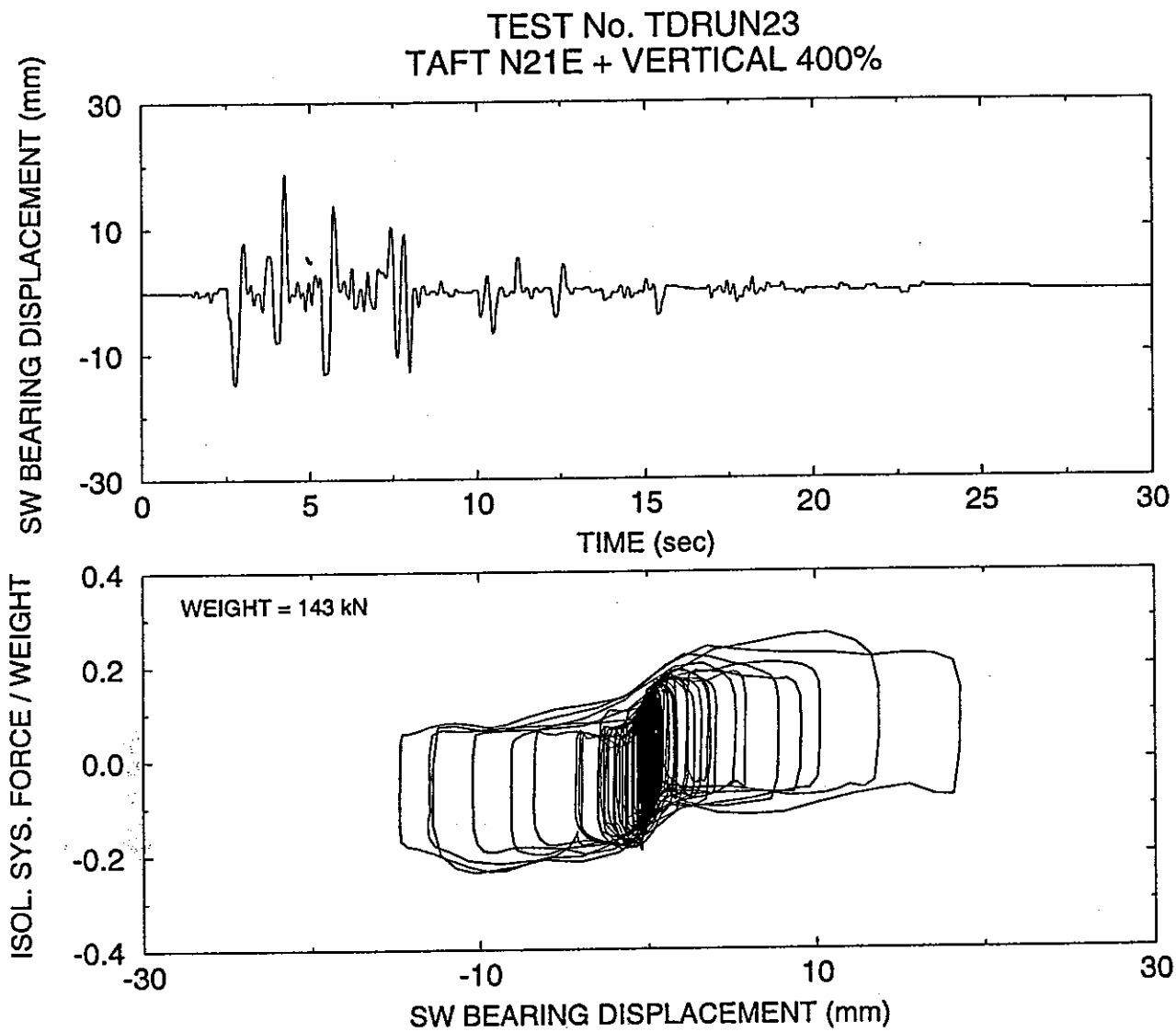
TEST No. TDRUN23
TAFT N21E + VERTICAL 400%
SW BEARING DISPLACEMENT (mm)
30
10
-10
-30
0
5
10
15
20
25
30
TIME (sec)
ISOL. SYS. FORCE / WEIGHT
WEIGHT = 143 kN
0.4
0.2
0.0
-0.2
-0.4
-30
-10
10
30
SW BEARING DISPLACEMENT (mm)

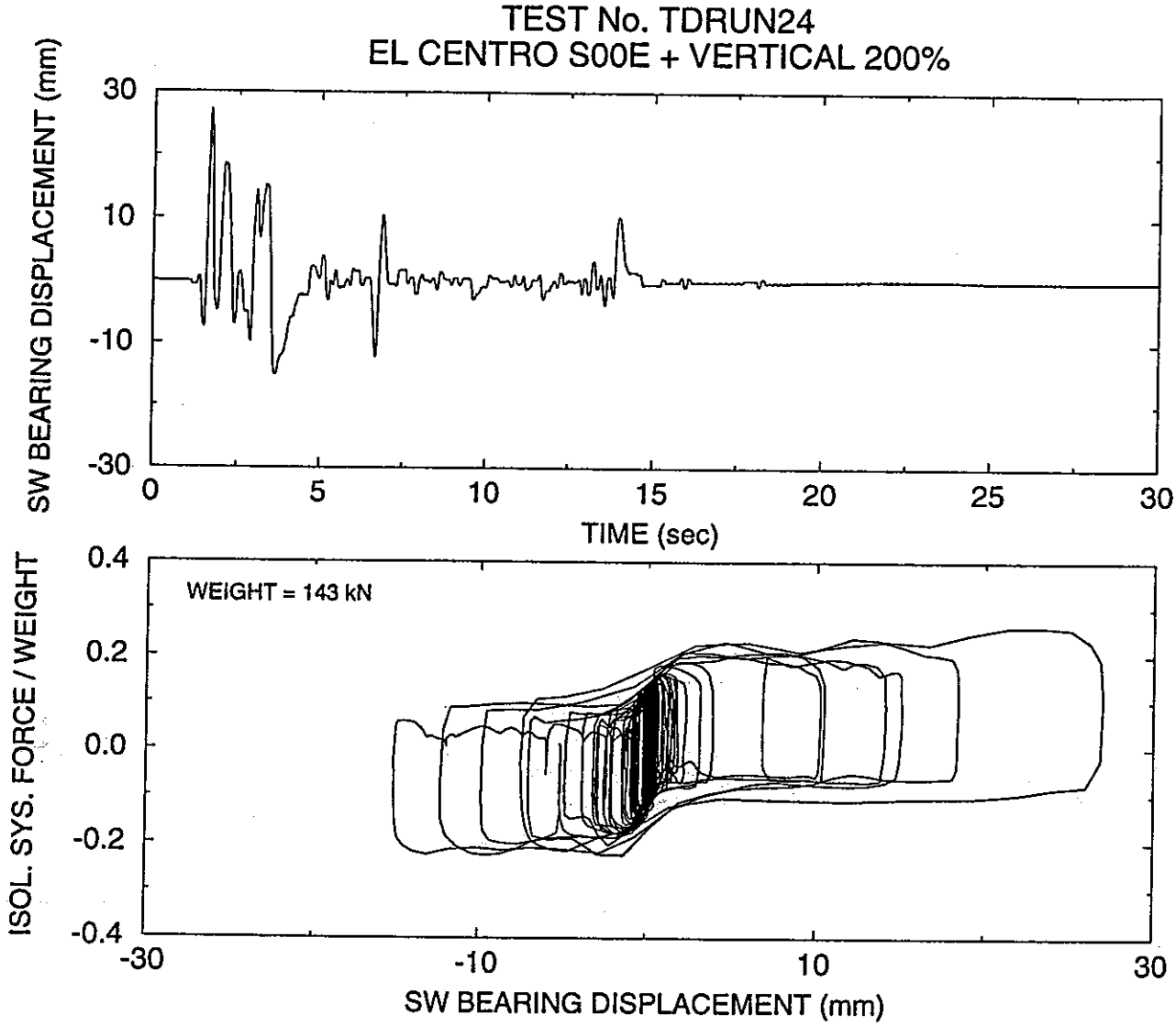
TEST No. TDRUN24
EL CENTRO S00E + VERTICAL 200%
SW BEARING DISPLACEMENT (mm)
30
10
-10
-30
0
5
10
15
20
25
30
TIME (sec)
ISOL. SYS. FORCE / WEIGHT
WEIGHT = 143 kN
0.4
0.2
0.0
-0.2
-0.4
-30
-10
10
30
SW BEARING DISPLACEMENT (mm)

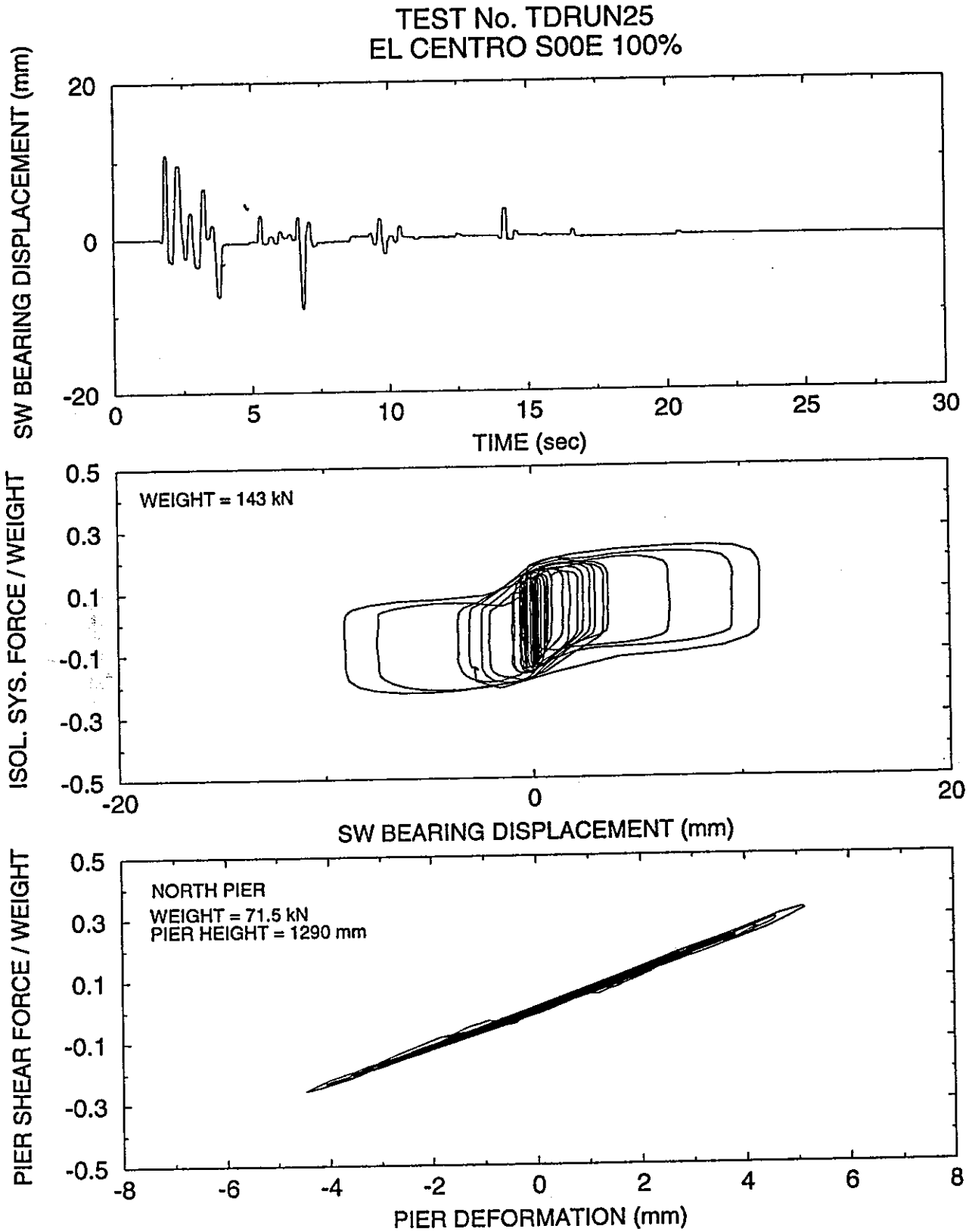
TEST No. TDRUN25
EL CENTRO S00E 100%
SW BEARING DISPLACEMENT (mm)
20
0
-20
0
5
10
15
20
25
30
TIME (sec)
ISOL. SYS. FORCE / WEIGHT
WEIGHT = 143 kN
0.5
0.3
0.1
-0.1
-0.3
-0.5
-20
0
20
SW BEARING DISPLACEMENT (mm)
PIER SHEAR FORCE / WEIGHT
NORTH PIER
WEIGHT = 71.5 kN
PIER HEIGHT = 1290 mm
0.5
0.3
0.1
-0.1
-0.3
-0.5
-8
-6
-4
-2
0
2
4
6
8
PIER DEFORMATION (mm)

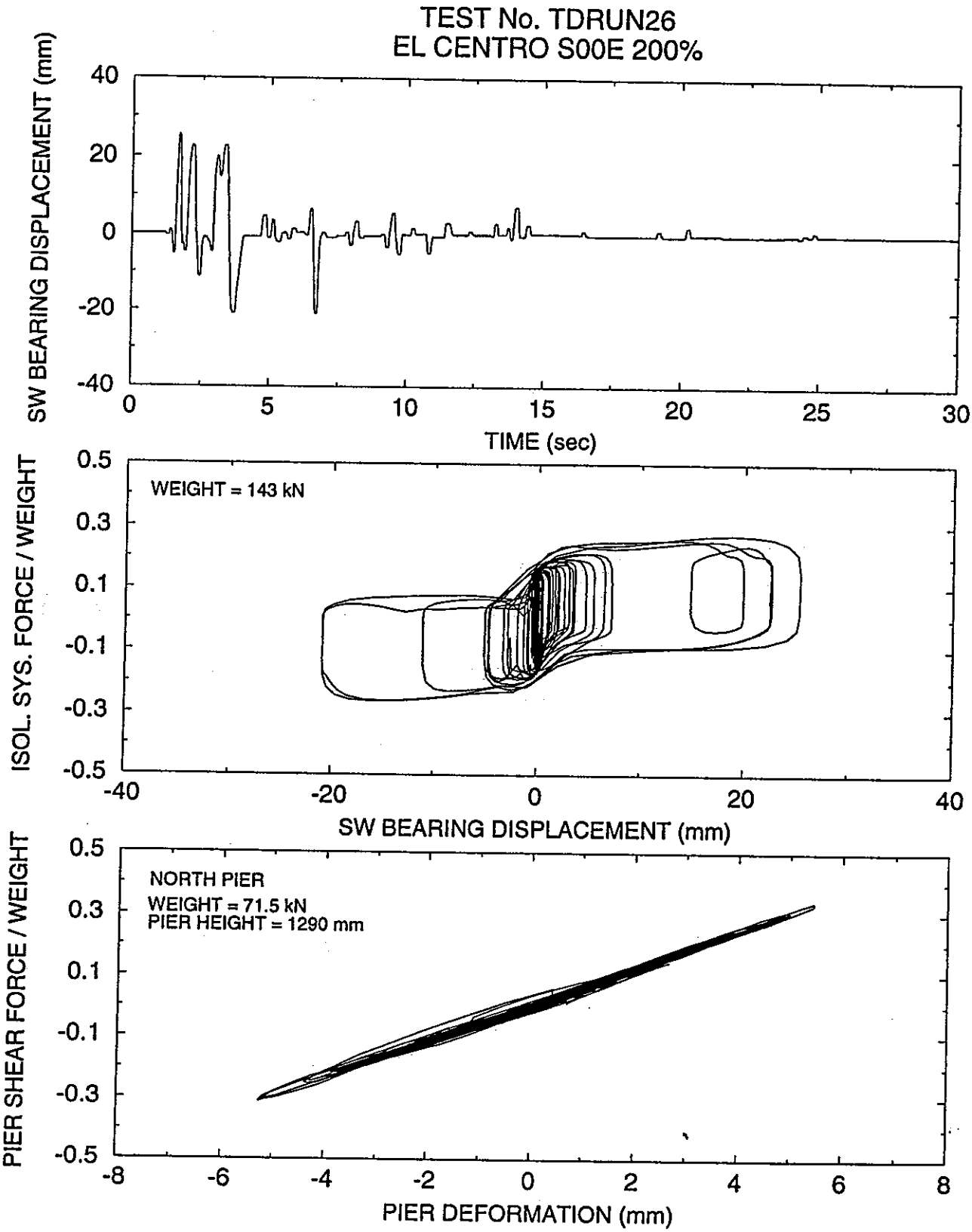
TEST No. TDRUN26
EL CENTRO S00E 200%
SW BEARING DISPLACEMENT (mm)
40
20
0
-20
-40
0
5
10
15
20
25
30
TIME (sec)
ISOL. SYS. FORCE / WEIGHT
WEIGHT = 143 kN
0.5
0.3
0.1
-0.1
-0.3
-0.5
-40
-20
0
20
40
SW BEARING DISPLACEMENT (mm)
PIER SHEAR FORCE / WEIGHT
NORTH PIER
WEIGHT = 71.5 kN
PIER HEIGHT = 1290 mm
0.5
0.3
0.1
-0.1
-0.3
-0.5
-8
-6
-4
-2
0
2
4
6
8
PIER DEFORMATION (mm)

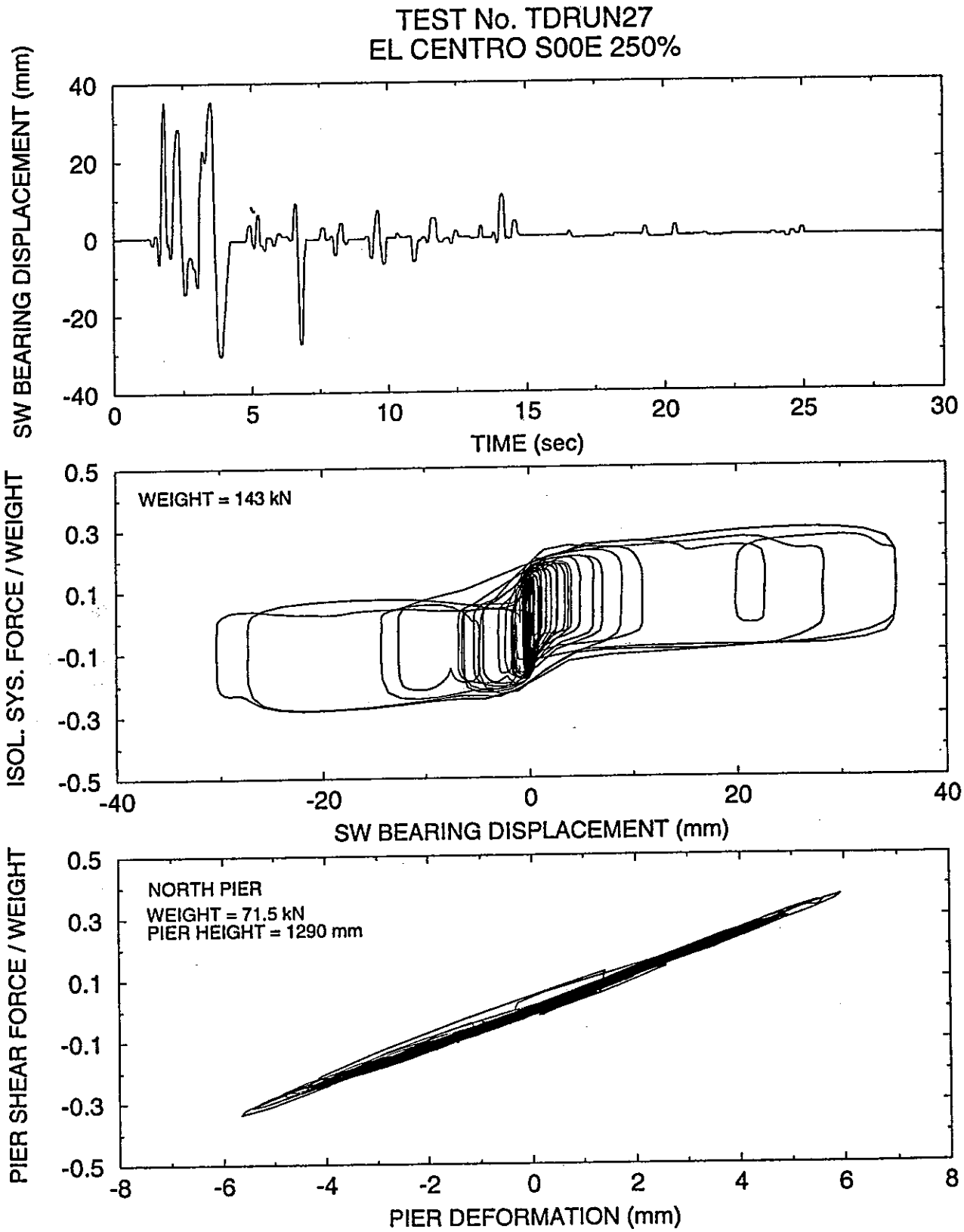
TEST No. TDRUN27
EL CENTRO S00E 250%
SW BEARING DISPLACEMENT (mm)
40
20
0
-20
-40
0
5
10
15
20
25
30
TIME (sec)
ISOL. SYS. FORCE / WEIGHT
WEIGHT = 143 kN
0.5
0.3
0.1
-0.1
-0.3
-0.5
-40
-20
0
20
40
SW BEARING DISPLACEMENT (mm)
PIER SHEAR FORCE / WEIGHT
NORTH PIER
WEIGHT = 71.5 kN
PIER HEIGHT = 1290 mm
0.5
0.3
0.1
-0.1
-0.3
-0.5
-8
-6
-4
-2
0
2
4
6
8
PIER DEFORMATION (mm)

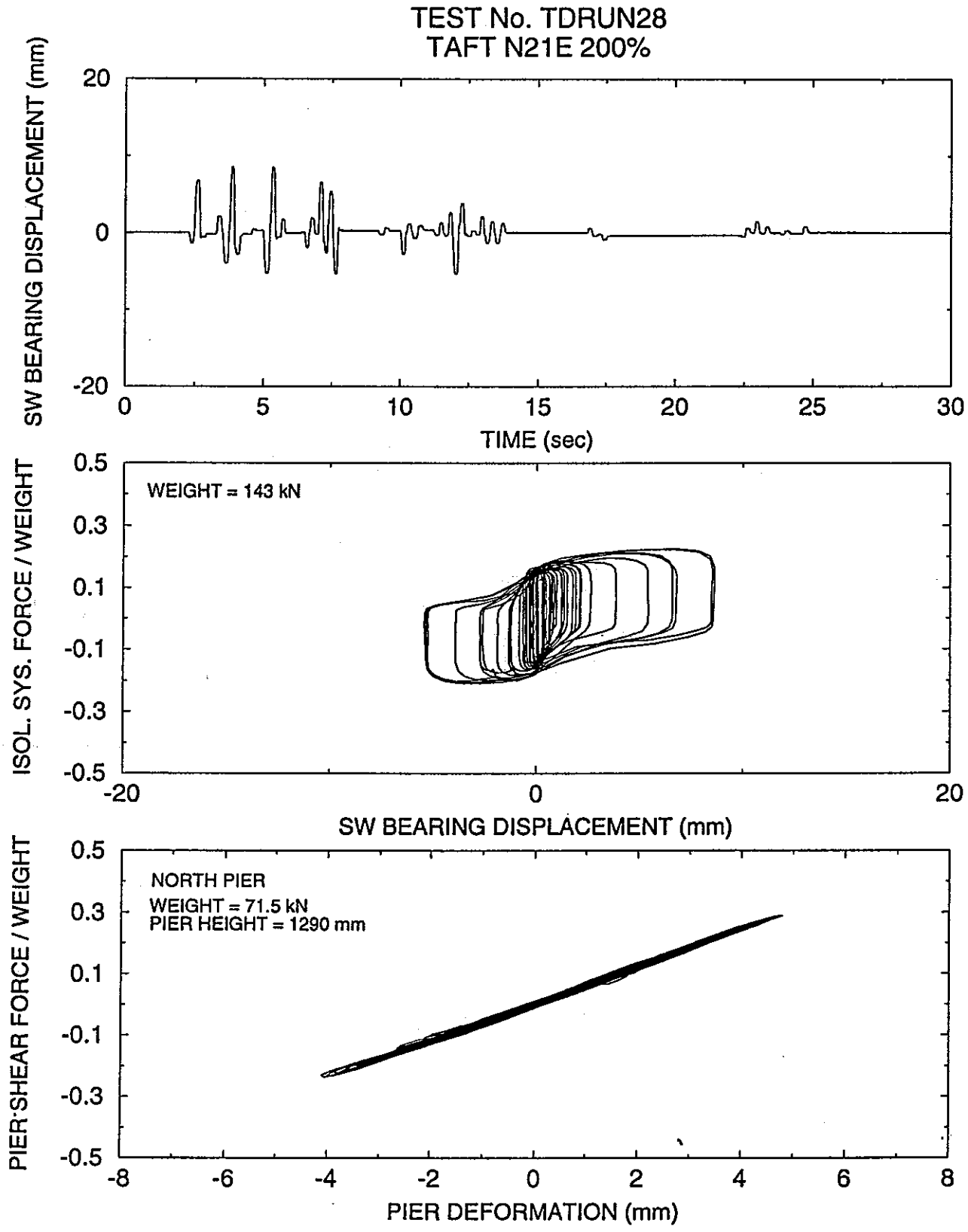
TEST No. TDRUN28
TAFT N21E 200%
SW BEARING DISPLACEMENT (mm)
20
0
-20
0
5
10
15
20
25
30
TIME (sec)
ISOL. SYS. FORCE / WEIGHT
WEIGHT = 143 kN
0.5
0.3
0.1
-0.1
-0.3
-0.5
-20
0
20
SW BEARING DISPLACEMENT (mm)
PIER SHEAR FORCE / WEIGHT
NORTH PIER
WEIGHT = 71.5 kN
PIER HEIGHT = 1290 mm
0.5
0.3
0.1
-0.1
-0.3
-0.5
-8
-6
-4
-2
0
2
4
6
8
PIER DEFORMATION (mm)

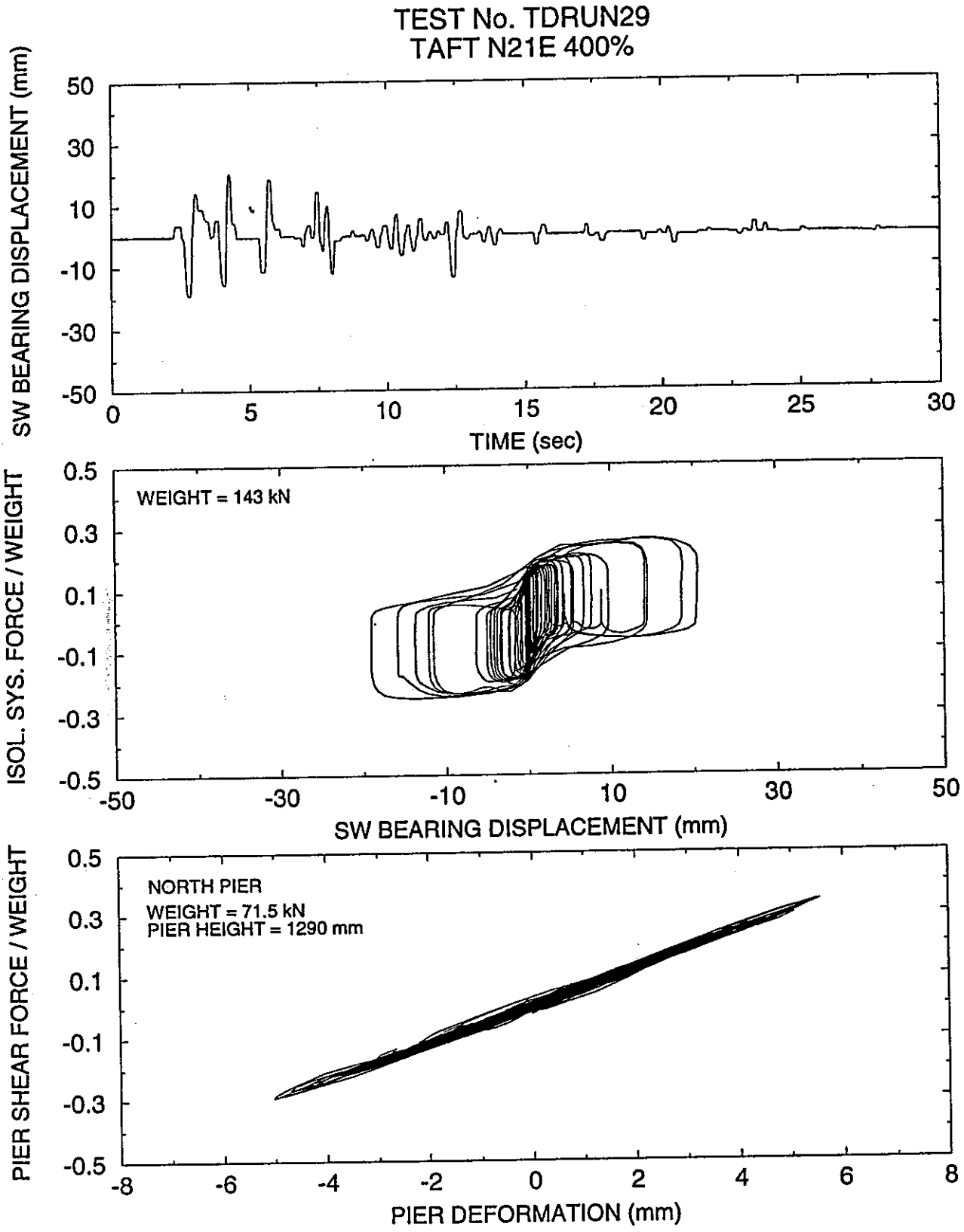
TEST No. TDRUN29
TAFT N21E 400%
SW BEARING DISPLACEMENT (mm)
50
30
10
-10
-30
-50
0
5
10
15
20
25
30
TIME (sec)
ISOL. SYS. FORCE / WEIGHT
WEIGHT = 143 kN
0.5
0.3
0.1
-0.1
-0.3
-0.5
-50
-30
-10
10
30
50
SW BEARING DISPLACEMENT (mm)
PIER SHEAR FORCE / WEIGHT
NORTH PIER
WEIGHT = 71.5 kN
PIER HEIGHT = 1290 mm
0.5
0.3
0.1
-0.1
-0.3
-0.5
-8
-6
-4
-2
0
2
4
6
8
PIER DEFORMATION (mm)

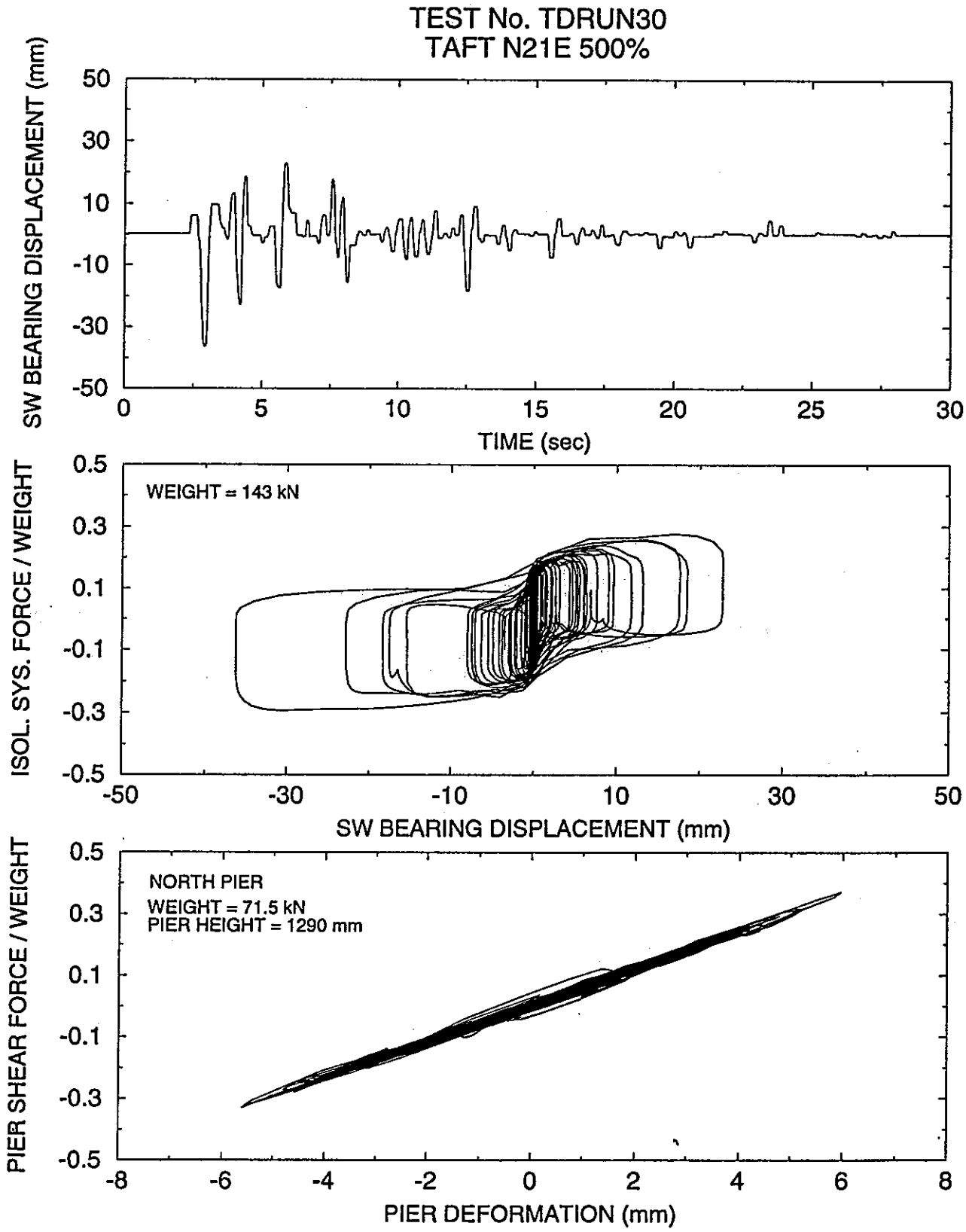
TEST No. TDRUN30
TAFT N21E 500%
SW BEARING DISPLACEMENT (mm)
50
30
10
-10
-30
-50
0
5
10
15
20
25
30
TIME (sec)
ISOL. SYS. FORCE / WEIGHT
WEIGHT = 143 kN
0.5
0.3
0.1
-0.1
-0.3
-0.5
-50
-30
-10
10
30
50
SW BEARING DISPLACEMENT (mm)
PIER SHEAR FORCE / WEIGHT
NORTH PIER
WEIGHT = 71.5 kN
PIER HEIGHT = 1290 mm
0.5
0.3
0.1
-0.1
-0.3
-0.5
-8
-6
-4
-2
0
2
4
6
8
PIER DEFORMATION (mm)

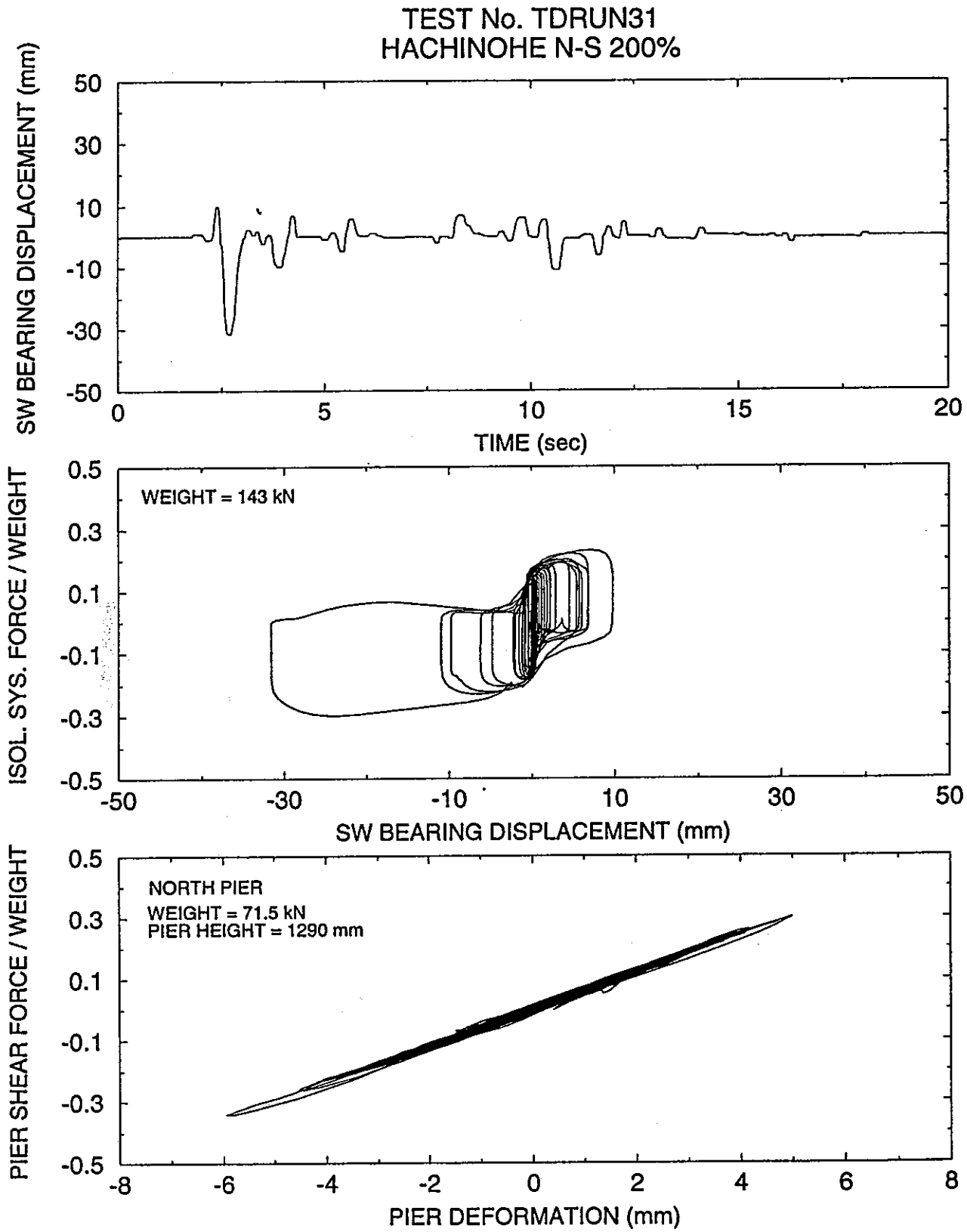
TEST No. TDRUN31
HACHINOHE N-S 200%
SW BEARING DISPLACEMENT (mm)
50
30
10
-10
-30
-50
0
5
10
15
20
TIME (sec)
ISOL. SYS. FORCE / WEIGHT
WEIGHT = 143 kN
0.5
0.3
0.1
-0.1
-0.3
-0.5
-50
-30
-10
10
30
50
SW BEARING DISPLACEMENT (mm)
PIER SHEAR FORCE / WEIGHT
NORTH PIER
WEIGHT = 71.5 kN
PIER HEIGHT = 1290 mm
0.5
0.3
0.1
-0.1
-0.3
-0.5
-8
-6
-4
-2
0
2
4
6
8
PIER DEFORMATION (mm)

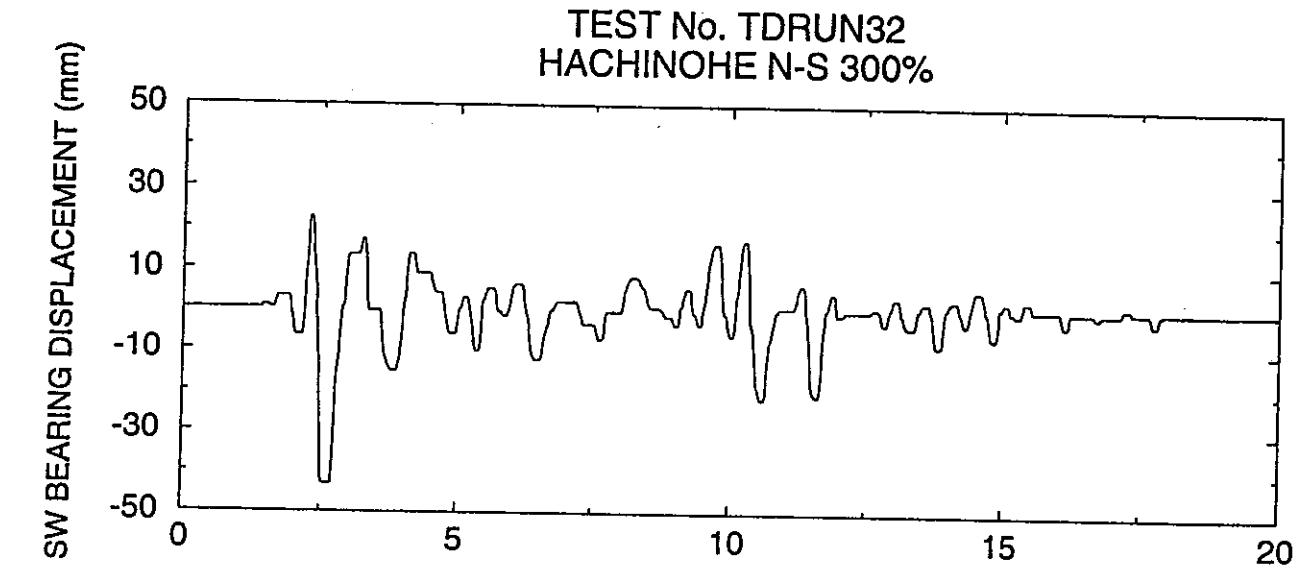
TEST No. TDRUN32
HACHINOHE N-S 300%
SW BEARING DISPLACEMENT (mm)
50
30
10
-10
-30
-50
0
5
10
15
20
TIME (sec)

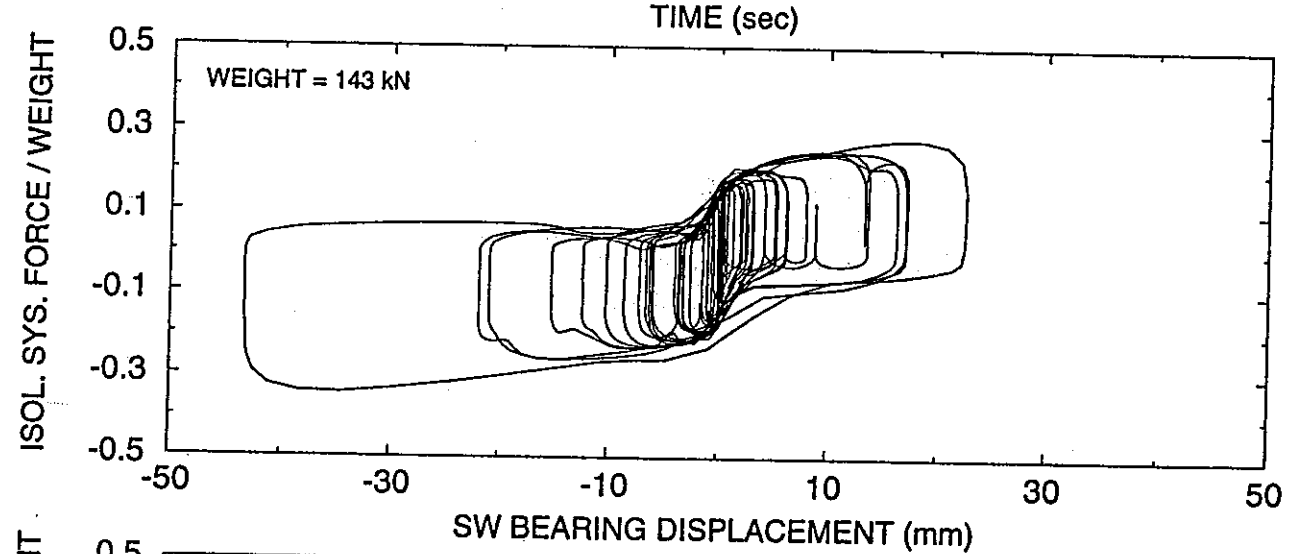
ISOL. SYS. FORCE / WEIGHT
WEIGHT = 143 kN
0.5
0.3
0.1
-0.1
-0.3
-0.5
-50
-30
-10
10
30
50
SW BEARING DISPLACEMENT (mm)

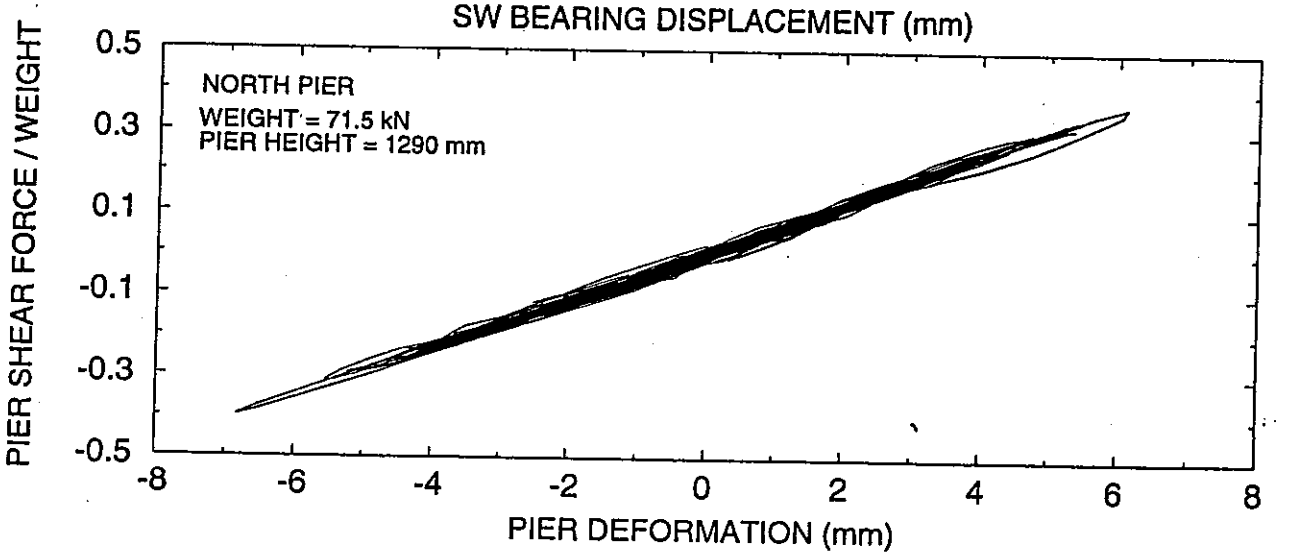
PIER SHEAR FORCE / WEIGHT
NORTH PIER
WEIGHT = 71.5 kN
PIER HEIGHT = 1290 mm
0.5
0.3
0.1
-0.1
-0.3
-0.5
-8
-6
-4
-2
0
2
4
6
8
PIER DEFORMATION (mm)

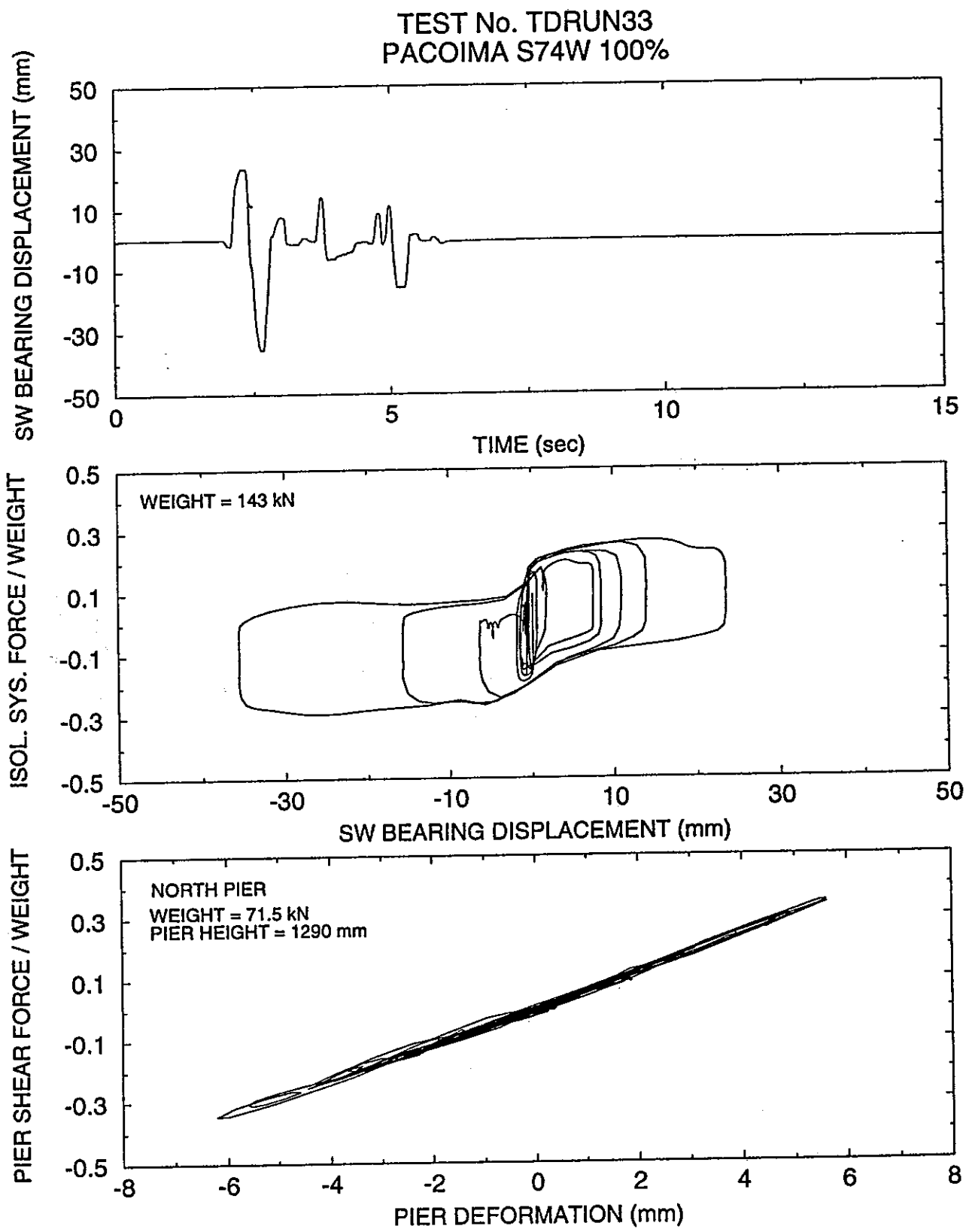
TEST No. TDRUN33
PACOIMA S74W 100%
SW BEARING DISPLACEMENT (mm)
50
30
10
-10
-30
-50
0
5
10
15
TIME (sec)
ISOL. SYS. FORCE / WEIGHT
WEIGHT = 143 kN
0.5
0.3
0.1
-0.1
-0.3
-0.5
-50
-30
-10
10
30
50
SW BEARING DISPLACEMENT (mm)
PIER SHEAR FORCE / WEIGHT
NORTH PIER
WEIGHT = 71.5 kN
PIER HEIGHT = 1290 mm
0.5
0.3
0.1
-0.1
-0.3
-0.5
-8
-6
-4
-2
0
2
4
6
8
PIER DEFORMATION (mm)

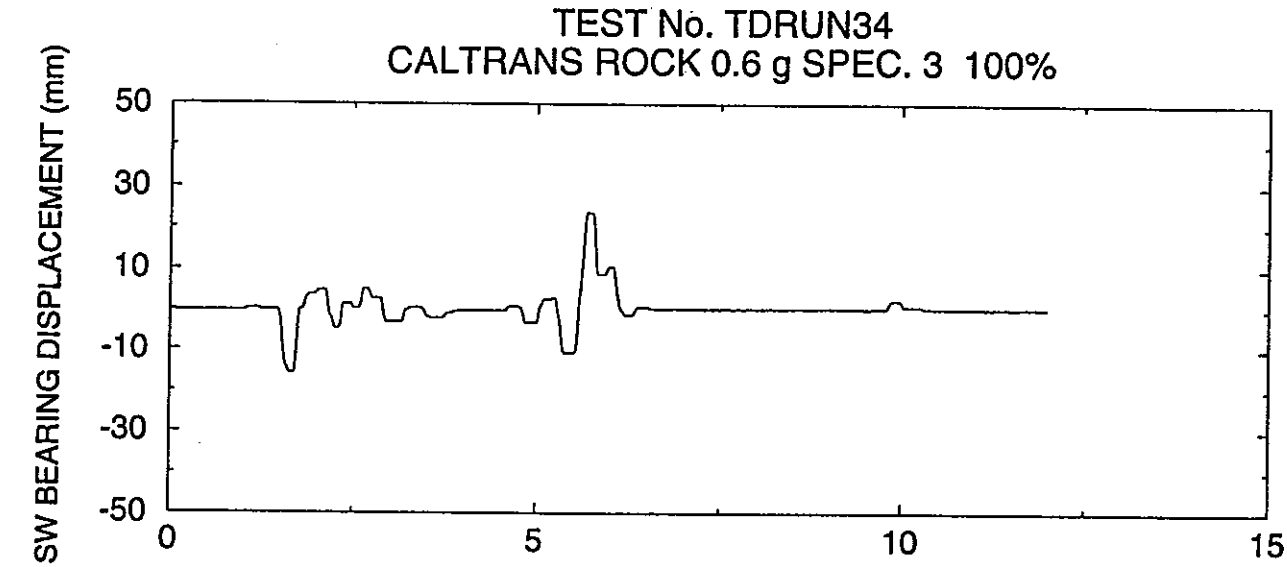
TEST No. TDRUN34
CALTRANS ROCK 0.6 g SPEC. 3 100%
SW BEARING DISPLACEMENT (mm)
50
30
10
-10
-30
-50
0
5
10
15
TIME (sec)

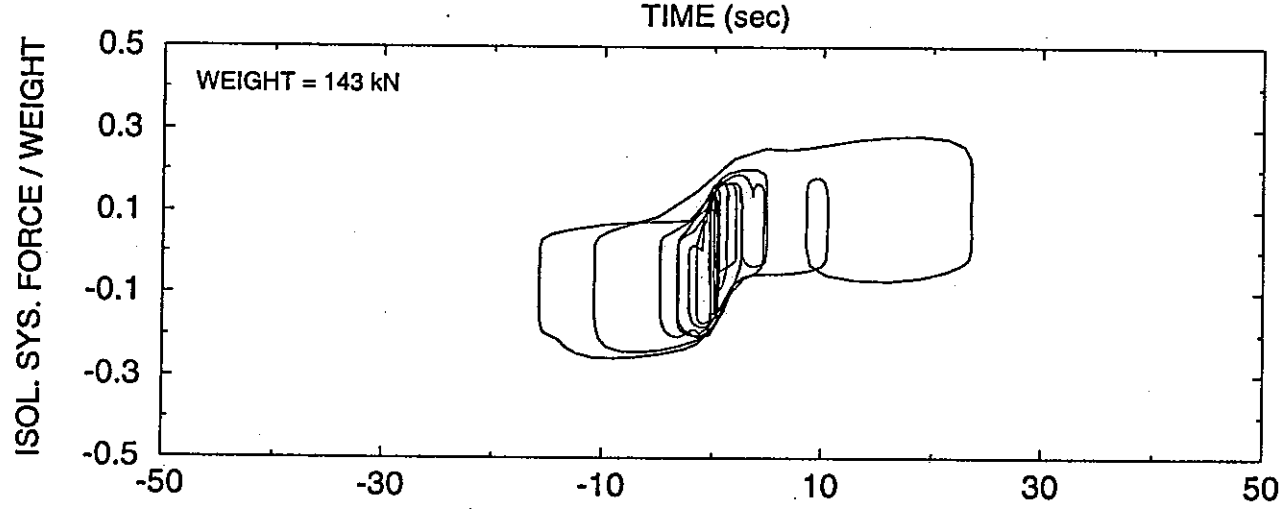
ISOL. SYS. FORCE / WEIGHT
WEIGHT = 143 kN
0.5
0.3
0.1
-0.1
-0.3
-0.5
-50
-30
-10
10
30
50
SW BEARING DISPLACEMENT (mm)

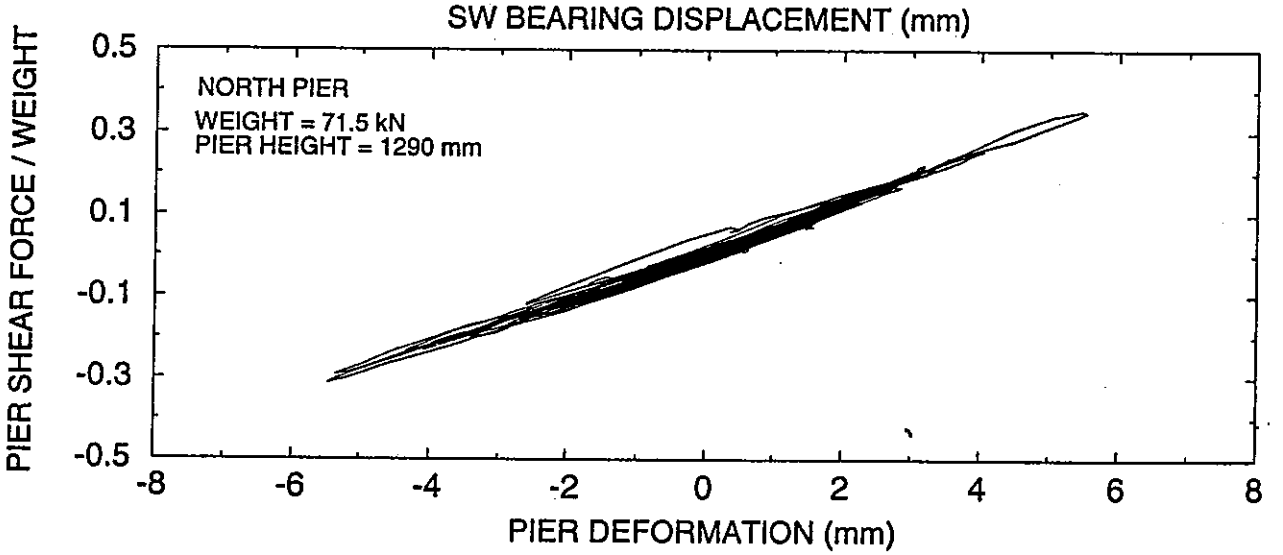
PIER SHEAR FORCE / WEIGHT
NORTH PIER
WEIGHT = 71.5 kN
PIER HEIGHT = 1290 mm
0.5
0.3
0.1
-0.1
-0.3
-0.5
-8
-6
-4
-2
0
2
4
6
8
PIER DEFORMATION (mm)

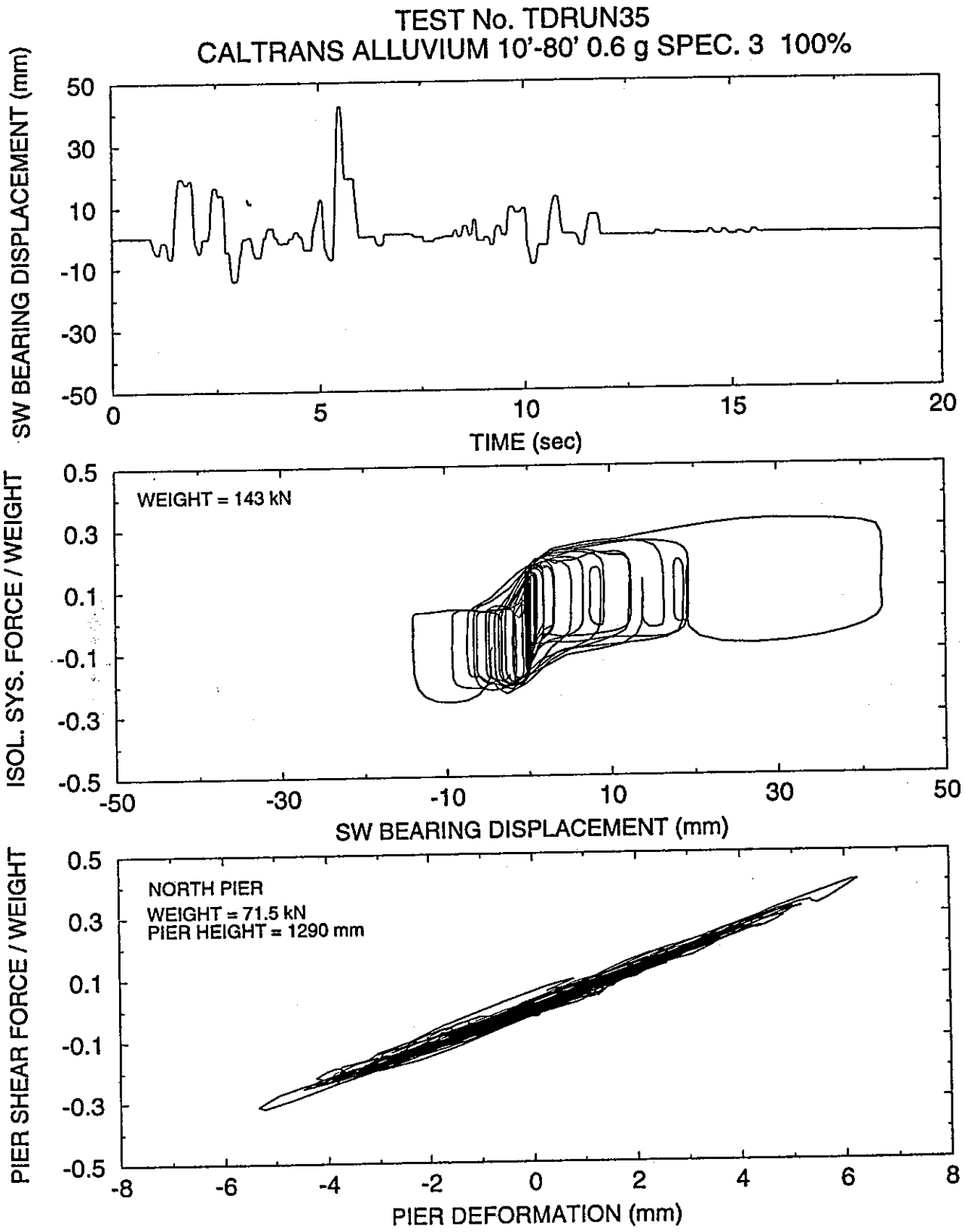
TEST No. TDRUN35
CALTRANS ALLUVIUM 10'-80' 0.6 g SPEC. 3 100%
SW BEARING DISPLACEMENT (mm)
50
30
10
-10
-30
-50
0
5
10
15
20
TIME (sec)
ISOL. SYS. FORCE / WEIGHT
WEIGHT = 143 kN
0.5
0.3
0.1
-0.1
-0.3
-0.5
-50
-30
-10
10
30
50
SW BEARING DISPLACEMENT (mm)
PIER SHEAR FORCE / WEIGHT
NORTH PIER
WEIGHT = 71.5 kN
PIER HEIGHT = 1290 mm
0.5
0.3
0.1
-0.1
-0.3
-0.5
-8
-6
-4
-2
0
2
4
6
8
PIER DEFORMATION (mm)

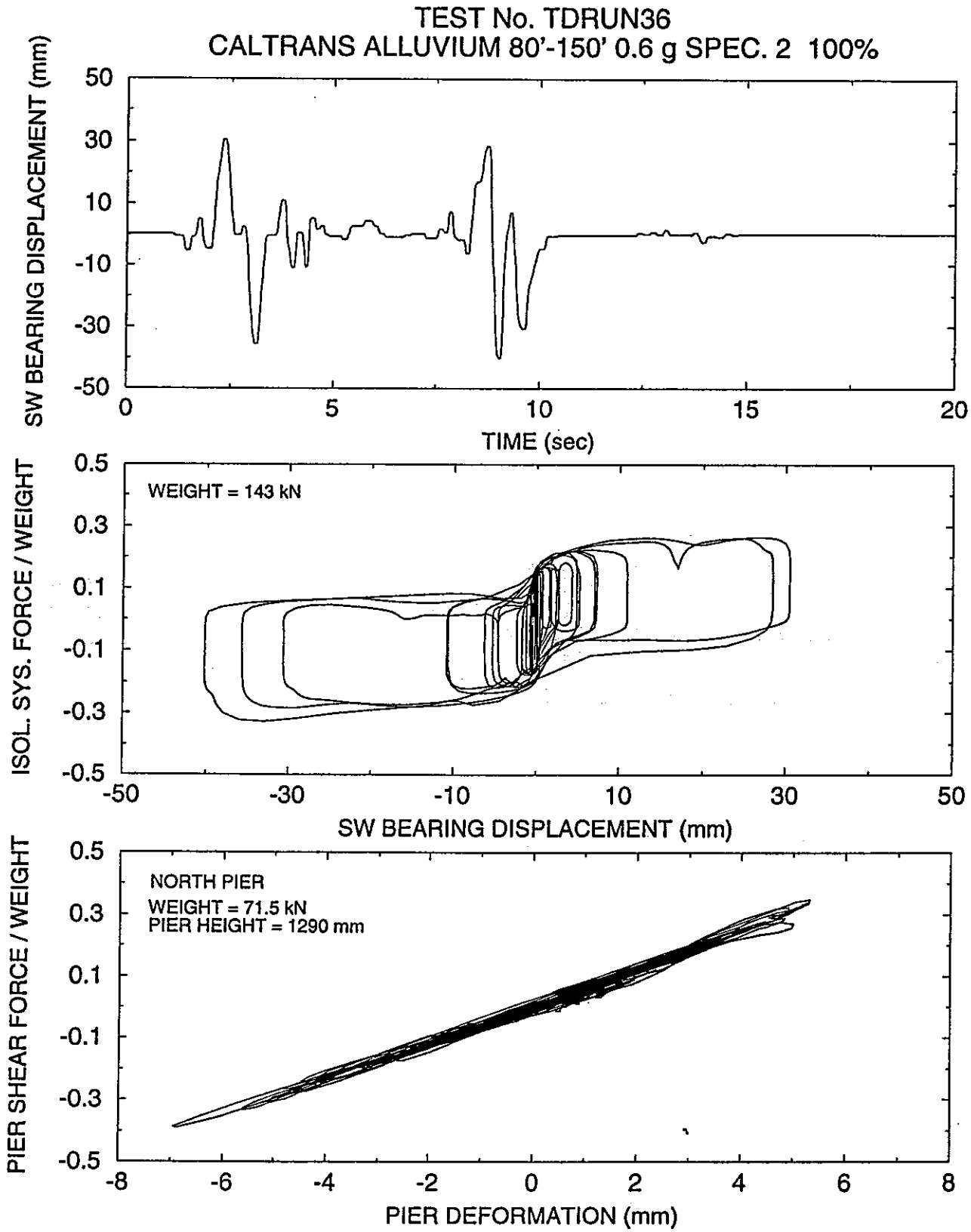
TEST No. TDRUN36
CALTRANS ALLUVIUM 80'-150' 0.6 g SPEC. 2 100%
SW BEARING DISPLACEMENT (mm)
50
30
10
-10
-30
-50
0
5
10
15
20
TIME (sec)
ISOL. SYS. FORCE / WEIGHT
WEIGHT = 143 kN
0.5
0.3
0.1
-0.1
-0.3
-0.5
-50
-30
-10
10
30
50
SW BEARING DISPLACEMENT (mm)
PIER SHEAR FORCE / WEIGHT
NORTH PIER
WEIGHT = 71.5 kN
PIER HEIGHT = 1290 mm
0.5
0.3
0.1
-0.1
-0.3
-0.5
-8
-6
-4
-2
0
2
4
6
8
PIER DEFORMATION (mm)

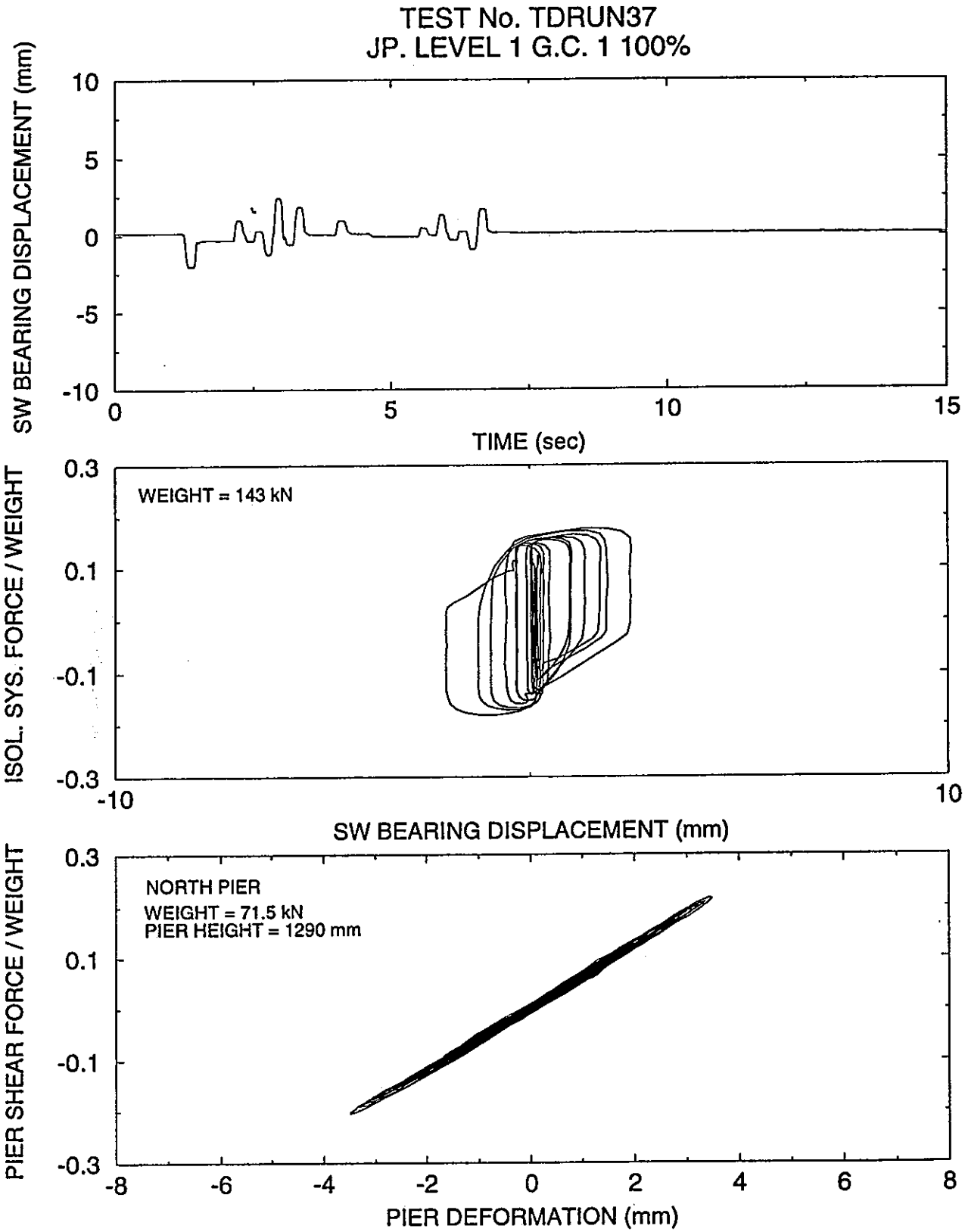
TEST No. TDRUN37
JP. LEVEL 1 G.C. 1 100%
SW BEARING DISPLACEMENT (mm)
10
5
0
-5
-10
0
5
10
15
TIME (sec)
ISOL. SYS. FORCE / WEIGHT
WEIGHT = 143 kN
0.3
0.1
-0.1
-0.3
-10
10
SW BEARING DISPLACEMENT (mm)
PIER SHEAR FORCE / WEIGHT
NORTH PIER
WEIGHT = 71.5 kN
PIER HEIGHT = 1290 mm
0.3
0.1
-0.1
-0.3
-8
-6
-4
-2
0
2
4
6
8
PIER DEFORMATION (mm)

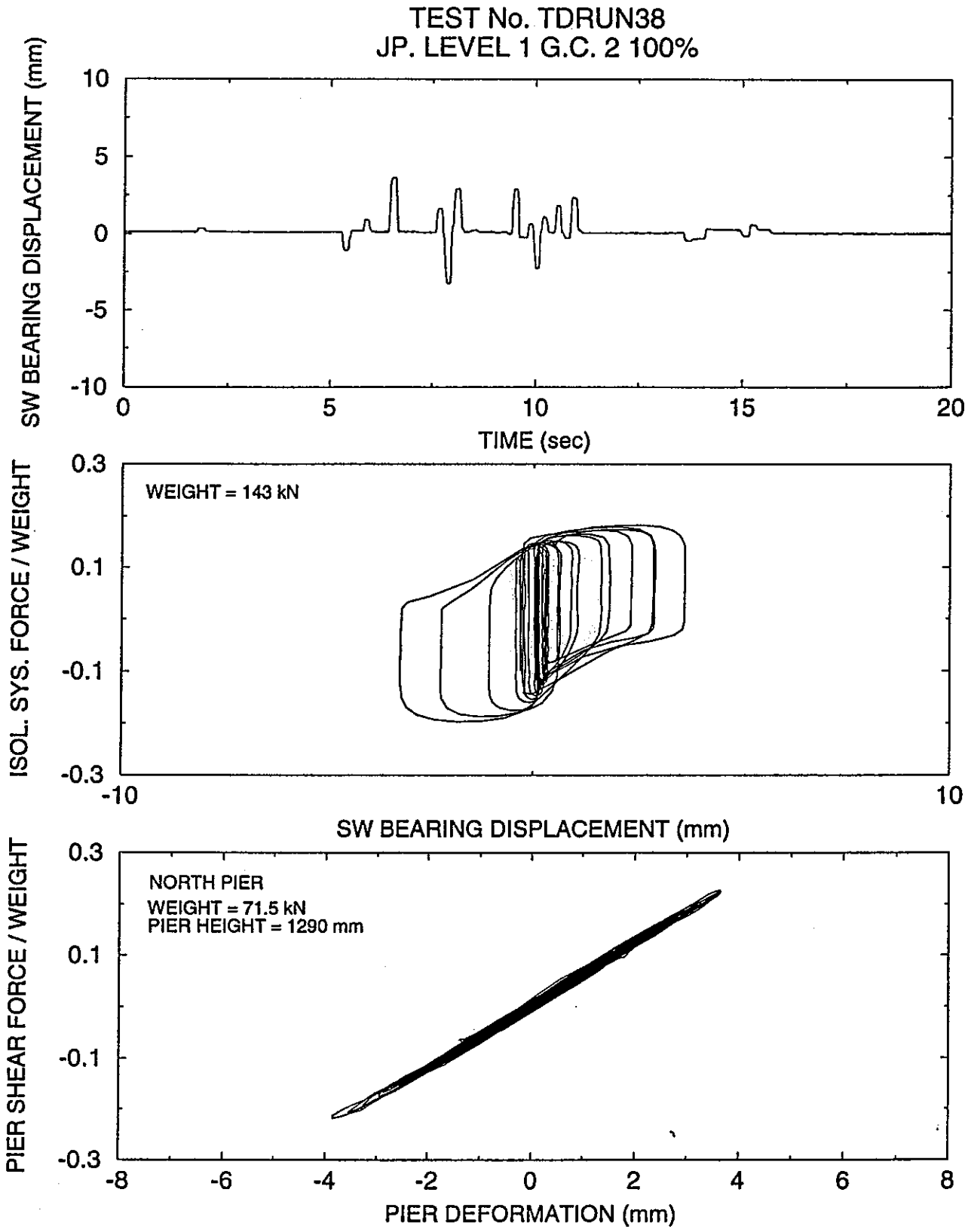
TEST No. TDRUN38
JP. LEVEL 1 G.C. 2 100%
SW BEARING DISPLACEMENT (mm)
10
5
0
-5
-10
0
5
10
15
20
TIME (sec)
ISOL. SYS. FORCE / WEIGHT
WEIGHT = 143 kN
0.3
0.1
-0.1
-0.3
-10
10
SW BEARING DISPLACEMENT (mm)
PIER SHEAR FORCE / WEIGHT
NORTH PIER
WEIGHT = 71.5 kN
PIER HEIGHT = 1290 mm
0.3
0.1
-0.1
-0.3
-8
-6
-4
-2
0
2
4
6
8
PIER DEFORMATION (mm)

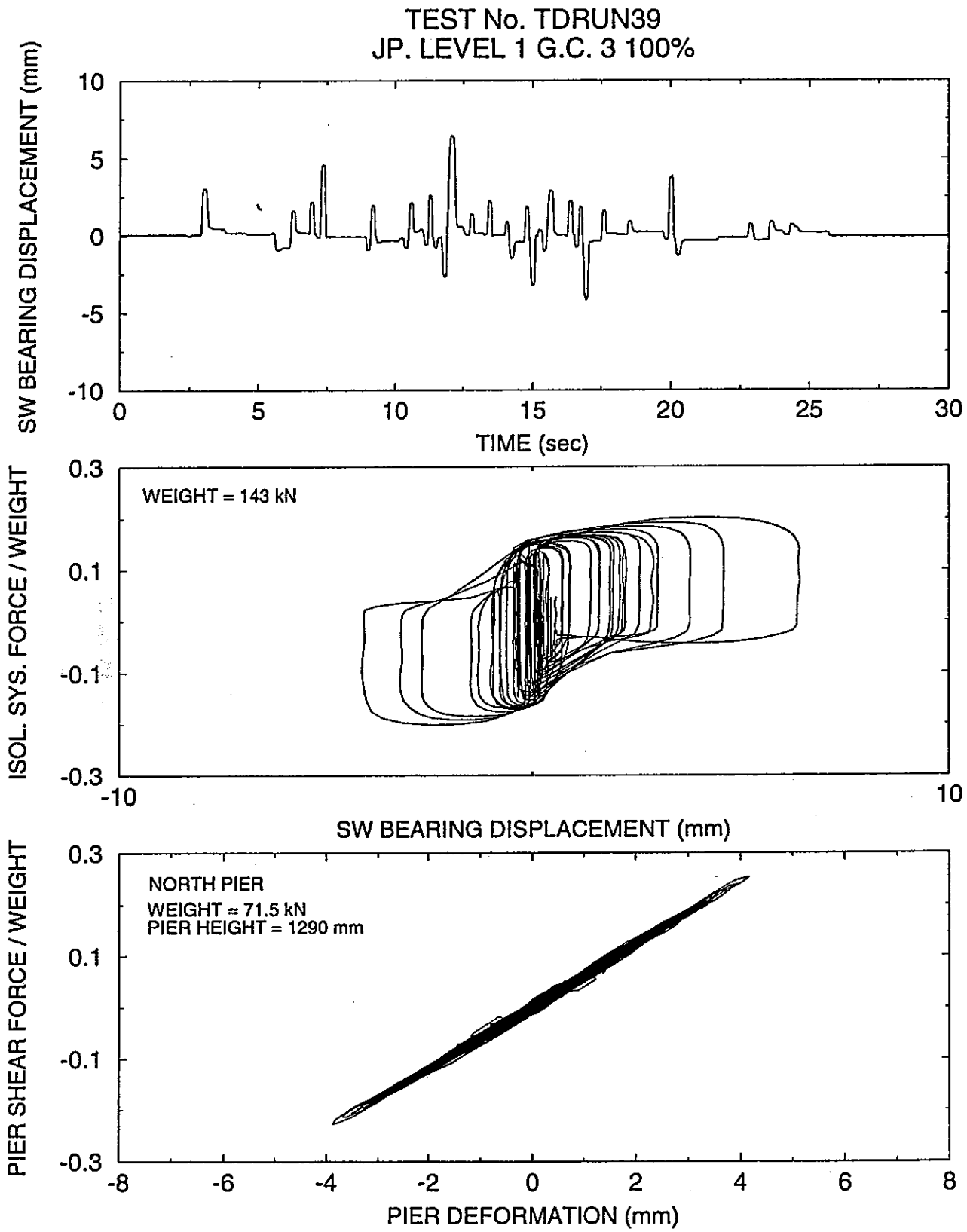
TEST No. TDRUN39
JP. LEVEL 1 G.C. 3 100%
SW BEARING DISPLACEMENT (mm)
10
5
0
-5
-10
0
5
10
15
20
25
30
TIME (sec)
ISOL. SYS. FORCE / WEIGHT
WEIGHT = 143 kN
0.3
0.1
-0.1
-0.3
-10
10
SW BEARING DISPLACEMENT (mm)
PIER SHEAR FORCE / WEIGHT
NORTH PIER
WEIGHT = 71.5 kN
PIER HEIGHT = 1290 mm
0.3
0.1
-0.1
-0.3
-8
-6
-4
-2
0
2
4
6
8
PIER DEFORMATION (mm)

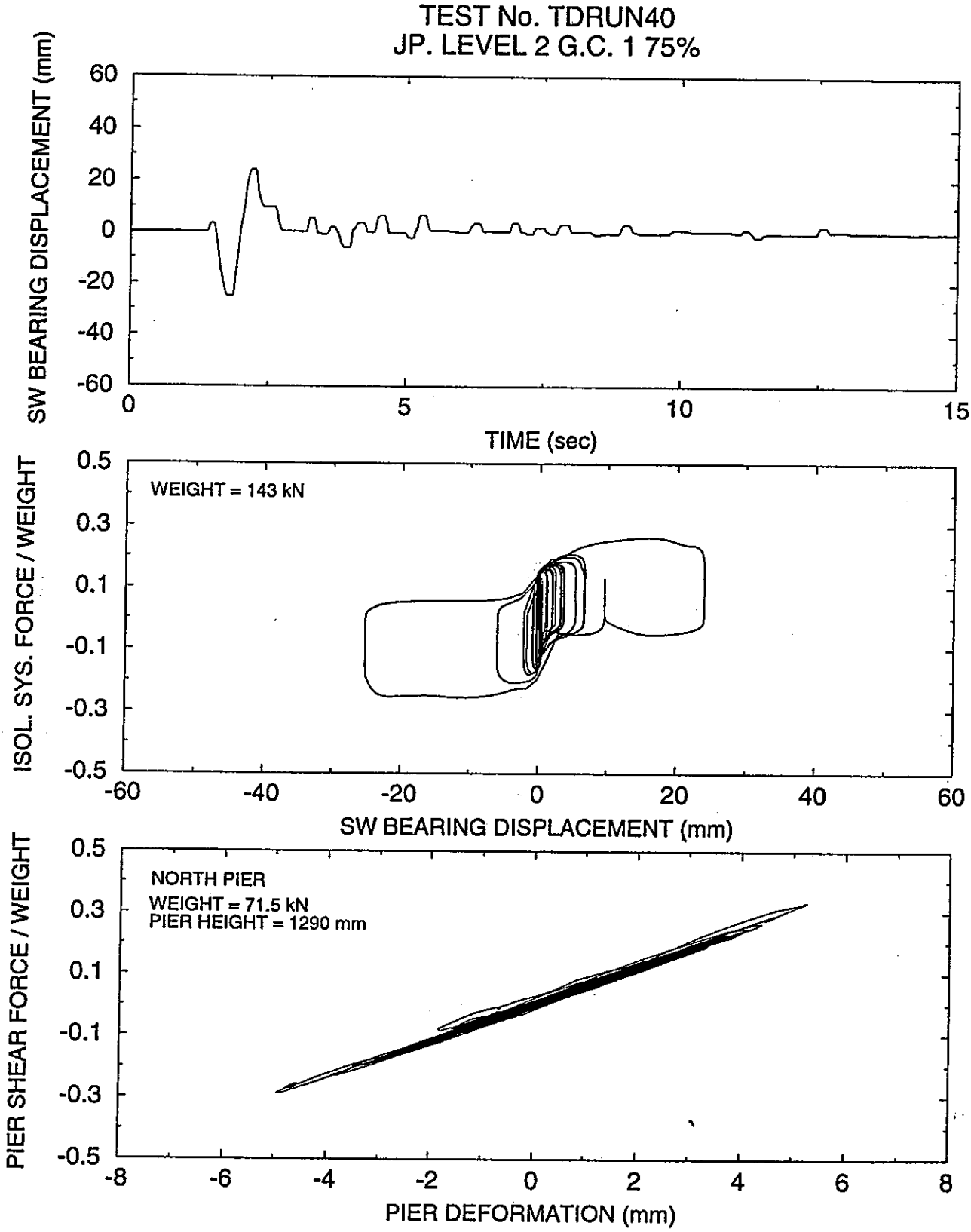
TEST No. TDRUN40
JP. LEVEL 2 G.C. 1 75%
SW BEARING DISPLACEMENT (mm)
60
40
20
0
-20
-40
-60
0
5
10
15
TIME (sec)
ISOL. SYS. FORCE / WEIGHT
WEIGHT = 143 kN
0.5
0.3
0.1
-0.1
-0.3
-0.5
-60
-40
-20
0
20
40
60
SW BEARING DISPLACEMENT (mm)
PIER SHEAR FORCE / WEIGHT
NORTH PIER
WEIGHT = 71.5 kN
PIER HEIGHT = 1290 mm
0.5
0.3
0.1
-0.1
-0.3
-0.5
-8
-6
-4
-2
0
2
4
6
8
PIER DEFORMATION (mm)

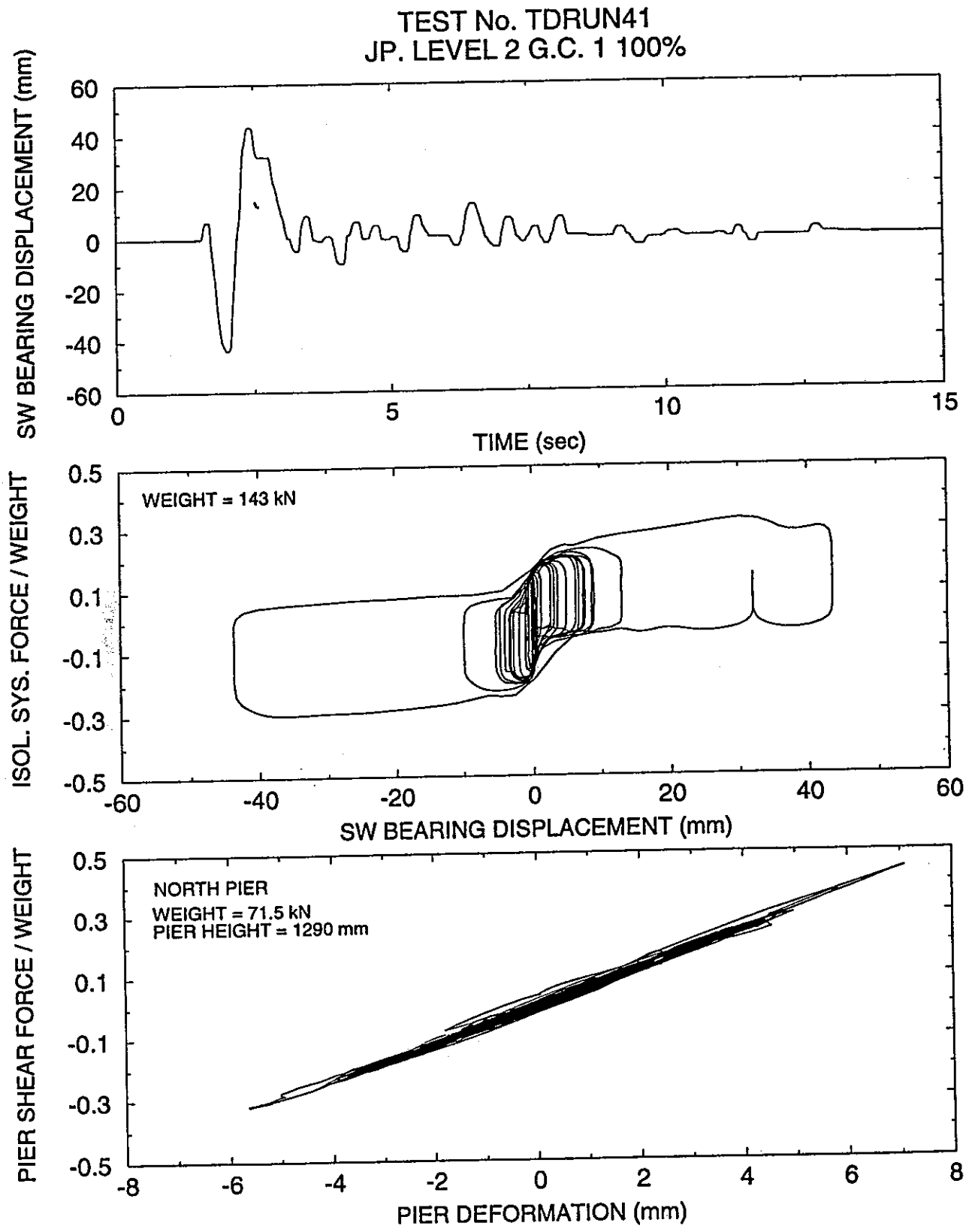
TEST No. TDRUN41
JP. LEVEL 2 G.C. 1 100%
SW BEARING DISPLACEMENT (mm)
60
40
20
0
-20
-40
-60
0
5
10
15
TIME (sec)
ISOL. SYS. FORCE / WEIGHT
WEIGHT = 143 kN
0.5
0.3
0.1
-0.1
-0.3
-0.5
-60
-40
-20
0
20
40
60
SW BEARING DISPLACEMENT (mm)
PIER SHEAR FORCE / WEIGHT
NORTH PIER
WEIGHT = 71.5 kN
PIER HEIGHT = 1290 mm
0.5
0.3
0.1
-0.1
-0.3
-0.5
-8
-6
-4
-2
0
2
4
6
8
PIER DEFORMATION (mm)

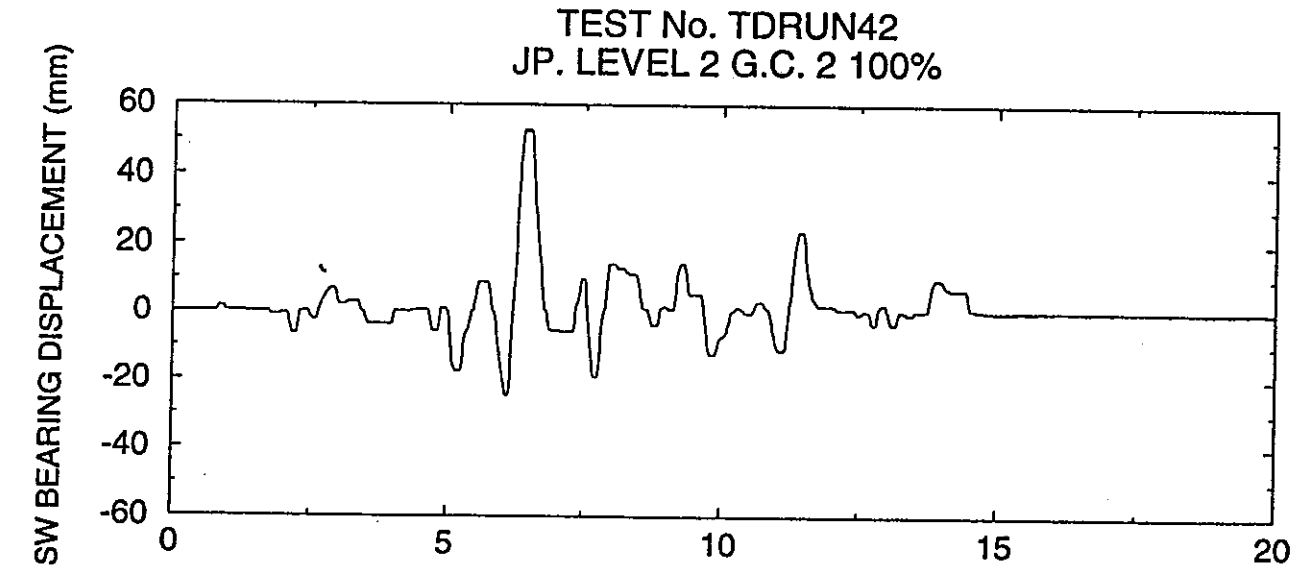
TEST No. TDRUN42
JP. LEVEL 2 G.C. 2 100%
SW BEARING DISPLACEMENT (mm)
60
40
20
0
-20
-40
-60
0
5
10
15
20
TIME (sec)

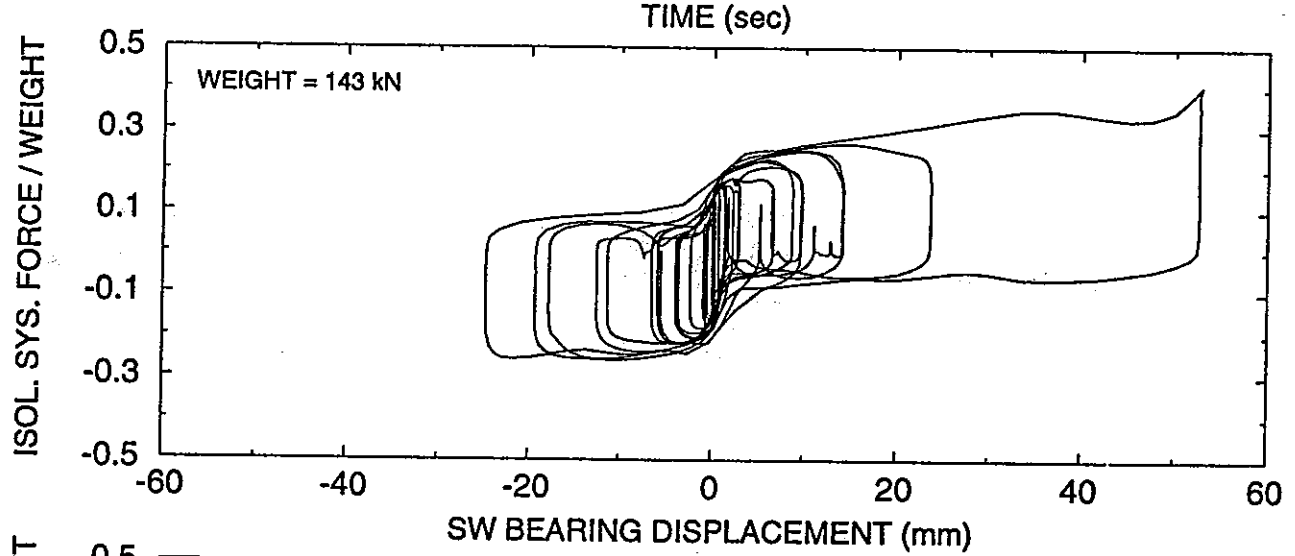
ISOL. SYS. FORCE / WEIGHT
WEIGHT = 143 kN
0.5
0.3
0.1
-0.1
-0.3
-0.5
-60
-40
-20
0
20
40
60
SW BEARING DISPLACEMENT (mm)

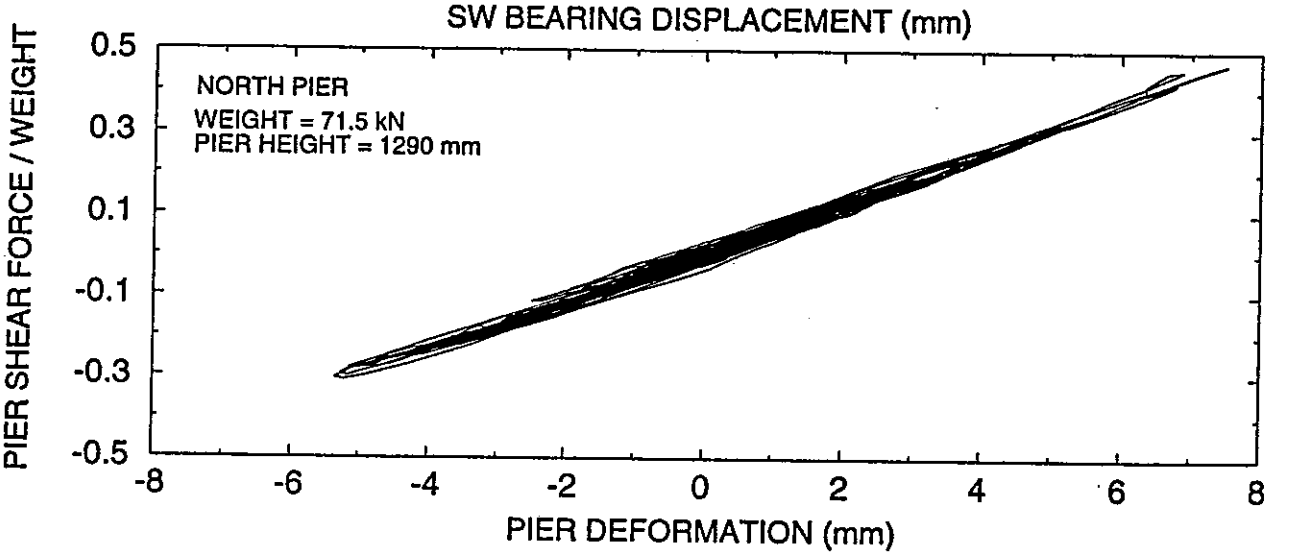
PIER SHEAR FORCE / WEIGHT
NORTH PIER
WEIGHT = 71.5 kN
PIER HEIGHT = 1290 mm
0.5
0.3
0.1
-0.1
-0.3
-0.5
-8
-6
-4
-2
0
2
4
6
8
PIER DEFORMATION (mm)

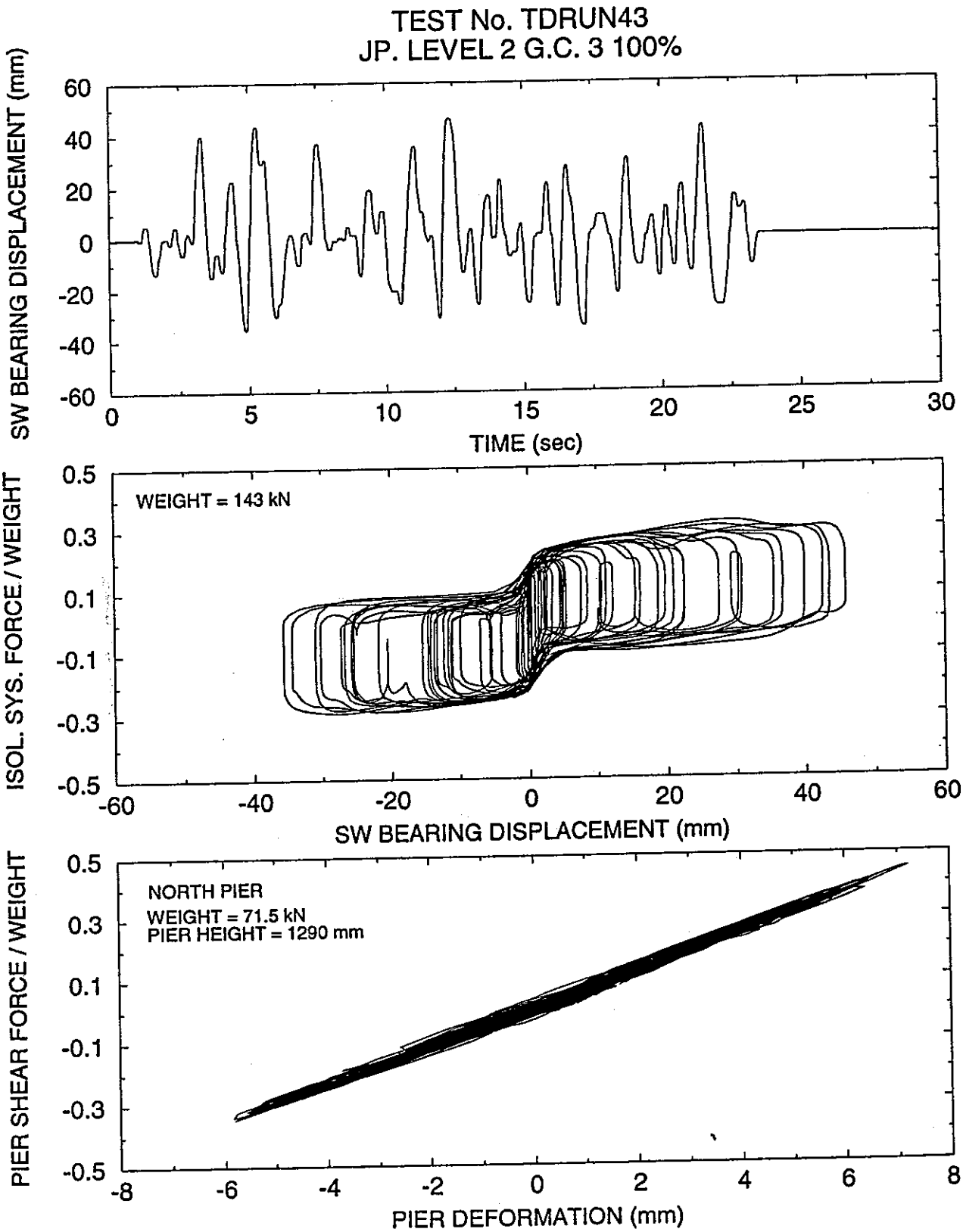
TEST No. TDRUN43
JP. LEVEL 2 G.C. 3 100%
SW BEARING DISPLACEMENT (mm)
60
40
20
0
-20
-40
-60
0
5
10
15
20
25
30
TIME (sec)
ISOL. SYS. FORCE / WEIGHT
WEIGHT = 143 kN
0.5
0.3
0.1
-0.1
-0.3
-0.5
-60
-40
-20
0
20
40
60
SW BEARING DISPLACEMENT (mm)
PIER SHEAR FORCE / WEIGHT
NORTH PIER
WEIGHT = 71.5 kN
PIER HEIGHT = 1290 mm
0.5
0.3
0.1
-0.1
-0.3
-0.5
-8
-6
-4
-2
0
2
4
6
8
PIER DEFORMATION (mm)

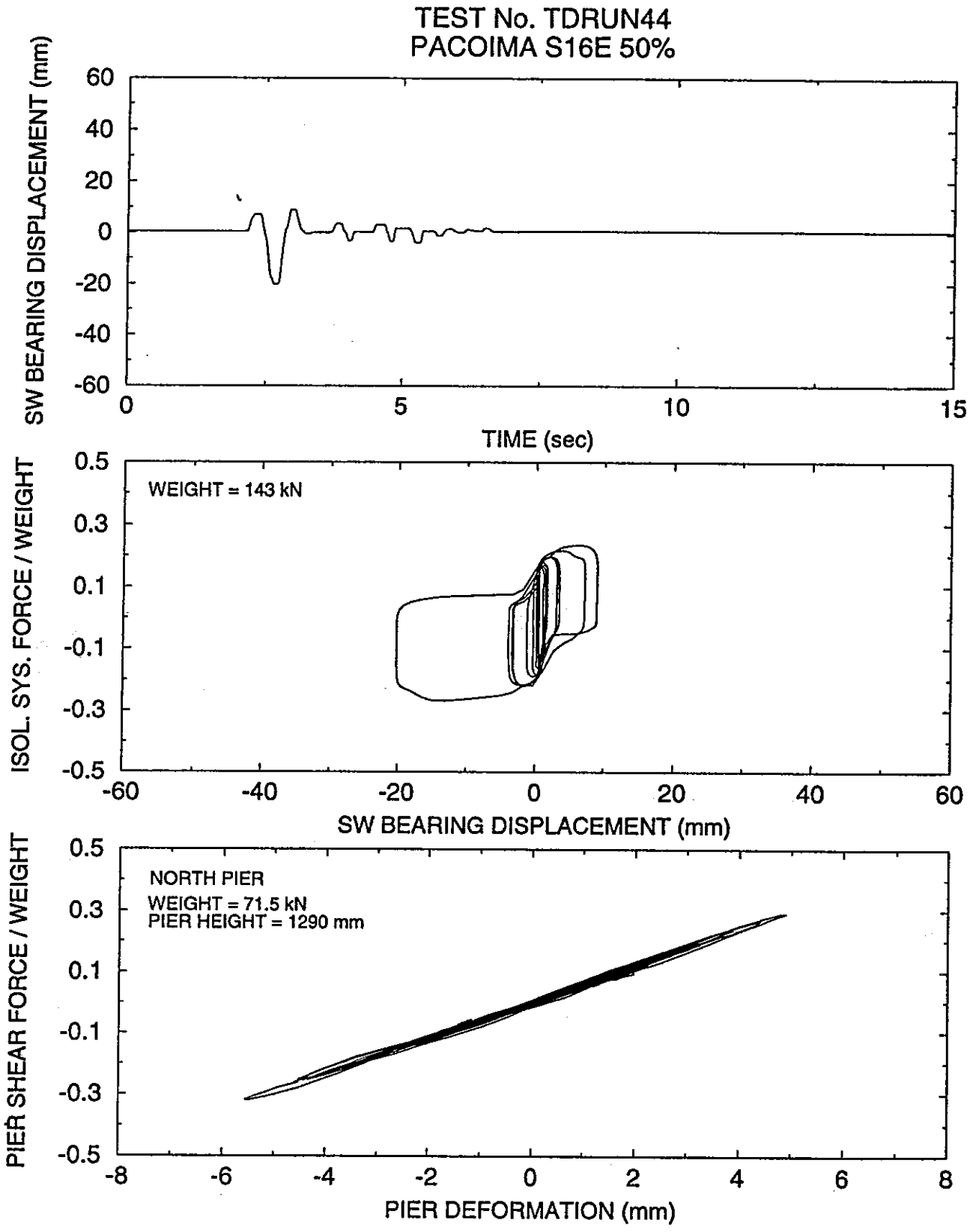
TEST No. TDRUN44
PACOIMA S16E 50%
SW BEARING DISPLACEMENT (mm)
60
40
20
0
-20
-40
-60
0
5
10
15
TIME (sec)
ISOL. SYS. FORCE / WEIGHT
WEIGHT = 143 kN
0.5
0.3
0.1
-0.1
-0.3
-0.5
-60
-40
-20
0
20
40
60
SW BEARING DISPLACEMENT (mm)
PIER SHEAR FORCE / WEIGHT
NORTH PIER
WEIGHT = 71.5 kN
PIER HEIGHT = 1290 mm
0.5
0.3
0.1
-0.1
-0.3
-0.5
-8
-6
-4
-2
0
2
4
6
8
PIER DEFORMATION (mm)

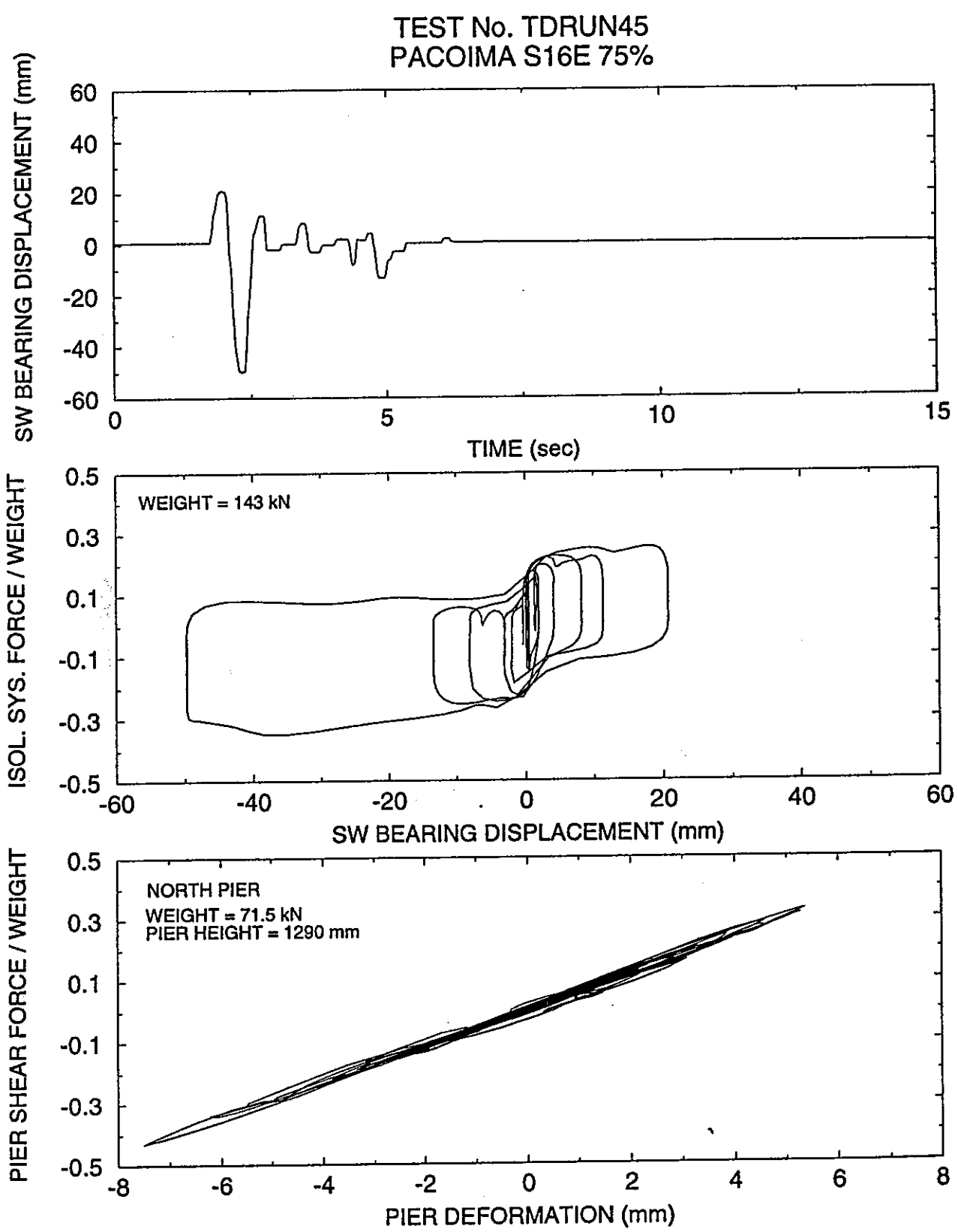
TEST No. TDRUN45
PACOIMA S16E 75%
SW BEARING DISPLACEMENT (mm)
60
40
20
0
-20
-40
-60
0
5
10
15
TIME (sec)
ISOL. SYS. FORCE / WEIGHT
WEIGHT = 143 kN
0.5
0.3
0.1
-0.1
-0.3
-0.5
-60
-40
-20
0
20
40
60
SW BEARING DISPLACEMENT (mm)
PIER SHEAR FORCE / WEIGHT
NORTH PIER
WEIGHT = 71.5 kN
PIER HEIGHT = 1290 mm
0.5
0.3
0.1
-0.1
-0.3
-0.5
-8
-6
-4
-2
0
2
4
6
8
PIER DEFORMATION (mm)

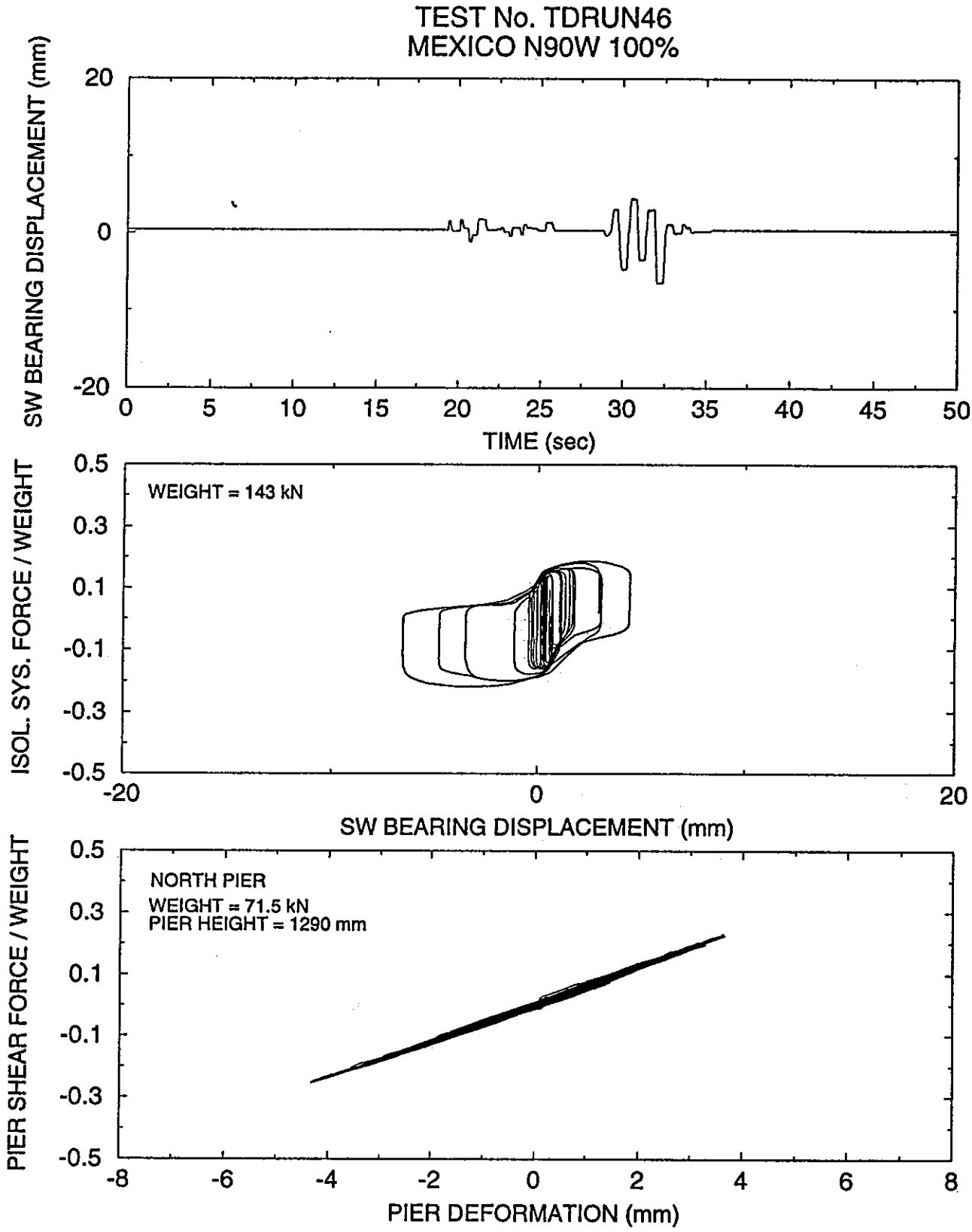
TEST No. TDRUN46
MEXICO N90W 100%
SW BEARING DISPLACEMENT (mm)
20
0
-20
0
5
10
15
20
25
30
35
40
45
50
TIME (sec)
ISOL. SYS. FORCE / WEIGHT
WEIGHT = 143 kN
0.5
0.3
0.1
-0.1
-0.3
-0.5
-20
0
20
SW BEARING DISPLACEMENT (mm)
PIER SHEAR FORCE / WEIGHT
NORTH PIER
WEIGHT = 71.5 kN
PIER HEIGHT = 1290 mm
0.5
0.3
0.1
-0.1
-0.3
-0.5
-8
-6
-4
-2
0
2
4
6
8
PIER DEFORMATION (mm)

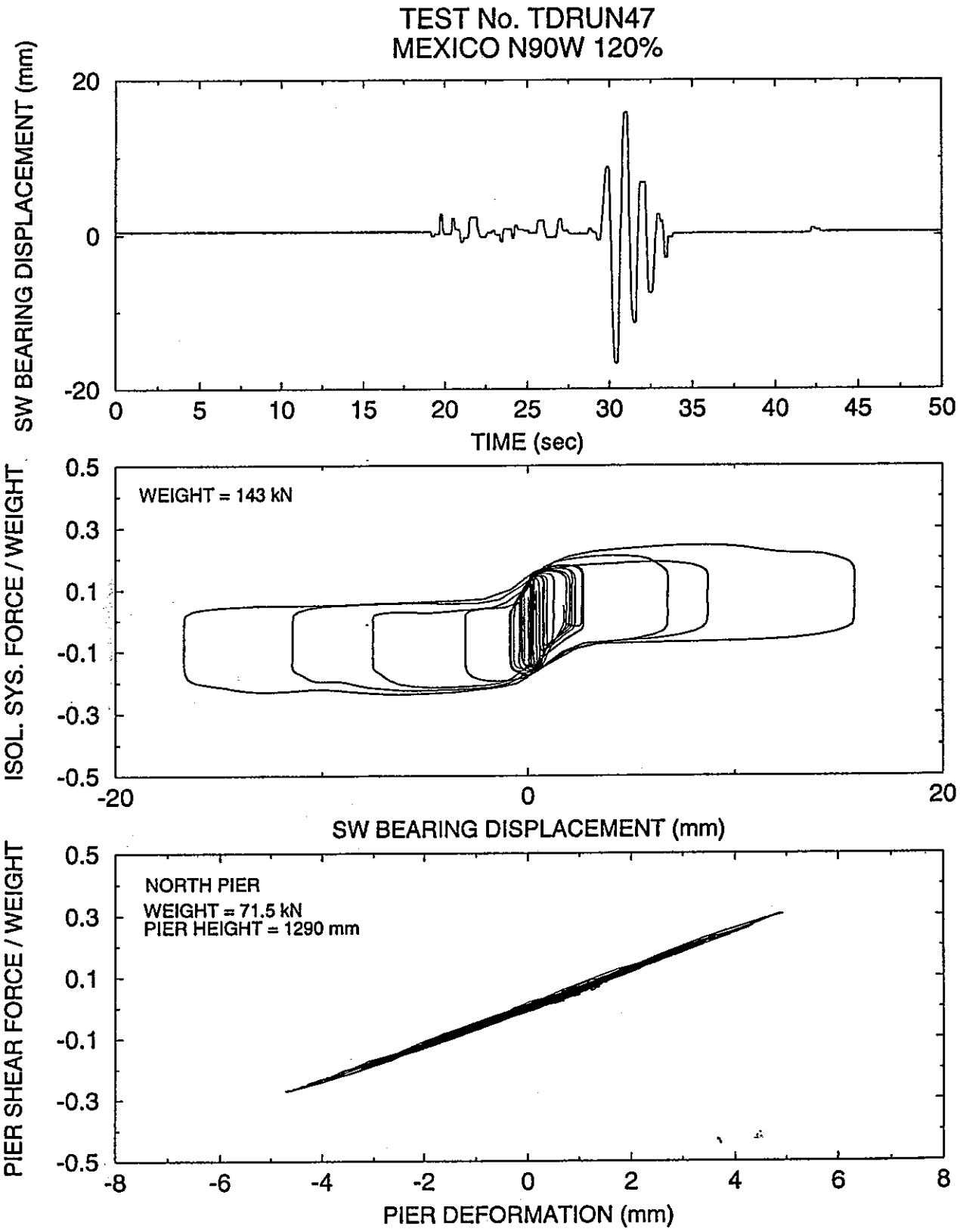
TEST No. TDRUN47
MEXICO N90W 120%
SW BEARING DISPLACEMENT (mm)
20
0
-20
0
5
10
15
20
25
30
35
40
45
50
TIME (sec)
ISOL. SYS. FORCE / WEIGHT
WEIGHT = 143 kN
0.5
0.3
0.1
-0.1
-0.3
-0.5
-20
0
20
SW BEARING DISPLACEMENT (mm)
PIER SHEAR FORCE / WEIGHT
NORTH PIER
WEIGHT = 71.5 kN
PIER HEIGHT = 1290 mm
0.5
0.3
0.1
-0.1
-0.3
-0.5
-8
-6
-4
-2
0
2
4
6
8
PIER DEFORMATION (mm)

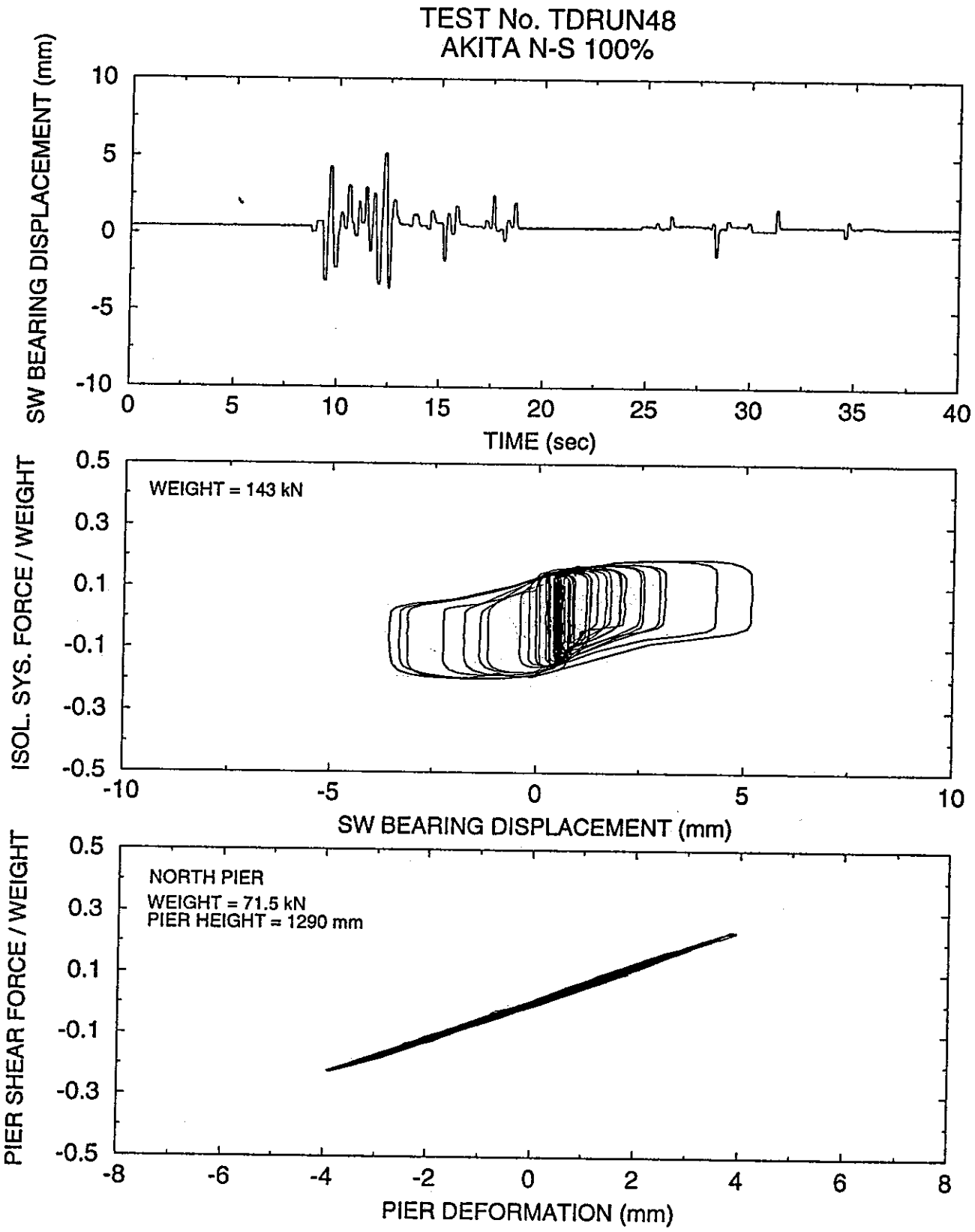
TEST No. TDRUN48
AKITA N-S 100%
SW BEARING DISPLACEMENT (mm)
10
5
0
-5
-10
0
5
10
15
20
25
30
35
40
TIME (sec)
ISOL. SYS. FORCE / WEIGHT
WEIGHT = 143 kN
0.5
0.3
0.1
-0.1
-0.3
-0.5
-10
-5
0
5
10
SW BEARING DISPLACEMENT (mm)
PIER SHEAR FORCE / WEIGHT
NORTH PIER
WEIGHT = 71.5 kN
PIER HEIGHT = 1290 mm
0.5
0.3
0.1
-0.1
-0.3
-0.5
-8
-6
-4
-2
0
2
4
6
8
PIER DEFORMATION (mm)

TEST No. TDRUN49
AKITA N-S 200%

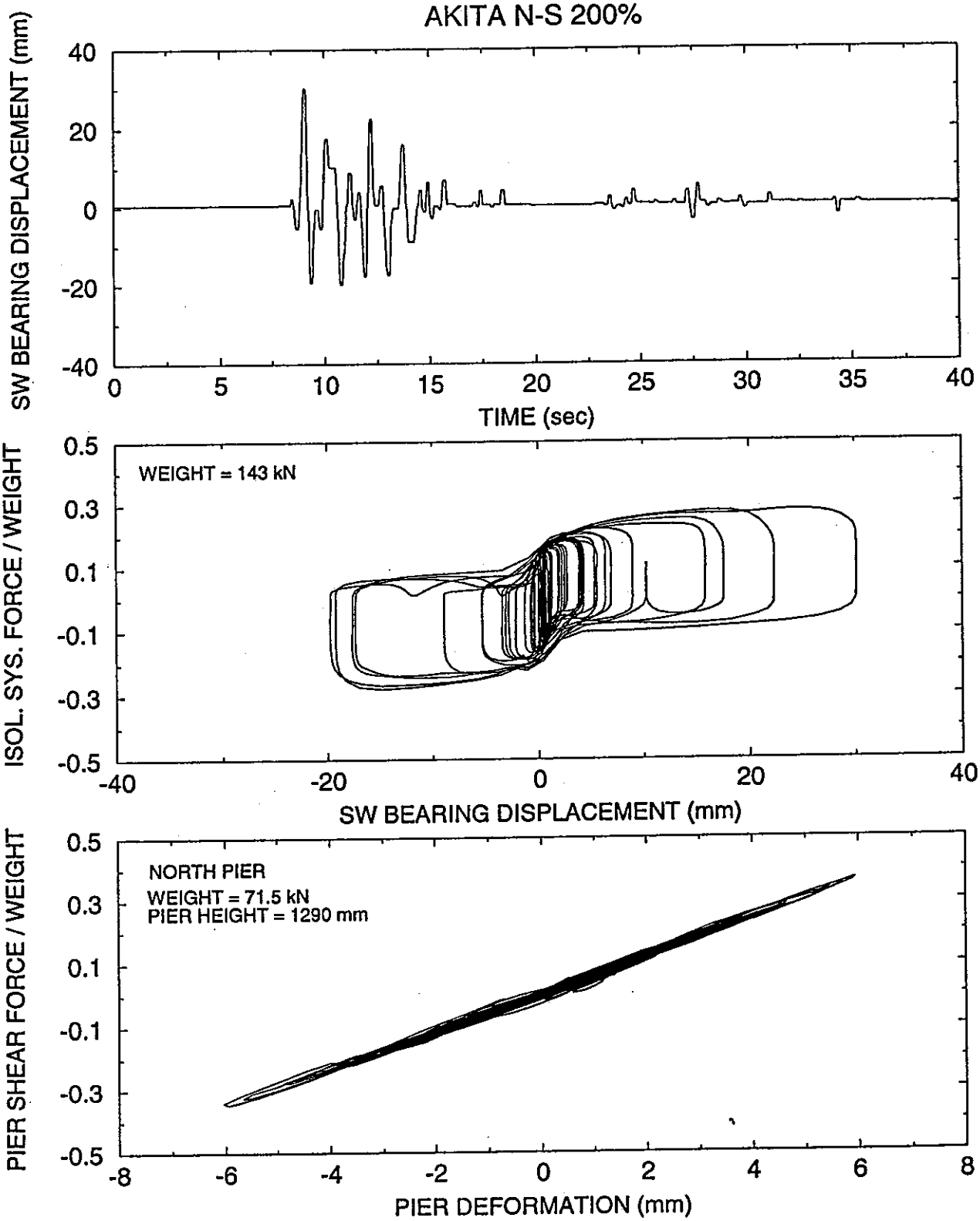

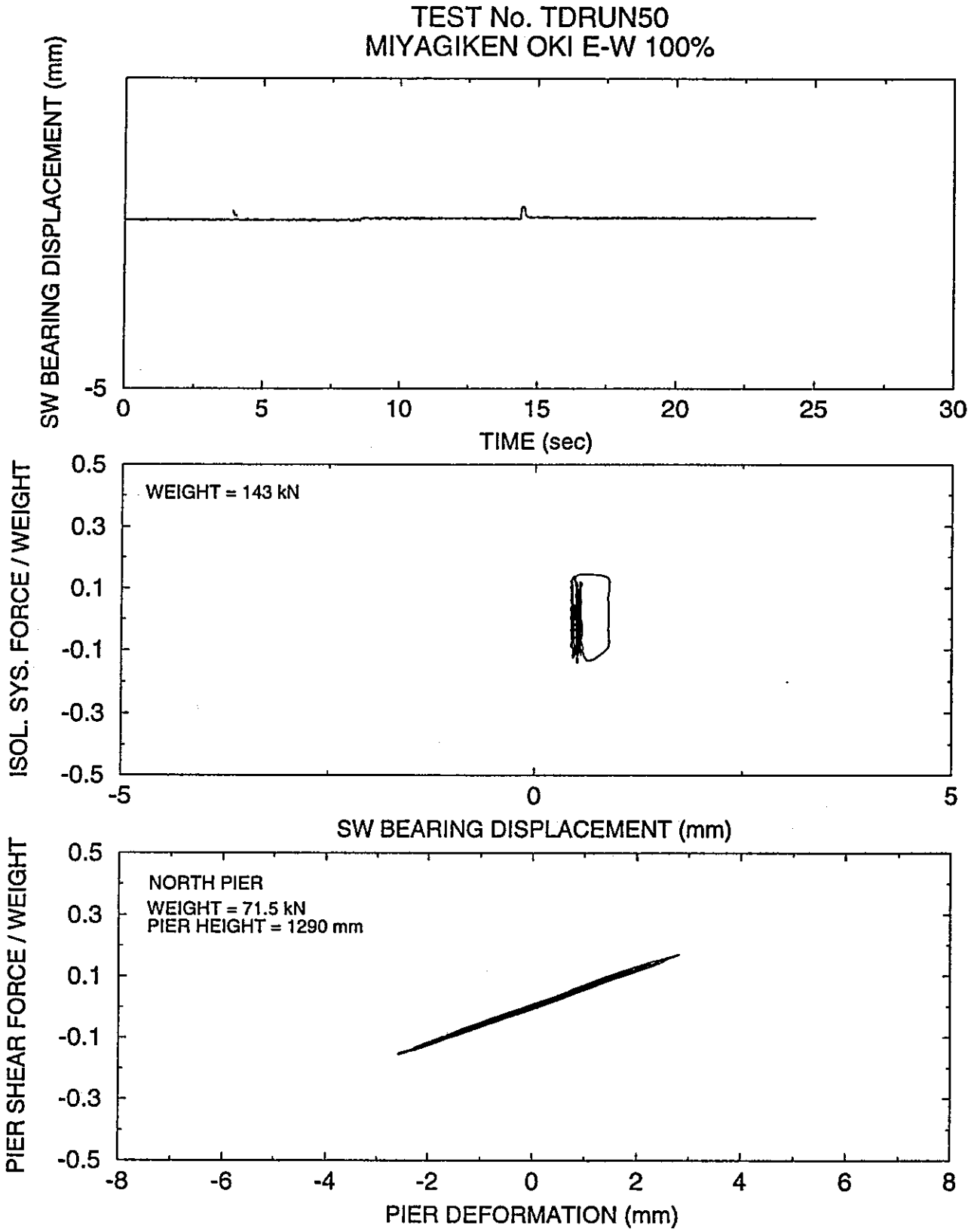
TEST No. TDRUN50
MIYAGIKEN OKI E-W 100%
SW BEARING DISPLACEMENT (mm)
-5
0
5
10
15
20
25
30
TIME (sec)
ISOL. SYS. FORCE / WEIGHT
WEIGHT = 143 kN
0.5
0.3
0.1
-0.1
-0.3
-0.5
-5
0
5
SW BEARING DISPLACEMENT (mm)
PIER SHEAR FORCE / WEIGHT
NORTH PIER
WEIGHT = 71.5 kN
PIER HEIGHT = 1290 mm
0.5
0.3
0.1
-0.1
-0.3
-0.5
-8
-6
-4
-2
0
2
4
6
8
PIER DEFORMATION (mm)

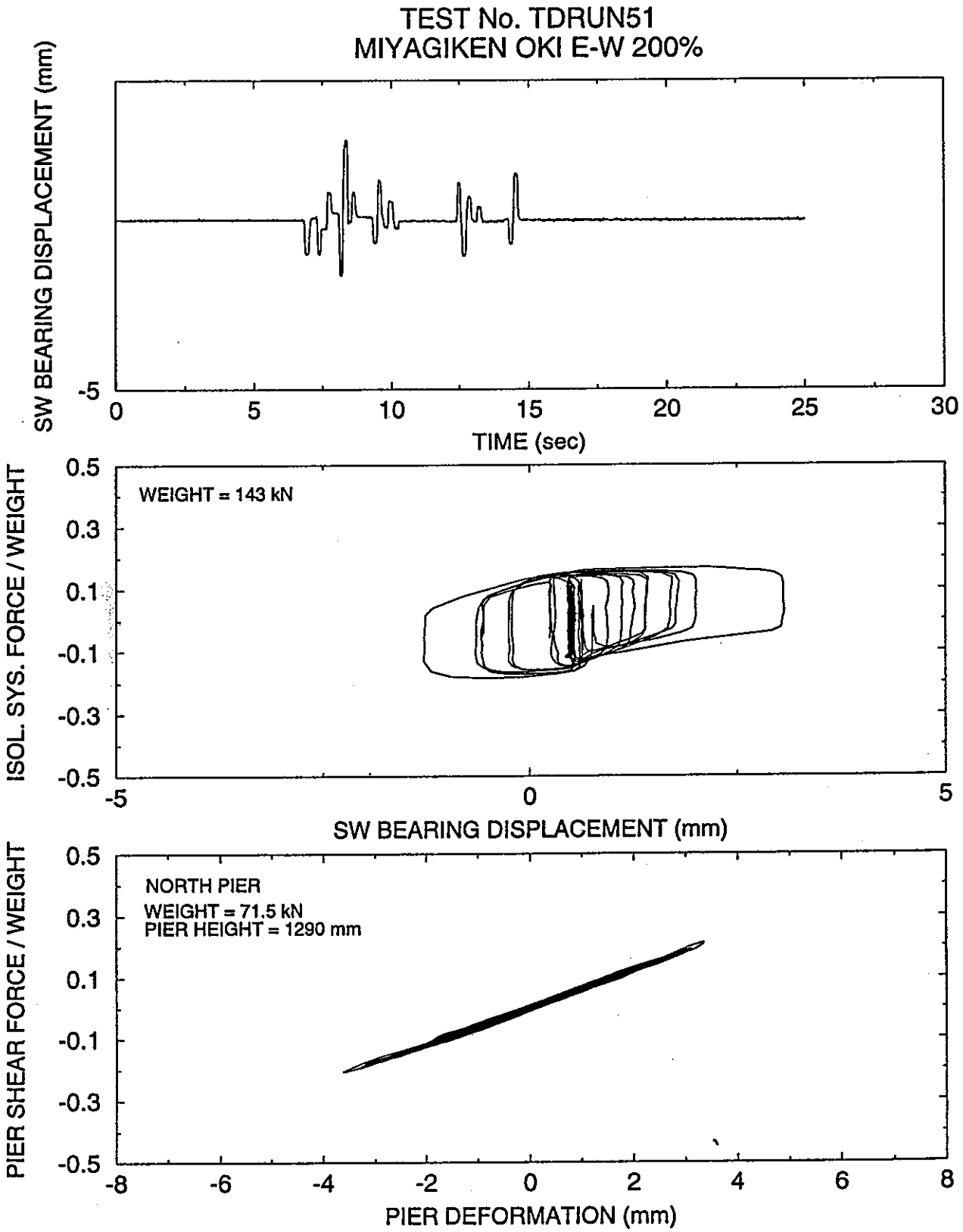
TEST No. TDRUN51
MIYAGIKEN OKI E-W 200%
SW BEARING DISPLACEMENT (mm)
-5
0
5
10
15
20
25
30
TIME (sec)
ISOL. SYS. FORCE / WEIGHT
WEIGHT = 143 kN
0.5
0.3
0.1
-0.1
-0.3
-0.5
-5
0
5
SW BEARING DISPLACEMENT (mm)
PIER SHEAR FORCE / WEIGHT
NORTH PIER
WEIGHT = 71.5 kN
PIER HEIGHT = 1290 mm
0.5
0.3
0.1
-0.1
-0.3
-0.5
-8
-6
-4
-2
0
2
4
6
8
PIER DEFORMATION (mm)

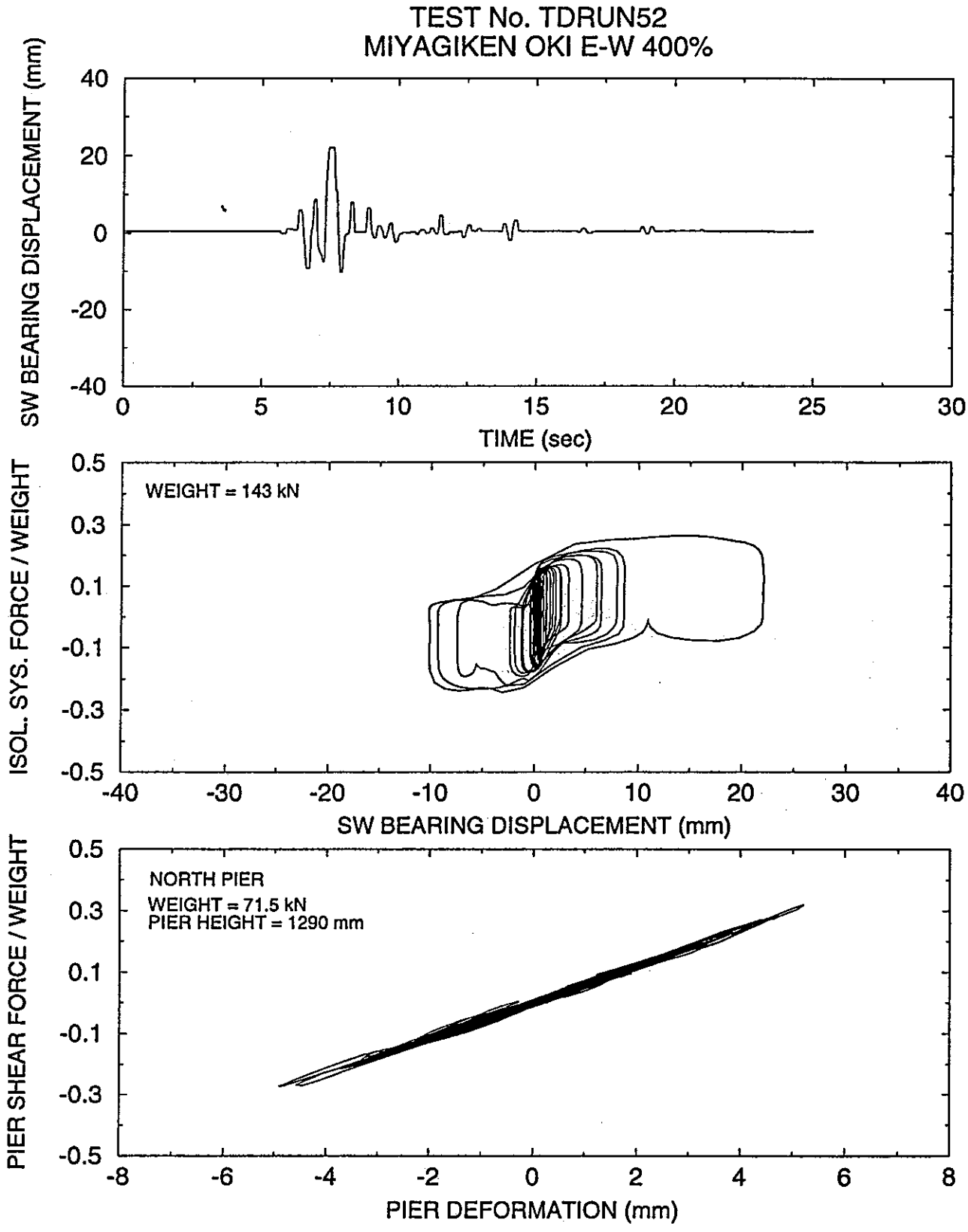
TEST No. TDRUN52
MIYAGIKEN OKI E-W 400%
SW BEARING DISPLACEMENT (mm)
40
20
0
-20
-40
0
5
10
15
20
25
30
TIME (sec)
ISOL. SYS. FORCE / WEIGHT
WEIGHT = 143 kN
0.5
0.3
0.1
-0.1
-0.3
-0.5
-40
-30
-20
-10
0
10
20
30
40
SW BEARING DISPLACEMENT (mm)
PIER SHEAR FORCE / WEIGHT
NORTH PIER
WEIGHT = 71.5 kN
PIER HEIGHT = 1290 mm
0.5
0.3
0.1
-0.1
-0.3
-0.5
-8
-6
-4
-2
0
2
4
6
8
PIER DEFORMATION (mm)

TEST No. TDRUN53
MIYAGIKEN OKI E-W 600%

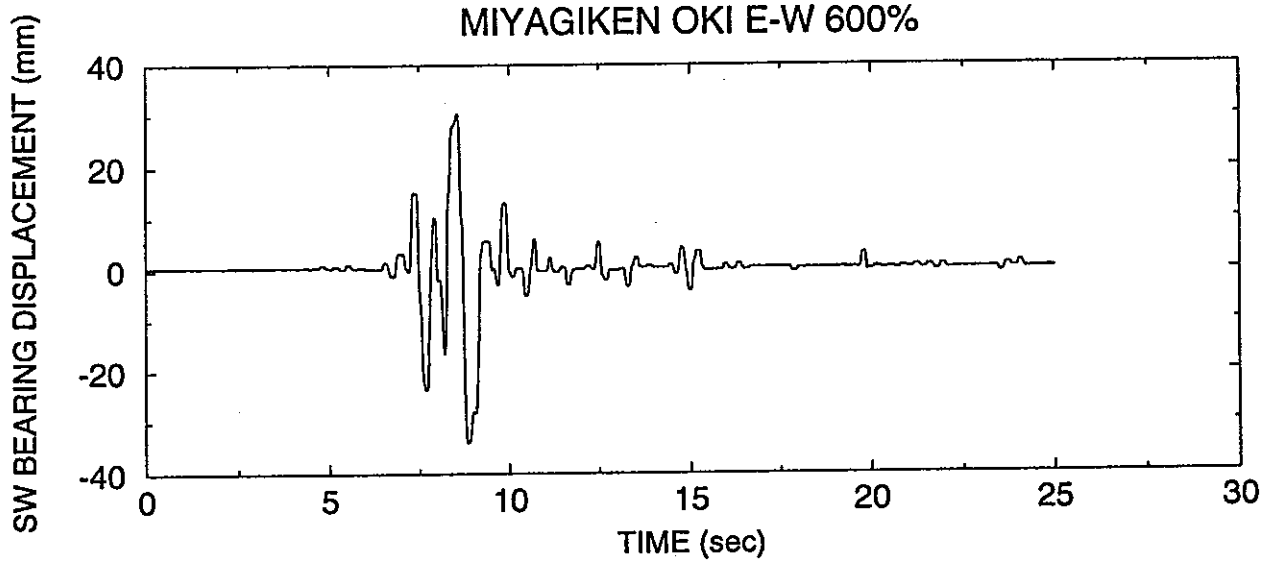

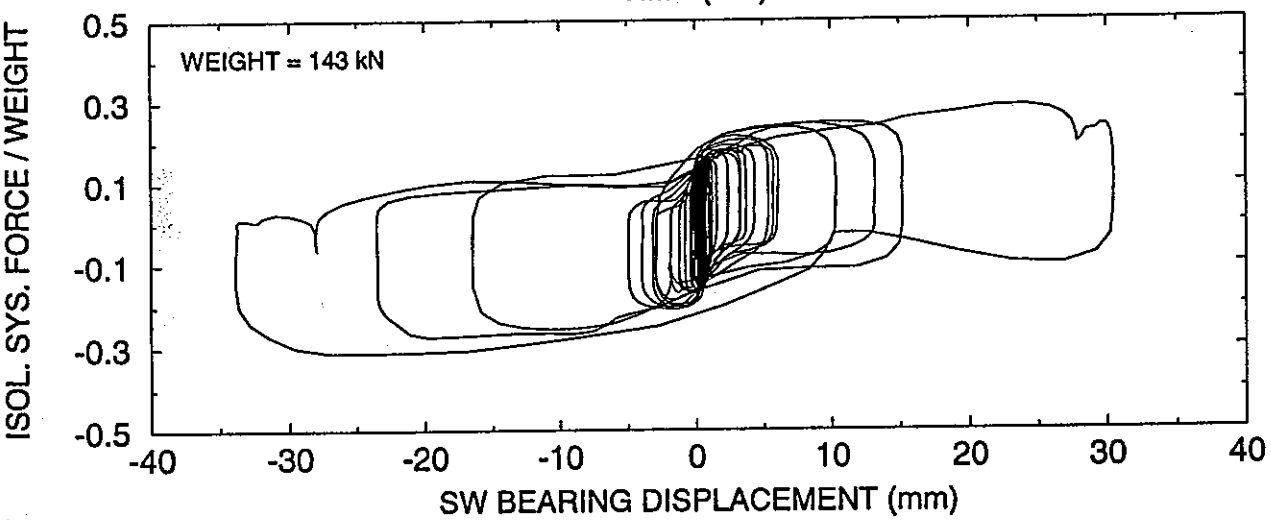

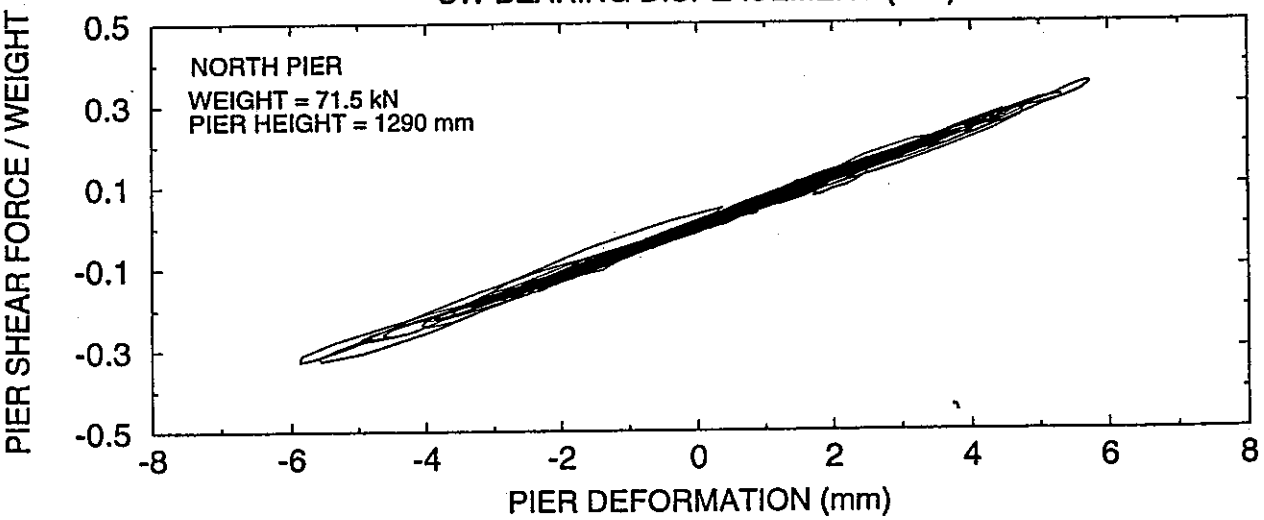

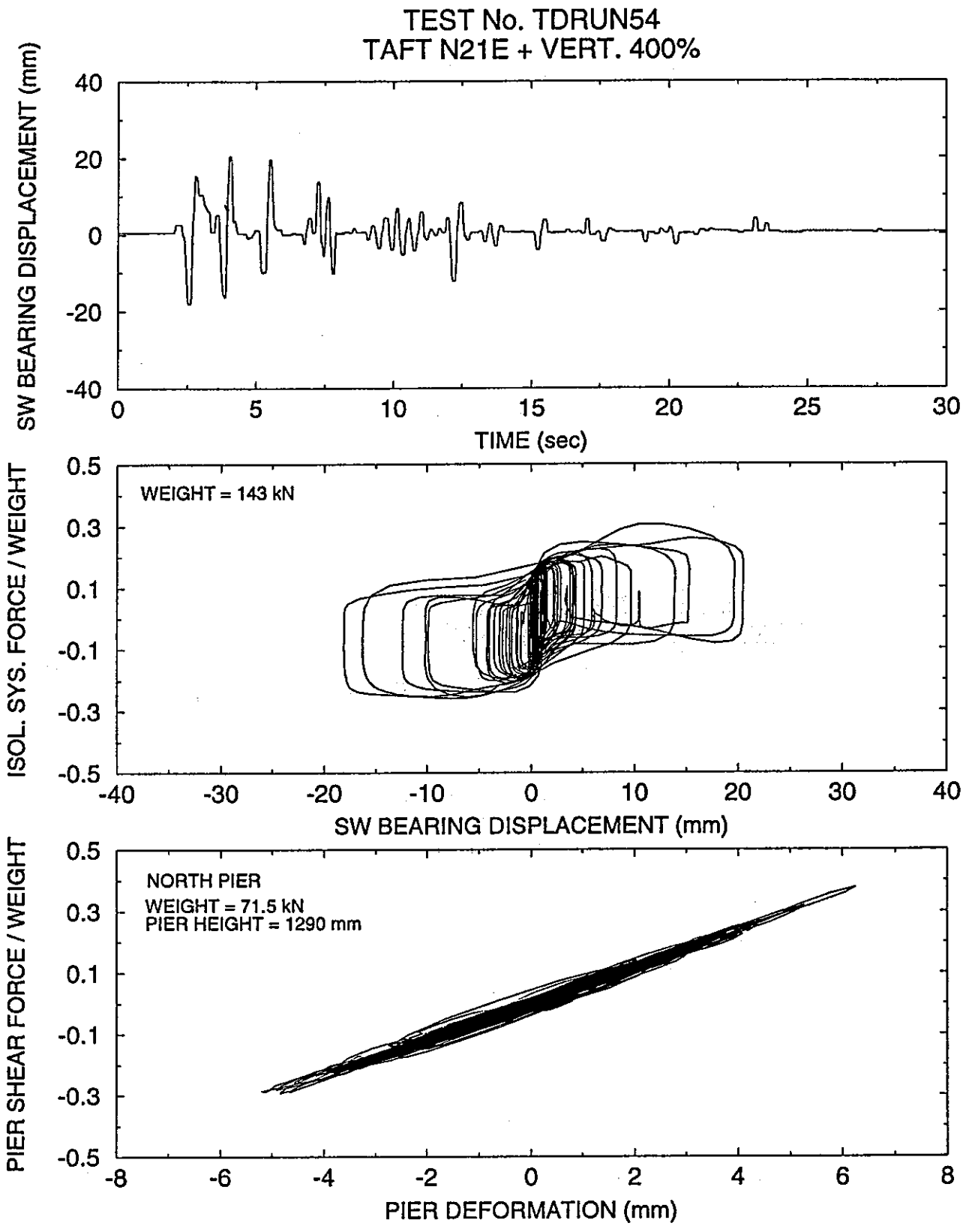
TEST No. TDRUN54
TAFT N21E + VERT. 400%
SW BEARING DISPLACEMENT (mm)
TIME (sec)
ISOL. SYS. FORCE / WEIGHT
WEIGHT = 143 kN
SW BEARING DISPLACEMENT (mm)
PIER SHEAR FORCE / WEIGHT
NORTH PIER
WEIGHT = 71.5 kN
PIER HEIGHT = 1290 mm
PIER DEFORMATION (mm)

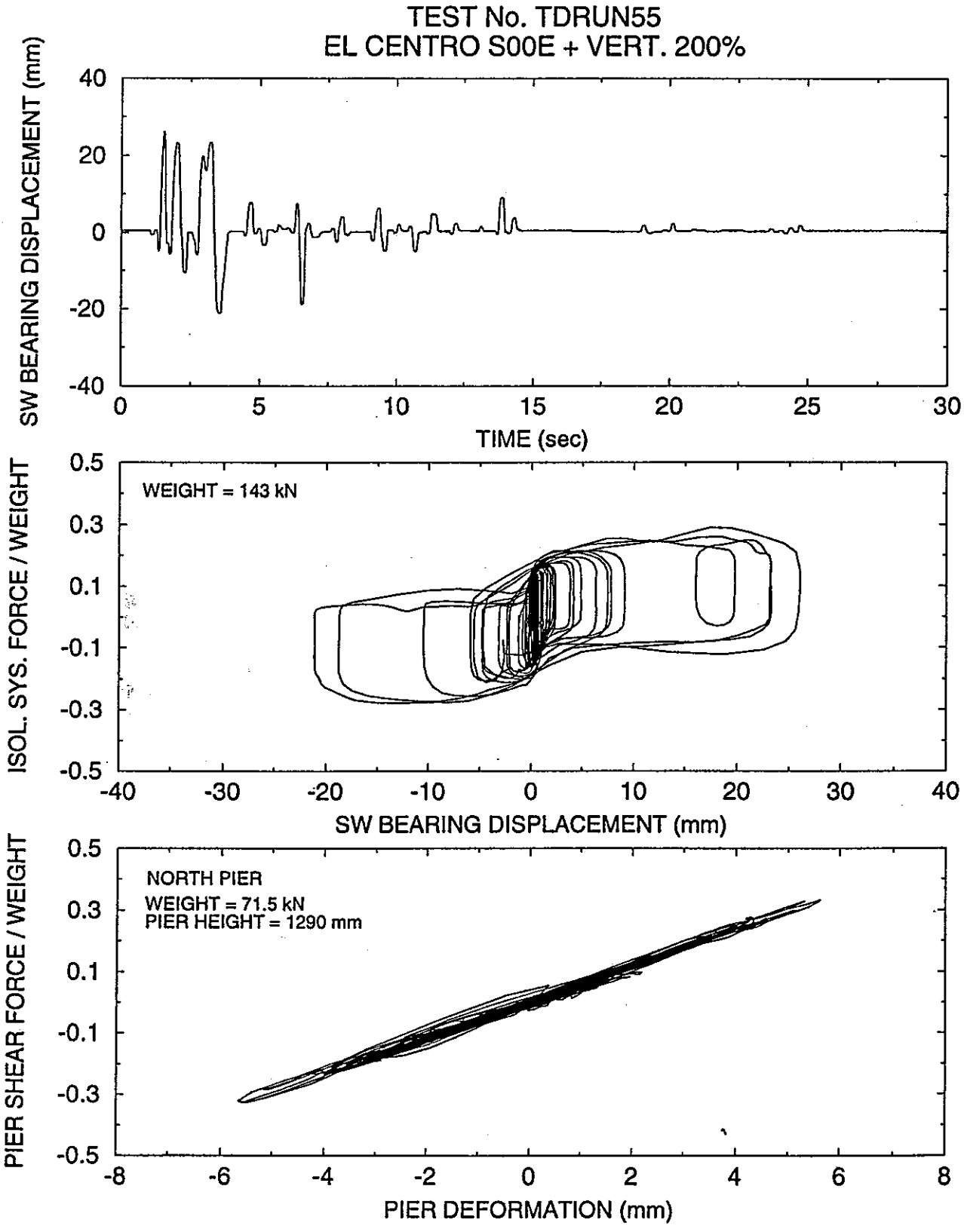
TEST No. TDRUN55
EL CENTRO S00E + VERT. 200%
SW BEARING DISPLACEMENT (mm)
40
20
0
-20
-40
0
5
10
15
20
25
30
TIME (sec)
ISOL. SYS. FORCE / WEIGHT
WEIGHT = 143 kN
0.5
0.3
0.1
-0.1
-0.3
-0.5
-40
-30
-20
-10
0
10
20
30
40
SW BEARING DISPLACEMENT (mm)
PIER SHEAR FORCE / WEIGHT
NORTH PIER
WEIGHT = 71.5 kN
PIER HEIGHT = 1290 mm
0.5
0.3
0.1
-0.1
-0.3
-0.5
-8
-6
-4
-2
0
2
4
6
8
PIER DEFORMATION (mm)

NATIONAL CENTER FOR EARTHQUAKE ENGINEERING RESEARCH
LIST OF TECHNICAL REPORTS

The National Center for Earthquake Engineering Research (NCEER) publishes technical reports on a variety of subjects related to earthquake engineering written by authors funded through NCEER. These reports are available from both NCEER's Publications Department and the National Technical Information Service (NTIS). Requests for reports should be directed to the Publications Department, National Center for Earthquake Engineering Research, State University of New York at Buffalo, Red Jacket Quadrangle, Buffalo, New York 14261. Reports can also be requested through NTIS, 5285 Port Royal Road, Springfield, Virginia 22161. NTIS accession numbers are shown in parenthesis, if available.

NCEER-87-0001 "First-Year Program in Research, Education and Technology Transfer," 3/5/87, (PB88-134275).

NCEER-87-0002 "Experimental Evaluation of Instantaneous Optimal Algorithms for Structural Control," by R.C. Lin, T.T. Soong and A.M. Reinhorn, 4/20/87, (PB88-134341).

NCEER-87-0003 "Experimentation Using the Earthquake Simulation Facilities at University at Buffalo," by A.M. Reinhorn and R.L. Ketter, to be published.

NCEER-87-0004 "The System Characteristics and Performance of a Shaking Table," by J.S. Hwang, K.C. Chang and G.C. Lee, 6/1/87, (PB88-134259). This report is available only through NTIS (see address given above).

NCEER-87-0005 "A Finite Element Formulation for Nonlinear Viscoplastic Material Using a Q Model," by O. Gyebi and G. Dasgupta, 11/2/87, (PB88-213764).

NCEER-87-0006 "Symbolic Manipulation Program (SMP) - Algebraic Codes for Two and Three Dimensional Finite Element Formulations," by X. Lee and G. Dasgupta, 11/9/87, (PB88-218522).

NCEER-87-0007 "Instantaneous Optimal Control Laws for Tall Buildings Under Seismic Excitations," by J.N. Yang, A. Akbarpour and P. Ghaemmaghami, 6/10/87, (PB88-134333). This report is only available through NTIS (see address given above).

NCEER-87-0008 "IDARC: Inelastic Damage Analysis of Reinforced Concrete Frame - Shear-Wall Structures," by Y.J. Park, A.M. Reinhorn and S.K. Kunnath, 7/20/87, (PB88-134325).

NCEER-87-0009 "Liquefaction Potential for New York State: A Preliminary Report on Sites in Manhattan and Buffalo," by M. Budhu, V. Vijayakumar, R.F. Giese and L. Baumgras, 8/31/87, (PB88-163704). This report is available only through NTIS (see address given above).

NCEER-87-0010 "Vertical and Torsional Vibration of Foundations in Inhomogeneous Media," by A.S. Veletsos and K.W. Dotson, 6/1/87, (PB88-134291).

NCEER-87-0011 "Seismic Probabilistic Risk Assessment and Seismic Margins Studies for Nuclear Power Plants," by Howard H.M. Hwang, 6/15/87, (PB88-134267).

NCEER-87-0012 "Parametric Studies of Frequency Response of Secondary Systems Under Ground-Acceleration Excitations," by Y. Yong and Y.K. Lin, 6/10/87, (PB88-134309).

NCEER-87-0013 "Frequency Response of Secondary Systems Under Seismic Excitation," by J.A. HoLung, J. Cai and Y.K. Lin, 7/31/87, (PB88-134317).

NCEER-87-0014 "Modelling Earthquake Ground Motions in Seismically Active Regions Using Parametric Time Series Methods," by G.W. Ellis and A.S. Cakmak, 8/25/87, (PB88-134283).

NCEER-87-0015 "Detection and Assessment of Seismic Structural Damage," by E. DiPasquale and A.S. Cakmak, 8/25/87, (PB88-163712).

NCEER-87-0016 "Pipeline Experiment at Parkfield, California," by J. Isenberg and E. Richardson, 9/15/87, (PB88-163720). This report is available only through NTIS (see address given above).

NCEER-87-0017 "Digital Simulation of Seismic Ground Motion," by M. Shinozuka, G. Deodatis and T. Harada, 8/31/87, (PB88-155197). This report is available only through NTIS (see address given above).

NCEER-87-0018 "Practical Considerations for Structural Control: System Uncertainty, System Time Delay and Truncation of Small Control Forces," J.N. Yang and A. Akbarpour, 8/10/87, (PB88-163738).

NCEER-87-0019 "Modal Analysis of Nonclassically Damped Structural Systems Using Canonical Transformation," by J.N. Yang, S. Sarkani and F.X. Long, 9/27/87, (PB88-187851).

NCEER-87-0020 "A Nonstationary Solution in Random Vibration Theory," by J.R. Red-Horse and P.D. Spanos, 11/3/87, (PB88-163746).

NCEER-87-0021 "Horizontal Impedances for Radially Inhomogeneous Viscoelastic Soil Layers," by A.S. Veletsos and K.W. Dotson, 10/15/87, (PB88-150859).

NCEER-87-0022 "Seismic Damage Assessment of Reinforced Concrete Members," by Y.S. Chung, C. Meyer and M. Shinozuka, 10/9/87, (PB88-150867). This report is available only through NTIS (see address given above).

NCEER-87-0023 "Active Structural Control in Civil Engineering," by T.T. Soong, 11/11/87, (PB88-187778).

NCEER-87-0024 "Vertical and Torsional Impedances for Radially Inhomogeneous Viscoelastic Soil Layers," by K.W. Dotson and A.S. Veletsos, 12/87, (PB88-187786).

NCEER-87-0025 "Proceedings from the Symposium on Seismic Hazards, Ground Motions, Soil-Liquefaction and Engineering Practice in Eastern North America," October 20-22, 1987, edited by K.H. Jacob, 12/87, (PB88-188115).

NCEER-87-0026 "Report on the Whittier-Narrows, California, Earthquake of October 1, 1987," by J. Pantelic and A. Reinhorn, 11/87, (PB88-187752). This report is available only through NTIS (see address given above).

NCEER-87-0027 "Design of a Modular Program for Transient Nonlinear Analysis of Large 3-D Building Structures," by S. Srivastav and J.F. Abel, 12/30/87, (PB88-187950).

NCEER-87-0028 "Second-Year Program in Research, Education and Technology Transfer," 3/8/88, (PB88-219480).

NCEER-88-0001 "Workshop on Seismic Computer Analysis and Design of Buildings With Interactive Graphics," by W. McGuire, J.F. Abel and C.H. Conley, 1/18/88, (PB88-187760).

NCEER-88-0002 "Optimal Control of Nonlinear Flexible Structures," by J.N. Yang, F.X. Long and D. Wong, 1/22/88, (PB88-213772).

NCEER-88-0003 "Substructuring Techniques in the Time Domain for Primary-Secondary Structural Systems," by G.D. Manolis and G. Juhn, 2/10/88, (PB88-213780).

NCEER-88-0004 "Iterative Seismic Analysis of Primary-Secondary Systems," by A. Singhal, L.D. Lutes and P.D. Spanos, 2/23/88, (PB88-213798).

NCEER-88-0005 "Stochastic Finite Element Expansion for Random Media," by P.D. Spanos and R. Ghanem, 3/14/88, (PB88-213806).

NCEER-88-0006 "Combining Structural Optimization and Structural Control," by F.Y. Cheng and C.P. Pantelides, 1/10/88, (PB88-213814).

NCEER-88-0007 "Seismic Performance Assessment of Code-Designed Structures," by H.H-M. Hwang, J-W. Jaw and H-J. Shau, 3/20/88, (PB88-219423).

NCEER-88-0008 "Reliability Analysis of Code-Designed Structures Under Natural Hazards," by H.H-M. Hwang, H. Ushiba and M. Shinozuka, 2/29/88, (PB88-229471).

NCEER-88-0009 "Seismic Fragility Analysis of Shear Wall Structures," by J-W Jaw and H.H-M. Hwang, 4/30/88, (PB89-102867).

NCEER-88-0010 "Base Isolation of a Multi-Story Building Under a Harmonic Ground Motion - A Comparison of Performances of Various Systems," by F-G Fan, G. Ahmadi and I.G. Tadjbakhsh, 5/18/88, (PB89-122238).

NCEER-88-0011 "Seismic Floor Response Spectra for a Combined System by Green's Functions," by F.M. Lavelle, L.A. Bergman and P.D. Spanos, 5/1/88, (PB89-102875).

NCEER-88-0012 "A New Solution Technique for Randomly Excited Hysteretic Structures," by G.Q. Cai and Y.K. Lin, 5/16/88, (PB89-102883).

NCEER-88-0013 "A Study of Radiation Damping and Soil-Structure Interaction Effects in the Centrifuge," by K. Weissman, supervised by J.H. Prevost, 5/24/88, (PB89-144703).

NCEER-88-0014 "Parameter Identification and Implementation of a Kinematic Plasticity Model for Frictional Soils," by J.H. Prevost and D.V. Griffiths, to be published.

NCEER-88-0015 "Two- and Three- Dimensional Dynamic Finite Element Analyses of the Long Valley Dam," by D.V. Griffiths and J.H. Prevost, 6/17/88, (PB89-144711).

NCEER-88-0016 "Damage Assessment of Reinforced Concrete Structures in Eastern United States," by A.M. Reinhorn, M.J. Seidel, S.K. Kunnath and Y.J. Park, 6/15/88, (PB89-122220).

NCEER-88-0017 "Dynamic Compliance of Vertically Loaded Strip Foundations in Multilayered Viscoelastic Soils," by S. Ahmad and A.S.M. Israil, 6/17/88, (PB89-102891).

NCEER-88-0018 "An Experimental Study of Seismic Structural Response With Added Viscoelastic Dampers," by R.C. Lin, Z. Liang, T.T. Soong and R.H. Zhang, 6/30/88, (PB89-122212). This report is available only through NTIS (see address given above).

NCEER-88-0019 "Experimental Investigation of Primary - Secondary System Interaction," by G.D. Manolis, G. Juhn and A.M. Reinhorn, 5/27/88, (PB89-122204).

NCEER-88-0020 "A Response Spectrum Approach For Analysis of Nonclassically Damped Structures," by J.N. Yang, S. Sarkani and F.X. Long, 4/22/88, (PB89-102909).

NCEER-88-0021 "Seismic Interaction of Structures and Soils: Stochastic Approach," by A.S. Veletsos and A.M. Prasad, 7/21/88, (PB89-122196).

NCEER-88-0022 "Identification of the Serviceability Limit State and Detection of Seismic Structural Damage," by E. DiPasquale and A.S. Cakmak, 6/15/88, (PB89-122188). This report is available only through NTIS (see address given above).

NCEER-88-0023 "Multi-Hazard Risk Analysis: Case of a Simple Offshore Structure," by B.K. Bhartia and E.H. Vanmarcke, 7/21/88, (PB89-145213).

NCEER-88-0024 "Automated Seismic Design of Reinforced Concrete Buildings," by Y.S. Chung, C. Meyer and M. Shinozuka, 7/5/88, (PB89-122170). This report is available only through NTIS (see address given above).

NCEER-88-0025 "Experimental Study of Active Control of MDOF Structures Under Seismic Excitations," by L.L. Chung, R.C. Lin, T.T. Soong and A.M. Reinhorn, 7/10/88, (PB89-122600).

NCEER-88-0026 "Earthquake Simulation Tests of a Low-Rise Metal Structure," by J.S. Hwang, K.C. Chang, G.C. Lee and R.L. Ketter, 8/1/88, (PB89-102917).

NCEER-88-0027 "Systems Study of Urban Response and Reconstruction Due to Catastrophic Earthquakes," by F. Kozin and H.K. Zhou, 9/22/88, (PB90-162348).

NCEER-88-0028 "Seismic Fragility Analysis of Plane Frame Structures," by H.H-M. Hwang and Y.K. Low, 7/31/88, (PB89-131445).

NCEER-88-0029 "Response Analysis of Stochastic Structures," by A. Kardara, C. Bucher and M. Shinozuka, 9/22/88, (PB89-174429).

NCEER-88-0030 "Nonnormal Accelerations Due to Yielding in a Primary Structure," by D.C.K. Chen and L.D. Lutes, 9/19/88, (PB89-131437).

NCEER-88-0031 "Design Approaches for Soil-Structure Interaction," by A.S. Veletsos, A.M. Prasad and Y. Tang, 12/30/88, (PB89-174437). This report is available only through NTIS (see address given above).

NCEER-88-0032 "A Re-evaluation of Design Spectra for Seismic Damage Control," by C.J. Turkstra and A.G. Tallin, 11/7/88, (PB89-145221).

NCEER-88-0033 "The Behavior and Design of Noncontact Lap Splices Subjected to Repeated Inelastic Tensile Loading," by V.E. Sagan, P. Gergely and R.N. White, 12/8/88, (PB89-163737).

NCEER-88-0034 "Seismic Response of Pile Foundations," by S.M. Mamoon, P.K. Banerjee and S. Ahmad, 11/1/88, (PB89-145239).

NCEER-88-0035 "Modeling of R/C Building Structures With Flexible Floor Diaphragms (IDARC2)," by A.M. Reinhorn, S.K. Kunnath and N. Panahshahi, 9/7/88, (PB89-207153).

NCEER-88-0036 "Solution of the Dam-Reservoir Interaction Problem Using a Combination of FEM, BEM with Particular Integrals, Modal Analysis, and Substructuring," by C-S. Tsai, G.C. Lee and R.L. Ketter, 12/31/88, (PB89-207146).

NCEER-88-0037 "Optimal Placement of Actuators for Structural Control," by F.Y. Cheng and C.P. Pantelides, 8/15/88, (PB89-162846).

NCEER-88-0038 "Teflon Bearings in Aseismic Base Isolation: Experimental Studies and Mathematical Modeling," by A. Mokha, M.C. Constantinou and A.M. Reinhorn, 12/5/88, (PB89-218457). This report is available only through NTIS (see address given above).

NCEER-88-0039 "Seismic Behavior of Flat Slab High-Rise Buildings in the New York City Area," by P. Weidlinger and M. Ettouney, 10/15/88, (PB90-145681).

NCEER-88-0040 "Evaluation of the Earthquake Resistance of Existing Buildings in New York City," by P. Weidlinger and M. Ettouney, 10/15/88, to be published.

NCEER-88-0041 "Small-Scale Modeling Techniques for Reinforced Concrete Structures Subjected to Seismic Loads," by W. Kim, A. El-Attar and R.N. White, 11/22/88, (PB89-189625).

NCEER-88-0042 "Modeling Strong Ground Motion from Multiple Event Earthquakes," by G.W. Ellis and A.S. Cakmak, 10/15/88, (PB89-174445).

NCEER-88-0043 "Nonstationary Models of Seismic Ground Acceleration," by M. Grigoriu, S.E. Ruiz and E. Rosenblueth, 7/15/88, (PB89-189617).

NCEER-88-0044 "SARCF User's Guide: Seismic Analysis of Reinforced Concrete Frames," by Y.S. Chung, C. Meyer and M. Shinozuka, 11/9/88, (PB89-174452).

NCEER-88-0045 "First Expert Panel Meeting on Disaster Research and Planning," edited by J. Pantelic and J. Stoyle, 9/15/88, (PB89-174460).

NCEER-88-0046 "Preliminary Studies of the Effect of Degrading Infill Walls on the Nonlinear Seismic Response of Steel Frames," by C.Z. Chrysostomou, P. Gergely and J.F. Abel, 12/19/88, (PB89-208383).

NCEER-88-0047 "Reinforced Concrete Frame Component Testing Facility - Design, Construction, Instrumentation and Operation," by S.P. Pessiki, C. Conley, T. Bond, P. Gergely and R.N. White, 12/16/88, (PB89-174478).

NCEER-89-0001 "Effects of Protective Cushion and Soil Compliancy on the Response of Equipment Within a Seismically Excited Building," by J.A. HoLung, 2/16/89, (PB89-207179).

NCEER-89-0002 "Statistical Evaluation of Response Modification Factors for Reinforced Concrete Structures," by H.H-M. Hwang and J-W. Jaw, 2/17/89, (PB89-207187).

NCEER-89-0003 "Hysteretic Columns Under Random Excitation," by G-Q. Cai and Y.K. Lin, 1/9/89, (PB89-196513).

NCEER-89-0004 "Experimental Study of 'Elephant Foot Bulge' Instability of Thin-Walled Metal Tanks," by Z-H. Jia and R.L. Ketter, 2/22/89, (PB89-207195).

NCEER-89-0005 "Experiment on Performance of Buried Pipelines Across San Andreas Fault," by J. Isenberg, E. Richardson and T.D. O'Rourke, 3/10/89, (PB89-218440). This report is available only through NTIS (see address given above).

NCEER-89-0006 "A Knowledge-Based Approach to Structural Design of Earthquake-Resistant Buildings," by M. Subramani, P. Gergely, C.H. Conley, J.F. Abel and A.H. Zaghw, 1/15/89, (PB89-218465).

NCEER-89-0007 "Liquefaction Hazards and Their Effects on Buried Pipelines," by T.D. O'Rourke and P.A. Lane, 2/1/89, (PB89-218481).

NCEER-89-0008 "Fundamentals of System Identification in Structural Dynamics," by H. Imai, C-B. Yun, O. Maruyama and M. Shinozuka, 1/26/89, (PB89-207211).

NCEER-89-0009 "Effects of the 1985 Michoacan Earthquake on Water Systems and Other Buried Lifelines in Mexico," by A.G. Ayala and M.J. O'Rourke, 3/8/89, (PB89-207229).

NCEER-89-R010 "NCEER Bibliography of Earthquake Education Materials," by K.E.K. Ross, Second Revision, 9/1/89, (PB90-125352).

NCEER-89-0011 "Inelastic Three-Dimensional Response Analysis of Reinforced Concrete Building Structures (IDARC-3D), Part I - Modeling," by S.K. Kunnath and A.M. Reinhorn, 4/17/89, (PB90-114612).

NCEER-89-0012 "Recommended Modifications to ATC-14," by C.D. Poland and J.O. Malley, 4/12/89, (PB90-108648).

NCEER-89-0013 "Repair and Strengthening of Beam-to-Column Connections Subjected to Earthquake Loading," by M. Corazao and A.J. Durrani, 2/28/89, (PB90-109885).

NCEER-89-0014 "Program EXKAL2 for Identification of Structural Dynamic Systems," by O. Maruyama, C-B. Yun, M. Hoshiya and M. Shinozuka, 5/19/89, (PB90-109877).

NCEER-89-0015 "Response of Frames With Bolted Semi-Rigid Connections, Part I - Experimental Study and Analytical Predictions," by P.J. DiCorso, A.M. Reinhorn, J.R. Dickerson, J.B. Radziminski and W.L. Harper, 6/1/89, to be published.

NCEER-89-0016 "ARMA Monte Carlo Simulation in Probabilistic Structural Analysis," by P.D. Spanos and M.P. Mignolet, 7/10/89, (PB90-109893).

NCEER-89-P017 "Preliminary Proceedings from the Conference on Disaster Preparedness - The Place of Earthquake Education in Our Schools," Edited by K.E.K. Ross, 6/23/89, (PB90-108606).

NCEER-89-0017 "Proceedings from the Conference on Disaster Preparedness - The Place of Earthquake Education in Our Schools," Edited by K.E.K. Ross, 12/31/89, (PB90-207895). This report is available only through NTIS (see address given above).

NCEER-89-0018 "Multidimensional Models of Hysteretic Material Behavior for Vibration Analysis of Shape Memory Energy Absorbing Devices, by E.J. Graesser and F.A. Cozzarelli, 6/7/89, (PB90-164146).

NCEER-89-0019 "Nonlinear Dynamic Analysis of Three-Dimensional Base Isolated Structures (3D-BASIS)," by S. Nagarajaiah, A.M. Reinhorn and M.C. Constantinou, 8/3/89, (PB90-161936). This report is available only through NTIS (see address given above).

NCEER-89-0020 "Structural Control Considering Time-Rate of Control Forces and Control Rate Constraints," by F.Y. Cheng and C.P. Pantelides, 8/3/89, (PB90-120445).

NCEER-89-0021 "Subsurface Conditions of Memphis and Shelby County," by K.W. Ng, T-S. Chang and H-H.M. Hwang, 7/26/89, (PB90-120437).

NCEER-89-0022 "Seismic Wave Propagation Effects on Straight Jointed Buried Pipelines," by K. Elhmadi and M.J. O'Rourke, 8/24/89, (PB90-162322).

NCEER-89-0023 "Workshop on Serviceability Analysis of Water Delivery Systems," edited by M. Grigoriu, 3/6/89, (PB90-127424).

NCEER-89-0024 "Shaking Table Study of a 1/5 Scale Steel Frame Composed of Tapered Members," by K.C. Chang, J.S. Hwang and G.C. Lee, 9/18/89, (PB90-160169).

NCEER-89-0025 "DYNAID: A Computer Program for Nonlinear Seismic Site Response Analysis - Technical Documentation," by Jean H. Prevost, 9/14/89, (PB90-161944). This report is available only through NTIS (see address given above).

NCEER-89-0026 "1:4 Scale Model Studies of Active Tendon Systems and Active Mass Dampers for Aseismic Protection," by A.M. Reinhorn, T.T. Soong, R.C. Lin, Y.P. Yang, Y. Fukao, H. Abe and M. Nakai, 9/15/89, (PB90-173246).

NCEER-89-0027 "Scattering of Waves by Inclusions in a Nonhomogeneous Elastic Half Space Solved by Boundary Element Methods," by P.K. Hadley, A. Askar and A.S. Cakmak, 6/15/89, (PB90-145699).

NCEER-89-0028 "Statistical Evaluation of Deflection Amplification Factors for Reinforced Concrete Structures," by H.H.M. Hwang, J-W. Jaw and A.L. Ch'ng, 8/31/89, (PB90-164633).

NCEER-89-0029 "Bedrock Accelerations in Memphis Area Due to Large New Madrid Earthquakes," by H.H.M. Hwang, C.H.S. Chen and G. Yu, 11/7/89, (PB90-162330).

NCEER-89-0030 "Seismic Behavior and Response Sensitivity of Secondary Structural Systems," by Y.Q. Chen and T.T. Soong, 10/23/89, (PB90-164658).

NCEER-89-0031 "Random Vibration and Reliability Analysis of Primary-Secondary Structural Systems," by Y. Ibrahim, M. Grigoriu and T.T. Soong, 11/10/89, (PB90-161951).

NCEER-89-0032 "Proceedings from the Second U.S. - Japan Workshop on Liquefaction, Large Ground Deformation and Their Effects on Lifelines, September 26-29, 1989," Edited by T.D. O'Rourke and M. Hamada, 12/1/89, (PB90-209388).

NCEER-89-0033 "Deterministic Model for Seismic Damage Evaluation of Reinforced Concrete Structures," by J.M. Bracci, A.M. Reinhorn, J.B. Mander and S.K. Kunnath, 9/27/89.

NCEER-89-0034 "On the Relation Between Local and Global Damage Indices," by E. DiPasquale and A.S. Cakmak, 8/15/89, (PB90-173865).

NCEER-89-0035 "Cyclic Undrained Behavior of Nonplastic and Low Plasticity Silts," by A.J. Walker and H.E. Stewart, 7/26/89, (PB90-183518).

NCEER-89-0036 "Liquefaction Potential of Surficial Deposits in the City of Buffalo, New York," by M. Budhu, R. Giese and L. Baumgrass, 1/17/89, (PB90-208455).

NCEER-89-0037 "A Deterministic Assessment of Effects of Ground Motion Incoherence," by A.S. Veletsos and Y. Tang, 7/15/89, (PB90-164294).

NCEER-89-0038 "Workshop on Ground Motion Parameters for Seismic Hazard Mapping," July 17-18, 1989, edited by R.V. Whitman, 12/1/89, (PB90-173923).

NCEER-89-0039 "Seismic Effects on Elevated Transit Lines of the New York City Transit Authority," by C.J. Costantino, C.A. Miller and E. Heymsfield, 12/26/89, (PB90-207887).

NCEER-89-0040 "Centrifugal Modeling of Dynamic Soil-Structure Interaction," by K. Weissman, Supervised by J.H. Prevost, 5/10/89, (PB90-207879).

NCEER-89-0041 "Linearized Identification of Buildings With Cores for Seismic Vulnerability Assessment," by I-K. Ho and A.E. Aktan, 11/1/89, (PB90-251943).

NCEER-90-0001 "Geotechnical and Lifeline Aspects of the October 17, 1989 Loma Prieta Earthquake in San Francisco," by T.D. O'Rourke, H.E. Stewart, F.T. Blackburn and T.S. Dickerman, 1/90, (PB90-208596).

NCEER-90-0002 "Nonnormal Secondary Response Due to Yielding in a Primary Structure," by D.C.K. Chen and L.D. Lutes, 2/28/90, (PB90-251976).

NCEER-90-0003 "Earthquake Education Materials for Grades K-12," by K.E.K. Ross, 4/16/90, (PB91-251984).

NCEER-90-0004 "Catalog of Strong Motion Stations in Eastern North America," by R.W. Busby, 4/3/90, (PB90-251984).

NCEER-90-0005 "NCEER Strong-Motion Data Base: A User Manual for the GeoBase Release (Version 1.0 for the Sun3)," by P. Friberg and K. Jacob, 3/31/90 (PB90-258062).

NCEER-90-0006 "Seismic Hazard Along a Crude Oil Pipeline in the Event of an 1811-1812 Type New Madrid Earthquake," by H.H.M. Hwang and C-H.S. Chen, 4/16/90(PB90-258054).

NCEER-90-0007 "Site-Specific Response Spectra for Memphis Sheahan Pumping Station," by H.H.M. Hwang and C.S. Lee, 5/15/90, (PB91-108811).

NCEER-90-0008 "Pilot Study on Seismic Vulnerability of Crude Oil Transmission Systems," by T. Ariman, R. Dobry, M. Grigoriu, F. Kozin, M. O'Rourke, T. O'Rourke and M. Shinozuka, 5/25/90, (PB91-108837).

NCEER-90-0009 "A Program to Generate Site Dependent Time Histories: EQGEN," by G.W. Ellis, M. Srinivasan and A.S. Cakmak, 1/30/90, (PB91-108829).

NCEER-90-0010 "Active Isolation for Seismic Protection of Operating Rooms," by M.E. Talbott, Supervised by M. Shinozuka, 6/8/9, (PB91-110205).

NCEER-90-0011 "Program LINEARID for Identification of Linear Structural Dynamic Systems," by C-B. Yun and M. Shinozuka, 6/25/90, (PB91-110312).

NCEER-90-0012 "Two-Dimensional Two-Phase Elasto-Plastic Seismic Response of Earth Dams," by A.N. Yiagos, Supervised by J.H. Prevost, 6/20/90, (PB91-110197).

NCEER-90-0013 "Secondary Systems in Base-Isolated Structures: Experimental Investigation, Stochastic Response and Stochastic Sensitivity," by G.D. Manolis, G. Juhn, M.C. Constantinou and A.M. Reinhorn, 7/1/90, (PB91-110320).

NCEER-90-0014 "Seismic Behavior of Lightly-Reinforced Concrete Column and Beam-Column Joint Details," by S.P. Pessiki, C.H. Conley, P. Gergely and R.N. White, 8/22/90, (PB91-108795).

NCEER-90-0015 "Two Hybrid Control Systems for Building Structures Under Strong Earthquakes," by J.N. Yang and A. Danielians, 6/29/90, (PB91-125393).

NCEER-90-0016 "Instantaneous Optimal Control with Acceleration and Velocity Feedback," by J.N. Yang and Z. Li, 6/29/90, (PB91-125401).

NCEER-90-0017 "Reconnaissance Report on the Northern Iran Earthquake of June 21, 1990," by M. Mehrain, 10/4/90, (PB91-125377).

NCEER-90-0018 "Evaluation of Liquefaction Potential in Memphis and Shelby County," by T.S. Chang, P.S. Tang, C.S. Lee and H. Hwang, 8/10/90, (PB91-125427).

NCEER-90-0019 "Experimental and Analytical Study of a Combined Sliding Disc Bearing and Helical Steel Spring Isolation System," by M.C. Constantinou, A.S. Mokha and A.M. Reinhorn, 10/4/90, (PB91-125385).

NCEER-90-0020 "Experimental Study and Analytical Prediction of Earthquake Response of a Sliding Isolation System with a Spherical Surface," by A.S. Mokha, M.C. Constantinou and A.M. Reinhorn, 10/11/90, (PB91-125419).

NCEER-90-0021 "Dynamic Interaction Factors for Floating Pile Groups," by G. Gazetas, K. Fan, A. Kaynia and E. Kausel, 9/10/90, (PB91-170381).

NCEER-90-0022 "Evaluation of Seismic Damage Indices for Reinforced Concrete Structures," by S. Rodriguez-Gomez and A.S. Cakmak, 9/30/90, PB91-171322).

NCEER-90-0023 "Study of Site Response at a Selected Memphis Site," by H. Desai, S. Ahmad, E.S. Gazetas and M.R. Oh, 10/11/90, (PB91-196857).

NCEER-90-0024 "A User's Guide to Strongmo: Version 1.0 of NCEER's Strong-Motion Data Access Tool for PCs and Terminals," by P.A. Friberg and C.A.T. Susch, 11/15/90, (PB91-171272).

NCEER-90-0025 "A Three-Dimensional Analytical Study of Spatial Variability of Seismic Ground Motions," by L-L. Hong and A.H.-S. Ang, 10/30/90, (PB91-170399).

NCEER-90-0026 "MUMOID User's Guide - A Program for the Identification of Modal Parameters," by S. Rodriguez-Gomez and E. DiPasquale, 9/30/90, (PB91-171298).

NCEER-90-0027 "SARCF-II User's Guide - Seismic Analysis of Reinforced Concrete Frames," by S. Rodriguez-Gomez, Y.S. Chung and C. Meyer, 9/30/90, (PB91-171280).

NCEER-90-0028 "Viscous Dampers: Testing, Modeling and Application in Vibration and Seismic Isolation," by N. Makris and M.C. Constantinou, 12/20/90 (PB91-190561).

NCEER-90-0029 "Soil Effects on Earthquake Ground Motions in the Memphis Area," by H. Hwang, C.S. Lee, K.W. Ng and T.S. Chang, 8/2/90, (PB91-190751).

NCEER-91-0001 "Proceedings from the Third Japan-U.S. Workshop on Earthquake Resistant Design of Lifeline Facilities and Countermeasures for Soil Liquefaction, December 17-19, 1990," edited by T.D. O'Rourke and M. Hamada, 2/1/91, (PB91-179259).

NCEER-91-0002 "Physical Space Solutions of Non-Proportionally Damped Systems," by M. Tong, Z. Liang and G.C. Lee, 1/15/91, (PB91-179242).

NCEER-91-0003 "Seismic Response of Single Piles and Pile Groups," by K. Fan and G. Gazetas, 1/10/91, (PB92-174994).

NCEER-91-0004 "Damping of Structures: Part 1 - Theory of Complex Damping," by Z. Liang and G. Lee, 10/10/91, (PB92-197235).

NCEER-91-0005 "3D-BASIS - Nonlinear Dynamic Analysis of Three Dimensional Base Isolated Structures: Part II," by S. Nagarajaiah, A.M. Reinhorn and M.C. Constantinou, 2/28/91, (PB91-190553).

NCEER-91-0006 "A Multidimensional Hysteretic Model for Plasticity Deforming Metals in Energy Absorbing Devices," by E.J. Graesser and F.A. Cozzarelli, 4/9/91, (PB92-108364).

NCEER-91-0007 "A Framework for Customizable Knowledge-Based Expert Systems with an Application to a KBES for Evaluating the Seismic Resistance of Existing Buildings," by E.G. Ibarra-Anaya and S.J. Fenves, 4/9/91, (PB91-210930).

NCEER-91-0008 "Nonlinear Analysis of Steel Frames with Semi-Rigid Connections Using the Capacity Spectrum Method," by G.G. Deierlein, S-H. Hsieh, Y-J. Shen and J.F. Abel, 7/2/91, (PB92-113828).

NCEER-91-0009 "Earthquake Education Materials for Grades K-12," by K.E.K. Ross, 4/30/91, (PB91-212142).

NCEER-91-0010 "Phase Wave Velocities and Displacement Phase Differences in a Harmonically Oscillating Pile," by N. Makris and G. Gazetas, 7/8/91, (PB92-108356).

NCEER-91-0011 "Dynamic Characteristics of a Full-Size Five-Story Steel Structure and a 2/5 Scale Model," by K.C. Chang, G.C. Yao, G.C. Lee, D.S. Hao and Y.C. Yeh," 7/2/91, (PB93-116648).

NCEER-91-0012 "Seismic Response of a 2/5 Scale Steel Structure with Added Viscoelastic Dampers," by K.C. Chang, T.T. Soong, S-T. Oh and M.L. Lai, 5/17/91, (PB92-110816).

NCEER-91-0013 "Earthquake Response of Retaining Walls; Full-Scale Testing and Computational Modeling," by S. Alampalli and A-W.M. Elgamal, 6/20/91, to be published.

NCEER-91-0014 "3D-BASIS-M: Nonlinear Dynamic Analysis of Multiple Building Base Isolated Structures," by P.C. Tsopelas, S. Nagarajaiah, M.C. Constantinou and A.M. Reinhorn, 5/28/91, (PB92-113885).

NCEER-91-0015 "Evaluation of SEAOC Design Requirements for Sliding Isolated Structures," by D. Theodossiou and M.C. Constantinou, 6/10/91, (PB92-114602).

NCEER-91-0016 "Closed-Loop Modal Testing of a 27-Story Reinforced Concrete Flat Plate-Core Building," by H.R. Somaprasad, T. Toksoy, H. Yoshiyuki and A.E. Aktan, 7/15/91, (PB92-129980).

NCEER-91-0017 "Shake Table Test of a 1/6 Scale Two-Story Lightly Reinforced Concrete Building," by A.G. El-Attar, R.N. White and P. Gergely, 2/28/91, (PB92-222447).

NCEER-91-0018 "Shake Table Test of a 1/8 Scale Three-Story Lightly Reinforced Concrete Building," by A.G. El-Attar, R.N. White and P. Gergely, 2/28/91, (PB93-116630).

NCEER-91-0019 "Transfer Functions for Rigid Rectangular Foundations," by A.S. Veletsos, A.M. Prasad and W.H. Wu, 7/31/91.

NCEER-91-0020 "Hybrid Control of Seismic-Excited Nonlinear and Inelastic Structural Systems," by J.N. Yang, Z. Li and A. Danielians, 8/1/91, (PB92-143171).

NCEER-91-0021 "The NCEER-91 Earthquake Catalog: Improved Intensity-Based Magnitudes and Recurrence Relations for U.S. Earthquakes East of New Madrid," by L. Seeber and J.G. Armbruster, 8/28/91, (PB92-176742).

NCEER-91-0022 "Proceedings from the Implementation of Earthquake Planning and Education in Schools: The Need for Change - The Roles of the Changemakers," by K.E.K. Ross and F. Winslow, 7/23/91, (PB92-129998).

NCEER-91-0023 "A Study of Reliability-Based Criteria for Seismic Design of Reinforced Concrete Frame Buildings," by H.H.M. Hwang and H-M. Hsu, 8/10/91, (PB92-140235).

NCEER-91-0024 "Experimental Verification of a Number of Structural System Identification Algorithms," by R.G. Ghanem, H. Gavin and M. Shinozuka, 9/18/91, (PB92-176577).

NCEER-91-0025 "Probabilistic Evaluation of Liquefaction Potential," by H.H.M. Hwang and C.S. Lee," 11/25/91, (PB92-143429).

NCEER-91-0026 "Instantaneous Optimal Control for Linear, Nonlinear and Hysteretic Structures - Stable Controllers," by J.N. Yang and Z. Li, 11/15/91, (PB92-163807).

NCEER-91-0027 "Experimental and Theoretical Study of a Sliding Isolation System for Bridges," by M.C. Constantinou, A. Kartoum, A.M. Reinhorn and P. Bradford, 11/15/91, (PB92-176973).

NCEER-92-0001 "Case Studies of Liquefaction and Lifeline Performance During Past Earthquakes, Volume 1: Japanese Case Studies," Edited by M. Hamada and T. O'Rourke, 2/17/92, (PB92-197243).

NCEER-92-0002 "Case Studies of Liquefaction and Lifeline Performance During Past Earthquakes, Volume 2: United States Case Studies," Edited by T. O'Rourke and M. Hamada, 2/17/92, (PB92-197250).

NCEER-92-0003 "Issues in Earthquake Education," Edited by K. Ross, 2/3/92, (PB92-222389).

NCEER-92-0004 "Proceedings from the First U.S. - Japan Workshop on Earthquake Protective Systems for Bridges," Edited by I.G. Buckle, 2/4/92, (PB94-142239, A99, MF-A06).

NCEER-92-0005 "Seismic Ground Motion from a Haskell-Type Source in a Multiple-Layered Half-Space," A.P. Theoharis, G. Deodatis and M. Shinozuka, 1/2/92, to be published.

NCEER-92-0006 "Proceedings from the Site Effects Workshop," Edited by R. Whitman, 2/29/92, (PB92-197201).

NCEER-92-0007 "Engineering Evaluation of Permanent Ground Deformations Due to Seismically-Induced Liquefaction," by M.H. Baziar, R. Dobry and A-W.M. Elgamal, 3/24/92, (PB92-222421).

NCEER-92-0008 "A Procedure for the Seismic Evaluation of Buildings in the Central and Eastern United States," by C.D. Poland and J.O. Malley, 4/2/92, (PB92-222439).

NCEER-92-0009 "Experimental and Analytical Study of a Hybrid Isolation System Using Friction Controllable Sliding Bearings," by M.Q. Feng, S. Fujii and M. Shinozuka, 5/15/92, (PB93-150282).

NCEER-92-0010 "Seismic Resistance of Slab-Column Connections in Existing Non-Ductile Flat-Plate Buildings," by A.J. Durrani and Y. Du, 5/18/92.

NCEER-92-0011 "The Hysteretic and Dynamic Behavior of Brick Masonry Walls Upgraded by Ferrocement Coatings Under Cyclic Loading and Strong Simulated Ground Motion," by H. Lee and S.P. Prawel, 5/11/92, to be published.

NCEER-92-0012 "Study of Wire Rope Systems for Seismic Protection of Equipment in Buildings," by G.F. Demetriades, M.C. Constantinou and A.M. Reinhorn, 5/20/92.

NCEER-92-0013 "Shape Memory Structural Dampers: Material Properties, Design and Seismic Testing," by P.R. Witting and F.A. Cozzarelli, 5/26/92.

NCEER-92-0014 "Longitudinal Permanent Ground Deformation Effects on Buried Continuous Pipelines," by M.J. O'Rourke, and C. Nordberg, 6/15/92.

NCEER-92-0015 "A Simulation Method for Stationary Gaussian Random Functions Based on the Sampling Theorem," by M. Grigoriu and S. Balopoulou, 6/11/92, (PB93-127496).

NCEER-92-0016 "Gravity-Load-Designed Reinforced Concrete Buildings: Seismic Evaluation of Existing Construction and Detailing Strategies for Improved Seismic Resistance," by G.W. Hoffmann, S.K. Kunnath, A.M. Reinhorn and J.B. Mander, 7/15/92, (PB94-142007, A08, MF-A02).

NCEER-92-0017 "Observations on Water System and Pipeline Performance in the Limón Area of Costa Rica Due to the April 22, 1991 Earthquake," by M. O'Rourke and D. Ballantyne, 6/30/92, (PB93-126811).

NCEER-92-0018 "Fourth Edition of Earthquake Education Materials for Grades K-12," Edited by K.E.K. Ross, 8/10/92.

NCEER-92-0019 "Proceedings from the Fourth Japan-U.S. Workshop on Earthquake Resistant Design of Lifeline Facilities and Countermeasures for Soil Liquefaction," Edited by M. Hamada and T.D. O'Rourke, 8/12/92, (PB93-163939).

NCEER-92-0020 "Active Bracing System: A Full Scale Implementation of Active Control," by A.M. Reinhorn, T.T. Soong, R.C. Lin, M.A. Riley, Y.P. Wang, S. Aizawa and M. Higashino, 8/14/92, (PB93-127512).

NCEER-92-0021 "Empirical Analysis of Horizontal Ground Displacement Generated by Liquefaction-Induced Lateral Spreads," by S.F. Bartlett and T.L. Youd, 8/17/92, (PB93-188241).

NCEER-92-0022 "IDARC Version 3.0: Inelastic Damage Analysis of Reinforced Concrete Structures," by S.K. Kunnath, A.M. Reinhorn and R.F. Lobo, 8/31/92, (PB93-227502, A07, MF-A02).

NCEER-92-0023 "A Semi-Empirical Analysis of Strong-Motion Peaks in Terms of Seismic Source, Propagation Path and Local Site Conditions, by M. Kamiyama, M.J. O'Rourke and R. Flores-Berrones, 9/9/92, (PB93-150266).

NCEER-92-0024 "Seismic Behavior of Reinforced Concrete Frame Structures with Nonductile Details, Part I: Summary of Experimental Findings of Full Scale Beam-Column Joint Tests," by A. Beres, R.N. White and P. Gergely, 9/30/92, (PB93-227783, A05, MF-A01).

NCEER-92-0025 "Experimental Results of Repaired and Retrofitted Beam-Column Joint Tests in Lightly Reinforced Concrete Frame Buildings," by A. Beres, S. El-Borgi, R.N. White and P. Gergely, 10/29/92, (PB93-227791, A05, MF-A01).

NCEER-92-0026 "A Generalization of Optimal Control Theory: Linear and Nonlinear Structures," by J.N. Yang, Z. Li and S. Vongchavalitkul, 11/2/92, (PB93-188621).

NCEER-92-0027 "Seismic Resistance of Reinforced Concrete Frame Structures Designed Only for Gravity Loads: Part I - Design and Properties of a One-Third Scale Model Structure," by J.M. Bracci, A.M. Reinhorn and J.B. Mander, 12/1/92, (PB94-104502, A08, MF-A02).

NCEER-92-0028 "Seismic Resistance of Reinforced Concrete Frame Structures Designed Only for Gravity Loads: Part II - Experimental Performance of Subassemblages," by L.E. Aycardi, J.B. Mander and A.M. Reinhorn, 12/1/92, (PB94-104510, A08, MF-A02).

NCEER-92-0029 "Seismic Resistance of Reinforced Concrete Frame Structures Designed Only for Gravity Loads: Part III - Experimental Performance and Analytical Study of a Structural Model," by J.M. Bracci, A.M. Reinhorn and J.B. Mander, 12/1/92, (PB93-227528, A09, MF-A01).

NCEER-92-0030 "Evaluation of Seismic Retrofit of Reinforced Concrete Frame Structures: Part I - Experimental Performance of Retrofitted Subassemblages," by D. Choudhuri, J.B. Mander and A.M. Reinhorn, 12/8/92, (PB93-198307, A07, MF-A02).

NCEER-92-0031 "Evaluation of Seismic Retrofit of Reinforced Concrete Frame Structures: Part II - Experimental Performance and Analytical Study of a Retrofitted Structural Model," by J.M. Bracci, A.M. Reinhorn and J.B. Mander, 12/8/92, (PB93-198315, A09, MF-A03).

NCEER-92-0032 "Experimental and Analytical Investigation of Seismic Response of Structures with Supplemental Fluid Viscous Dampers," by M.C. Constantinou and M.D. Symans, 12/21/92, (PB93-191435).

NCEER-92-0033 "Reconnaissance Report on the Cairo, Egypt Earthquake of October 12, 1992," by M. Khater, 12/23/92, (PB93-188621).

NCEER-92-0034 "Low-Level Dynamic Characteristics of Four Tall Flat-Plate Buildings in New York City," by H. Gavin, S. Yuan, J. Grossman, E. Pekelis and K. Jacob, 12/28/92, (PB93-188217).

NCEER-93-0001 "An Experimental Study on the Seismic Performance of Brick-Infilled Steel Frames With and Without Retrofit," by J.B. Mander, B. Nair, K. Wojtkowski and J. Ma, 1/29/93, (PB93-227510, A07, MF-A02).

NCEER-93-0002 "Social Accounting for Disaster Preparedness and Recovery Planning," by S. Cole, E. Pantoja and V. Razak, 2/22/93, (PB94-142114, A12, MF-A03).

NCEER-93-0003 "Assessment of 1991 NEHRP Provisions for Nonstructural Components and Recommended Revisions," by T.T. Soong, G. Chen, Z. Wu, R-H. Zhang and M. Grigoriu, 3/1/93, (PB93-188639).

NCEER-93-0004 "Evaluation of Static and Response Spectrum Analysis Procedures of SEAOC/UBC for Seismic Isolated Structures," by C.W. Winters and M.C. Constantinou, 3/23/93, (PB93-198299).

NCEER-93-0005 "Earthquakes in the Northeast - Are We Ignoring the Hazard? A Workshop on Earthquake Science and Safety for Educators," edited by K.E.K. Ross, 4/2/93, (PB94-103066, A09, MF-A02).

NCEER-93-0006 "Inelastic Response of Reinforced Concrete Structures with Viscoelastic Braces," by R.F. Lobo, J.M. Bracci, K.L. Shen, A.M. Reinhorn and T.T. Soong, 4/5/93, (PB93-227486, A05, MF-A02).

NCEER-93-0007 "Seismic Testing of Installation Methods for Computers and Data Processing Equipment," by K. Kosar, T.T. Soong, K.L. Shen, J.A. HoLung and Y.K. Lin, 4/12/93, (PB93-198299).

NCEER-93-0008 "Retrofit of Reinforced Concrete Frames Using Added Dampers," by A. Reinhorn, M. Constantinou and C. Li, to be published.

NCEER-93-0009 "Seismic Behavior and Design Guidelines for Steel Frame Structures with Added Viscoelastic Dampers," by K.C. Chang, M.L. Lai, T.T. Soong, D.S. Hao and Y.C. Yeh, 5/1/93, (PB94-141959, A07, MF-A02).

NCEER-93-0010 "Seismic Performance of Shear-Critical Reinforced Concrete Bridge Piers," by J.B. Mander, S.M. Waheed, M.T.A. Chaudhary and S.S. Chen, 5/12/93, (PB93-227494, A08, MF-A02).

NCEER-93-0011 "3D-BASIS-TABS: Computer Program for Nonlinear Dynamic Analysis of Three Dimensional Base Isolated Structures," by S. Nagarajaiah, C. Li, A.M. Reinhorn and M.C. Constantinou, 8/2/93, (PB94-141819, A09, MF-A02).

NCEER-93-0012 "Effects of Hydrocarbon Spills from an Oil Pipeline Break on Ground Water," by O.J. Helweg and H.H.M. Hwang, 8/3/93, (PB94-141942, A06, MF-A02).

NCEER-93-0013 "Simplified Procedures for Seismic Design of Nonstructural Components and Assessment of Current Code Provisions," by M.P. Singh, L.E. Suarez, E.E. Matheu and G.O. Maldonado, 8/4/93, (PB94-141827, A09, MF-A02).

NCEER-93-0014 "An Energy Approach to Seismic Analysis and Design of Secondary Systems," by G. Chen and T.T. Soong, 8/6/93, (PB94-142767, A11, MF-A03).

NCEER-93-0015 "Proceedings from School Sites: Becoming Prepared for Earthquakes - Commemorating the Third Anniversary of the Loma Prieta Earthquake," Edited by F.E. Winslow and K.E.K. Ross, 8/16/93.

NCEER-93-0016 "Reconnaissance Report of Damage to Historic Monuments in Cairo, Egypt Following the October 12, 1992 Dahshur Earthquake," by D. Sykora, D. Look, G. Croci, E. Karaesmen and E. Karaesmen, 8/19/93, (PB94-142221, A08, MF-A02).

NCEER-93-0017 "The Island of Guam Earthquake of August 8, 1993," by S.W. Swan and S.K. Harris, 9/30/93, (PB94-141843, A04, MF-A01).

NCEER-93-0018 "Engineering Aspects of the October 12, 1992 Egyptian Earthquake," by A.W. Elgamal, M. Amer, K. Adalier and A. Abul-Fadl, 10/7/93, (PB94-141983, A05, MF-A01).

NCEER-93-0019 "Development of an Earthquake Motion Simulator and its Application in Dynamic Centrifuge Testing," by I. Krstelj, Supervised by J.H. Prevost, 10/23/93.

NCEER-93-0020 "NCEER-Taisei Corporation Research Program on Sliding Seismic Isolation Systems for Bridges: Experimental and Analytical Study of a Friction Pendulum System (FPS)," by M.C. Constantinou, P. Tsopelas, Y-S. Kim and S. Okamoto, 11/1/93, (PB94-142775, A08, MF-A02).

NCEER-93-0021 "Finite Element Modeling of Elastomeric Seismic Isolation Bearings," by L.J. Billings, Supervised by R. Shepherd, 11/8/93, to be published.

NCEER-93-0022 "Seismic Vulnerability of Equipment in Critical Facilities: Life-Safety and Operational Consequences," by K. Porter, G.S. Johnson, M.M. Zadeh, C. Scawthorn and S. Eder, 11/24/93.

NCEER-93-0023 "Hokkaido Nansei-oki, Japan Earthquake of July 12, 1993, by P.I. Yanev and C.R. Scawthorn, 12/23/93.

NCEER-94-0001 "An Evaluation of Seismic Serviceability of Water Supply Networks with Application to the San Francisco Auxiliary Water Supply System," by I. Markov, Supervised by M. Grigoriu and T. O'Rourke, 1/21/94.

NCEER-94-0002 "NCEER-Taisei Corporation Research Program on Sliding Seismic Isolation Systems for Bridges: Experimental and Analytical Study of Systems Consisting of Sliding Bearings, Rubber Restoring Force Devices and Fluid Dampers," Volumes I and II, by P. Tsopelas, S. Okamoto, M.C. Constantinou, D. Ozaki and S. Fujii, 2/4/94.

NCEER-94-0003 "A Markov Model for Local and Global Damage Indices in Seismic Analysis," by S. Rahman and M. Grigoriu, 2/18/94.

NCEER-94-0004 "Proceedings from the NCEER Workshop on Seismic Response of Masonry Infills," edited by D.P. Abrams, 3/1/94.

NCEER-94-0005 "The Northridge, California Earthquake of January 17, 1994: General Reconnaissance Report," edited by J.D. Goltz, 3/11/94.

NCEER-94-0006 "Seismic Energy Based Fatigue Damage Analysis of Bridge Columns: Part I - Evaluation of Seismic Capacity," by G.A. Chang and J.B. Mander, 3/14/94.

NCEER-94-0007 "Seismic Isolation of Multi-Story Frame Structures Using Spherical Sliding Isolation Systems," by T.M. Al-Hussaini, V.A. Zayas and M.C. Constantinou, 3/17/94.

NCEER-94-0008 "The Northridge, California Earthquake of January 17, 1994: Performance of Highway Bridges," edited by I.G. Buckle, 3/24/94.

NCEER-94-0009 "Proceedings of the Third U.S.-Japan Workshop on Earthquake Protective Systems for Bridges," edited by I.G. Buckle and I. Friedland, 3/31/94.

NCEER-94-0010 "3D-BASIS-ME: Computer Program for Nonlinear Dynamic Analysis of Seismically Isolated Single and Multiple Structures and Liquid Storage Tanks," by P.C. Tsopelas, M.C. Constantinou and A.M. Reinhorn, 4/12/94.

NCEER-94-0011 "The Northridge, California Earthquake of January 17, 1994: Performance of Gas Transmission Pipelines," by T.D. O'Rourke and M.C. Palmer, 5/16/94.

NCEER-94-0012 "Feasibility Study of Replacement Procedures and Earthquake Performance Related to Gas Transmission Pipelines," by T.D. O'Rourke and M.C. Palmer, 5/25/94.

NCEER-94-0013 "Seismic Energy Based Fatigue Damage Analysis of Bridge Columns: Part II - Evaluation of Seismic Demand," by G.A. Chang and J.B. Mander, 6/1/94, to be published.

NCEER-94-0014 "NCEER-Taisei Corporation Research Program on Sliding Seismic Isolation Systems for Bridges: Experimental and Analytical Study of a System Consisting of Sliding Bearings and Fluid Restoring Force/Damping Devices," by P. Tsopelas and M.C. Constantinou, 6/13/94.